Structure function relationship of recombinant sRAGE

A thesis submitted for the Doctor of Philosophy

Dinamithra Gedara Sujeewani Rasika Premaratne

April 2016

School of Biological Sciences, Monash University, Melbourne, Australia

School of Biomedical Sciences, Monash University, Melbourne, Australia

Baker IDI Heart and Diabetes Institute, Melbourne, Australia

Notice 1

Notice 2

I certify that I have made all reasonable efforts to secure copyright permissions for third-party content included in this thesis and have not knowingly added copyright content to my work without the owner's permission.

Table of Contents

Abstract

The receptor for advanced glycation end-products (RAGE) is a member of the immunoglobulin super family of cell surface receptors. It acts as the direct mediator of physiological and pathological responses such as inflammation, chemotaxis, neurite outgrowth, angiogenesis, apoptosis and proliferation. RAGE is known to bind with structurally and functionally diverse ligands, such as advanced glycation end-products (AGEs), high mobility group family proteins including HMGB-1/amphoterin, matrix proteins, such as amyloid β peptides, and members of the S100/calgranulin protein family. The up-regulation of RAGE via its ligands and thereby its role in development of disease pathologies in humans is well understood. The blockage of RAGE is considered a therapeutic approach to overcome RAGE-related disease development. One major isoform of RAGE, known as soluble RAGE (sRAGE) acts as a decoy receptor by scavenging RAGE ligands, and prevents them from binding to RAGE or other cell surface receptors. Recent studies have revealed that sRAGE might be useful in treating pathologies caused through RAGE-ligand interactions. Therefore, sRAGE has potential therapeutic properties.

In the present study, sRAGE was successfully expressed in hairy root cultures to obtain a yield of ~300 µg purified protein from ~100 g of hairy roots. Plant expression systems, including tobacco hairy root cultures, have the advantage of producing glycosylated proteins similar to mammalian expression system. Although the complex modification of glycans differs between plants and mammals, the core glycans and the frequency and sites of glycosylation are identical. Purified plant-made sRAGE predominantly existed in its monomeric form (as determined by SDS-PAGE analysis) with a molecular weight of ~45 kDa. Enzymatic *N*-linked deglycosylation assays using PNGase F suggests that the sRAGE produced was *N*-linked glycosylated.

sRAGE was also successfully expressed in *E. coli*-Rosetta-gami strain as a HaloTag® fusion protein, yielding ~0.3 g L^{-1} (monomeric form), with a purity of 90 %. In contrast to plant-made sRAGE, *E. coli*-made sRAGE produced putative protein aggregates along with the monomeric form. As expected the *E. coli* expression system produced non-glycosylated sRAGE.

The purified monomeric form of plant and *E. coli* derived sRAGE was used to perform *in vitro* ligand binding studies with HMGB-1 and S100A8/A9 complex to determine the affinities of these glycosylated and non-glycosylated sRAGE proteins to the ligands. It was shown that glycosylated plant-made sRAGE has a higher affinity to both HMGB-1 and S100A8/A9 than *E. coli*-made or deglycosylated plant-made sRAGE. The observed higher affinity was statistically significant for HMGB-1. However, the observed higher affinity of plant-made sRAGE to S100A8/A9 complex was not statistically significant compared to *E. coli*-made sRAGE or the deglycosylated (non-denatured) plant-made sRAGE. The higher affinity of plant-made sRAGE to ligands was related to the *N*-linked glycosylation of sRAGE.

The effects of extracellular components and conditions on sRAGE-ligand binding was tested by the addition of EDTA and several cations. In our study, Mg^{2+}/Zn^{2+} enhanced *in vitro* binding of sRAGE-S100A8/A9 complex with a similar capacity to Ca^{2+}/Zn^{2+}. The importance of Ca^{2+}/Zn^{2+} cations for RAGE binding to S100A9 has been reported previously. The inhibitory effect of EDTA (2.0 mM) observed for HMGB-1 binding could be tested *in vivo* studies in future, as a potential treatment for RAGE-mediated inflammatory diseases.

This is the first report of the expression of biologically active recombinant sRAGE in a plant expression system. Our research has found that if sRAGE is to be used as a therapeutic protein in the future, plant expression system could be used as a potential production platform. The enhanced binding potential of the *N*-linked glycosylated plant-made sRAGE showed the importance of glycosylation on the activity of the protein. Therefore, in future studies, glycoengineering could be investigated to introduce important glycans and then to enhance the activity of sRAGE. Thus, a bio-better potential therapeutic protein could be produced in a plant expression system.

Declaration

I, D. G. S. Rasika Premaratne, declare that this thesis contains no material that has been accepted for the award of any degree or diploma in any other University and, to the best of my knowledge and belief, contains no material which has been previously published or written by another person, except where due reference is made in the text of the thesis.

D.G.S. Rasika Premaratne

Abbreviations

aa	Amino acids
2AB	2-aminobenzamine
AD	Alzheimer's disease
AEC	Anion-exchange chromatography
AGEs	Advanced glycation end-products
Ala	Alanine
APS	Ammonium persulfate
Arg	Arginine
Asn	Asparagine
Asp	Aspartic acid
AT2	Angiotensin II type 2 receptor
BEVS	Baculovirus expression vector systems
BHK	Baby hamster kidney
BMPR2	Bone morphogenetic protein R2
BSA	Bovine serum albumin
CAMS	Cell adhesion molecules
CD	Circular dichroism spectroscopy
CHD	Coronary heart disease
CHF	Chronic heart failure
CHO	Chinese hamster ovary
CML	$N\varepsilon$-(carboxymethyl) lysine
CVD	Cardio vascular disease
DNA	Deoxyribonucleic acids
DPP	Dolichol pyrophosphate
DTT	Dithiothreitol
ECL	Enhanced chemiluminescence

EDTA	Ethylenediaminetetraacetic acid
ELISA	Enzyme-linked immunosorbent assays
EMA	European Medicines Agency
EpCAM	Epithelial cell adhesion molecule
ER	Endoplasmic reticulum
ES/MS	Electro spray mass spectroscopy
FDA	Food and Drug Administration
FFI	2-(2-furoyl)-4-(5)-(2-furanyl)-1H-imidazole
FH1	Formin homology domain-1
FMDV	Foot-and-mouth disease virus
FPLC	Fast protein liquid chromatography
Fuc	Fucose
Gal	Galactose
Glc	Glucose
GlcNAc	Glucose *N*-Acetylglucosamine
Gln	Glutamine
Gly	Glycine
GST	Glutathione S-transferase
HEK	Human embryonic kidney
HEPES	(4-(2-hydroxyethyl)-1-piperazineethanesulfonic acid)
hGh	Human growth hormone
His	Histidine
HMEC-1	Human dermal microvascular endothelial cells
HMGB-1	High mobility group box protein-1
HPT	Hygromycin B phosphotransferase
HPV	Human Papillomavirus
HRP	Horseradish peroxidase

ICAM-1	Intercellular adhesion molecule-1
Ig	Immunoglobulin
IKK	Inhibitor of kappa B kinase
IMAC	Immobilized metal chelate affinity chromatography
ITC	Isothermal titration calorimetry
IκB	Inhibitor of κB
JAK	Janus kinase
JNK	c-Jun N-terminal kinase
JUNK	Jun-N-terminal kinase
kDa	Kilo dalton
LB	Luria-Bertani medium
LTB	Heat-labile toxin B Subunit
LVEF	Left ventricular ejection fraction
mAb	Monoclonal antibody
MAC-1	Macrophage-1 antigen
MALDI/MS	Matrix-assisted laser desorption ionization/mass spectrometry
MAPK	Mitogen-activated protein kinase
mAU	Milli Absorbance units
MBP	Maltose-binding protein
mDia 1	Mammalian Diaphanous-related formin 1
μg	Microgram
MHC	Major Histocompatibility complex
mILs	Mouse interleukins
mRNA	Messenger RNA
MRP	Migration inhibitory factor-related protein
MS medium	Murashige and Skoog medium
MW	Molecular weight

MWCO	Molecular weight cut-off
NADPH	Nicotinamide adenine dinucleotide phosphate
N-CAM	Neural adhesion molecules
NeuAc	N-Acetylneuraminic acid
NF-κB	Nuclear factor κB
nM	Nanomolar
NMD	Nonsense-mediated decay pathway
NMR	Nuclear magnetic resonance
NusA	N-utilisation substance A
P13K	Phosphoinositide 3-kinase
PA	Protective antigen
PBS	Phosphate buffered saline
PBST	Phosphate buffered saline solution with Tween 20
PCR	Polymerase chain reaction
PDB	Protein data bank archive
PDE7A1	Phosphodiesterase 7A1 enzyme
PDI	Protein disulfide isomerase
pI	Isoelectric point
PMSF	Phenylmethylsulfonyl fluoride
PPI's	Peptidyl prolyl *cis/trans* isomerases
PRRs	Pattern recognition receptors
PTMs	Post-translational modifications
PVDF	Polyvinylidene fluoride
PVPP	Polyvinylpolypyrrolidone
RAGE	Receptor for advanced glycation end-products
RNA	Ribonucleic acid
ROS	Reactive oxygen species

RuBisCO	Ribulose-1,5-bisphosphate carboxylase/oxygenase
SAPK	Stress-activated protein kinase
SAXS	Small angle X-ray scattering
SDS-PAGE	Sodium dodecyl sulfate polyacrylamide gel electrophoresis
SEC	Size-exclusion chromatography
Si-RNA	Small interfering RNA
SMCs	Smooth muscle cells
SOD	Superoxide dismutase
SPR	Surface plasmon resonance
sRAGE	Soluble receptor for advanced glycation end-products
STAT	Signal transducer and activator of transcription
TEMED	Tetramethylethylenediamine
Thr	Threonine
TMB	3,3',5,5'-tetramethylbenzidine
TPA	Tissue plasminogen activator
t-RNAs	Transfer ribonucleic acids
TSP	Total soluble protein
UTR	Untranslated region
v/v	Volume per volume
VCAM-1	Vascular cell adhesion molecule-1
VLA-4	Very late antigen 4
w/v	Weight per volume
Xyl	Xylose

CHAPTER 1

Introduction

1.1 Receptor for advanced glycation end-products (RAGE)

The receptor for advanced glycation end-products (RAGE) acts as the direct mediator of physiological and pathological responses, such as inflammation, chemotaxis, neurite outgrowth, angiogenesis, apoptosis and proliferation (Schmidt *et al*., 2001; Schmidt *et al*., 2000). However, whether or not it influences these processes as part of normal physiological functions is unknown. RAGE is a member of the immunoglobulin (Ig) super family of cell surface receptors and is the best studied receptor of advanced glycation end-products (AGEs). (Neeper *et al*., 1992; Schmidt *et al*., 2000; Schmidt *et al*., 1992). AGEs are formed when proteins or lipids come into contact with an aldose sugar, this results in the non-enzymatic glycation and oxidization of the protein/lipid through reversible Schiff bases followed by Amadori rearrangement (Figure 1.1a) (Bierhaus *et al*., 1998; Schmidt *et al*., 1994). These early glycation products undergo further modifications, such as rearrangement, dehydration and condensation, to produce irreversibly cross-linked AGEs, such as $N\varepsilon$-(carboxymethyl) lysine (CML), which has been significantly modified whilst 2-(2-furoyl)-4-(5)-(2-furanyl)-1H-imidazole (FFI) has not (Figure 1.1b) (Brownlee *et al*., 1985; Goldin *et al*., 2006).

1.2 RAGE related pathologies

RAGE is produced in a wide range of differentiated adult cells in a regulated manner. It is produced in mature type 1 pneumocytes (Buckley & Ehrhardt, 2010), embryonic cells (Stogsdill *et al*., 2012) and in the human brain (Ding & Keller, 2005). Elevated RAGE production is also associated with inflammation related pathological conditions such as diabetic complications (Stern *et al*., 2002), vascular disease (Hegab *et al*., 2012), neurodegenerative disorders like Alzheimer's (Deane *et al*., 2012; Lue *et al*., 2001; Yan *et al*., 1997), cancer (Huttunen *et al*., 2002; Logsdon *et al*., 2007; Taguchi *et al*., 2000) or impaired wound healing (Goova *et al*., 2001). In contrast to healthy tissues, RAGE expression is lower in lung tumours (Bartling *et al*., 2005) and in idiopathic pulmonary fibrosis (Englert *et al*., 2008; Queisser *et al*., 2008). Changes in RAGE expression are highly correlated with the expression of RAGE ligands, suggesting that the RAGE ligands have an active role in disease development (Queisser *et al*., 2008).
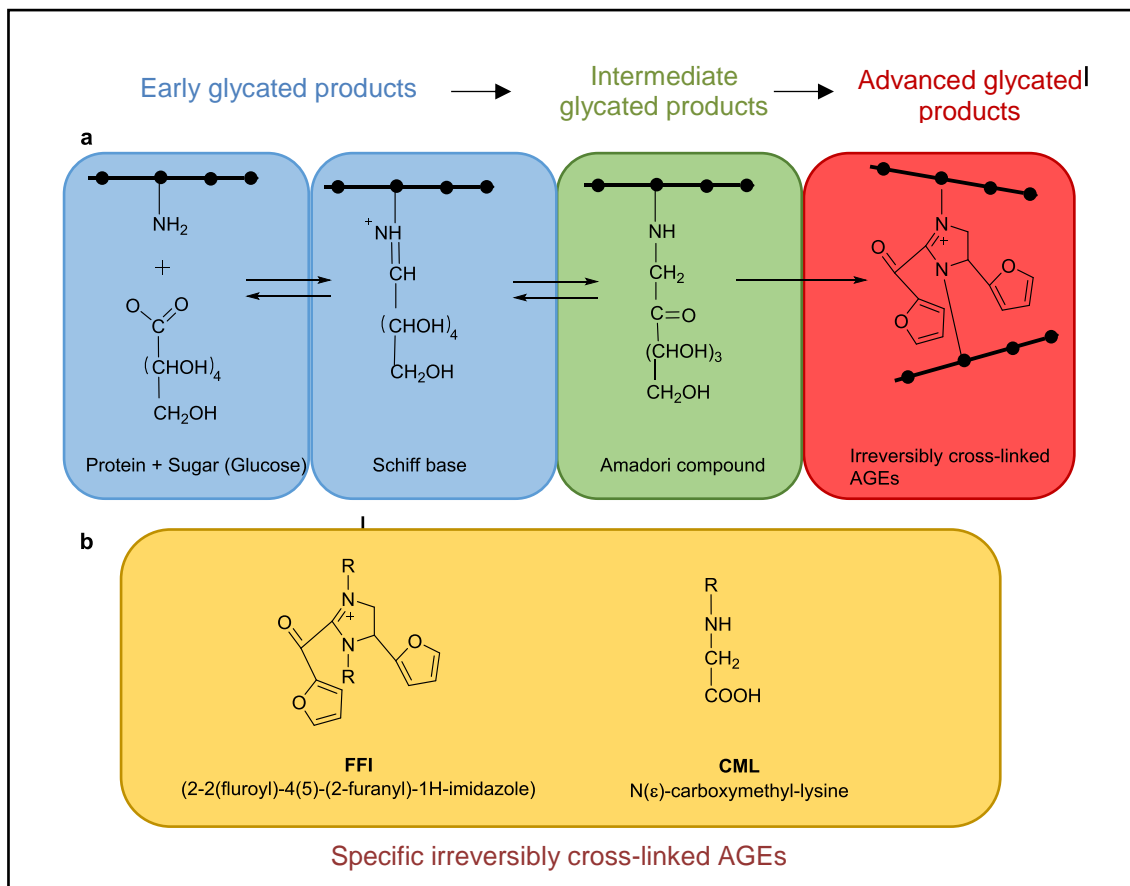
Figure 1.1 (a) The formation of advanced glycation end-products (AGEs) in the Maillard reaction. Early glycated end products are formed by the condensation of reducing sugars with amino groups of macromolecules. This forms reversible Schiff base adducts that undergo further rearrangement, dehydration and condensation reactions resulting in the irreversible formation of AGEs that are capable of physically crosslinking amino groups. (b) Example of the structure of two irreversibly cross-linked AGEs, FFI, and CML (Modified from Bierhaus *et al.*, 1998).

1.3 Cellular signalling of RAGE

RAGE signalling pathways are highly dependent on cell type and the dose of ligand-receptor complex. Therefore, RAGE inhibition may cause a reduction of precursor molecules of different pathways, which may be useful in normal physiological functions (Xie *et al.*, 2013). The complexity of the RAGE signalling network makes it difficult to design therapeutics to target RAGE and its ligands.

The cross-linked AGEs can trigger RAGE-dependent oxidative stress leading to pathologies such as diabetic complications, cardiovascular diseases (CVD) and vascular

complications like retinopathy and nephropathy (Figure 1.2) (Daffu *et al*., 2013; Forbes *et al*., 2003; Sakurai *et al*., 2003; Stitt 2010; Tan *et al*., 2007; Thomas, 2011). This occurs through the production of AGEs by diverse array of stimuli (eg: high glucose, aging, inflammation and oxidative stress). At a sufficient concentration AGEs bind to and activate RAGE. Binding of AGEs to RAGE generates intracellular reactive oxygen species (ROS) and depletes antioxidant defence mechanisms (Lander *et al*., 1997). As a result, glutathione levels are reduced. Glutathione depletion in turn reduces the recycling of glyoxalase-1 and affects the *in situ* activity (Figure 1.2). RAGE activation is demonstrated by interaction between the cytoplasmic domain and the Mammalian Diaphanous-related formin 1 (mDia1), which triggers the signalling pathway leading to activation of NADPH oxidase and the generation of ROS. AGEs are then released from the cell and can stimulate the recruitment of RAGE-expressing inflammatory cells which, in turn activates the release of RAGE ligands, such as S100A8/A9 and HMGB-1 (Figure 1.2). The release of RAGE ligands and the continued production of AGEs lead to further binding to RAGE and further cycles of the amplification loops that then contributes to the observed pathologies, including diabetic complications, cardiovascular disease and aging (Daffu *et al*., 2013).
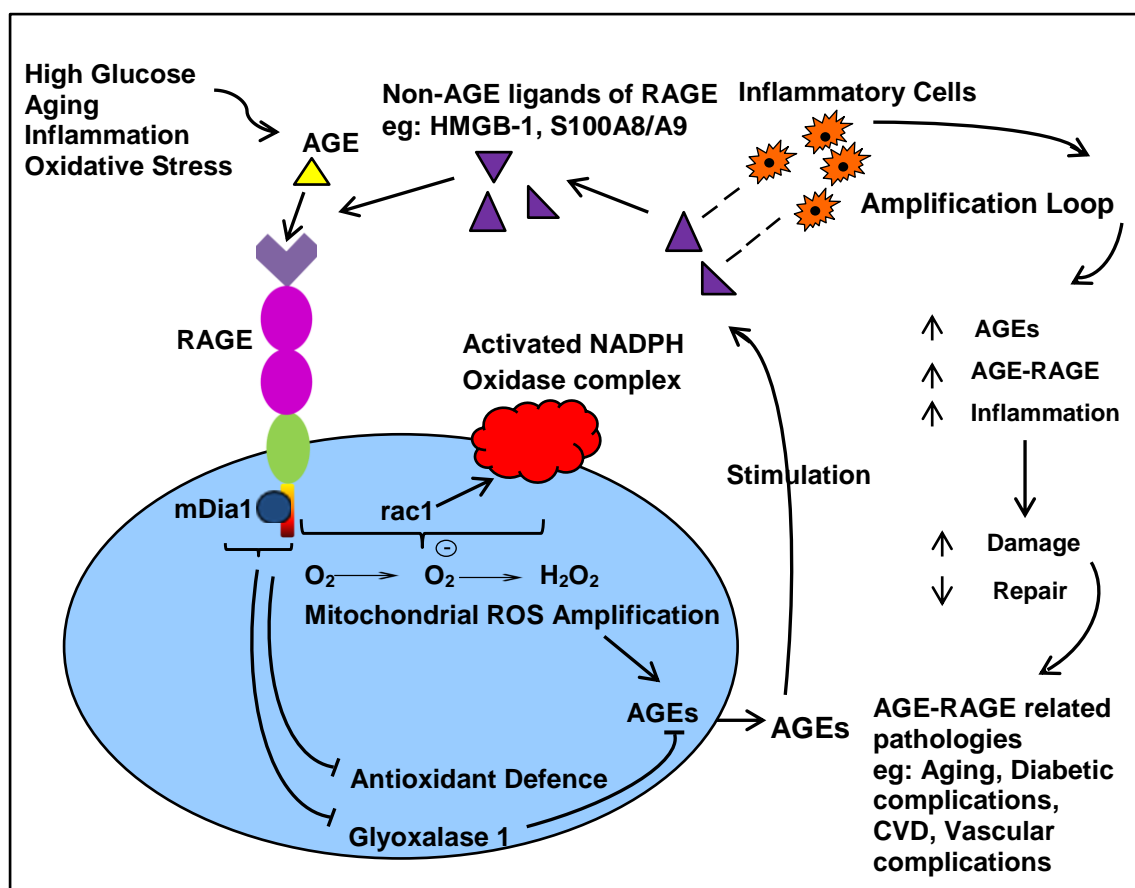
Figure 1.2 Diagrammatic representation of the AGE-RAGE oxidative stress and amplification loops linked to the pathogenesis of chronic diseases. Stimulation of AGEs and subsequent binding to RAGE increases reactive oxygen species (ROS) leading to further production of AGEs and the release of non-AGE (RAGE) ligands from inflammatory cells. This triggers the amplification loop leading to numerous pathologies. (Modified from Daffu *et al.*, 2013).

The up-regulation of RAGE via its ligands and thereby its role in disease development in humans is well understood. The blockage of RAGE is considered a therapeutic approach to overcome RAGE-related disease development in humans (Sturchler *et al*., 2008; Taguchi *et al*., 2000; Yamagishi *et al*., 2008). Therefore, understanding the cellular signalling events, triggered through RAGE activation is important. Using transgenic animal models and *in vitro* assays, many studies have investigated the intracellular signalling of RAGE with respect to cell migration, inflammation, proliferation, apoptosis and autophagy (Hofmann *et al*., 1999; Huang *et al*., 1999; Huttunen *et al*., 1999; Kislinger *et al*. 1999; Lander *et al*., 1997). These studies have identified and characterised some of

the signalling components involved in both immune response and the continued activation of inflammation. AGE-RAGE interaction activates intracellular signal transduction pathways, including extracellular signal-regulated kinase 1/2 (ERK1/2), the p38 mitogen-activated protein kinase (MAPK), Janus kinase/signal transducer and activator of transcription (JAK/STAT), Rho GTPases, and nuclear factor-κB (NF-κB) (Figure 1.3) (Hofmann *et al*., 1999; Huang *et al*., 1999; Huttunen *et al*., 1999; Kislinger *et al*., 1999; Lander *et al*., 1997). When HMGB-1 or S100A8/A9 binds to RAGE, it is able to activate the mitogen-activated protein kinase (MAPK) signalling cascades that converge on the IκB kinase complex (IKK) to inhibit the inhibitor of κB (IκB) and thereby releasing and activating nuclear factor κB (NF-κB) (Ishihara *et al*., 2003; Lander *et al*., 1997; Li *et al*., 2004;). p38 MAPK involves the induction of NF-κB activation by Nε-(carboxymethyl) lysine (CML) through RAGE in human monocyte leukaemia cells (Yeh *et al*., 2001). Apart from p38, p44/p42 MAPKs are shown to mediate RAGE-NF-κB transcriptional activation and cytokine secretion from monocytes (Yeh *et al*., 2001). The induction of vascular cell adhesion molecule-1 (VCAM-1) in mouse aortic endothelial cells by RAGE ligands could be suppressed by the c-jun N-terminal kinase (JNK) inhibitor SP600125, or with JNK siRNA (Harja *et al*., 2008). This supports the involvement of JNK in RAGE related inflammation through the MAPK pathway (p38 and P44/p42).
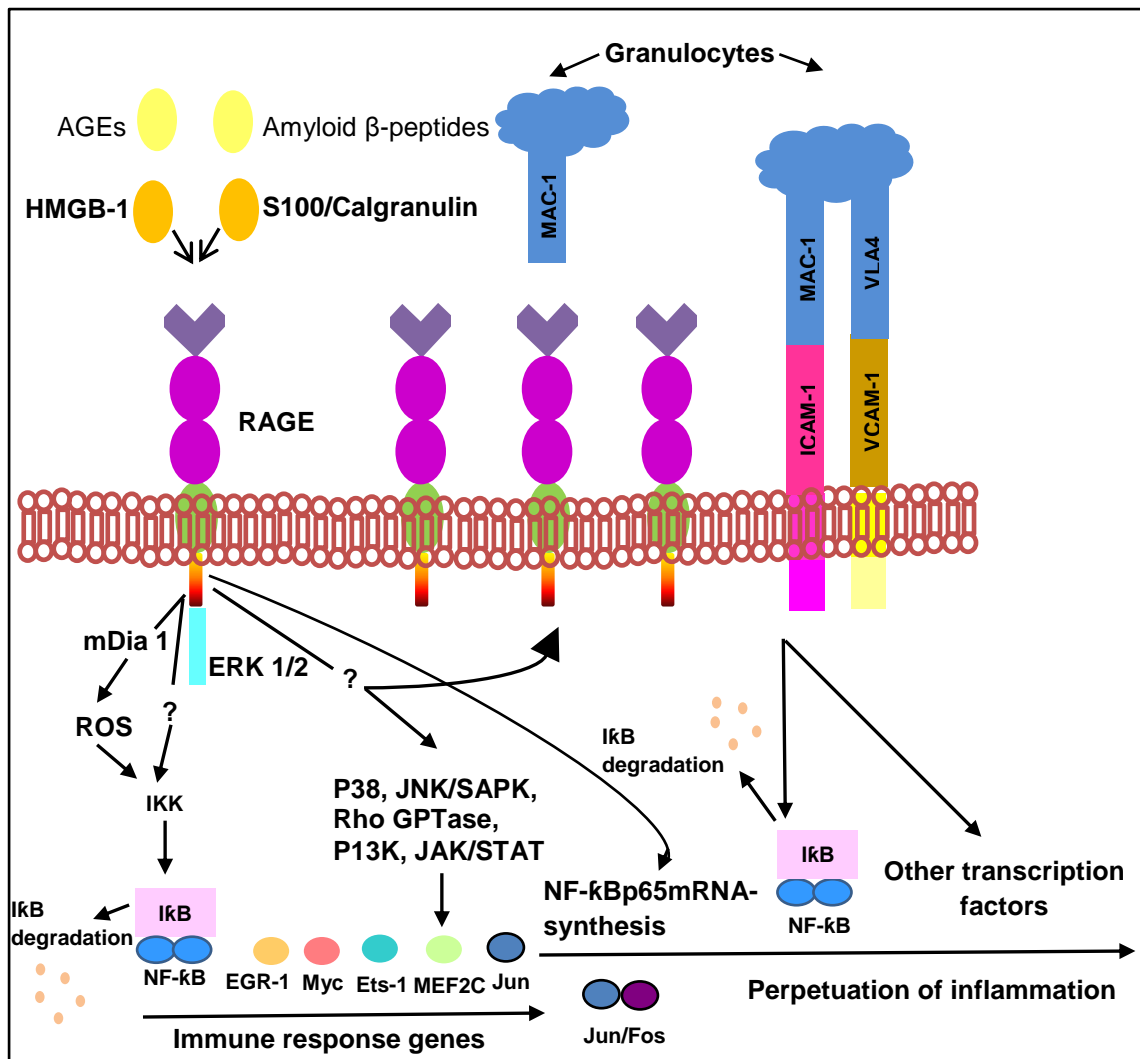
Figure 1.3 Intracellular signalling pathways of RAGE. This diagram mainly shows the inflammatory pathways involving the NF-κB and the MAPK pathways. AGE, advanced glycation end-products; HMGB-1, high mobility group box protein 1; mDia 1, mammalian diaphanous-related formin 1; ERK 1/2, extracellular signal-regulated kinase 1/2; ROS, reactive oxygen species; IKK, inhibitor of kappa B kinase; IκB, inhibitor of kappa B; MAPK, the p38, p44/42 mitogen-activated protein kinase; JAK/STAT, Janus kinase/signal transducer and activator of transcription; Rho GTPases; NF-κB, nuclear factor-κB; JAK, Janus kinase; JNK, c-jun N-terminal kinase; SAPK, stress-activated protein kinase; STAT, signal transducer and activator of transcription, MAC-1, macrophage-1 antigen; ICAM-1, intercellular adhesion molecule 1; VCAM-1, vascular cell adhesion molecule 1 and VLA-4, very late antigen 4 (Modified from Bopp *et al.*, 2008).

Mammalian Diaphanous-related formin 1 (mDia 1) was identified as one of the key mediators of RAGE-mediated intracellular signalling (Figure 1.2; Hudson *et al*., 2008a) and this explains how full-length RAGE induces signalling transduction cascades in the absence of intrinsic tyrosine kinases. mDia 1 (140 kDa) belongs to the formin protein

family of actin and microtubule polymerisation factor and regulates a number of processes, including cell migration and division (Higgs, 2005). The proline-rich two formin homology domains (FH1 and FH2) are required for this mDia 1 polymerisation activity (Higgs, 2005; Wallar & Alberts, 2003). The FH1 domain of mDia 1 is known to interact with the cytoplasmic tail of RAGE and subsequent signalling affects the function of vascular smooth muscle cells (SMCs). Further, Arg-5 and Gln-6 of the full-length RAGE were identified as the essential residues for the association between FH1 and full-length RAGE to occur (Rai *et al*., 2012). This molecular detail of the RAGE-mDia 1 interactions opens up new possibilities for RAGE-dependent pathologies.

1.4 Structure of RAGE

1.4.1 Structure of RAGE gene

The RAGE gene has been cloned and characterised from mouse lung as early as 1992 (Neeper *et al*., 1992). The human RAGE gene (also known as AGER) encodes a type 1 transmembrane protein that is located on chromosome 6 in the major histocompatibility complex (MHC) class III region (Sugaya *et al*., 1994). It is composed of a 5' flanking region that regulates its transcription and a short three prime untranslated region (3'-UTR) and eleven exons. The resulting protein is composed of 404 amino acids with a molecular mass of 55 kDa (Neeper *et al*., 1992; Sugaya *et al*., 1994). RAGE is a member of the immunoglobulin (Ig) super family of cell surface receptors (Neeper *et al*., 1992; Schmidt *et al*., 1992) and it shows a high degree of structural and sequence similarity to neural cell adhesion molecules (N-CAM) (Ding & Keller, 2005). Recently, it was shown that RAGE is only present in mammals and it is closely related to the family of cell adhesion molecules (CAMS) (Sessa *et al*., 2014).

1.4.2 Domain structure of RAGE protein

The extracellular domain of RAGE consists of an N-terminal ''V'' type domain, (residues, 23-116), which is located most distal to the plasma membrane and two ''C'' type domains, C1 (residues 124-221) and C2 (residues 227-317) (Figure 1.4) (Hudson *et al*., 2008a; Neeper *et al*., 1992; Schmidt *et al*., 1992). Based on limited proteolysis, dynamic light scattering, circular dichroism (CD) spectroscopy, and nuclear magnetic resonance (NMR) studies, it has been shown that the V and C1-domains are integrated to form a single

structural unit (VC1). In contrast, C2 is a fully independent domain and it is attached to the VC1-domains through a flexible linker (Dattilo *et al*., 2007; Neeper *et al*., 1992).
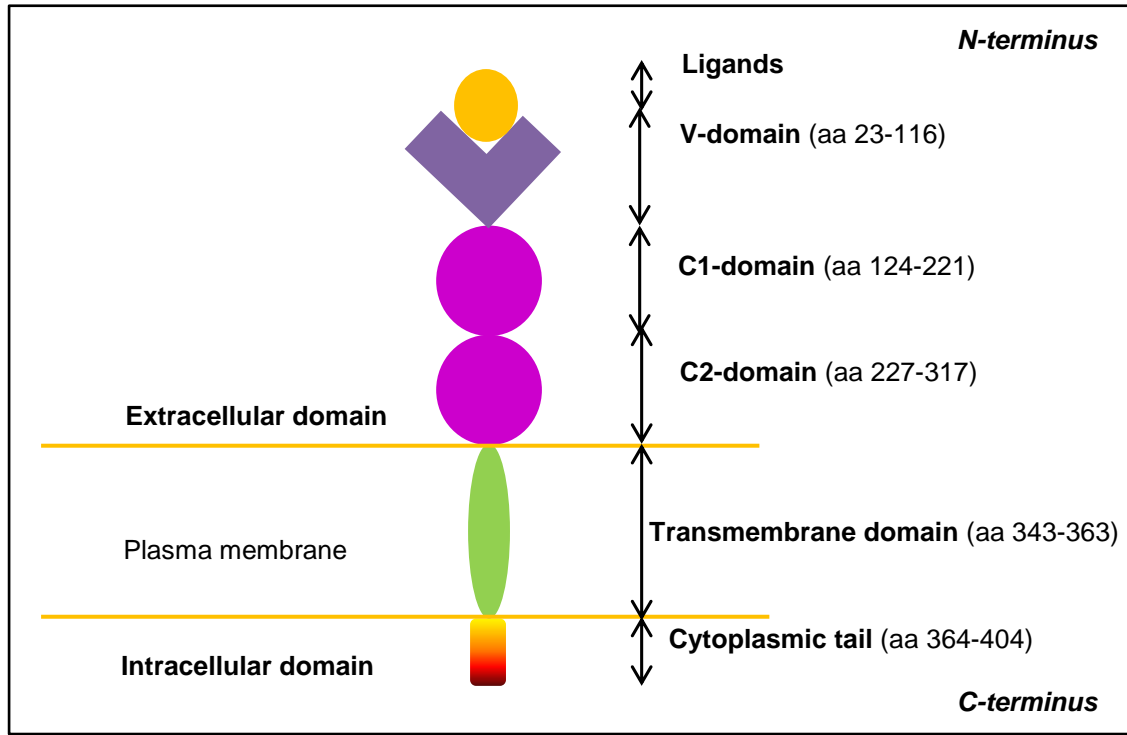
Figure 1.4 Schematic representation of full-length RAGE (FL-RAGE). Numbers showing the amino acid (aa) sequences of full-length RAGE, aa 404. Full-extracellular domain (aa 1-342) composed of a signal peptide (aa 1–22), a single transmembrane domain (aa 343-363) and a cytoplasmic domain (aa 364-404) (Modified from Hudson *et al.*, 2008b).

Apart from the common extracellular domain, full-length RAGE (FL-RAGE) contains a single transmembrane domain and a short cytoplasmic tail (intracellular domain) (Neeper *et al*., 1992; Schmidt *et al*., 1992), which is reported to be essential for intracellular signalling. This involves the activation of nuclear factor-κB (NF-κB), mitogen activated protein kinase (MAPK) and Jun-N-terminal kinase (JUNK) (Gao *et al*., 2008; Lander *et al*., 1997; Origlia *et al*., 2008).

1.4.3 Structure and the ligand binding properties of the VC1-domains

Protein expression encompassing the V and C1-domains (amino acids 23-221; Koch *et al*., 2010) and the V and C1 domains with additional amino acid residues (23-231; MBP-RAGE 12) of RAGE (Park *et al*., 2010) in *Escherichia coli* expression system has

generated two similar crystal structures of the VC1-domains of RAGE (assigned PDB codes 3O3U and 3CJJ, respectively). Both the proteins in PDB entries 3CJJ and 3O3U are structurally similar. However, the 3CJJ structure has a slightly longer C-terminus, and lacks the 3_{10} helix in the C'D region (Koch *et al*., 2010; Park *et al*., 2010). Analysis of these structures in Protein Data Bank archive (PDB; http://www.rcsb.org/pdb/) revealed that the VC1-domains exist as an elongated molecule with a highly conserved large hydrophobic patch and a large basic patch (Koch *et al*., 2010; Park *et al*., 2010).

The V-domain (Figure 1.5), contains a "V" type Ig fold; both the front sheet and back sheet of the domain are made up of β-strands. Back-side β-strands are relatively short, resulting in longer inter-strand loops. The V-domain is well structured through extensive hydrogen bonding. β-strands B and F are connected by a well-conserved disulphide linkage. One such disulphide linkage is present in each of the V, C1 and C2-domains. Small one turn 3_{10} helix common for Ig variable domains is present between the β-strands E and F (Figure 1.5) (Park *et al*., 2010).

The C-domain (Figure 1.5) consists of a "C" type Ig fold, and its back and front sheets are made up of β- strands. A, B, C and D strands make the front sheet and G, F, C and C' strands comprise the back sheet (Park *et al*., 2010).
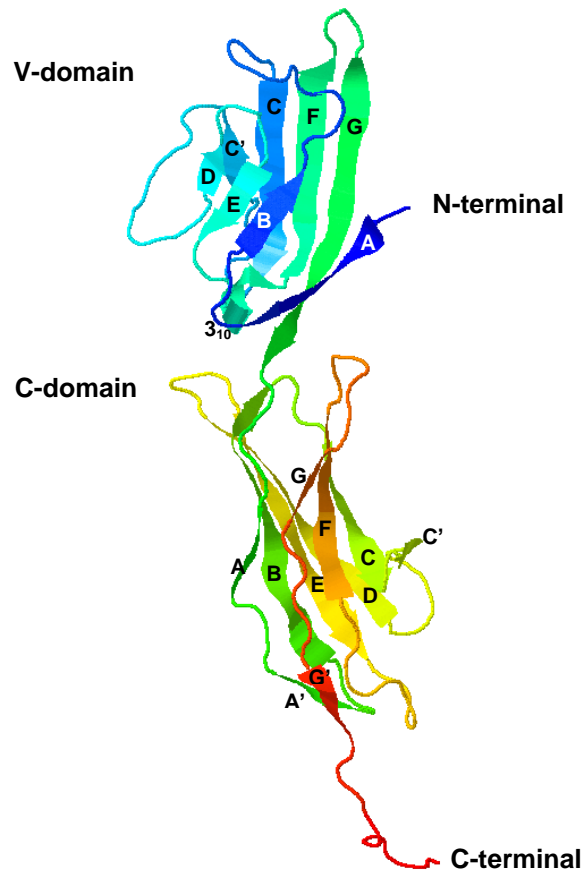
Figure 1.5 Ribbon diagram representation of the crystal structure of the MBP-RAGE. MBP has been removed from the model for clarity. The sequence was obtained from http://www.ncbi.nlm.nih.gov/ and the structure was modelled using Phyre2, Protein Homology/analogY Recognition Engine, Version 2.0 (http://www.sbg.bio.ic.ac.uk/phyre2/html/page.cgi?id=index).

The V-domain is the principle site of ligand binding. Almost all of the identified RAGE ligands bind either to the V-domain or to the C1-domain or both (Leclerc *et al*., 2009). AGEs bind only to the V domain (Xie *et al*., 2008) and S100 proteins bind to V, C1, or both (Dattilo *et al*., 2007; Koch *et al*., 2010; Ostendorp *et al*., 2007; Xie *et al*., 2007). However, S100A6 is the only ligand identified to date that engages the C2-domain (Leclerc *et al*., 2007).

Recent studies have shown that the charge separation within the extracellular domain of RAGE is important in ligand recognition. The V-domain carries a net positive charge at neutral pH due to its high content of arginine and lysine residues (Park *et al*., 2010). This

is in agreement with the presence of a basic patch on one side of the VC1 tandem domains (PDB entries: 3O3U and 3CJJ) (Koch *et al*., 2010; Park *et al*., 2010). In contrast, the C2-domain carries mainly acidic residues, and is negatively charged according to the NMR structure in solution phase (2ENS; PDB; http://www.rcsb.org/pdb/). A recent NMR-based structure of the complex of glycated peptide with the V-domain revealed that negatively charged ligand residues are electrostatically recognized by a positively charged V-domain surface patch (Xue *et al*., 2011). A series of peptide ligand backbone contacts have also been described. The structure of VC1 and NMR-based models of the VC1-S100B complex suggests that clustering of basic residues on the binding surface of VC1-domains and highly acidic surface of S100B are the major driving forces in formation of this receptor-ligand complex (Koch *et al*., 2010). Competition experiments using gel shift assays suggest that RAGE interaction with AGE is driven by the recognition of negative charges on AGE-proteins (Park *et al*., 2010). This kind of structural information is critical to understanding the mechanisms of RAGE signalling and to design and optimise effective therapeutic agents against RAGE-caused pathologies.

1.5 RAGE isoforms

More than twenty isoforms of RAGE have been identified to date (Hudson *et al*., 2008b). However, the majority of these isoforms are unlikely to be detected as proteins, since the sequence of these variants are potential targets of the nonsense-mediated decay (NMD) pathway. The lack of signal sequence in exon 1 in some other isoforms causes premature degradation of the respective protein (Sparvero *et al*., 2009).

Three major isoforms of RAGE have been identified as expressed proteins in cultured human endothelial cells and pericytes; N-terminally truncated RAGE, Full-length RAGE (FL-RAGE) and soluble RAGE (sRAGE; includes two forms, endogenous secretory RAGE [esRAGE] and proteolytically cleaved C-truncated RAGE alternatively called cleaved-type soluble RAGE) (Hudson *et al*., 2008b; Park *et al*., 2004; Schlueter *et al*., 2003; Yonekura *et al*., 2003) (Figure 1.6).
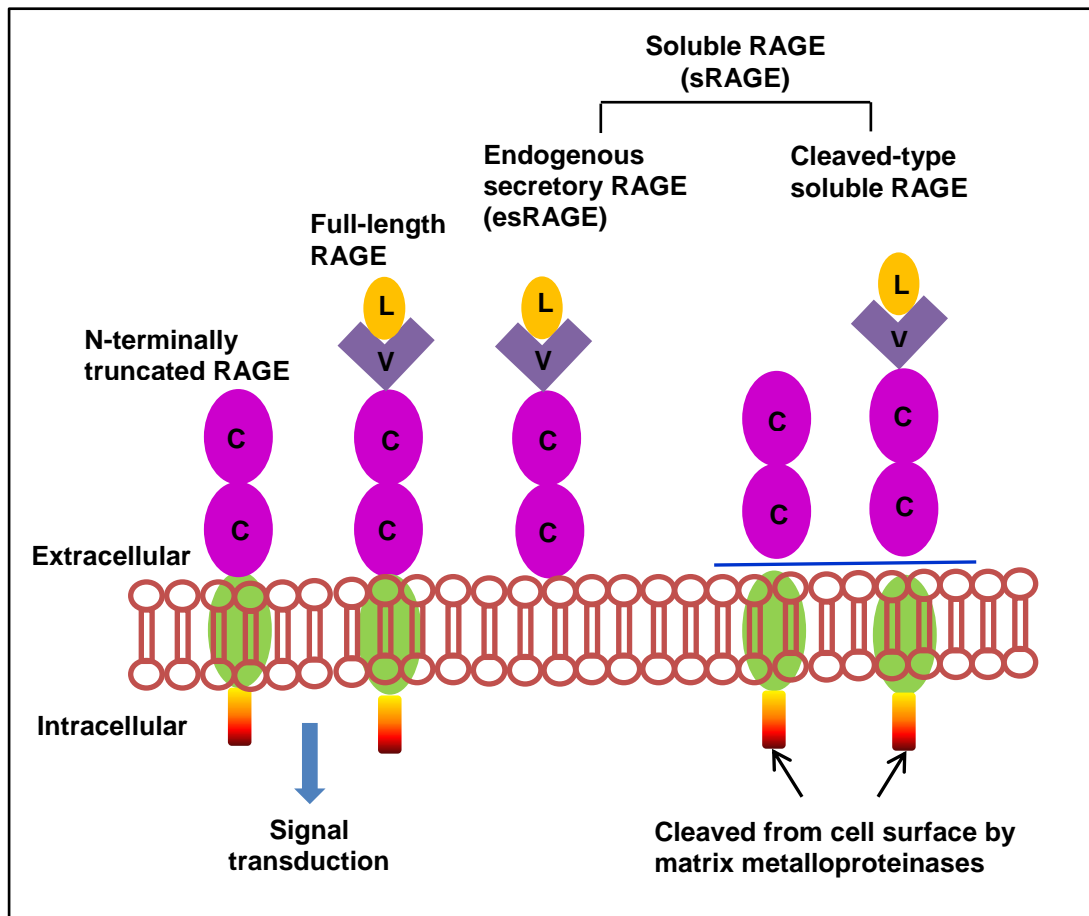
Figure 1.6 The structures of the major isoforms of RAGE; full-length RAGE, N-terminally truncated RAGE, endogenous secretory RAGE and cleaved-type soluble RAGE. V is the V-domain, C is the C-domain and L is the ligand/s (Modified from Basta, 2008).

N-truncated RAGE is identical to FL-RAGE except for the absence of the V-type immunoglobulin domain. N-truncated RAGE cannot bind to ligands because of the absence of the V-type domain. Soluble receptor for advanced glycation end-products (sRAGE) consists of an extracellular domain only and has the ability to bind to RAGE ligands.

1.6 Soluble receptor for advanced glycation end-products (sRAGE)

The soluble receptor for advanced glycation end-products (sRAGE) belongs to the immunoglobulin (Ig) super family and is composed only of the extracellular domain of RAGE. It is 35 kDa in size (Sarkany *et al*., 2011; Schmidt *et al*., 1992). The lack of intracellular and transmembrane domains means that sRAGE is secreted extracellularly

(Ding & Keller, 2005; Neeper *et al*., 1992; Schmidt *et al*., 1992). It has the ability to scavenge RAGE ligands thus preventing them from binding to RAGE or other cell surface receptors, but in the absence of an intracellular domain it will not trigger any post-signalling cascades. Thus, it acts a decoy receptor for RAGE ligands, rather than a selective RAGE blocker and, effectively neutralises the detrimental effects of cell-bound RAGE/ligand interactions. It competes with FL- RAGE for ligand binding and thereby, blunts the RAGE-dependent signal transductions (Ding & Keller, 2005). Thus, sRAGE is believed to have therapeutic potential in RAGE-dependent pathologies (Buckley & Ehrhardt, 2010).

The concentrations of sRAGE isoforms are lower than that of the FL-RAGE and are tissue specific. The total ratio of sRAGE to FL-RAGE varies between 1.72 in the myometrium and 0.56 in the lymph node (Schlueter *et al*., 2003). Changes in sRAGE to RAGE ratio or the association between concentrations of circulating sRAGE and disease outcomes serve as a biomarker in many RAGE-related human diseases (Colhoun *et al*, 2011; Lam *et al*., 2013; Schmidt 2015; Thomas *et al*., 2011).

1.6.1 sRAGE, disease pathologies and its potential as a biomarker

A number of studies have focused on understanding the role of sRAGE as a biomarker and potential predictor of RAGE related human disease development or disease outcomes, for example diabetic vascular complications, septic shock, stroke, cancer and kidney complications (Moy *et al*., 2013; Penfold *et al*., 2010; Schmidt, 2015; Thomas *et al*., 2011; Yamamoto *et al*., 2011 Yonchuk *et al*., 2015). However, the role of the AGE-RAGE system in heart failure is not known in detail. In an attempt to fulfil this objective, concentrations of sRAGE in the plasma of patients with chronic heart failure (CHF) and its correlation to left ventricular ejection fraction (LVEF) was investigated (Falcone *et al*., 2013). Data showed a positive correlation between concentrations of sRAGE in the plasma and LVEF in the CHF patient population. The sRAGE plasma concentrations were shown to be significantly lower in CHF and severe left ventricular systolic dysfunction patients compared to those in patients with moderate left ventricular dysfunction. Therefore, Falcone *et al*. (2013) believe that sRAGE could also be used as a tool in prognostic stratification in patients affected by CHF.

The accumulation of AGEs is believed to be a key modulator in the initiation and progression of diabetic nephropathy. According to recent findings, RAGE is a key

modulator of AT2 (angiotensin II type 2) receptor expression (Sourris *et al*., 2010). This newly identified RAGE-AT2 axis is believed to be involved in the development and progression of diabetic nephropathy. AT2 receptor deficiency is associated with enhanced renal disease in diabetic mouse models. Therefore, they concluded that RAGE deficiency protects the AT2 receptor expression (Sourris *et al*., 2010).

The activation of RAGE and the development and progression of diabetic complications is understood. In a study by Thomas *et al*. (2011), it was demonstrated that increased concentrations of sRAGE are associated with cardiovascular mortality in Type 1 diabetes patients. This observation was consistent, regardless of the other predictive variables of cardiovascular mortality like age, glycaemic control, systemic inflammation, triglycerol and HDL-cholesterol concentrations. The AGEs receptor polymorphism was shown to be associated with the circulating concentration of sRAGE (in agreement with previous findings), but not with mortality outcomes. It was concluded, that this reflects hyper activation of the AGE-RAGE axis in diabetes patients, leading to progressive development of vascular complications, auto-induced RAGE production and subsequent sRAGE shedding into the circulation (Thomas *et al*., 2011).

The effect of insulin on the serum levels of sRAGE (in total) and also specifically esRAGE in Chinese patients with Type 1 diabetes were investigated and then, the effect of insulin on the generation of sRAGE and esRAGE was evaluated *in vitro* (Lam *et al*., 2013). Their findings revealed that patients have higher serum concentrations of sRAGE and esRAGE. They concluded that *in vitro* insulin increases both the FL-RAGE and esRAGE and also stimulates the shedding of sRAGE from the membrane-bound RAGE (Lam *et al*., 2013). These findings are in agreement with the findings of Thomas *et al*. (2011). Therefore, the presence of serum levels of sRAGE could be used as a biomarker of Type 1 diabetes recognition.

The level of sRAGE and esRAGE were evaluated as predictive biomarkers of coronary heart disease (CHD) risk in patients with Type 2 Diabetes (Colhoun *et al*., 2011). They utilised a randomised controlled clinical trial of statin therapy in type 2 diabetes patients without prior cardio vascular disease (CVD). The results revealed that higher levels of sRAGE and esRAGE were associated with incident CHD but not stroke in Type 2 diabetes. They suggest that their finding reflects a potential usefulness of the circulating serum levels of sRAGE and esRAGE as biomarkers.

All these studies reflect the potential importance of the serum concentrations of sRAGE as a biomarker. sRAGE is believed to have therapeutic potential in RAGE-dependent pathologies. Thus, the understanding of the structure-function relationship of sRAGE and ligands are important. A number of systems have been used such as Yeast, *E. coli* and insect cell cultures (Ostendorp *et al*., 2006; Renard *et al*., 1997; Wilton *et al*., 2006). However, most of the studies have focused on understanding the structure-function relationship of the RAGE-ligand axis by using RAGE expressed in *E. coli* expression systems, where the effect of post-translational modifications of RAGE protein such as glycosylation are not considered (Koch *et al*., 2010; Kumano-Kuramochi *et al*., 2009; Park *et al*., 2010). To address this issue, the present study focused on understanding the effect of glycosylation of sRAGE protein on ligand binding by comparing sRAGE from *E. coli* with that produced in hairy roots.

1.7 Ligands of RAGE

Although, it was first described as a receptor for AGEs, RAGE also binds high mobility group family proteins including HMGB-1/amphoterin, members of the S100/calgranulin protein family, and matrix proteins such as amyloid β-peptides (Stern *et al*., 2002). All the members of these families are not identified as specific RAGE ligands; instead many of them bind to other receptors and thus have RAGE-independent effects as well (Hegab *et al*., 2012). Studies suggest that RAGE is behaving as a pattern recognition receptor (PRR); this is indicated by the structural diversity of its ligands, and its ability to recognise a class of ligands including AGEs (Deane *et al*., 2012).

AGE-RAGE biology has been studied for more than 20 years, however, very little is known about the structural biology of AGE-RAGE complexes due to the extensive heterogeneity of AGEs created by glycation reactions. HMGB-1 and S100A8/A9 complex were selected as ligands for the present study; firstly, these ligands are less heterogeneous compared to the AGEs. Secondly, HMGB-1 is the only member of the high mobility group box protein family that acts as a ligand of RAGE. Thirdly, S100A8/A9 complex serves as the least studied ligand of RAGE compared to the other proteins of S100 protein family.

1.7.1 High mobility group box protein-1 (HMGB-1)

HMGB-1 is a basic, non-histone chromosome protein, of 215 amino acid residues (~25 kDa in molecular weight). It is a highly conserved protein and there are only two amino acid differences between mouse and human HMGB-1. Human HMGB-1 shows an 80 % sequence similarity with HMGB-2 and HMGB-3 (Read *et al*., 1993). HMGB-1 consists of three structural domains, two tandem HMG-box domains, and a well-conserved acidic, short C-terminal tail. HMG-box A and box B domains are well conserved and spaced by a flexible linker. The two N-terminal domains contain several arginine and lysine residues, which are required for DNA binding and are made up of three α-helices arranged in an L-shaped configuration (Figure 1.7 B). The C-terminal tail consists of 20 consecutive aspartic and glutamic acid residues (Figure 1.7 A); a C-terminal acidic tail of this length and composition is rarely seen in nature (Sparvero *et al*., 2009; Read *et al*., 1993).

Studies have shown that HMGB-1 and RAGE have an active role in disease pathology including cell death, brain damage (Muhammad *et al.*, 2008), ischemia-reperfusion injury of the heart (Andrassy *et al*., 2008), cancer (Choi *et al*., 2011), inflammation and infection (Andersson & Tracey, 2011).

HMGB-1, as a non-histone DNA binding protein plays a structural role in the nucleus, and facilitates the assembly of nucleoproteins (Thomas, 2001; Thomas & Travers, 2001). Interactions between the acidic tail and boxes A and B are believed to regulate the HMGB-1 and DNA binding (Thomas, 2001; Thomas & Travers, 2001). Post-translational modifications, such as oxidation of HMGB-1, are found to be responsible for its various functional aspects, like intracellular localisation, cytokine activity and DNA interaction (Sparvero *et al.*, 2009). However, there are many unanswered questions, including whether the activity of HMGB-1 through RAGE is related to the specific structural features of these proteins and whether there are any other proteins or carriers involved. In our study, we attempt to understand the effect of glycosylation of sRAGE on HMGB-1 binding.

A

```
MGKGDPKKPR GKMSSYAFFV QTCREEHKKK HPDASVNFSE FSKKCSERWK

TMSAKEKGKF EDMAKADKAR YEREMKTYIP PKGETKKKFK DPNAPKRPPS

AFFLFCSEYR PKIKGEHPGL SIGDVAKKLG EMWNNTAADD KQPYEKKAA**K**

**LKEKYEKDIA AYRAKGKPDA AKKGVVKAEK SKK**KKEEEED EEDEEDEEEE

EDEEDEDEEE DDDDE
```
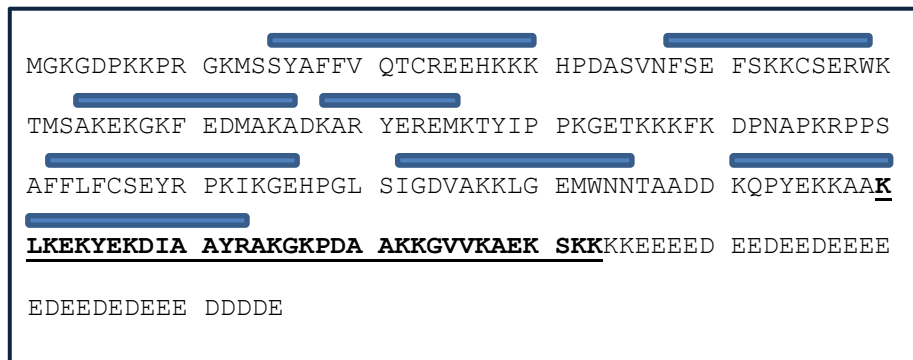
B
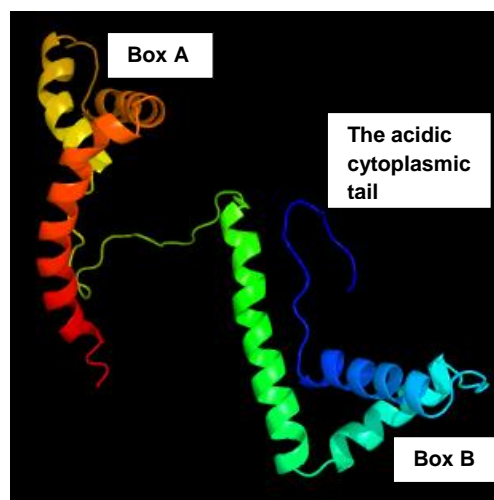
Figure 1.7 A. Schematic structure of HMGB-1, which is composed of the HMGB-1 Box A – blue; HMGB-1 Box B – yellow; Acidic cytoplasmic tail – magenta; RAGE binding site –bold and underline; Alpha helices (Delineated using http://www.rcsb.org/pdb/protein/P09429; Expasy Protein model portal http://www.expasy.org/resources). B. Solution structure of HMGB-1, showing α-helices arranged in L-shaped configuration. Sequence for HMGB-1 from http://www.ncbi.nlm.nih.gov/. The structure was modelled using Phyre 2, Protein Homology/analogY Recognition Engine, Version 2.0 at http://www.sbg.bio.ic.ac.uk/phyre2/html/page.cgi?id=index.

1.7.2 S100A8/A9 complex

S100A8 (myeloid related protein 8, MRP8) and S100A9 (MRP14) belong to the calcium binding S100 protein family. They are expressed in a wide variety of cell types, especially circulating neutrophils and during early differentiation of monocytes (Odink *et al*., 1987; Roth *et al*., 2003). Similar to other S100 proteins, S100A8 and S100A9 are characterised by the presence of two EF-hand calcium-binding sites. The C-terminal EF hand or the EF-hand II has a higher affinity for calcium binding compared to the N-terminal EF hand or the EF-hand I (Heizmann *et al*., 2002).

Like other S100 proteins S100A8 and S100A9 proteins form dimers as well as higher order oligomers. Laboratory studies using a yeast two hybrid system, CD spectroscopy, fluorescence spectroscopy and NMR analysis studies have shown that formation of a heterodimer complex of S100A8 and S100A9 is dependent on the presence or absence of calcium (Hunter & Chazin, 1998; Propper *et al*., 1999). Further, it was revealed that this basic form of heterodimer undergoes oligomerisation in the presence of calcium to form a heterotetramer (Strupat *et al*., 2000; Vogl *et al.*, 1999). Later, MALDI-MS, ESI-MS and fluorescence spectroscopy revealed that zinc-binding also induces the formation of S100A8/S100A9 tetramer similar to calcium-binding (Vogl *et al*., 2006). With the elucidation of the crystal structure of the S100A8/A9 heterotetramer, two different putative zinc binding sites, each consisting of three His residues and one Asp side-chain, were identified (Korndorfer *et al*., 2007). This tetramer form of S100A8/A9 is essential for biological activity (Leukert *et al*., 2006).

S100A12, S100B, S100A1 and S100P are the S100 proteins so far identified to have a direct interaction with RAGE (Arumugam *et al*., 2004; Dattilo *et al*., 2007; Hofmann *et al*., 1999). Recently, RAGE signalling and activation of NF-κB involvement in S100A8/A9-promoted cell growth has been recognised (Ghavami *et al*., 2008). Furthermore, a study using mouse models and human tissue samples, found that RAGE carboxylated glycans and S100A8/A9 mediate tumor-stromal interactions, leading to inflammation associated colon carcinogenesis (Turovskaya *et al*., 2008). The involvement of S100A8/A9 in cardiomyocyte dysfunction via RAGE was also identified (Boyd *et al*., 2008).

1.8 Recombinant protein production

In this study human sRAGE was expressed in a plant expression system and an *Escherichia coli* expression system to obtain glycosylated and non-glycosylated recombinant sRAGE, respectively, with the expectation of performing *in vitro* ligand binding studies to understand the structure-function relationship of sRAGE and the selected ligands, HMGB-1 or S100A8/A9 complex. Here, the importance of recombinant protein production and possible protein production platforms are described in detail.

The development of biotechnology has meant that different protein expression systems can be used to produce recombinant proteins on an industrial scale to meet the therapeutic needs of patients (Andersen & Krummen, 2002). Clinical administration of a therapeutic protein could be a promising therapy for diseases that occur as a result of deficiencies in the productions of a particular polypeptide, the synthesis of a mutant protein, or the generation of a non-functional protein. Therefore, there is a potential for therapeutic proteins to play a crucial role in correcting an acquired or an inherited deficiency of a native protein or produce a possible antagonist/competitive receptor (Leader *et al*., 2008; Schellekens, 2002).

Initially, therapeutic proteins were derived from natural sources; for example, proteins like insulin from the pancreas, human serum albumin from plasma, and glucocerebrosidase from human placenta (Alderson *et al*., 2004; Beutler *et al*., 1977; Ferrer-Miralles *et al*., 2009). Most of these human proteins are known to have a significant pharmaceutical value; unfortunately, they are hard to obtain and purify, in a large enough scale, from natural resources. However, with the development of recombinant DNA technology, the first recombinant therapeutic protein, insulin, was developed using an *E. coli* expression system. In 1982 the recombinant insulin protein received U.S. Food and Drug Administration (FDA) approval for the treatment of diabetes (FDA Bulletin, 1982). To date, there are five major production platforms that are utilised as hosts to produce recombinant proteins. These include, *E. coli*, yeast, mammalian cell cultures, insect cell cultures and fungal expression systems (Bhattacharya *et al*., 2005; Casademunt *et al*., 2012; Ecamilla-Trevino *et al*., 2000; Kjeldsen, 2000; Okazaki *et al*., 2012; Peters *et al*., 2010; Porro *et al*., 2005; Unger *et al*., 2012; Vanz *et al*., 2008; Ward *et al*., 2004; Zhang *et al*., 2003).

The adaptability and the scalability of different expression systems, make it possible to generate therapeutic proteins on a large-scale industrial setting. As a result, a large number of therapeutic proteins have been introduced into the market after the release of recombinant insulin. There has been a tremendous increase in the number of biopharmaceuticals produced during the last three decades (Ferrer-Miralles *et al*., 2009). However, scientists and engineers are still working to produce novel, and cheaper, drugs with improved production systems.

1.8.1 *Escherichia coli*

As previously mentioned, *E. coli* was the host used in the production of the first recombinant therapeutic protein, insulin, approved by FDA in 1982 (FDA Bulletin, 1982). Until the mid-90s, *E. coli* was the dominant and most attractive host for the production of therapeutic proteins. The gram negative bacterium still remains the most attractive and common host system because of its rapid growth, inexpensive growth substrates, the easy maintenance of bacterial cultures, simplicity of scaling up to an industrial output, and the well characterised genome of *E. coli*, along with a large number of cloning vectors and expression strains (Baneyx, 1999; Baneyx & Mujacic, 2004). The availability of the complete sequence data of *E. coli* genome along with a large array of genetic tools, make it possible to create many modifications to this host system (Jana & Deb, 2005). According to Ferrer-Miralles *et al*. (2009), the number of recombinant pharmaceuticals licenced up to January 2009 by the FDA and European Medicines Agency (EMA) that have been produced in *E. coli* (28) is second to the numbers generated by mammalian cell systems (59). Recent reports show that from 2010 to July 2014, mammalian cell systems still account for the majority (51.5 %) of approved biopharmaceuticals, whilst it only 29 % for produced in *E. coli* (Walsh, 2014).

The production of more complex and functional proteins, especially those from eukaryotic sources, has often been difficult and challenging because of the inability of the *E. coli* protein expression systems to fold these products into their native 3D conformation (Jana & Deb, 2005; Swartz, 2001). In addition, *E. coli* is not capable of performing post-translational modifications such as generating or attaching mammalian glycosylation chains (Jenkins & Curling, 1994). However, this is only an issue for those products that require glycosylation. Therefore, *E. coli* is still the first choice as a protein expression system for many products and applications, where glycosylation is not necessary.

However, attempts have been made to produce *N*-linked glycoproteins in *E. coli* by the introduction of short glycosylation tags (GlycTags), containing the preferred *Campylobacter jejuni N*-glycosylation consensus sequence, D-Q-N-A-T (Fisher *et al*., 2011). The pathogenic ε-proteobacterium *Campylobacter jejuni* was the first bacterium found to have an *N*-linked glycosylation pathway (Szymanski *et al*., 1999). Although long established in eukaryotes, *N*-linked protein glycosylation in bacteria is a relatively recent discovery (Baker *et al*., 2013).

Many of the over-expressed recombinant proteins in the *E. coli* expression system undergo proteolytic degradation and misfolding, or associate with each other to form insoluble aggregates known as inclusion bodies. As a result, the proteins fail to acquire the correct conformation. Therefore, these proteins are often functionally inactive (Baneyx & Mujacic, 2004). Inclusion body formation commonly occurs in the reducing cytoplasm of *E. coli* and is mostly prevalent among large multi-domain and overexpressed proteins (Baneyx & Mujacic, 2004). However, many strategies have been undertaken to improve the yields, solubility and to facilitate *in vivo* folding of more complex proteins in *E. coli* expression system. The most common methods for improving yields of soluble protein during expression are by lowering the temperature to 30 ºC (Schein, 1989) or even to 15 ºC (Shirano & Shibata, 1990), using different expression strains (Rosano & Ceccarelli, 2009) and co-expressing the proteins with chaperones and foldases (Baneyx & Palumbo, 2003; Kondo *et al.*, 2000). However, use of fusion tags is the best available tool that enhances the solubility of expressed proteins. Maltose-binding protein-Tag (MBP) (Kapust & Waugh, 1999), Glutathione S-transferase-Tag (GST) (Hammarstrom *et al*., 2002) or a combination of hexa-histidine-maltose-binding protein affinity-Tags (His (6)-MBP) (Sun *et al*., 2011) are the most commonly used tags. Attempts have been made to refold proteins from inclusion bodies by dissolving the protein in concentrated solutions of denaturants with reducing agents, (Demain & Vaishnav, 2009). In this way, Hygromycin B phosphotransferase (HPT) protein expressed in *E. coli* gained in purity by 95 % after refolding (Zhuo *et al*., 2005). This *E. coli* derived HPT showed biological activities similar to that of the HPT produced by transgenic rice (Zhuo *et al*., 2005). Similarly, catalytic refolding resulted in a better yield and enrichment of a human 3',5'-cyclic nucleotide phosphodiesterase 7A1 (PDE7A1) enzyme (Richter *et al*., 2002). Likewise, three human class I histocompatibility antigen HLA-A2-peptide complexes were able to be crystallized after refolding the protein

aggregates (Garboczi *et al*., 1992). These strategies had improved the efficacy of the *E. coli* expression system, in terms of yields, solubility and *in vivo* folding of proteins.

In this study an *E. coli* expression system was selected to express non-glycosylated sRAGE and to perform in *vitro* ligand binding studies. Then, the binding potentials of non-glycosylated *E. coli*-made sRAGE and glycosylated plant-made sRAGE were compared.

1.8.2 Yeast expression system

Yeast is a single-celled eukaryotic expression system that is easy to manipulate genetically and demonstrates rapid cell growth on inexpensive media (Demain & Vaishnav, 2009). In contrast to *E. coli* expression systems, yeast expression systems are known to perform many post-translational modifications; such as *N*-glycosylation, O-glycosylation, acetylation and phosphorylation. Therefore, yeast produces even complex foreign proteins that are identical or very similar to native products. A large number of heterologous proteins can be produced at a lower cost in the yeast system, compared to insect and mammalian cell cultures (Graumann & Premstaller, 2006). However, yeast expression systems are less useful because of their inability to modify proteins with human glycosylation structures. Instead they produce over-glycosylated proteins (yeast *N*-glycosylation is of high-mannose type) (Wildt & Gerngross, 2005).

1.8.3 Insect cell cultures

Insect cell-baculovirus expression vector systems (BEVS) have a greater potential as an expression platform to produce recombinant proteins with complex post-translational modifications than the yeast expression system (Graumann & Premstaller, 2006). However, insect cells mostly produce simple *N*-glycans, which can cause allergenic reactions in humans as opposed to the complex *N*-glycans commonly produced by mammalian cells (Harrison & Jarvis, 2006). Therefore, enormous efforts have been made to understand the process, potential and limits of *N*-glycosylation in insect cell systems. As a consequence, novel insect cell lines, transformed with mammalian β-1,4-galactosyltransferase, α-2,6-sialyltransferase and *N*-acetylglucosaminyltransferase genes, have been developed to produce proteins with terminally sialylated *N*-glycans (Hollister *et al*., 2002). Extensive studies are underway to generate more authentic recombinant

glycoproteins using insect cell-baculovirus expression vector systems (Assenberg *et al*., 2013).

1.8.4 Mammalian cell cultures

Mammalian cell lines are considered as the gold standard for the production of recombinant mammalian proteins. The human tissue plasminogen activator (TPA) was the first therapeutic protein derived from the mammalian cells that received market approval in 1986. Today, 60-70 % of therapeutic proteins are produced in mammalian cells. The Chinese hamster ovary (CHO) was the first cell line utilised for the production of therapeutics. Subsequently, mouse myeloma (NSO), baby hamster kidney (BHK), human embryonic kidney (HEK-293) and human retinal cell lines have gained regulatory approval for the production of recombinant proteins (Wurm, 2004).

A well-established media composition, high-yield producing cell lines and improvements in bioreactors technology have made it possible to generate kilograms of authentic human therapeutics from larger bioreactors (Altamirano *et al*., 2000; Geiger *et al*., 2012; Hayashi & Sato 1976; Rauch *et al*., 2011; Smelko *et al*., 2011). However, mammalian cell culture is limited by the high cost involved with the initial set-up including consumables, long cycle times and limited control over glycosylation (Aricescu *et al*., 2006; Li *et al*., 2010).

1.8.5 Plant expression systems

The increasing demand for biopharmaceuticals has provided the impetus to seek a variety of expression platforms, like *E. coli*, yeast, insect cells and mammalian systems, capable of producing authentic therapeutics at a lower cost. An additional alternative production system is plant-based platforms, which have emerged in the last few decades (reviewed by Yusibov *et al*., 2011; Paul & Ma, 2011). As a result, the first plant derived potential pharmaceutical, human growth hormone (hGh) was expressed in tobacco in 1986 (Barta *et al*., 1986).

Over the past 20 years, the potential of plant expression systems to produce therapeutically useful proteins including antibodies, enzymes and vaccines, has been extensively studied. Antibodies such as IgG, IgA and IgM, and enzymes like trypsin are examples of compounds produced using plant expression systems (Khoudi *et al*., 1999; Ma *et al*., 1998; Ma *et al*., 1995; Verch *et al*., 1998; Woodard *et al*., 2003). Vaccines have also been produced in plants and include VP1 of foot-and-mouth disease virus (FMDV)

(Carrillo *et al*., 1998), protective antigen (PA), the principal virulence factor of *Bacillus anthracis* (pp-PA 83) (Chichester *et al*., 2013), Norwalk virus capsid protein (Mason *et al*., 1996, Rigano *et al*., 2013), rabbit virus glycoprotein (McGarvey *et al*., 1995), *E. coli* heat-labile enterotoxin (LT-B) (Haq *et al*., 1995), Hepatitis B surface antigen (Richter *et al*., 2000), Cholera B subunit (Arakawa *et al*., 1997), measles (Webster *et al*., 2005; Webster *et al*., 2002), Human Papillomavirus (HPV) (Liu *et al*., 2005; Maclean *et al*., 2007), and influenza virus (Mortimer *et al*., 2012; Redkiewicz *et al*., 2014). As a result of the development of plant expression systems, CaroRx, the world's first clinically tested plantibody has been approved for healthcare (Ma & Lehner, 1990). CaroRx is a monoclonal antibody (mAb) that binds to *Streptococcus mutans,* the primary causative agent of bacterial decay. Similarly, Taliglucerase alfa, the recombinant glucocerebrosidase produced in carrot cell cultures (Protalix BioTherapeutics; Fox, 2012), to treat Gaucher's disease, recently got FDA approval, to administer parenterally, this has been considered a milestone in plant-based therapeutics.

The production of recombinant proteins in plants has many advantages over other expression systems. Reduced capital relative to fermentation techniques, rapid scale up of production systems and the use of non-toxic plant material are some of these advantages. Products free from oncogenic DNA sequence and prions make plants a safer system for therapeutic protein production, compared to the insect cells and mammalian systems (Fischer *et al*., 2004; Ma *et al*., 2003; Sack *et al*., 2015, Stoger *et al*., 2014 ; Tekoah *et al*., 2015). However, plant expression systems are limited by the production of plant specific glycans that are different from native mammalian glycans during the *N*-glycan maturation steps (Nagels *et al*., 2012).

We specifically selected a plant expression system to express sRAGE as, firstly, it is relatively cost effective compared to insect and mammalian cell cultures, secondly, it is free of harmful pathogens and importantly, thirdly, it has the ability to perform glycosylation. Plant-made recombinant proteins are generally folded correctly, undergo specific post-translational modification including glycosylation and self-associate into biologically active forms *in planta* (Holtz *et al*., 2015; Yao *et al*., 2015). Thus, in this study sRAGE was expressed in stable hairy root cultures of *Nicotiana tabacum* plants.

1.8.5.1 Stable plant expression systems

Stable transformation involves the permanent integration of the foreign DNA segment/transgene into the plant genome. As a result, the acquired novel character is transferred to the next generation. Stable transformation of the nuclear genome and the chloroplast genome are the commonly used methods.

Nuclear transformation involves the preparation of a suitable explant material, delivery of DNA or gene of interest, selection of transformed tissues and regeneration of the explant. The gene of interest or foreign DNA can be introduced into the explant material by *Agrobacterium tumefaciens* mediated transformation or through the biolistic method. The T-DNA region of *A. tumefaciens*, along with the gene of interest, is transported to the plant cell by exploiting the natural capability of the bacterium to transfer DNA into the plant cell. *A. tumefaciens* is the causal agent of crown gall disease of many eudicots. The symptoms of the disease are caused by the insertion of a small segment of DNA known as the T-DNA, from a plasmid, into the plant cell, which is incorporated at a semi-random location into the plant genome (Chilton *et al*., 1977; Schell *et al*., 1979).

Alternatively, using the biolistic method, metal particles coated with DNA are delivered to plant cells using a gene gun (particle bombardment) (Sanford, 1990). The transformed single cells are then regenerated into complete fertile plants by tissue culture techniques. One disadvantage of this method is that the transgenes can be integrated at random positions and multiple copies can be inserted into the plant genome. However, transgenic plants have the advantage of producing proteins at a relatively low cost.

Chloroplasts are organelles present in photosynthetic plant cells; they capture energy from light to fix atmospheric CO_2 and convert it into sugars. Existing technologies for chloroplast transformation use the particle bombardment delivery of DNA into organelles. Chloroplast transformation methods have unique advantages, the major one being that the maternal inheritance of chloroplasts reduces the risk of potential transgene escape through pollen dissemination (Daniell, 2006). Chloroplast transformation was first achieved in *Chlamydomonas reinhardtii* (Boynton *et al*., 1988), however, only a few higher plants have the ability to undergo chloroplast transformation, and mostly it is restricted to tobacco plants *Nicotiana tabacum* (Svab & Maliga 1993; Pengelly *et al.,* 2014). High-level expression of recombinant proteins, the feasibility of expressing multiple proteins from polysystronic mRNAs and production of proteins with post-translational

modifications, including formation of disulfide bonds, are some of the advantages of this system (Arlen *et al.*, 2007; De Cosa *et al.*, 2001; Ruhlman *et al.*, 2007; Staub *et al.*, 2000). *E. coli* LT-B antigen, *Clostridium tetani* toxin Fragment C, *Bacillus anthracis* (anthrax) protective antigen and superoxide dismutase (SOD; an industrially useful enzyme) have been successfully produced in transgenic tobacco chloroplasts (Daniell, 2006; Madanala *et al.*, 2015; Tregoning *et al.*, 2003; Watson *et al.*, 2004).

1.8.5.1.1 Hairy root cultures

Agrobacterium rhizogenes is a Gram negative soil bacterium that produces hairy root disease in dicotyledonous plants. *A. rhizogenes* induces the formation of proliferative multi-branched adventitious roots known as 'hairy roots' at the site of infection (Chilton *et al.*, 1982). In the rhizosphere (the narrow region of soil that is directly influenced by root secretions and associated soil microorganisms), plants may suffer from wounds by soil pathogens or other sources. This leads to the secretion of phenolic compounds like acetosyringone that attract the bacteria. Under such conditions, certain bacterial genes are turned on, leading to the transfer of its T-DNA from its root inducing plasmid (Ri plasmid) into the plant, through the wound. After integration of T-DNA into the plant genome, plants show overdevelopment of a root system known as hairy roots (Cardarelli *et al.*, 1987; Sevon & Oksman-Caldentey, 2002). These neoplastic (cancerous) roots show distinctive features, such as high growth rates, unlimited branching, and biochemical and genetic stability (Sharma *et al.*, 2013). Hairy roots resemble normal roots in terms of morphology and biosynthetic machinery, producing similar secondary metabolites compared to wild-type roots. As a result, hairy roots were used to develop *in vitro* hairy root cultures for a large number of plants for the commercial-scale production of secondary metabolites (Guzman *et al.*, 2011; Giri & Narasu, 2000; Komaraiah *et al.*, 2003; Lin *et al.*, 2003; Moyano *et al.*, 2003; Sudha *et al.*, 2003), as well as recombinant proteins including antibodies (Gaume *et al.*, 2003; Martinez *et al.*, 2005; Putalun *et al.*, 2003). Hairy roots cultured in controlled growth conditions prevent transgene or active protein dissemination to the environment. It is the major advantage of this expression system (Guillon *et al.*, 2006). However, the major constraint for commercial exploitation of hairy root cultures is the development and scaling up of cultures, including the development of bioreactors that permit the growth of interconnected tissues unevenly distributed throughout the reactor (Srivastava & Srivastava, 2007).

sRAGE was initially expressed in stable transgenic *N. tabacum* lines by Webster & Pickering (pers. comm.). Ribulose-1,5-bisphosphate carboxylase oxygenase (RuBisCO) was co-purified when *N. tabacum* leaves were used to purify sRAGE. RuBisCO is the most abundant protein in leaves that accounts for 50 % of soluble leaf protein in C3 plants and 30 % in C4 plants (Gowik & Westhoff, 2011). To overcome contamination of the sRAGE protein with RuBisCO, the high yielding stable lines of *N. tabacum* were transformed to develop hairy root cultures utilising *Agrobacterium rhizogenes* by Webster & Pickering (pers. comm.). In the present study, sRAGE was expressed in hairy root cultures of *Nicotiana tabacum* on a large scale to obtain a high yield of sRAGE with similar patterns of glycosylation as the native protein.

1.8.5.2 Transient plant expression systems

As the name implies, transient expression is the expression of genes of interest for a short period of time. The gene of interest is not transferred to the next generation; therefore, new plants need to be transfected prior to each round of protein production. Transient protein expression is a potential alternative to stable expression for the production of therapeutic proteins (Chen *et al*., 2013; Joh & VanderGheynst, 2006). Transient protein expression in plants can be achieved either by using biolistic delivery of "naked DNA", agroinfiltration (*Agrobacterium* mediated infiltration), or infection of the plants with viral vectors. This delivery system is preferential to stable transfection when a shorter process time is required, for example, drug discovery, and assay development or for high-throughput screening (Gils *et al*., 2005; Gleba *et al*., 2007; Leuzinger *et al*., 2013).

In virus-based transient expression, a virus systemically infects the plant cells. Many transcripts of the gene of interest are generated and recombinant protein is produced as a by-product by viral replication. Multiple viral-provector modules can be targeted to different subcellular locations in the plant cell, such as the apoplast, cytoplast and chloroplast, thus, more than one protein can be produced at a time (Gleba *et al*., 2005; Marillonnet *et al*., 2005). This easy manipulation and the small size of plant viruses make viral-based transient expression systems attractive systems for heterologous protein production (Lico *et al*., 2008). Alternatively, viral vectors facilitate the generation of higher yields of proteins more efficiently and at a lower cost than mammalian systems (Dong *et al*., 2005; Gils *et al*., 2005; Gleba *et al*., 2007; Koya *et al*., 2005; Ma *et al*., 2005; Ma *et al*., 2003; Sainsbury & Lomonossoff, 2008; Santi *et al*., 2007; Werner *et al*., 2011).

Plasmodium yoelii merozoite surface protein is an example that expressed in high yield (10 % TSP or 1-2 mg / g of fresh weight) using MagnICON® deconstructed viral vector system in the Webster laboratory (Webster *et al*., 2009). This yield is ~40-fold increase compared to that produced with nuclear transformation of *N. tabacum* (Wang *et al*., 2008).

A. tumefaciens-based transient expression systems involve the transfer of the genes of interest along with the bacterium T-DNA region to the plant cell nucleus through agroinfiltration (Kapila *et al*., 1997). Here, the T-DNA copies do not integrated into the nucleus and instead are transcribed to produce proteins transiently and serve as a rapid recombinant protein expression technique (Sainsbury & Lomonossoff, 2014). This system allows production of more than one protein in the same plant simultaneously; alternatively, they can be targeted to different compartments, like the cytosol, apoplast, endoplasmic reticulum (ER), chloroplast or the vacuole by fusing the gene(s) of interest with the appropriate signal peptides. Therefore, *A. tumefaciens*-based transient expression systems assist in finding the cellular compartment where that protein is best produced (Lee & Gelvin, 2008).

1.9 The effect of post-translational modifications on the structure and function of proteins

Post-translational modifications (PTMs) of proteins are the covalent modifications that yield derivatives of individual amino acid residues in the polypeptide chain. These modifications include attachment of fatty acids, proteolysis, glycosylation, acetylation and hydroxylation (Gomord *et al*., 2010). However, glycosylation is the most complex and commonly observed form of post-translational modification (Schedin-Weiss *et al*., 2014). Glycosylation is an enzymatic process that attaches glycans to the side chains of the protein and differs from glycation. The PTMs of proteins play an important role in regulating stability, interactions and function of proteins (Akiyama *et al*., 2009; Jacobs *et al*., 2009; Lanctot *et al*., 2005).

In this study, sRAGE was expressed in a plant expression system with the expectation of obtaining glycosylated sRAGE to perform *in vitro* ligand binding assays to determine the effect of glycosylation of sRAGE on ligand binding. The effects of *N*-linked glycosylation on the properties of proteins in general are described in detail in the following paragraph.

1.9.1 *N*-linked glycosylation

N-glycosylation, the enzymatic attachment of an oligosaccharide precursor (Glc3Man9N-5) acetylglucosamine [Glc3Man9GlcNAc] onto a specific Asparagine (Asn) residue, which is a constituent of the potential *N*-glycosylation specific sequence (Asn-X-Ser/Thr) of a protein, is a major post-translational modification in eukaryotes (Gomord *et al*., 2010). In humans, more than 50 % of proteins are estimated to be *N*-glycosylated (Apweiler *et al*., 1999). In contrast to DNA, RNA or protein synthesis, glycosylation is not under direct transcriptional control and is not based on a template (Loos & Steinkellner, 2012). Instead non-template driven *N*-glycosylation normally results in the synthesis of a heterogeneous collection of different carbohydrate structures (heterogeneously glycosylated mixture) on an otherwise homogeneous protein backbone (microheterogeneity) (Bosch *et al*., 2013). This microheterogeneity may comprise several thousand glycoforms given the high number of possible glycans attached to proteins, and manifold functions can be attributed to the carbohydrate moiety: folding, stability, conformation, solubility, quality control, half-life, oligomerization or functionality. The presence of *N*-glycans regulates *in vivo* functionality of proteins as observed for mouse interleukins (mILs; Gao *et al*., 2008). A hematopoietic stimulant, Darbepoetin is an example of a protein produced with an extended half-life and increased efficacy, upon engineering additional glycosylation sites (Sinclair & Elliott, 2005). *N*-glycans contribute to the volume and charge of glycoproteins, which may be important for ligand binding and conformational stability (Agarwal *et al*., 2008; Hu *et al*., 1994; Hu & Norrby, 1994; Srikrishna *et al*., 2002).

1.9.1.1 N-linked glycosylation of plant and mammalian proteins

N-glycosylation of proteins produced in plant cells share considerable similarity with that of mammalian cells (Bosch *et al*., 2013; Webster & Thomas, 2012). In both plant and mammalian cells, *N*-glycosylation begins in the ER with the addition of a dolichol-linked oligosaccharide precursor to the potential *N*-glycosylation Asn residue. The formation of the precursor complex initiates the sequential addition of two *N*-Acetylglucosamines (GlcNAcs), five mannose residues to the ER membrane-bound dolichol pyrophosphate (DPP) at the cytosolic face of the ER (Figure 1.8). Subsequently the heptasaccharide dolichol-linked structure is translocated to the luminal side of the ER. In the ER, four more mannoses and three glucoses are linked, creating the fully assembled dolichol-linked precursor (Nagels *et al*., 2012). The oligosaccharide precursors of the resulting

glycoproteins then undergo several maturation steps in the ER and Golgi apparatus (Figure 1.8).

The initial steps in the formation and processing of *N*-glycans in humans and plants are the same. However, prominent differences appear in the latter steps of maturation within the Golgi apparatus (Gomord & Faye, 2004; Nagels *et al*., 2012). Thus, biosynthesis of oligomannosidic (mannose residues attached to the pentasaccharide sugar core) *N*-glycan structures is conserved, but the complex type end products display very distinct differences between plants and humans. In plants, the proximal GlcNAc residue is attached with an α1,3-linked fucose while in mammals this is an α1,6-linked fucose. In plants, the proximal mannose residue of the core is attached with a β1,2-xylose (Bosch *et al*., 2013; Gomord & Faye, 2004). Furthermore, plants can attach β1,3-linked galactose and α1,4-linked fucose residues to the terminal GlcNAcs while for mammals mainly β1,4-linked galactose and N-Acetylneuraminic acid (NeuAc, the predominant sialic acid residue) are added to the terminal GlcNAcs (Nagels *et al*., 2012; Saint-Jore-Dupas *et al*., 2007). Interestingly, human *N*-glycan structures are of multi-antennary nature while in plants these structures carry only two antennae (Figure 1.8). These differences occur because plants lack the enzymes that catalyse such modifications. Although the final structure of *N*-glycans in mammals and plants are different from each other, they share a remarkably high degree of homology during processing along the secretory pathway.
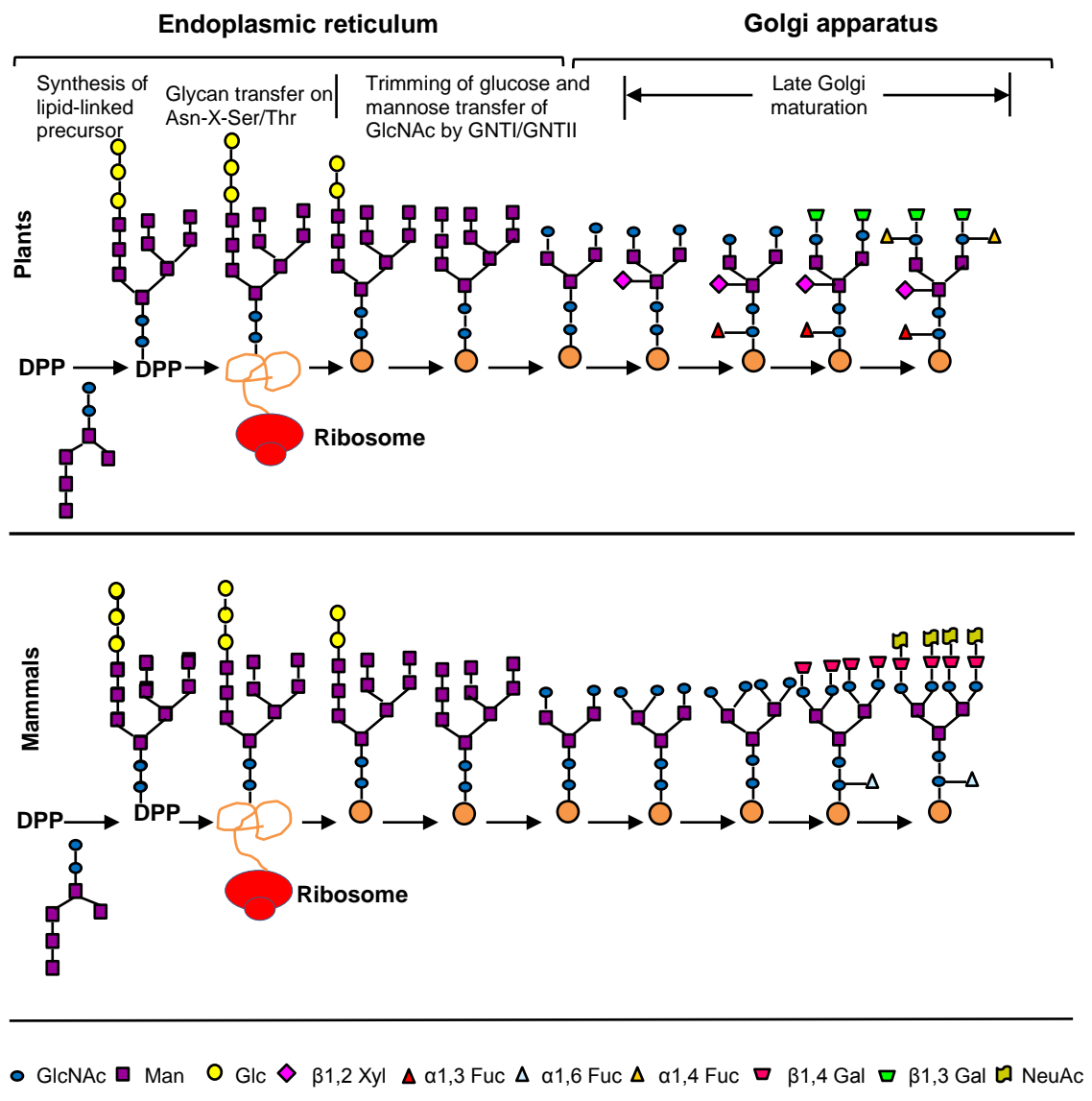
Figure 1.8 A comparison of protein *N*-glycosylation in plants and mammals. The formation and the processing of *N*-linked glycans in the ER and the Golgi apparatus in plants and mammals are similar. Differences in *N*-glycosylation in plants and mammals occur with the formation of complex *N*-glycans within the Golgi apparatus during the late maturation step. *N*-glycosylation starts with the formation of a lipid-linked oligosaccharide precursor and then is transferred on specific Asn-X-Ser/Thr residues of the nascent growing polypeptide. Then, *N*-glycans are trimmed off with the removal of all of the glucosyl and most of the mannosyl residues. Plants form bi-antennae complex *N*-glycans with the attachments of β1,3 Gal and α1,4 Fuc and mammals form multi-antennae structures with GlucNAc, β1,4 Gal and NeuAc residues. Glc; Glucose, GlcNAc; *N*-Acetylglucosamine, Gal; Galactose, Fuc; Fucose, NeuAc; *N*-Acetylneuraminic acid, Xyl; Xylose (Modified from Gomord & Faye, 2004).

Attempts were made by Strasser *et al.* (2004) to eliminate or disrupt the plant specific xylose and core α1,3-fucose from recombinant glycoproteins. These glycans are not present in humans and therefore, considered as unwanted on proteins intended for therapeutic use. Thus, *Arabidopsis thaliana* knock-out plants lacking β1,2-xylosyltransferase and core α1,3-fucosyltransferase (XylT and α1,3-FucT) that are responsible for the synthesis of these glycan epitopes have been generated (Strasser *et al.*, 2004). Recently, six proteins were introduced from the mammalian sialylation pathway into plants that allow the biosynthesis of sialic acid, its activation, transport into the Golgi, and finally its transfer onto terminal galactose. Terminal sialylation is the final and the most complex step of human *N*-glycosylation. Most of the drugs require sialylated oligosaccharides for optimal therapeutic potency (Castilho *et al.*, 2010). These results can be considered as a milestone in plant glycoengineering. Introduction of mammalian sialylation pathways and elimination of specific *N*-glycan residues have placed plants in a particularly favourable position for the production of the next generation mAbs and "bio-betters".

Although the complex modification of glycans differs between plants and mammals as explained above, the core glycans and the frequency and sites of glycosylation are identical. This has been exploited in our research by fusing a SEKDEL sequence to recombinant sRAGE, resulting in the retention of the desired protein in the ER of the plant cells, to generate core glycans similar to mammals. There are two putative *N*-glycosylation sites present in the full-length RAGE protein. One is located in the amino terminus, adjacent to the V-region like domain of RAGE; the other site is located within the V-domain of RAGE (Appendix I) (Schlueter *et al.*, 2003; Turovskaya *et al.*, 2008). Several studies have shown that the presence of *N*-glycans on RAGE enhance the binding of ligands to RAGE, which will be discussed in chapter 4 in detail.

1.10 Aims of the research project

The specific aims of this project were,

1. To obtain high yields of purified recombinant sRAGE. sRAGE was expressed in *Nicotiana tabacum* hairy root cultures and in an *E. coli* expression system.

2. To understand the structural basis for the interaction between recombinant sRAGE and the ligands, HMGB-1 or S100A8/A9 complex by,

    i. Comparing the binding activity of *E. coli*-made and plant-made sRAGE to HMGB-1 or S100A8/A9 complex and relating these activities to glycosylation of sRAGE.

    ii. Determining the effect of extracellular environmental components (specifically, divalent cations and EDTA) and pH conditions on both plant and *E. coli*-made sRAGE binding to HMGB-1 or S100A8/A9 complex.

3. To determine the full-extracellular domain structure of plant-made sRAGE by small angle X-ray scattering (SAXS) analysis.

CHAPTER 2

Further development and optimisation of recombinant sRAGE protein derived from hairy root cultures of *Nicotiana tabacum*

2.1 INTRODUCTION

The receptor for advanced glycation end-products (RAGE) is a member of the immunoglobulin (Ig) super family of the cell surface receptors (Neeper *et al*., 1992; Schmidt *et al*., 1992). Upon binding with ligands, such as advanced glycation end-products (AGEs), matrix proteins, members of the S100 proteins and high mobility group family proteins (HMGB-1), RAGE causes development of severe chronic pathologies, including diabetic complications, Alzheimer's disease and tumors (Leclerc *et al*., 2010; Sparvero *et al*., 2009). One isoform of RAGE; the soluble receptor for advanced glycation end-products (sRAGE) is of interest to researchers because of its ability to prevent the binding of RAGE-ligands to RAGE or other cell surface receptors (Ding & Keller, 2005). sRAGE acts as a dummy receptor and prevents the activation of RAGE. Hence, sRAGE has potential therapeutic properties (Geroldi *et al*., 2006; Lih-Fen *et al*., 2009). However, to be used therapeutically, the production and purification of high quality sRAGE is paramount.

Various expression systems for the production of recombinant proteins are available, each with specific advantages as well as disadvantage (see 1.8.1 to 1.8.5). The major advantage in using plant based expression systems is that the recombinant protein has similar patterns of glycosylation as the native protein. However, there are no published reports detailing the use of plant systems for the production of any of the RAGE isoforms. In the present study, sRAGE was expressed in hairy root cultures of *Nicotiana tabacum* and extraction and purification methods were further developed with the aim of producing high yields of sRAGE, with similar glycosylation patterns as the native protein. Studies have shown that glycosylation of RAGE proteins are important for its activity (Srikrishna *et al*., 2010; Srikrishna *et al*., 2002)

Unpublished results by Webster and Mulcair (pers. comm.) indicate that it is possible to obtain sRAGE (0.6 % of total soluble protein) from *N. tabacum* hairy root cultures, which,

following purification resulted in ~300 µg sRAGE. In this pilot study Webster and Mulcair used a sodium ascorbate based protein extraction buffer followed by anion-exchange chromatography (AEC) and size-exclusion chromatography (SEC) to purify sRAGE, but the yields achieved in this experiment has not been able to be replicated. Therefore, the aim of the experiments reported in this chapter, was to further develop and optimise the anion-exchange chromatography protocol to maximise the yield of sRAGE and obtain enough purified sRAGE for further analysis. Optimisation of the protocol involved modifications to the purification steps and also the extraction buffer components. Heparin Sepharose and Immobilized Metal Affinity Chromatography (IMAC)/His-Tag purification methods were also used for further purification of sRAGE. The final optimised protocol was developed by systematically testing each step of the extraction and purification process.

Anion-exchange chromatography (AEC) separates substances based on their net surface charge and is one of the most frequently used techniques for the purification of proteins, peptides, nucleic acids and other charged biomolecules, offering high resolution and group separations with high loading capacity (Bonnerjea *et al*., 1986). The tightness of the binding between the substance and the resin is based on the strength of the negative charge of the substance. Proteins are eluted mainly by increasing the ionic strength (salt concentration) of the buffer or by changing the pH. The salt concentration in the elution buffer is gradually increased and the negative ions (e.g. Cl^-) compete with the protein in binding to the resin. The pH of the solution can gradually be decreased, which results in a more positive charge on the protein, releasing it from the resin. In the present study, these parameters were modified for the elution of sRAGE.

Size-exclusion or gel-filtration is a chromatographic method in which molecules in solution are separated according to their size (Barth & Boyes, 1992). Size-exclusion chromatography is widely used for the purification and analysis of large molecules or macromolecular complexes, such as proteins and industrial polymers. It has a number of major advantages as a protein purification method, including a distinct separation of large and small molecules, while using minimal volumes of eluents, well-defined separation times and narrow bands in the resulting chromatograms (Alberts *et al*., 2002; Striegel *et al*., 2009). Here, SEC was selected as a second step of sRAGE purification, following removal of impurities by the AEC method.

2.2 MATERIALS AND METHODS

2.2.1 Growth of hairy root cultures of *N. tabacum* expressing sRAGE

Nicotiana tabacum plants were stably transformed to express sRAGE and leaf tissue from these plants was co-cultivated with *Agrobacterium rhizogenes* to generate hairy roots (Webster unpublished). These hairy root cultures were grown in Murashige and Skoog (MS) medium with selection using 100 µg mL^{-1} cefotaxime and 25 µg mL^{-1} kanamycin (Appendix III).

Prior to large scale sRAGE expression, randomly selected hairy root cultures were harvested and monitored for the production of sRAGE by enzyme-linked immunosorbent assay (ELISA) (see below). Following confirmation of the presence of sRAGE, hairy roots were subcultured in 250 mL universal jars (440 jars per batch) containing 25 mL of Murashige and Skoog (MS) medium (PhytoTechnology Laboratories$^{®}$) supplemented with 100 µg mL^{-1} cefotaxime and 25 µg mL^{-1} kanamycin. These cultures were grown for 18-21 days (Figure 2.1) at 25 ºC on an orbital shaker (Thermoline Scientific) at a speed of 80 rpm. Harvested hairy roots were repeatedly blotted to remove extracellular moisture (Chintapakorn & Hamill, 2003), weighed and snap frozen in liquid nitrogen. Hairy roots (1.0 g - 1.5 g) was produced from a single jar; 3 kg of hairy roots were obtained from six harvests (440 jars x 6 harvests). Approximately 50 g of hairy roots was wrapped in aluminium foil, snap frozen and stored at -80 ºC for sRAGE protein extraction.

Figure 2.1 Hairy root cultures in Murashige and Skoog medium (18 days old).

2.2.2 Extraction of sRAGE from hairy root cultures of *N. tabacum*

Frozen hairy roots (~100 g in total per extraction) were ground in a pre-chilled coffee grinder (Breville Coffee 'n' Spice Grinder) to get a coarse powder. Powdered hairy roots were transferred to a pre-chilled ceramic mortar containing 250 mL ice cold sodium ascorbate based extraction buffer (50 mM Tris, pH 9.0, 100 mM sodium ascorbate, 0.1 % Triton X-100, protein inhibitor cocktail according to manufacturer's instructions (cOmplete ULTRA Tablets [cat. # 5892953001]), Roche, EDTA free: 1 tablet per 50 mL extraction buffer). Sodium ascorbate was included in the extraction buffer to avoid oxidation of polyphenols and their interference with protein extractions (Cremer & Van de Walle, 1985). In addition, using sodium ascorbate rather than ascorbic acid is recommended because it does not change the pH of the buffer (Guzman *et al.*, 2011). The roots were further ground with the buffer resulting in the pre-total soluble protein (pre-TSP) mixture, which was filtered through two layers of Miracloth (Calbiochem) twice and then centrifuged at 10,000 g at 4 ℃ for 45 minutes. The supernatant was collected as the total soluble protein (TSP) fraction. The pellet was resuspended in ~50 mL of extraction buffer and centrifuged at 10,000 g at 4 ℃ for 45 minutes and the second TSP fraction was collected. Both TSP fractions were pooled for further analysis and purification.

2.2.2.1 Modifications to the total protein extraction and purification protocol

Modifications to the purification steps were made to try to improve the final sRAGE yield of TSP. Firstly Whatman no. 1 filters and 0.2 µm Nalgene™ 25 mm Syringe Filters (Thermo Fisher Scientific) were used as alternative clarification methods in place of centrifugation. Whatman no. 1 filter paper was placed in a glass funnel attached to the neck of an Erlenmeyer flask and the TSP fraction filtered through it. Extraction buffer (20 mL) was passed through the 0.2 µm syringe filter to facilitate efficient filtration and then the pre-TSP fraction was passed through the filter. Secondly, the time and speed of the centrifugation was modified in order to determine whether any protein was lost from the supernatant during the centrifugation process. The pre-TSP fraction was centrifuged for 5 minutes, 15 minutes, 30 minutes and 45 minutes at a speed of 8,000 g and 10,000 g to obtain the TSP fraction.

2.2.2.2 Modification of the extraction buffer

The components of buffers used for protein extractions may have an effect on the efficiency of the AEC purification process. In order to optimise the TSP extraction the following variations were made individually to the buffer: (i) addition of 20 mM ethylenediaminetetraacetic acid (EDTA) (a metal chelator and a protease inhibitor), (ii) the addition of 3 % (w/v) polyvinylpolypyrrolidone (PVPP) (mol. Wt. 36, 000, Sigma) (binds phenolics and therefore reduces protein precipitation) and (iii) a decrease in the Triton X-100 concentration from 0.1 % to 0.05 % (Triton X-100 facilitates extraction and solubilisation of membrane proteins but these proteins can be either modified or inactivated by higher concentrations of Triton X-100).

The pH of the extraction buffer may also effect protein yield. The starting pH should be at least 1 pH unit above the isoelectric point (pI) for anion- exchangers (Lampson & Tytell 1965). Therefore, the hairy root extraction buffer and the AEC purification buffer were changed from 9.0 to 8.6 considering that the pI of sRAGE is 7.6, to investigate if this pH change has any effect on the yield recovery of sRAGE.

To determine the efficacy of the above modifications, total soluble protein was extracted from ~5 g of hairy roots, independently for each variable. The TSP for each extraction was used to determine the effect of the modifications of the purification steps and also the extraction buffer components on the yield improvement in the TSP fraction on a small scale prior to scaling up for AEC analysis.

2.2.2.3 Dialysis and concentration of the TSP fraction

The TSP fraction was dialysed to exchange the protein extract to the AEC purification buffer, and then concentrated before being loaded onto the anion-exchange column. The TSP fraction was dialysed against 50 mM Tris, pH 9.0 overnight at 4 ºC and was concentrated up to ~30 - 40 mL using 50 mL Amicon Ultra 10,000 MWCO centrifugal filter devices (Merck Millipore). Then, concentrated TSP fraction was centrifuged at 4,000 g for 10 minutes before being loaded onto the anion-exchange column for further purification. sRAGE concentration before and after anion-exchange chromatography purification was quantified by ELISA (see 2.2.5.2).

2.2.3 Purification of sRAGE from the total soluble protein extracted from hairy root cultures of *N. tabacum*

sRAGE extracted from hairy roots of *N. tabacum* was purified by anion-exchange chromatography followed by size-exclusion chromatography methods developed by Webster and Mulcair (pers. comm.). In the present study, in addition to AEC and SEC methods, Heparin Sepharose (GE Healthcare) and Immobilized Metal Affinity Chromatography (IMAC)/His-Tag system (Qiagen) were tested to further purify sRAGE and optimise conditions.

2.2.3.1 Anion-exchange chromatography

Two systems were used; (i) a 10 mL MT 20 column (Bio-scale^{TM} MT High Resolution Empty Column; Bio-Rad) attached to a FPLC system (ÄKTA, GE Healthcare) and (ii) a 10 mL needleless syringe attached to a pressure manifold to apply pressure and to control the flow rate of the column (Figure 2.2). Both columns were packed with Q-Sepharose (GE Healthcare) and pre-equilibrated with 50 mM Tris pH 9.0. The TSP fraction was loaded onto the columns at a flow rate of 5 mL min^{-1} and then washed with ten column volumes of 50 mM Tris pH 9.0. The buffers used in AEC purification were filtered through 250 mL Steritop^{TM} Sterile Vacuum Bottle-Top Filters (0.22 µm) (EMD Millipore). Using the FPLC system sRAGE was eluted by automatic increases in sodium chloride (NaCl) concentrations up to 1 M NaCl. For the needless syringe/pressure manifold system, sRAGE was eluted stepwise with 200 mM increments of NaCl in 50 mM Tris, pH 9.0 (applied manually starting with 200 mM NaCl in 50 mM Tris pH 9.0, and increasing to 1 M NaCl in 50 mM Tris pH 9.0). At each increment five column volumes of buffer were used at a flow rate of 5 mL min^{-1}. Fractions for both systems were collected as follows: flow-through (50 mL), wash (100 mL) and eluent 1 to 5 (E1 to E5 each of 50 mL) were collected manually. Eluent 1 (E1) and eluent 2 (E2) were obtained by running the column with 50 mL of 50 mM Tris/0.2 M NaCl and 50 mM Tris/0.4 M NaCl respectively. Eluent 3 (E3), eluent 4 (E4) and eluent 5 (E5) were obtained by running the column with 50 mL of 50 mM Tris/0.6 M NaCl, 50 mL of 50 mM Tris/0.8 M NaCl and 50 mL of 50 mM Tris/1.0 M NaCl.

Figure 2.2 Pressure manifold utilised to carry out protein purification.

If a specific protein extraction modification was shown to improve the yield of sRAGE in the TSP fraction, then sRAGE was extracted using ~15 g of hairy roots for AEC purification to determine if the yield improvement was consistent even after AEC purification. In addition, the pH of the extraction buffer and the AEC buffer was changed from 9.0 to 8.6, which may facilitate the efficient elution of protein. Once the protocol was optimised, AEC purification was carried out to determine the repeatability of the established anion-exchange chromatography protocol on a large scale using the extract of ~100 g of hairy roots. Fractions were analyzed by the Bradford total soluble protein assay (Bio-Rad) and by ELISA (see below).

2.2.3.2 Size-exclusion chromatography

A Superdex 200 10/300 pre-packed column (GE Healthcare) was attached to a FPLC (ÄKTA, GE Healthcare). SEC buffer; 50 mM Tris pH 9.0, 150 mM NaCl and 5 % glycerol was filtered through 250 mL Steritop™ Sterile Vacuum Bottle-Top Filters (0.22 µm; EMD Millipore). The column was equilibrated with ten column volumes of 50 mM Tris pH 9.0, 150 mM NaCl and 5 % glycerol. Following the anion-exchange, fractions were pooled, concentrated to ~1 - 2 mL using 15 mL, Amicon Ultra 10,000 MWCO centrifugal filter devices (Merck Millipore) and loaded onto the SEC column at a rate of 1 mL min^{-1}. sRAGE was eluted in 50 mM Tris pH 9.0, 150 mM NaCl and 5 % glycerol at a rate of 1 mL min^{-1}.

2.2.3.3 Heparin Sepharose chromatography

Heparin Sepharose is preferably used to purify proteins that show a natural affinity for heparin, such as DNA binding proteins. sRAGE has the ability to bind both double stranded DNA and single stranded RNA (Park *et al*., 2010). Therefore, it was

hypothesised that Heparin Sepharose could be utilised successfully to purify sRAGE. Moreover, Heparin Sepharose has previously been used to purify recombinant mouse sRAGE (Hanford *et al*., 2004). Therefore, a Heparin Sepharose column was used as the third step (after AEC and SEC purification) of purification.

A 1 mL HiTrap™ Heparin Sepharose column (GE Healthcare) was attached to the FPLC (ÄKTA, GE Healthcare) and equilibrated with ten column volumes of buffer A (phosphate buffered saline (PBS) pH 7.4; Appendix III) with 5 % glycerol and 0.1 mM phenylmethylsulfonyl fluoride (PMSF), followed by ten column volumes of buffer B (PBS pH 7.4, 1 M NaCl, 5 % glycerol and 0.1 mM PMSF) and again with twenty column volumes of buffer A according to the manufacturer's protocol (GE Healthcare). Buffer A and buffer B were filtered through 250 mL Steritop™ Sterile Vacuum Bottle-Top Filters (0.22 μm; EMD Millipore) before being used.

Following the size-exclusion chromatography separation, fractions containing sRAGE as determined by SDS-PAGE analysis and ELISA were pooled and concentrated to ~1 - 2 mL using 15 mL Amicon 10,000 Ultra MWCO centrifugal filter devices (Merck Millipore), and loaded onto the column at a flow rate of 0.5 mL min^{-1}. sRAGE was eluted under a linear concentration gradient of 100 % buffer A to 100 % buffer B according to the manufacturer's protocol. Fractions were analyzed by SDS-PAGE to detect purity of the protein (see 2.2.4.1) and western blotting to detect the presence of the protein of interest using antibodies (see 2.2.4.2).

2.2.3.4 Immobilized metal affinity chromatography purification

Eight histidine-residues (His-Tag) in the C-terminal end of the sRAGE gene were included in the design of the sRAGE construct (Appendix I) to facilitate purification by Immobilized Metal Affinity Chromatography (IMAC). Webster and Mulcair (pers. comm.) attempted to purify sRAGE directly from total soluble proteins by IMAC-based purification, but were only able to obtain poorly purified sRAGE with a yield recovery of less than 5 % of the 0.6 % sRAGE present in the TSP. Therefore, as a first step in sRAGE purification from total protein extracts the IMAC-based purification failed. However, it was expected that this IMAC-based purification method would successfully purify sRAGE once most of the impurities had been removed by AEC and SEC methods. Therefore, AEC followed by SEC purified sRAGE was further purified by Ni-NTA Sepharose (Qiagen) chromatography as per the manufacturer's guidelines as follows.

Approximately, 1 mL of Ni-NTA resin (Qiagen) was added to a 15 mL tube and centrifuged at 1,000 *g* for 1 minute. The column was then washed three times with Milli-Q water followed by three washes with 10 mL Ni-NTA lysis buffer; phosphate buffered saline (PBS), pH 7.4, 10 mM imidazole supplied with the Ni-NTA spin kit (Qiagen). Size-exclusion chromatography purified and concentrated sRAGE was added directly onto the Ni-NTA Sepharose, pre-equilibrated with Ni-NTA lysis buffer. The 15 mL tube was subjected to end-over-end mixing for 20 minutes on a tube rotator, to facilitate batch binding of sRAGE. It was washed with 10 mL of Ni-NTA wash buffer (PBS, pH 7.4, 10 mM imidazole) three times. His-Tagged sRAGE was recovered by adding 2 mL of Ni-NTA elution buffer (PBS, pH 7.4, 75 mM imidazole) and centrifuged (1,000 *g* for 5 minutes) at 4 ℃. To recover any remaining bound sRAGE, an additional 5 mL of PBS, pH 7.4 supplemented with 300 mM imidazole was added, and re-centrifuged at 4 ℃. The supernatants from these two steps were stored separately at 4 ℃ for analysis. All the buffers used in the IMAC-based purification were filtered through 250 mL Steritop™ Sterile Vacuum Bottle-Top Filters (0.22 µm; EMD Millipore) before being used. Eluent 1 (E1), eluted with PBS, pH 7.4, 75 mM imidazole (2 mL) and Eluent 2 (E2) eluted with PBS, pH 7.4, 300 mM imidazole (5 mL) were collected manually and analysed by enzyme-linked immunosorbent assays (ELISA) as per methods described either in 2.2.5.2 or in 2.2.5.3.

2.2.4 Characterisation of plant-made sRAGE

Purified sRAGE was characterised by sodium dodecyl sulfate polyacrylamide gel electrophoresis (SDS-PAGE) and western blot analysis.

2.2.4.1 SDS-PAGE analysis

Aliquots of 15 µL of sRAGE protein sample were transferred into a 1.5 mL eppendorf tube and 5 µL of 4X SDS-PAGE loading buffer (125 mM Tris-HCl pH 6.8, 4 % SDS, 0.01 % bromophenol blue, 10 % glycerol and 10 % β-mercaptoethanol) was added. Samples were heated at 95 °C for 5 minutes, centrifuged briefly in a bench top centrifuge at 4,000 *x g* before loading onto a 12 % SDS-PAGE gel (Separating gel: 40 % acrylamide, 1.5 M Tris pH 6.8, 10 % SDS, 10 % ammonium persulfate (APS) and tetramethylethylenediamine (TEMED); Stacking gel: 40 % acrylamide, 0.5 M Tris pH 6.8, 10 % SDS, 10 % APS and TEMED). Alongside the samples 7 µL of protein molecular mass markers (Bio-Rad, Precision Plus Protein™ Dual Xtra standard) were loaded and

electrophoresis was performed at 200 V, for 50 minutes using Bio-Rad Mini-PROTEAN® three cells cassette with running buffer (10 % Tris glycine: 25 mM Tris, 192 mM glycine and 0.1 % SDS). After separation, the gel was removed from the cassette and stained with 0.5 % Coomassie Brilliant Blue R-250 for 30 minutes and destained with destain buffer (20 % methanol and 10 % glacial acetic acid).

2.2.4.2 Western blot analysis with SNAP i.d. Protein Detection System

For western blot analysis samples were run as described above. The gel was removed from the cassette and soaked in running buffer (25 mM Tris, 192 mM glycine and 0.1 % SDS) for 10 minutes followed by 15 minutes in transfer buffer (25 mm Tris, 192 mM glycine, 0.1 % SDS and 20 % methanol). Four pieces of filter papers larger than the Immobilon®-P, PVDF (Polyvinylidene fluoride) membrane (Merck Millipore) were prepared. The membrane was cut slightly larger than the gel. The membrane was washed in 70 % methanol for 3 - 4 minutes and then washed with Milli-Q water before it was soaked in transfer buffer. The fibre pads, PVDF membrane and filter papers were soaked in the transfer buffer for approximately 15 minutes. The western cassette was assembled as follows, fibre pad, two filter papers, gel, membrane, two filter papers, and the fibre pad. When each layer was added, any air bubbles were removed. A magnetic stirrer was added and the gel was subjected to electrophoresis at 70 V, for 45 minutes at 4 °C.

After protein transfer, the membrane was removed from the cassette and placed in 30 mL of 0.3 % skim milk in blotting buffer (25 mM Tris, 0.15 M NaCl and 0.1 % Tween 20, pH 7.4) for 30 minutes at 4 °C. Then the membrane was placed in a pre-wet SNAP i.d. cassette with a fibre spacer (EMD Millipore). Once the cassette was inserted into the vacuum system, 30 mL of blotting buffer was added and vacuum was applied. The blot was washed three times with 20 mL of blotting buffer (25 mM Tris, 0.15 M NaCl and 0.1 % Tween 20, pH 7.4). Mouse anti-human RAGE antibody (R & D System) was diluted to 0.5 µg mL^{-1} (in 0.3 % milk in blotting buffer) and added to the membrane and incubated for 6 minutes. A vacuum was then applied and the membrane was washed three times with 20 mL of blotting buffer, followed by the addition of 3 mL of goat anti-mouse IgG (Fc specific) peroxidase conjugated antibody (Sigma), diluted 1:60,000 in 0.3 % milk in blotting buffer and incubated for 6 minutes. The vacuum was applied again and the membrane washed three times with 20 mL of the blotting buffer.

The probed membrane was then transferred to a container where it was incubated with 500 µL of ECL (Enhanced Chemiluminescence) reagent (GE Healthcare) for 5 minutes. Then, the membrane was sandwiched between overhead transparencies and excess solution was squeezed out by wiping with a lint free tissue. Kodak Biomax light film (Eastman Kodak, USA) was exposed to the membrane, in a dark room at 3 and 5 minute intervals, and then developed in an X-ray film developer machine (AGFA CP 1000, Gevaert, Belgium).

2.2.5 Quantification of sRAGE

2.2.5.1 Bradford total soluble protein assay

Concentrations of TSP were determined by using a Bradford based commercial kit method (Bio-Rad protein assay) (Guzman *et al*., 2011). Known concentrations (ranging from $0.0 \, mg \, mL^{-1}$ to $0.5 \, mg \, mL^{-1}$) of bovine serum albumin (BSA, Sigma) solutions were prepared in a 96 well microtiter plate (Interpath Services) to generate a standard curve. 10 µL of each of the sample were diluted 1:10 or 1:50 in 1X phosphate buffered saline (Appendix III) and added to the wells along with the standard in duplicate. Concentrated protein dye reagent (Bio-Rad) was diluted 1:5 with Milli-Q water and filtered through a Whatman No. 2 filter paper and 200 µL of diluted dye reagent was added to the samples and standards. The plate was incubated for 5 minutes to develop a colour change and the absorbance was measured at a wavelength of 595 nm using a plate reader (Multiskan Ascent, Thermo Fisher Scientific). Total soluble protein concentrations of the samples were calculated using the standard curve.

2.2.5.2 Sandwich ELISA for sRAGE

The sandwich ELISA assay specific for sRAGE was developed by Webster & Pickering (pers. comm.) to quantify the amount of sRAGE present in the hairy roots samples. Mouse anti-human RAGE antibody (R & D System) was diluted 1:500 with PBS. Anti-human RAGE biotinylated antibody (R & D System) and HRP-conjugated streptavidin (R & D System) was diluted 1:500 and 1:200 respectively with 1 % BSA (Sigma) in PBS. The standard curve was within the range of $78 \, pg \, mL^{-1}$ to $5{,}000 \, pg \, mL^{-1}$ of recombinant human RAGE Fc Chimera (R & D System). Protein samples were diluted 1:100, 1:200 and 1:400.

A high binding 96 well ELISA plate (Interpath Services) was coated with 50 µL of Mouse anti-human RAGE antibody (R & D System) and incubated overnight at 4 °C. Wells were aspirated and washed three times with PBS containing 0.05 % tween 20 (PBST). The plate was blocked with 1 % BSA (Sigma) in PBS for 90 minutes at room temperature and washed with PBST three times. One hundred microliters of standards, control or samples (including dilutions) were added in duplicate, incubated for 90 minutes at room temperature and then washed three times with PBST. Anti-human RAGE biotinylated antibody (100 µL; R & D System) was added, incubated for 90 minutes at room temperature and washed three times with PBST, followed by the addition of 100 µL of HRP-conjugated streptavidin (R & D System), further incubated for 20 minutes at room temperature and washed three times with PBST. TMB (3,3′,5,5′-tetramethylbenzidine, Sigma) substrate (100 µL) was added to each well and incubated for 30 minutes at room temperature. Finally, 50 µL of 1N H_2SO_4 was added and the absorbance was measured at a wavelength of 450 nm using a plate reader (Multiskan Ascent, Thermo Fisher Scientific).

2.2.5.3 Quantikine ELISA for sRAGE

Selected samples were further quantified using an expensive gold standard, commercial ELISA kit (Quantikine, R & D Systems) as per the manufacturer's guidelines as follows:

Color reagent A (stabilized hydrogen peroxide) and B (stabilized chromogen [tetramethylbenzidine]) were mixed together in equal volumes (substrate solution) within 15 minutes of use. The standard curve was within the range of 78 pg mL^{-1} to 5,000 pg mL^{-1} of Human RAGE Fc Chimera. Protein samples were diluted 1:200 and 1:400. Standard, control or experimental samples (including dilutions; 50 µL) was added, in duplicate, to a 96 well polystyrene microplate, pre-coated with a monoclonal antibody specific for human RAGE. This was followed by addition of 100 µL of assay diluent, RD1-60 (a buffered protein base with preservatives and blue dye) and the plate was covered with an adhesive strip and incubated for 2 hours at room temperature. Wells were aspirated and washed with wash buffer four times. After addition of 200 µL of RAGE conjugate (a polyclonal antibody specific for human RAGE conjugated to horseradish peroxidase), the plate was incubated for another 2 hours at room temperature. Washing procedure was repeated as described above. Substrate solution (200 µL) was added and the plate incubated for 30 minutes. Finally, 50 µL of stop solution (2N H_2SO_4) was added

and the absorbance was measured at a wavelength of 450 nm using a plate reader (Multiskan Ascent, Thermo Fisher Scientific) within 30 minutes.

2.2.5.4 Calculation of sRAGE yield and recovery as a percentage of total soluble protein

The yield of sRAGE in hairy roots was expressed as a percentage of TSP (% TSP) by dividing the amount of sRAGE detected by the ELISA, by the amount of total soluble protein detected by Bradford assay and multiplied by 100, after adjustment for any dilutions.

$$sRAGE\ yield\ of\ TSP\ (\%) = \frac{sRAGE\ (\mu g)\ from\ ELISA}{TSP\ (\mu g)} \times 100$$

The percentage recovery of sRAGE after AEC purification was calculated as follows,

$$Recovery\ of\ sRAGE\ (\%) = \frac{sRAGE\ E1 + E2\ (\mu g)}{sRAGE\ in\ TSP\ loaded\ onto\ AEC\ column\ (\mu g)} \times 100$$

2.2.6 Statistical analysis

GraphPad Prism version 6 was used for all the statistical analyses performed. The two-tailed *t*-test was used to evaluate the statistical differences between the two groups of data. Probabilities of $P<0.05$ of the observed differences were considered significant.

2.3 RESULTS

The calculated molecular weight of sRAGE protein expressed in hairy roots is 34.5 kDa with a pI (isoelectric point) value of 7.6 as determined by ExPASy-Compute pI/Mw tool (http://web.expasy.org/compute_pi/). A SEKDEL sequence was fused to the C-terminal end of the sRAGE protein, to ensure the protein is retained in the endoplasmic reticulum (ER) of the plant cells, where core glycans are added (Braakman *et al*., 1992; Lodish *et al*., 2000; Sitia & Braakman 2003). The formation and processing of these *N*-glycans in humans and plants are the same. Native human sRAGE undergoes more complex modifications within the Golgi apparatus to generate mammalian specific *β*1,4-linked galactose and sialic acid residues (Saint-Jore-Dupas *et al*., 2007).

2.3.1 The yield of sRAGE using the previously developed AEC protocol

The original AEC protocol (Webster and Mulcair pers. Comm.) used a 10 mL MT 20 column (Bio-scale[TM] MT High Resolution Empty Column; Bio-Rad) packed with Q-Sepharose (GE Healthcare) attached to a FPLC system (ÄKTA, GE Healthcare). Repeating this protocol in two independent experiments, in the present study, resulted in low yields of purified sRAGE (Table 2.1). Analysis of all the fractions collected, including the pre-TSP fraction (prior to centrifugation) and the TSP fraction (after centrifugation), using sandwich ELISA, indicated that in Experiment 1, where ~100 g of hairy roots was used in the extraction, the pre-TSP fraction contained 1670 µg of sRAGE (Table 2.1). When this pre-TSP fraction was subjected to centrifugation, the resultant TSP fraction contained only 946 µg of sRAGE, with 724 µg (43 %) of sRAGE lost. A further, 900 µg of sRAGE was lost within the column resulting in only 21 µg of purified sRAGE collectively in eluent one (E1) and eluent two (E2). In Experiment 2, half the amount of hairy roots (50 g) was used in the extraction, resulting in 598 µg of sRAGE detected in the pre-TSP fraction. Centrifugation again resulted in a loss of approximately 40 % of sRAGE and again following AEC purification the majority of sRAGE was lost in the column, with only 15 µg of purified sRAGE obtained from Experiment 2. The 21 µg and 15 µg of sRAGE observed in the pooled E1 and E2 in experiment 1 and 2, respectively, was very low compared to the yield of sRAGE (~300 µg purified sRAGE) reported by Webster and Mulcair (pers. comm.). It is possible that the protein extracts contained impurities that resulted in binding or blocking of the column, therefore, to optimise the

protocol and increase the yield of sRAGE, the protein extraction and purification procedures were modified.

Table 2.1 Yield of sRAGE (μg) in AEC purification steps based on quantification by ELISA.

Fractions	Experiment 1		Experiment 2	
	sRAGE (μg)	Yield lost (%)	sRAGE (μg)	Yield lost (%)
Pre-TSP (prior to centrifugation)	1670	Centrifugation = 43	598	Centrifugation = 40
Tsp (Pre-TSP fraction after centrifugation)	946		362	
Anion-exchange chromatography (AEC) values				
Flow-through	12	Within the column = 95	40	Within the column = 83
Wash	3		8	
E1 (50mM Tris/0.2M NaCl)	**17**		**13**	
E2 (50mM Tris/0.4M NaCl)	**4**		**2**	
Weight of hairy roots used	~100 g		~50 g	

2.3.2 The yield of sRAGE with the modified protein clarification protocol

The low yield of sRAGE obtained using the method of Webster and Mulcair suggested that this previously developed extraction and AEC protocol was not ideal. Therefore, it was decided to optimise the protocol to enhance the yield of sRAGE by changing various variables.

2.3.2.1 Clarification of the pre-TSP fraction using Whatman no. 1 filters and 0.2 μm filters

To minimise the loss of sRAGE observed during centrifugation, alternative filtration methods were used to clarify the pre-TSP fraction; Whatman no.1 filter papers and 0.2 μm Nalgene™ 25 mm Syringe filters (Thermo Scientific). Whatman no.1 filter papers were shown to be incapable of filtering larger volumes of hairy root extracts. Similarly, the 0.2 μm Nalgene™ 25 mm Syringe filters did not clarify the pre-TSP fraction. In both cases this is due to clogging of the filters with solid particles and other cell debris.

2.3.2.2 *Changing the centrifugation force and/or length of the time*

To understand the effect of centrifugation force on sRAGE recovery, different centrifugation forces were applied for different time periods. Centrifugation speeds of 8,000 g and 10,000 g were applied for 5 minutes, 15 minutes, 30 minutes and 45 minutes compared to the original centrifugation force of 10,000 g for 45 minutes. The amounts of sRAGE present before centrifugation (pre-TSP fraction) and after centrifugation (TSP fraction) of the protein extraction were calculated using ELISA and these values were used to calculate the average percentage recovery of sRAGE (Figure 2.3).
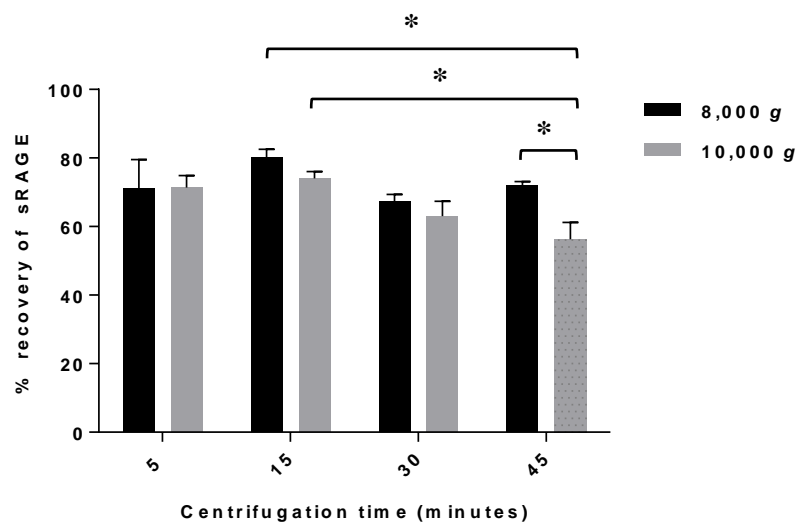
Figure 2.3 Effect of centrifugation force and time on percentage recovery of sRAGE. Error bars show the standard error of mean values (n=3). sRAGE values from the modified centrifugation conditions were compared to the total yield seen in the centrifugation conditions for the original protocol (10,000 *g* for 45 minutes). Significance is denoted by an asterisk (*P<0.05, by *t*-test).

When the pre-TSP fraction was centrifuged using the original centrifugation force of 10,000 g for 45 minutes, 56 % of sRAGE was recovered relative to the amount prior to centrifugation. However, a lower centrifugation force (8,000 g) generated a higher percentage of sRAGE recovery, for all centrifugation times, except at 5 minutes, where equal percentage recovery of sRAGE was observed for both the forces (Figure 2.3). These results suggest that, 10,000 g force has an adverse effect on the recovery of sRAGE compared to 8,000 g force.

The length of centrifugation time is also important. A higher percentage of sRAGE recovery was observed at 15 minutes for both the 10,000 g and 8,000 g force. When the centrifugation time was increased to 30 minutes, the percentage of recovery decreased for both speeds. However, at 45 minutes percentage yield dropped significantly for 10,000 g only. Therefore, 8,000 g for 15 minutes was selected as the best conditions for centrifuge to clarify the pre-TSP fraction as this had the highest percentage recovery of sRAGE (80 %).

2.3.3 Changing the protein extraction buffer and anion-exchange column variables

To reduce the 95/83 % loss (Experiment 1 and 2, respectively) of sRAGE within the column (Table 2.1), several variables were modified prior to running the samples on the anion-exchange column. This included changing the components of the protein extraction buffer (addition of EDTA, PVPP and reduction of Triton X-100), the addition of dialysis steps and the concentration of the TSP fraction, and changing the pH of the extraction buffer and the AEC purification buffer.

2.3.3.1 Adding EDTA to the extraction buffer

The addition of 20 mM EDTA increased the yield of sRAGE in the pre-TSP fraction. The yield of sRAGE was 5.3 µg in the pre-TSP fraction from ~0.5 g of hairy roots extracted with EDTA, whilst the sRAGE present in the pre-TSP fraction in the absence of EDTA was found to be 3.3 µg (Figure 2.4).
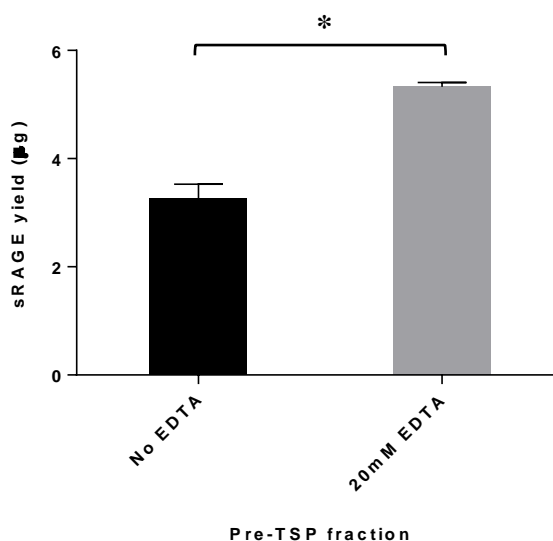
Figure 2.4 Yield of sRAGE (µg) present in the pre-TSP fraction in the presence and absence of EDTA based on quantification by ELISA. Error bars show the standard error of mean values (n=3). Significantly different sRAGE (µg) compared to the control (no EDTA) is denoted by an asterisk (* P<0.05 by *t*-test).

The TSP fraction of an extraction from ~15 g of hairy roots was loaded onto the anion-exchange column, to determine the effect of EDTA on AEC purification and subsequent recovery of yield. The total recovery of sRAGE (%) after anion-exchange purification was higher when EDTA was included (9.3 %) than the experiment without any EDTA (6.25 %), in the extraction buffer (Table 2.2). However, in both the experiments, more than 75 % of the loaded sRAGE (No-EDTA =189 µg of sRAGE and EDTA added =173 µg of sRAGE) was lost in the flow-through rather than retained on the column.

Table 2.2 Yield of sRAGE (µg) in AEC purification steps, with added EDTA in the extraction buffer, based on quantification by ELISA.

Fractions	No EDTA	EDTA
	sRAGE yield (µg)	
Pre-TSP	263	230
TSP	248	211
Flow-through	**189**	**173**
Wash	9	8
E1 (50 mM Tris/0.2 M NaCl)	13.5	18.4
E2 (50 mM Tris/0.4 M NaCl)	2	1.3
Pooled E3, E4 and E5 (50 mM Tris/0.6 M to 1 M NaCl)	2	1.3
	sRAGE (%)	
Total % recovery of sRAGE	**6.25**	**9.3**
Weight of hairy roots used = ~15 g		

2.3.3.2 The yield of sRAGE with added PVPP in the extraction buffer

With the addition of PVPP, the yield of sRAGE (~0.5 g of hairy roots) was significantly increased in the pre-TSP from 5.25 µg to 7.23 µg (Figure 2.5), as quantified by ELISA. However, when this modification was used on a larger scale (~15 g of hairy roots) and also purified by AEC, this yield improvement due to addition of PVPP was not observed (Table 2.3). The overall total percentage recovery of sRAGE from ~15 g of hairy roots, quantified by ELISA, was found to be low (2.85 %) with added PVPP. The percentage recovery was comparatively higher when PVPP was excluded (6.25 %) (Table 2.3). The addition of PVPP increased the yield of sRAGE in the pre-TSP fraction from 263 µg to 343 µg. The total yield also increased in the TSP fraction from 248 µg to 333 µg. However, loss of sRAGE in the flow-through increased from 189 µg to 242 µg with added PVPP (Table 2.3). Overall, more than 70 % of sRAGE loaded onto the column was lost in the flow-through, regardless of the presence or absence of PVPP in the extraction buffer and

the overall sRAGE yield with PVPP was much lower than that obtained if PVPP was not added (Table 2.3).
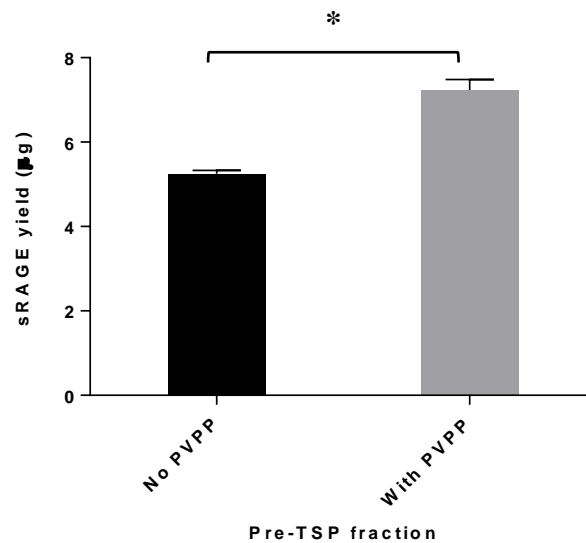
Figure 2.5 Yield of sRAGE (µg) present in the pre-TSP in the presence and absence of PVPP in the extraction buffer, based on quantification by ELISA. Error bars show the standard error of mean values (n=3). Significant difference in sRAGE (µg) yield with PVPP compared to the control (No PVPP) is denoted by an asterisk (P<0.05 by *t*-test).

Table 2.3 Yield of sRAGE (µg) in AEC purification steps, with added PVPP in the extraction buffer, based on quantification by ELISA.

Fractions	No PVPP	PVPP
	sRAGE yield (µg)	
Pre-TSP	263	343
TSP	248	333
Flow-through	189	242
Wash	9	17.5
E1 (50 mM Tris/0.2 M NaCl)	13.5	7
E2 (50 mM Tris/0.4 M NaCl)	2	2.5
Pooled E3, E4 and E5 (50 mM Tris/0.6 M to 1 M NaCl)	2	0.8
	sRAGE (%)	
Total % recovery of sRAGE	**6.25**	**2.85**
Weight of hairy roots used = ~15 g		

2.3.3.3 The yield of sRAGE with lower concentration of Triton X-100

The yield of sRAGE in the TSP fraction was found to be 190 µg when 0.05 % Triton X-100 was added to the extraction buffer (Table 2.4). Loss of sRAGE in the flow-through and the wash fractions was collectively reduced to 31 %. Eighty one micrograms of sRAGE was recovered in total from E1 and E2, which equates to 43 % overall recovery of sRAGE. This yield (81 µg of sRAGE from ~15 g of hairy roots) is proportionally higher than that obtained by Webster and Mulcair (pers. comm.; ~300 µg of sRAGE from ~100 g of hairy roots.

Table 2.4 Yield of sRAGE in AEC purification steps with added 0.05 % Triton X-100 in the extraction buffer, based on quantification by ELISA.

Fractions	Triton X-100 (0.1 %)	Triton X-100 (0.05 %)
	sRAGE yield (µg)	
Pre-TSP	263	253
TSP	248	190
Flow-through	189	30
Wash	9	28
E1 (50 mM Tris/0.2 M NaCl)	13.5	59
E2 (50 mM Tris/0.4 M NaCl)	2	22
Pooled E3, E4 and E5 (50 mM Tris/0.6 M to 1 M NaCl)	2	3
	sRAGE (%)	
Total % recovery of sRAGE	**6.25**	**43**
Weight of hairy roots used = ~15 g		

2.3.3.4 The yield of sRAGE with change of pH of the extraction buffer and AEC purification buffer

When, the pH of the hairy root protein extraction buffer and AEC purification buffer was reduced to 8.6, a total of 149 µg (88.7%) of sRAGE was lost in the flow-through and wash fractions. A lower yield of sRAGE (4.5 µg; 2.7 % recovery) was obtained from E1 and E2 (Table 2.5). Thus, lowering the pH of the extraction buffer and AEC purification buffer was not effective in improving the recovery of sRAGE.

Table 2.5 Yield of sRAGE (µg) in AEC purification steps, with change of pH of extraction buffer and AEC purification buffer, based on quantification by ELISA.

Fractions	sRAGE (µg)	% of sRAGE in fraction
Pre-TSP	181	
TSP	168	93
Flow-through	126	88.7
Wash	23	
E1 (50 mM Tris/0.2 M NaCl)	3.5	**2.7**
E2 (50 mM Tris/0.4 M NaCl)	1	
Pooled E3, E4 and E5 (50 mM Tris/0.6 M to 1 M NaCl)	1	
Weight of hairy roots used = ~15 g		

2.3.3.5 The yield of sRAGE with dialysis, concentration and centrifugation of the TSP fraction

Dialysis, concentration and centrifugation of the TSP fraction before loading the sample onto the anion-exchange column resulted in a total yield of sRAGE of 17 µg (16.8 % total recovery) (Table 2.6). However, a high percentage of sRAGE (70 %) was still lost in the flow-through and the wash (Table 2.6).

Table 2.6 Yield of sRAGE (µg) in AEC purification steps, when dialysed, concentrated and centrifuged TSP fraction loaded based on quantification by ELISA.

Fractions	sRAGE (µg)	% of sRAGE in fraction
Pre-TSP	110	
TSP	101	92
Flow-through	59	
Wash	11	**70**
E1 (50 mM Tris/0.2 M NaCl)	14	
E2 (50 mM Tris/0.4 M NaCl)	3	16.8
Pooled E3, E4 and E5 (50 mM Tris/0.6 M to 1 M NaCl)	1.2	
Weight of hairy roots used = ~15g		

2.3.4 Large scale sRAGE purification using the modified AEC protocol

Results from the above experiments show that reducing the Triton X-100 to 0.05 % in the protein extraction buffer, and the addition of dialysis, centrifugation and concentration of the TSP fraction, using the 50 mL Amicon 10,000 MWCO concentrators (Merck Millipore), result in higher yields of sRAGE. The protein extraction and AEC protocol developed by Webster and Mulcair (pers. comm.) was therefore modified to include these steps. Anion-exchange column purification was carried out using TSP extracted from ~100 g of hairy roots following this modified protocol in order to verify that the improved yield could be replicated in large scale protein extraction and purification.

The TSP fraction (~300 mL) contained 861 µg of sRAGE, 653 µg (corresponding to 76 % recovery) was present after dialysis, and 449 µg of sRAGE was obtained after concentration (Table 2.7). sRAGE (449 µg) was loaded onto the anion-exchange column and the protein was predominantly eluted in E1 and E2 resulting in 399 µg of sRAGE (Table 2.7). A small amount (10 µg) of sRAGE was obtained from eluents 3 and 4 (E3 and E4). A total of 125 µg sRAGE was lost in the flow-through and wash. Overall ~46 % (from E1 and E2) of sRAGE was recovered after AEC purification with these

modifications. This is a 19 fold increase on the original protocol (Table 2.7). In subsequent purifications, similar yields of sRAGE were obtained, with an average of 414 µg of sRAGE (E1 and E2 collectively; corresponding to ~41 % recovery) was recovered after AEC purification in three independent experiments (Figure 2.6).

Table 2.7 Yield of sRAGE in large scale purification with modified AEC protocol.

Fractions	Original protocol sRAGE (µg)	% of sRAGE in fraction	Optimised protocol sRAGE (µg)	% of RAGE in fraction
TSP	946		861	
TSP after dialysis	-		653	76
Dialysed fraction after concentration	-		449	
Flow-through	12	1.6	39	30
Wash	3		86	
E1 (50 mM Tris/0.2 M NaCl)	17	**2.2**	306	**46**
E2 (50 mM Tris/0.4 M NaCl)	4		93	
Pooled E3 and E4 (50 mM Tris/0.6 M to 0.8 M NaCl)	-		10	
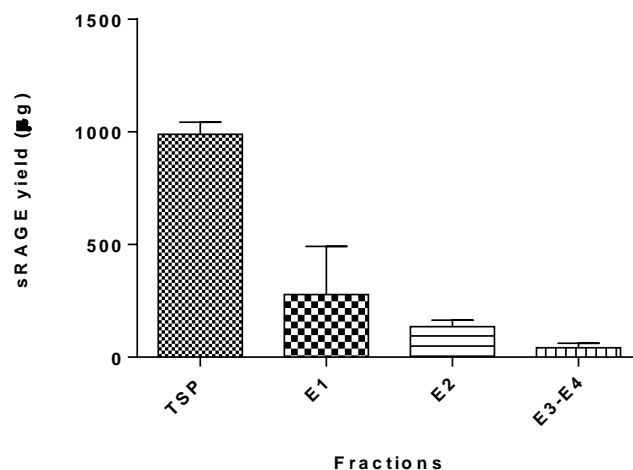
Figure 2.6 Yield of sRAGE (µg) in AEC purification steps based on quantification by ELISA (~100 g of hairy roots). TSP, clarified cell lysate extract with expressed sRAGE; E1 eluent 1; E2 eluent 2; E3-E4 pooled eluent 3 and 4. Error bars show the standard error of mean values (n=3).

2.3.4.1 SDS-PAGE and western blot analysis of plant-made sRAGE after AEC purification

To determine the purity and the molecular weight of the eluted proteins, the plant made sRAGE from the large scale modified AEC purification protocol was subjected to SDS-PAGE and fractions were visualised by Coomassie Brilliant Blue (Figure 2.7A). The five eluent fractions were individually concentrated and re-run on SDS-PAGE (Figure 2.7B). The pooled E1 and E2 fractions, and the E3 fraction following AEC (Panel A) were analysed by western blotting to confirm the molecular weight and the authenticity of sRAGE (Figure 2.8). The positive control (human sRAGE Fc Chimera (R & D System)) and a negative control (protein extracted from hairy roots not expressing sRAGE) were also included on the western blot.

A
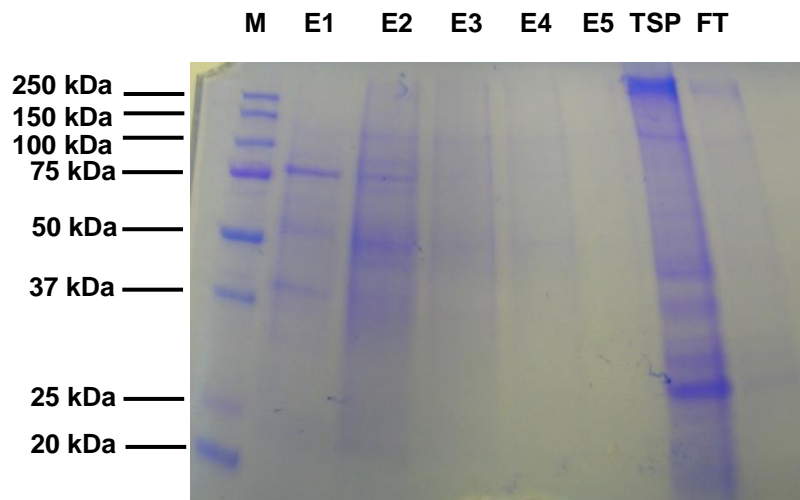
B
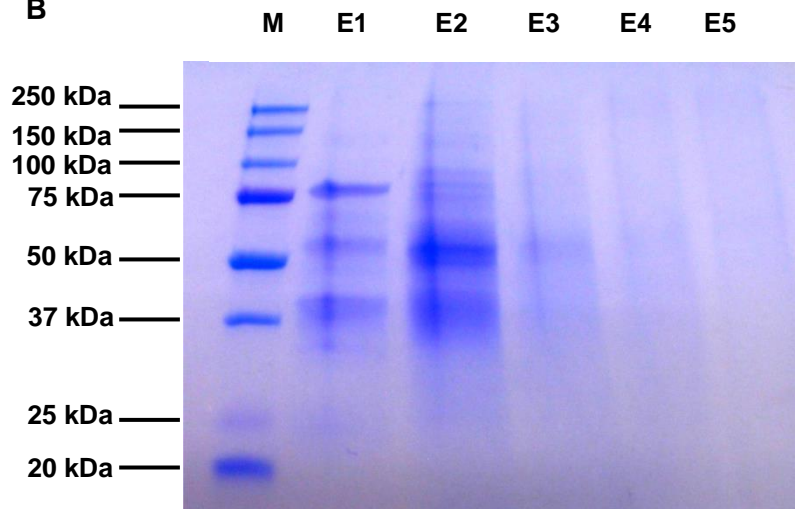
Figure 2.7 SDS-PAGE to visualise the plant-made sRAGE proteins purified by the modified protein extraction and AEC purification method. A. Lane M, protein molecular mass markers (kDa); E1 eluent 1; E2 eluent 2; E3 eluent 3; E4 eluent 4; E5 eluent 5 (eluents are not concentrated); TSP loaded onto the anion-exchange column; FT flow-through. B. Lane M, protein molecular mass markers (kDa); E1 eluent 1; E2 eluent 2; E3 eluent 3; E4 eluent 4; E5 eluent 5 (each eluent concentrated up to 0.5mL). The proteins were visualised with Coomassie Brilliant Blue.
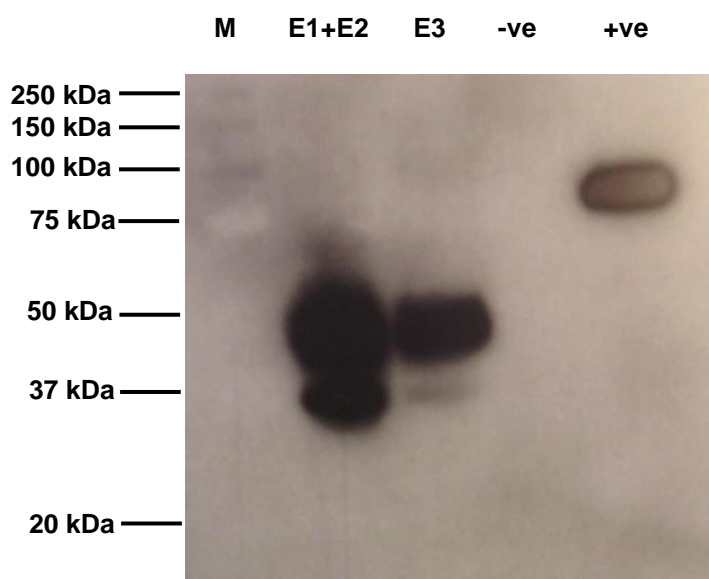
Figure 2.8 Western blotting using sRAGE antibodies to determine sRAGE presence and size after AEC purification. Lane M, protein molecular mass markers (kDa); E1+E2 pooled eluent 1 and eluent 2; E3 eluent 3; -ve negative control; +ve positive control. The protein molecular weight markers were visible on the western blot and were marked on the X-ray following alignment.

The sRAGE specific monoclonal antibody detected two bands in the pooled E1 and E2 (lane 1) at ~45 kDa and ~37 kDa and E3 contained a band of ~45 kDa and a faint band at ~37 kDa representing sRAGE (Figure 2.8). There were no bands observed for the negative control comprising proteins expressed by the hairy roots not expressing the sRAGE gene. Human sRAGE Fc Chimera (R & D system) was used as the positive control, and it was detected by the antibody as a ~80 kDa band, as expected.

2.3.5 Size-exclusion analysis of partially purified plant-made sRAGE

According to the results of the western blot (Figure 2.8), sRAGE appeared as ~45 kDa and ~37 kDa bands. Thus, bands other than ~45 kDa and ~37 kDa in the E1, E2 and E3 (Figure 2.7B) may have resulted from impurities. Therefore, AEC purified sRAGE (pooled E1 to E3) was further purified by size-exclusion chromatography (Figure 2.9) to remove these potential impurities.
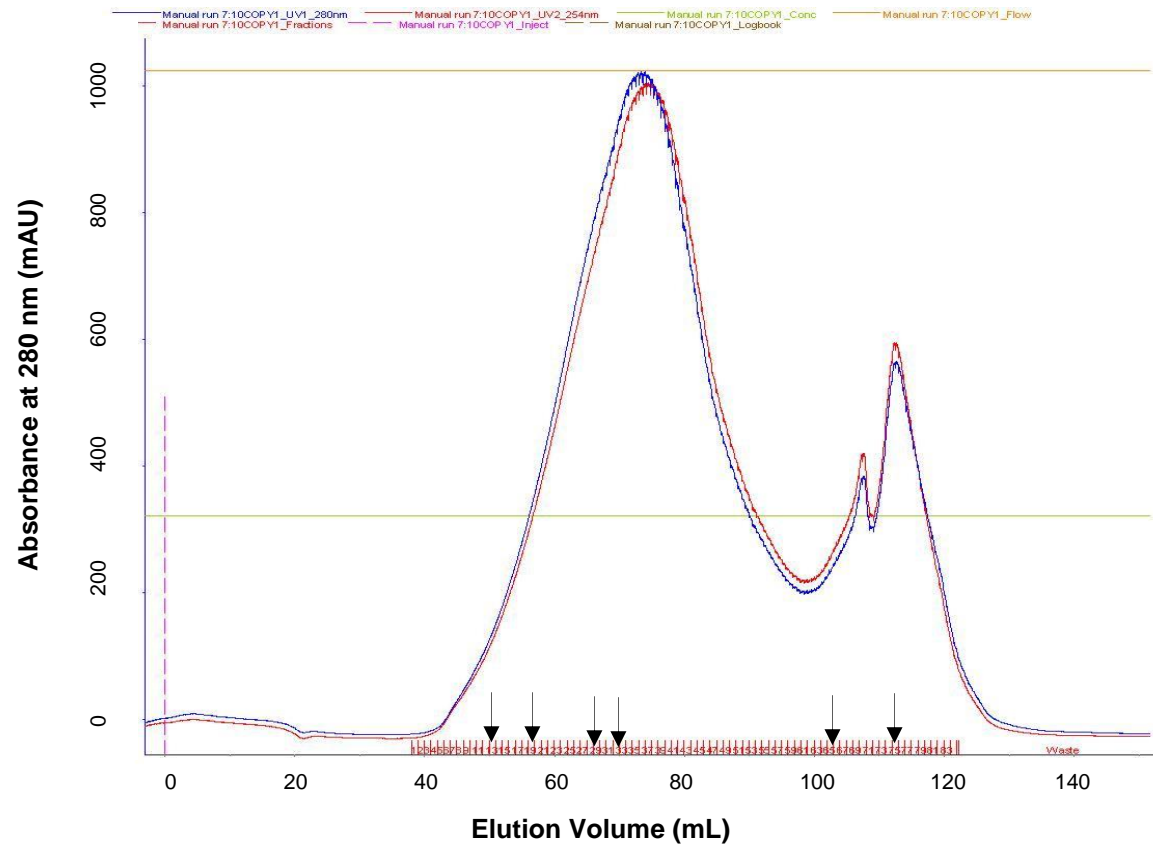
Figure 2.9 For size-exclusion chromatography, AEC purified sRAGE was applied to a Superdex 200 10/300 pre-packed column (GE Healthcare) and eluted with 50 mM Tris pH 9.0, 150 mM NaCl and 5 % glycerol at a rate of 1 mL min^{-1}. Protein elution was monitored by measuring absorbance at 280 nm, using an ÄKTA purifier FPLC system (GE Healthcare).

When AEC purified sRAGE was further purified by size-exclusion chromatography, one major peak starting from the fraction at ~53 mL and two other smaller peaks at ~105 mL fraction, ~115 mL fraction appeared in the resulting size-exclusion chromatogram (Figure 2.9). Five fractions, 53 mL, 59 mL, 61 mL, 69 mL and 73 mL, representing the major peak following size-exclusion chromatogram, as well as the 105 mL fraction, representing the smaller peak closest to the major peak of SEC chromatogram (Figure 2.9) were subjected to western blotting to determine the molecular weight and the authenticity of the protein.
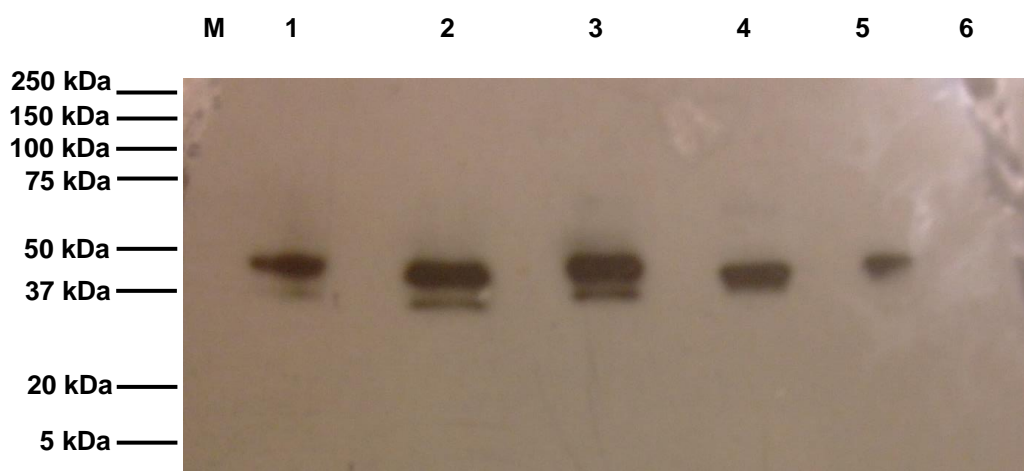
Figure 2.10 Western blotting using sRAGE antibodies to determine sRAGE presence and size after SEC purification. Lane M, protein molecular mass markers (kDa); lanes 1-6 different fractions based on the SEC chromatogram, lane 1, 53 mL; lane 2, 59 mL; lane 3, 61 mL; lane 4, 69 mL fraction; lane 5, 73 mL; lane 6, 105 mL. All these fractions were named according to the elution volume based on the size-exclusion chromatogram as shown in Figure 2.9. The location of the molecular weight markers were defined following alignment of the western blot and X-ray film.

The sRAGE specific antibody detected a band of ~45 kDa and a faint band at ~37 kDa in the 53 mL fraction (Figure 2.10, lane 1). These bands were also detected in the 59 mL and 61 mL fractions (lanes 2 and 3), where the ~37 kDa band was stronger. In the 69 mL and 73 mL fractions only the 45 kDa was detected by the antibody. This indicates that the major peak in the SEC chromatogram represents sRAGE protein. There were no bands observed in the 105 mL fraction and therefore, the peak observed for this fraction in SEC chromatogram (Figure 2.9) is likely to be an unrelated protein present as impurities.

The yield of size-exclusion purified sRAGE was found to be 324.6 µg (based on quantification by ELISA (see 2.2.5.2). This value is equal to ~80 % recovery of sRAGE relative to the amount of sRAGE loaded (~399 µg of sRAGE) onto the size-exclusion column.

2.3.6 sRAGE purification by Heparin Sepharose chromatography

Size-exclusion purified sRAGE was subjected to Heparin Sepharose column chromatography with the aim of obtaining highly purified (95 % purity) sRAGE. However, the Heparin Sepharose chromatogram did not show any peaks, clearly indicating that plant-made sRAGE does not bind to the Heparin Sepharose column (Figure 2.11). SDS-PAGE analysis of the fractions from the Heparin Sepharose column further verified that sRAGE did not bind to the column, with proteins only visible in the flow-through and wash fractions (data not shown).
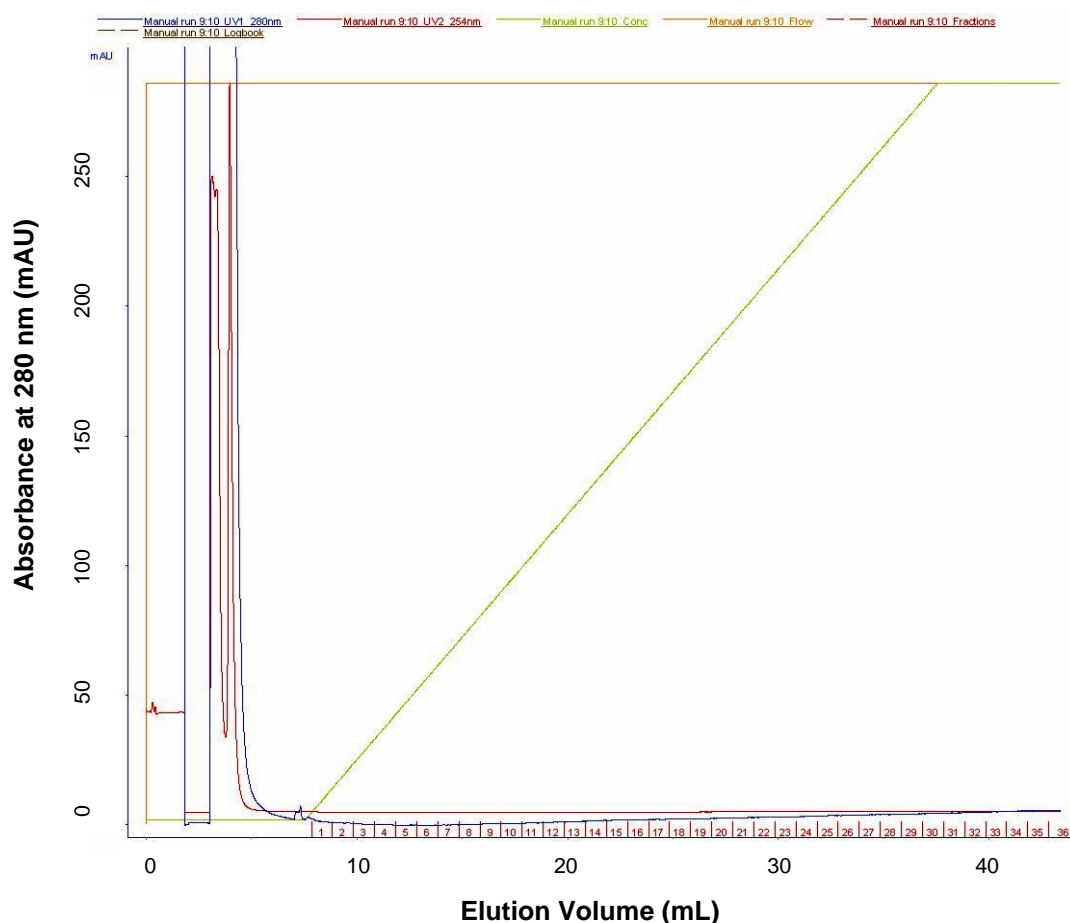
Figure 2.11 For Heparin Sepharose chromatography, SEC purified sRAGE was applied to a 1 mL HiTrap^{TM} Heparin column (GE Healthcare) and eluted with PBS pH 7.4, 1 M NaCl, 5 % glycerol and 0.1 mM PMSF at a rate of 0.5 mL min⁻¹. Protein elution is monitored by measuring absorbance at 280 nm, using an ÄKTA purifier FPLC system (GE Healthcare).

2.3.7 *Immobilized metal affinity chromatography purification*

An Immobilized Metal Affinity Chromatography (IMAC) method was used to further purify the sRAGE after SEC. The construct used to develop hairy root cultures of *N. tabacum* contained an eight histidine-Tag in its C-terminal end to allow purification of the protein by IMAC-based purification. When 102 µg of SEC purified sRAGE was subjected to IMAC-based purification, the majority of the sRAGE failed to bind to the resin and was present in the flow-through and wash. A low yield of sRAGE (6.7 µg) was recovered collectively from E1 and E2 (Table 2.8), representing 6.4 % recovery of sRAGE. This result supports the findings of Webster and Mulcair (pers. comm.) that sRAGE does not bind to Ni-NTA resin under these conditions.

Table 2.9 Yield of sRAGE (µg) in IMAC purification steps based on quantification by ELISA.

Fractions	sRAGE (µg)	% recovery of sRAGE
Amount of SEC purified sRAGE loaded to the IMAC	102	
Flow-through	75	
Wash	20.3	
E1	4.7	6.4
E2	2	

2.4 DISCUSSION

An optimised extraction protocol was developed in this study for the expression, purification and characterisation of plant-based sRAGE. This was required as the protocol developed by Webster and Mulcair (pers. comm.) could not be replicated by Mulcair or in the studies detailed here.

2.4.1 Optimisation of protein extraction and anion-exchange chromatography protocols

Using the original method developed by Webster and Mulcair (pers. comm.), 43 % and 40 % of sRAGE was lost during centrifugation and another 95 % and 83 %, for repeat experiments 1 and 2, respectively of loaded sRAGE was lost within the anion-exchange column (Table 2.1). The lost protein (95 % and 83 %) was not observed either in the flow-through or in the wash. It is possible that this low yield could have resulted from poor binding of the protein to the resin. When protein is not strongly bound to the resin, large amounts of protein should be present in the flow-through or wash. However, the flow-through contained only 12 µg and 40 µg of sRAGE, and wash contained 3 µg and 8 µg of sRAGE, which is a low value compared to 946 µg and 362 µg of sRAGE loaded onto the anion-exchange column in experiments 1 and 2, respectively. Alternative reasons for the low yield may be protein aggregation and multimeric-formation or strong protein binding to the resin. Multimeric forms of proteins and aggregates tend to be retained within the column due to the larger size of the molecules (Nybo, 2010) and this may have been the cause of the sRAGE retained within the column. Aggregates appear to be irreversible,

with very slow rates of disaggregation and the equilibrium favours the formation of aggregates rather than the formation of soluble monomeric forms (Schrodel & de Marco, 2005). Protein aggregates or the formation of larger structures often cause problems with the loss of the functionality/activity of the proteins. In the present study biologically active sRAGE was needed to perform *in vitro* ligand binding studies, therefore, the presence of protein aggregates was not tested and alternatively, the protein extraction buffer and the AEC purification protocol were modified to obtain soluble biologically active sRAGE.

Adjusting the buffer conditions, such as ionic strength, pH, and additives help in maintaining the stability and the subsequent elution of the protein from the column (Ritchie, 2012). The ionic strength of the elution buffer was increased to 1 M NaCl but this had no effect on the amount of sRAGE present in the elution fractions (E1-E5; Table 2.2). Therefore, the protein extraction and purification protocol was manipulated and several parameters changed individually, and the yield of sRAGE assessed for each.

It is necessary to clarify the pre-TSP fraction before loading onto the anion-exchange column for protein purification, therefore different centrifugation speeds and times were tested to optimise this step. Centrifugation is important to remove lipids and remaining particulate matter, such as cell debris from the pre-TSP, however, using the original conditions 43 % or 40 % of sRAGE was lost during centrifugation (Table 2.1). It was found that a reduced centrifugation force (8,000 *g*) and a shorter centrifugation time of 15 minutes was optimal, compared to the original protocol of a centrifugation force of 10,000 *g* for 45 minutes. These conditions resulted in ~80 % recovery of sRAGE (Figure 2.3) and this condition was used throughout the study.

The loss of sRAGE within the column was addressed by changing protein extraction and purification variables. First, the protein extraction buffer was modified by adding EDTA. EDTA reduces damages caused by oxidation to the proteins. Addition of EDTA is beneficial because oxidative changes to proteins can result in diverse functional consequences, such as inhibition of binding activities, increased susceptibility to aggregation and proteolysis (reviewed by Shacter, 2000). The yield of sRAGE in the TSP fraction was not increased when 20 mM EDTA was included in the extraction buffer and a relatively higher proportion of sRAGE (82 %) was lost in the flow-through from the anion-exchange column (Table 2.2) in the presence of EDTA. However, a high

percentage of sRAGE was lost in the flow-through (76 %) in the absence of EDTA as well. Therefore, this yield loss may have not be related to the addition of EDTA to the protein extraction buffer.

It was observed that the AEC column was discoloured following purification of the total soluble fraction and it is possible that this is due to the presence of phenolic compounds. Phenolic compounds are the most common secondary metabolites present in plant extracts that can affect both the protein extraction and the purification by anion-exchange chromatography (Wang *et al.*, 2008). In addition, lipoproteins and other lipid material can rapidly clog chromatography columns and it is advisable to remove them before beginning purification (Ward & Swiatek, 2009). To address this, polyvinylpolypyrrolidone (PVPP) was added to the protein extraction buffer to remove any phenolic compounds, lipoproteins and other lipid materials present in the extraction from the hairy roots. Addition of PVPP in the extraction buffer facilitates the formation of a precipitate resulting from hydrogen bonding between phenolics/lipoproteins and PVPP, which can be easily removed by centrifugation (Dash, 2013). This is a convenient method of eliminating troublesome phenolic compounds/lipoproteins during protein purification.

When PVPP was added to the extraction buffer 97 % of sRAGE was recovered in the TSP fraction (333 µg of sRAGE was recovered in the TSP out of 343 µg in pre-TSP, Table 2.3). This is similar to findings of Sharp & Doran (2001), who extracted a complete mouse IgG1 antibody from tobacco tissue cultures by using a polyvinylpolypyrrolidone (PVPP) and ascorbate based protein extraction buffer to remove phenolics and quinone. This extraction procedure was based on the method of Cremer and van de Walle (1985) and did not affect the yield of IgG1 (antibody concentrations as a percentage of total soluble protein was 2.4 ± 0.035 in the hairy roots) or the pattern of antibody bands observed. However, the yield of sRAGE after anion-exchange purification was not increased with the addition of PVPP. Quantification based on ELISA showed that a large amount of sRAGE was still lost in the flow-through (242 µg, 73 % of loss, Table 2.3) when PVPP was added. It was observed that the AEC column was not discoloured following addition of the PVPP but it did not result in an increase in protein binding to the resin. It is possible that a certain amount of PVPP may have been retained in the protein extract, preventing the binding of sRAGE to the Q-Sepharose resin. However, this seems unlikely as the addition of 50 mg mL^{-1} of PVPP in the extraction buffer to extract

Glutathione S-Transferase from Benoxacor-treated maize (*Zea mays*) has not been reported to have any detrimental effect when purified by AEC purification method (Irzyk & Fuerst, 1993). Similarly, addition of 1 % PVPP in the extraction buffer to extract membrane-bound peroxidase from date palm leaves (*Phoenix dactylifera* L.) did not result in any interference of PVPP in AEC and SEC purification protocols (Al-Senaidy, 2011). RuBisCO of higher land plants and the green macro alga were also successfully purified by AEC in the presence of 2 % PVPP in the extraction buffer (Uemura *et al*., 1996). The possible prevention of sRAGE binding to Q-Sepharose by PVPP has to be verified empirically in future studies. The protein yield was improved with the addition of PVPP but not the protein binding to the column. PVPP was not added to the extraction buffer to improve the recovery of sRAGE in AEC purification, considering the huge loss of sRAGE (73 %) in the flow-through.

The protein extraction buffer was also modified by changing the concentration of Triton X-100 from 0.1 % to 0.05 %. Triton X-100 was used in the original extraction buffer as a detergent as, importantly, it assists in the disruption of cellular membranes releasing more proteins (Gilbert *et al*., 2006). It also allows dispersion of water insoluble molecules, such as membrane proteins, into the aqueous medium by facilitating extraction and solubilisation (Hjelmeland & Chrambach, 1984; Koley & Bard, 2010; Thomas & McNamee, 1990). These factors are likely to increase the amount of TSP extracted. However, membrane proteins can be either modified or inactivated by detergent solubilisation due to the integrity of native lipid interactions being disturbed (Bowie, 2001; Garavito & Ferguson-Miller, 2001; Gohon & Popot, 2003). Thus, removal of detergents is important. Detergents like Triton X-100 have low critical micelle concentration and large aggregation numbers (140) (Maire *et al*., 1989). The micelles formed from these detergent molecules are too large to diffuse through the dialysis membranes and are therefore non-dialysable (Smith & Morrissey, 2004). Considering the non-dialysable property of Triton X-100, a lower concentration (0.05 % compared to 0.1 % in the original protocol) was utilised to determine the effect of 0.05 % Triton X-100 on the yield of sRAGE. It was found that the lower concentration of Triton X-100 markedly improved the yield of sRAGE after anion-exchange purification (43 % recovery, Table 2.4).

In the case of proteins, which are built up of many different amino acids containing weak acidic and basic groups, the net surface charge of proteins change gradually as the pH of the environment changes and therefore, proteins are said to be amphoteric (Fortis *et al*.,

2005). The pH at which a particular protein carries no net electrical charge is known as its isoelectric point (pI). At a pH above its isoelectric point, a protein will bind to a positively charged medium or anion-exchanger. Therefore, pH of the start buffer should be at least 1 pH unit above the pI of the target substance when using an anion-exchanger (Lampson & Tytell 1965). We used sodium ascorbate based protocol to extract sRAGE which is acidic; however, considering the pI of sRAGE (7.6), the final pH of the buffer was adjusted to 9.0. This pH adjustment is not only important to facilitate the binding of sRAGE to anion-exchange resin but is also important for the maintenance of the stability and activity of the protein considering the amino acid composition of sRAGE. sRAGE consists of 6 cysteine residues in total, 2 cysteine residues per domain, V, C1 and C2 (Appendix I). Cysteine has the ability to form disulfide bonds and therefore, plays a crucial role in protein-folding, which is important for protein structure (Fass, 2012; Walker *et al*., 1996). Under acidic conditions, these disulphide bonds of sRAGE can scramble and rearrange. Thus, theoretically, scrambling and rearranging of disulphide bonds of sRAGE should not occur under this basic pH (pH 9.0) condition.

Being an antioxidant, sodium ascorbate prevents the extraction buffer and extracted proteins from reacting with atmospheric oxygen (Guzman *et al*., 2011). Using sodium ascorbate rather than ascorbic acid is recommended because it does not change the pH of the buffer (Guzman *et al*., 2011). However, the amount of extracellular reducing agents such as ascorbate and thioredoxin affect spatial and temporal fluctuations with consequent effects on protein disulphide bonding (Trivedi *et al*., 2009). Nevertheless, reduction of disulphides of sRAGE by sodium ascorbate has not been investigated.

The pH of the Tris buffer changed from 9.0 to 8.6, to maintain the pH of the extraction buffer within one unit difference of the pI of sRAGE (7.6). The experimental data showed that lowering the pH of the extraction buffer did not generate an improved yield of sRAGE after anion-exchange purification (recovery of sRAGE was 2.7 % and 88.7 % of sRAGE was lost in the flow-through) (Table 2.5). It is possible that this lowering of the pH causes protein molecules to become more protonated during anion-exchange column purification. Therefore, protein interactions are not as strong with the positively charged resin and elute more easily from the column. Considering the loss of sRAGE in the flow-through following the decrease in the pH of the Tris buffer, this is not likely to be of benefit to sRAGE purification by anion-exchange chromatography method.

The TSP fraction was subjected to overnight dialysis to exchange the protein extract to the AEC purification buffer; 50 mM Tris, pH 9.0 at 4 ℃ (ideally, samples should be in the same conditions as the start buffer) and then concentrated and centrifuged at 4,000 g for 10 minutes before being loaded onto the anion-exchange column. With these modifications 16.8 % of sRAGE (Table 2.6) was recovered and it is a substantial improvement considering the previous % recovery of sRAGE (9.3 % recovery, Table 2.2 and 6.25 % recovery, Table 2.3).

From these results specific steps were included to optimise the protein extraction and AEC purification protocol; changes to centrifugation, from 10,000 g to 8,000 g for 15 min; modification of the sRAGE extraction buffer by reducing Triton X-100 from 0.1 % to 0.05 % (43 % recovery of sRAGE after AEC purification, Table 2.4); and overnight dialysis of the TSP fraction in the presence of 50 mM Tris, pH 9.0 at 4 ℃, followed by concentration using 15 mL Amicon 10,000 MWCO concentrators (Merck Millipore) and centrifugation for 10 minutes at 4,000 g. This modified protocol (Figure 2.12) was used throughout the study to purify sRAGE from hairy roots. The increased yield of sRAGE obtained with this modified protocol was consistent when subsequent purification was carried out on a large scale using ~100 g of hairy roots (46 % recovery of sRAGE, Table 2.7 and an average of 41 % recovery across all subsequent extractions of sRAGE, Figure 2.6).

Figure 2.12 A comparison of the original and modified AEC purification protocol. The major steps that have been changed are highlighted in boldface type.

Original Protocol	Modified protocol
Extraction buffer: 50 mM Tris, pH 9.0, 100 mM sodium ascorbate, 0.1 % Triton X-100, protein inhibitors	Extraction buffer: 50 mM Tris, pH 9.0, 100 mM sodium ascorbate, **0.05 % Triton X-100**, protein inhibitors
Transfer the pre-TSP fraction to centrifuge tubes, balance and centrifuge at 10,000 *g* for 45 minutes	Transfer the pre-TSP fraction to centrifuge tubes, balance, and centrifuge at **8,000 *g* for 15 minutes**
Collect supernatant (TSP) and spin again, if solid material is present	Collect supernatant (TSP) and spin again, if solid material is present
	Overnight dialysis against 50 mM Tris, pH 9.0 at 4 ºC
	Concentrate the dialysed TSP fraction using 15 mL, Amicon 10,000 MWCO concentrators
	Centrifuge at 4,000 *g* for 10 minutes
Load the TSP fraction onto the anion-exchange column	Load the TSP fraction onto the anion-exchange column
SEC purification	SEC purification
	Purified sRAGE for further analysis

2.4.2 Characterisation and further purification of plant-made sRAGE

The calculated molecular weight of sRAGE is 34.5 kDa as determined by ExPASy-Compute pI/Mw tool (http://web.expasy.org/compute_pi/). The molecular weights of the visualised bands suggested that sRAGE protein existed predominantly in its monomeric form. This was similar to the observations of Webster and Mulcair (pers. comm.) after size-exclusion purification of sRAGE. However, the molecular weight of one of the band observed for sRAGE (~45 kDa) was higher than the calculated theoretical molecular weight of sRAGE whilst the second band appears nearly correct (~37 kDa) (Figure 2.10). The V-domain of sRAGE contains two potential *N*-glycosylation sites (Park *et al*., 2011) and, it was speculated that sRAGE will be *N*-glycosylated *in planta* (see chapter 4).

The difference between the plant-made sRAGE as determined by SDS-PAGE (~45 kDa) and calculated molecular weight of sRAGE (34.5 kDa) was similar to the findings of

Hanford *et al*. (2004). In an attempt to extract, characterise and describe a mechanism of synthesis of sRAGE extracted from mouse lung tissues, they observed a discrepancy between the mass of mouse sRAGE as determined by SDS-PAGE (~45 kDa) and mass spectroscopy of glycosylated native sRAGE (~36 kDa) (Hanford *et al*., 2004). It appeared that there was some residual structure of sRAGE after denaturation with SDS and reduction with Dithiothreitol, making sRAGE appear larger in SDS-PAGE (Hanford *et al*., 2004). It is possible that this could be the reason for plant-made sRAGE to appear as a ~45 kDa band in SDS-PAGE (see chapter 4).

The yield of sRAGE after anion-exchange chromatography, followed by size-exclusion chromatography was 324.6 µg from ~100 g of hairy roots. Therefore, it is estimated that approximately 3 mg of plant-made sRAGE can be harvested from 1 kg of hairy roots. Further purification steps were considered to obtain at least 95 % pure sRAGE to conduct structural studies. These include the use of Heparin Sepharose (GE Healthcare) and IMAC-based purification (Qiagen) systems. When sRAGE was purified using the Heparin Sepharose column (GE Healthcare), it was eluted in the flow-through and wash (data not shown) suggesting that the plant-made sRAGE could not bind to the resin. There is evidence to show that phenolic compounds present in plant extracts affect both the protein extraction and the purification by anion-exchange chromatography (Wang *et al*., 2008). Based on that evidence it is possible to speculate, that this would be true for Heparin Sepharose purification as well, but this needs to be verified empirically in future studies.

Immobilized Metal Affinity Chromatography (IMAC) purification was selected as an alternative method to test further purification of sRAGE, since the Heparin Sepharose method failed. The sRAGE protein expressed in the plant expression system was initially designed with a tag of eight histidine residues at the C-terminal end for IMAC-based purification. However, when the total soluble protein (containing 0.6 % sRAGE) was purified by IMAC-based system, as an initial step of purification, only 5 % of the loaded plant-made sRAGE was recovered by Webster and Mulcair (pers. comm.). Although the IMAC-based purification system was not successful as an initial purification step, it was thought that this method might work, after most of the plant proteins and other impurities were removed by anion-exchange and size-exclusion chromatography. However, when IMAC-based purification was applied at this later stage of purification, only 6.4 % of

sRAGE (Table 2.9) was recovered. This yield is comparable to that achieved when it was used as the first purification step. Although, there are eight histidine residues at the C-terminal of the sRAGE, it may have been sterically hindered in a manner that prevented the access of Ni-NTA resin (Magdeldin & Moser, 2012). Therefore, neither Heparin Sepharose (GE Healthcare) nor IMAC-based purification (Qiagen) was able to be used as a third step of purification to obtain highly purified (95 % purity) sRAGE.

2.5 CONCLUSION

This modified protein extraction and AEC/SEC protocol significantly increased the yield of sRAGE (Table 2.7 and Figure 2.6). This plant-made sRAGE was predominantly present in monomeric form according to the molecular weights (~45 kDa and ~37 kDa) as determined by western blot analysis after SEC purification (Figure 2.10). The sRAGE appeared to be glycosylated, which is important for protein function (Srikrishna *et al*., 2010; Srikrishna *et al*., 2002). In this study plant-made sRAGE was successfully expressed and purified in sufficient quantity, to conduct *in vitro* binding activity studies with ligands (see chapter 4).

CHAPTER 3

Characterisation of human sRAGE expressed in an *E. coli* expression system

3.1 INTRODUCTION

sRAGE was expressed in an *E. coli* expression system to obtain non-glycosylated sRAGE to conduct *in vitro* ligand binding assays and then to compare the results with the similar assays performed with plant-made glycosylated sRAGE. Recombinant human sRAGE has been commercially produced in *E. coli* (Aviscera Bioscience). However, the concentration (200 µg mL^{-1}) and the quantity (100 µL) of available *E. coli*-made sRAGE is not sufficient to conduct *in vitro* ligand binding assays, which require at least 0.5 mg mL^{-1} of sRAGE. Therefore, sRAGE was over-expressed in an *E. coli* expression system to obtain 4-5 mL of sRAGE in a concentration of at least 0.5 mg mL^{-1}, to perform the binding assays.

Commonly *E. coli* recombinant proteins are produced using Immobilized Metal Affinity Chromatography (IMAC)/His Tag-based purification method. However, previous experiments showed that this method does not work efficiently to purify plant-made sRAGE, therefore the Halo-Tag (Promega) system was selected here.

HaloTag® is engineered from a bacterial dehalogenase (34 kDa) and it has the ability to covalently immobilise with Halo-link™ resin (Promega). This covalent linkage facilitates stringent washing steps allowing better protein recovery and low non-specific contamination. HaloTag® has been shown to be better than other recognised tags, such as GST and MBP, in terms of its yield, solubility and purity for 23 expressed human proteins (Ohana *et al*., 2009). In contrast to other solubility tags, it is known to express "difficult to express" human proteins (Chumanov *et al*., 2011). Considering these advantages, HaloTag® (Promega) was chosen to express sRAGE in an *E. coli* expression system.

This chapter details the optimisation of the protein expression and purification protocols and the characterisation of *E. coli*-made sRAGE.

3.2 MATERIALS AND METHODS

3.2.1 Generation of the sRAGE product for cloning into pFN18K HaloTag® T7 Flexi® vector

To generate the sRAGE region for cloning into pFN18K HaloTag® T7 Flexi® vector, PCR was used to amplify the desired region from an ICONR construct previously prepared in the Webster laboratory. The ICONR construct contains the full-extracellular domain of human RAGE including the native signal peptide of the RAGE gene. The glycerol stock of the ICONR construct was streaked on a Luria-Bertani (LB) agar plate (Appendix III) supplemented with 100 µg mL^{-1} of carbenicillin (PhytoTechnology Laboratories) and grown overnight at 37 ℃. A fresh single colony was used to inoculate 5 mL of liquid LB supplemented with 100 µg mL^{-1} of carbenicillin (PhytoTechnology Laboratories®), and incubated overnight at 37 ℃. Plasmid DNA was purified using a HiYield™ Plasmid Mini Kit (Real Genomics), quantified and checked for purity by Nano drop (ND 1000 Spectrophotometer, Biolab) using the A_{260} and A_{280} ratio. Fifty nanograms of ICONR was used as the template to perform the PCR.

The proof-reading DNA polymerase, KOD Hot Start (EMD Biosciences, Inc.), was used to perform PCR (as per the manufacturer's instructions) in a 50 µL reaction volume. sRAGE gene specific forward and reverse primers, including restriction sites for subsequent cloning (Table 3.1) were designed using ApE (A Plasmid Editor; http://biologylabs.utah.edu/jorgensen/wayned/ape/), synthesised by Sigma and used at a final concentration of 0.2 µM. The region amplified was from amino acid Ala 23 to Gly 331, which excludes the N terminal signal sequence. MgCl$_2$ concentration was 1.5 mM. PCR conditions were as follows: 95 ℃ for 2 minutes, 30 cycles of 95 ℃ for 20 seconds, 60 ℃ for 10 seconds, and 72 ℃ for 15 seconds. PCR was carried out in an iCycler thermal cycler (Bio-Rad). The sRAGE PCR product was purified using a HiYield™ Gel/PCR DNA Fragments Extraction kit (Real Genomics) as per the manufacturer's instructions, checked by gel electrophoresis and confirmed by sequencing.

Table 3.1 Primers: HTFd and HTRev were used to generate Halo-R construct. The restriction enzymes *Nco*I and *Pme*I are underlined.

Name	Sequence	Tm (ºC)
HTFd	5'–ACAGTCCATGGCACAAAACATCACAGCCC	75
HTRev	5'–ACGTGTTTAAACTAACCTGCAGTTGGCCC	71

3.2.2 Ligation of the sRAGE PCR product into pFN18K HaloTag® T7 Flexi® vector to generate the sRAGE construct

The pFN18K HaloTag® T7 Flexi® vector (Promega) (complete sequence; http://www.ncbi.nlm.nih.gov/nuccore/EU545993) encodes an N-terminal HaloTag®, which forms covalent bonds with corresponding HaloTag® ligands, allowing the immobilisation of expressed proteins. TEV Protease cleaves the target protein from the HaloTag® protein, which is bound to the HaloLink™ resin. Genes downstream of the HaloTag® are the lethal barnase gene (Figure 3.1), for the positive selection of the presence of the insert and the *rrnB* transcription terminator, to prevent *in vivo E. coli* transcription of the insert. It is a high copy number vector with kanamycin resistance (30 µg mL^{-1}).
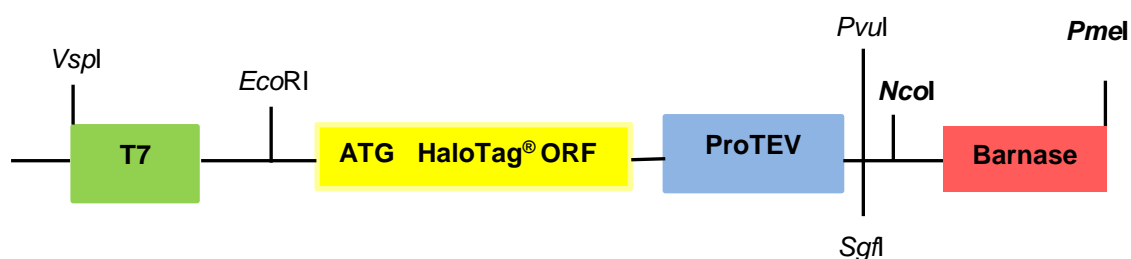
Figure 3.1 Sequence upstream and downstream of the HaloTag® gene. sRAGE gene is inserted between *Nco*I and *Pme*I restriction enzyme sites.

HaloTag Vector DNA and PCR products were digested under the conditions recommended by the manufacturer (New England Biolabs® Inc.), using the restriction enzymes *Nco*I and *Pme*I, with 0.1 mg of bovine serum albumin (BSA), for a minimum of 3 hours at 37°C. When these two enzymes are used for excision of the DNA fragments, sequential digestions need to be performed using a QIAquick PCR purification kit

(QIAGEN) to remove the buffers and the enzymes from the previous reaction. Digestion was confirmed by gel electrophoresis and purified DNA quantified by Nano drop (ND 1000 Spectrophotometer, Biolab). The sRAGE DNA fragment was ligated into the pFN18K HaloTag®T7 Flexi® vector system by incubating the digested PCR product (100 ng) and the vector (50 ng) for 1 hour, in the presence of T4 DNA Ligase (Promega) at room temperature, as per the Promega technical manual for Flexi® vector systems (product C8640).

3.2.3 Heat shock DNA transformation of *E. coli*-KRX strain

Single step *E. coli*-KRX competent cells supplied with the HaloTag® purification kit (Promega) were used to clone sRAGE as well as to express the resulting protein. Transformation was carried out using *E. coli*-KRX strains (Promega) in a single step.

Competent *E. coli*-KRX cells (Promega) were thawed on ice before the addition of DNA/ligation reaction mixture. The DNA and competent cells were incubated for 10 minutes on ice, heat shocked at 42 ℃ for 15 seconds and further incubated for 2 minutes on ice, then 450 µL of LB liquid medium was added. The mixture was incubated for 1 hour at 37 ℃ with shaking at 225 rpm. Cell mixtures were plated on LB agar supplemented with 30 µg mL^{-1} of kanamycin (Promega) and incubated overnight at 37 ℃.

3.2.4 PCR screening of the transformed bacterial colonies

Positive colonies containing the sRAGE were screened by PCR. Single colonies were suspended in 50 µL of Milli-Q water and, 1 µL was added to the PCR reaction containing Mango Taq™ DNA polymerase (Bioline) and the original primers used for cloning (Table 3.1). PCR was carried out in an iCycler thermal cycler (Bio-Rad) and products visualised by electrophoresis in 1.0 % agarose/TAE gel. PCR positive colonies were cultured overnight in 5 mL of LB liquid medium supplemented with 30 µg mL^{-1} of kanamycin (Promega). The sRAGE plasmid DNA was extracted using a QIAquick Spin Miniprep kit (QIAGEN), digested with the restriction endonucleases *Nco*I and *Pme*I and products were visualised by agarose gel electrophoresis to further verify the molecular size. The positive colonies were then stored as glycerol stocks at -80 ℃.

3.2.5 DNA Sequencing

Positive sRAGE constructs were sequenced to verify the presence and correct sequence of sRAGE by BigDye terminator cycle sequencing (Applied Biosystems) at the Micromon DNA sequencing facility (3730 Capillary Sequencer, Applied Biosystems) at Monash University. BigDye Premix (1 µL), 3.5 µL of 5X reaction buffer, template DNA (400 ng of double stranded DNA or 20 ng of PCR product), 5 pmoles of either forward or reverse primers and sterile Milli-Q water added to a volume of 20 µL. The cycle sequencing reaction was carried out as follows: 96 ºC for 1 minute, 30 cycles, 96 ºC for 10 seconds, 50 ºC for 5 seconds, 60 ºC for 4 minutes and 5 ºC for 2 minutes using an iCycler thermal cycler (Bio-Rad). Reactions were purified by sodium acetate/ethanol precipitation. The sodium acetate/ethanol solution was prepared by adding 3 µL of 3 M sodium acetate trihydrate (pH 5.2), 62.5 µL of 96 % (v/v) analytical grade ethanol and 14.5 µL of Milli-Q water. The sequencing reaction (20 µL) was added to 80 µL of the sodium acetate/ethanol solution in a 1.5 mL eppendorf tube, vortexed briefly and left to stand for 15 minutes at room temperature, then centrifuged at 13,000 g for 30 minutes and the supernatant discarded. The pellet was washed with 200 µL of 70 % (v/v) ethanol, briefly vortexed, then centrifuged at 13,000 g for 5 minutes and the supernatant discarded. The precipitated sequencing reaction was dried at 70 ºC for 1 minute, to allow any residual ethanol to evaporate. The sample was then submitted to Micromon DNA sequencing facility at Monash University.

3.2.6 Small scale expression and purification of sRAGE in *E. coli*-KRX strain
3.2.6.1 Culture conditions

A fresh single colony of sRAGE construct, grown overnight at 37 ºC on LB agar plate supplemented with 30 µg mL^{-1} of kanamycin (Promega), was used to inoculate LB liquid medium to prepare the starter culture. Starter culture was grown in 5 mL of LB liquid medium containing 30 µg mL^{-1} of kanamycin, overnight at 37 ºC, with shaking at 225 rpm. The culture was supplemented with 0.4 % D-glucose (Promega) in final concentration to further reduce the background expression of the protein.

The overnight starter culture was diluted 1:100 using 50 mL Terrific broth (Appendix III). Terrific broth was used instead of liquid LB medium because it generates a greater final cell mass. The diluted culture was supplemented with 30 µg mL^{-1} of kanamycin and

transferred to a 500 mL baffled conical flask to provide aeration. The culture was grown at 37 ℃, with shaking at 225 rpm until it reached an OD_{600} of 0.8 - 1.0.

Once the culture reached an OD_{600} of 0.8 - 1.0, it was transferred to an incubator shaker set at 18 ℃ and shaking continued at 225 rpm. When the culture reached an OD_{600} of 1.5, protein expression was induced by adding rhamnose (Promega), to a final concentration of 0.05 %. A lower concentration of rhamnose was used to induce the culture (recommended concentration was 0.1 %), in the hope that it would lower the rate of induction, thus assisting in the expression of soluble proteins like sRAGE (Schlegel *et al*., 2013). The culture was allowed to grow for 20 hours at 18 ℃ while shaking at 225 rpm. A temperature range of 15 ℃ to 25 ℃ was recommended by Promega for protein expression using Flexi vectors. However, a lower temperature of 18 ℃ was used to over-express sRAGE with the expectation of obtaining a higher yield. The lower temperatures produce more soluble proteins and enhance the solubility of a number of proteins, including human interferon α-2, subtilisin E, and ricin-A chain (Sorensen & Mortensen, 2005).

3.2.6.2 Harvesting and cell lysis by freeze and thaw method

Cells were harvested by centrifugation at 4,000 g for 20 minutes at 4 ℃ and the cell pellet weight recorded. The cell pellet was resuspended in 5 mL of HaloTag® purification buffer (50 mM HEPES pH 7.5 and 150 mM NaCl) supplemented with 100 µL of 10 mg mL^{-1} lysozyme (Promega) and 50 µL of 0.5 mg mL^{-1} RNase free DNase1 (New England Biolabs® Inc.). The cell suspension was incubated on ice for 10 minutes, then frozen on a dry ice/ethanol bath for 4 minutes and thawed in an ice/water bath with occasional mixing. Freezing and thawing steps were repeated for a total of four times. The cell lysate was centrifuged at 10,000 g for 25 minutes at 4 °C. The cell lysate supernatant was transferred to a fresh tube and kept on ice. The cell lysate supernatant (100 µL) was reserved on ice for further analysis by SDS-PAGE (see 2.2.4.1).

3.2.6.3 E. coli-made sRAGE purification by Halo-Tag purification system

HaloLink™ resin (4 mL; Promega) supplied as 25 % slurry in 25 % ethanol (Promega) was equilibrated in 10 mL of HaloTag® purification buffer in a 15 mL tube and centrifuged at 1,000 g for 5 minutes at room temperature. The cell lysate (5 mL) supernatant was added to 4 mL of HaloLink™ resin (Promega) and mixed by inverting

the tube. The tube was placed on a tube rotator for end-over-end mixing for 1 hour at room temperature. After 1 hour, the mixture was centrifuged at 1,000 g for 5 minutes and the supernatant was transferred to a fresh tube and reserved as the flow-through. Approximately 1 mL of freshly prepared cleavage solution (66 µL of TEV protease (Promega), 1,000 units with 1 mL HaloTag® purification buffer) was added to the settled resin and incubated on a tube rotator with end-over-end mixing at room temperature for 1 hour. The mix was then centrifuged at 3,000 g for 5 minutes and the supernatant was transferred to a 15 mL falcon tube and 1 mL of HaloTag® protein purification buffer was added again to the resin and the resin mix was centrifuged at 3,000 g for 5 minutes. The remaining sRAGE in the supernatant was collected and pooled into the previous supernatant; this was the eluent 1 (E1). A 100 µL aliquot of the E1 was left on ice, for downstream analysis by SDS-PAGE and ELISA, (see 2.2.4.1 and 2.2.5.2). HisLink™ resin (50 µL; Promega) was added to the E1 fraction and incubated on a tube rotator at room temperature for 20 minutes. The HisLink™ resin is to remove the TEV protease from the protein of interest (Figure 3.2) via its N-terminal (HQ) 5 tag. The tube was centrifuged at 1,000 g for 5 minutes to separate the resin and the supernatant. The supernatant is transferred into a new tube; this is the purified protein (E2). A 100 µL aliquot was removed and placed on ice, for further analysis by SDS-PAGE and ELISA.
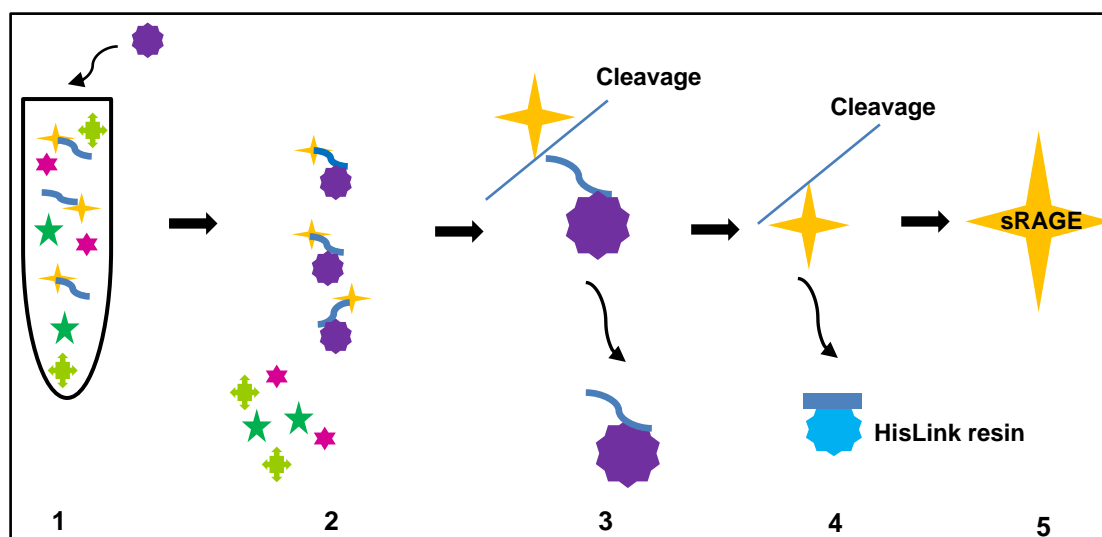
Figure 3.2 Schematic representations of HaloTag® purification steps (adapted from Promega). Step 1, immobilisation of HaloTag® fused sRAGE protein onto HaloLink™ resin; step 2, washing to remove the unbound proteins; step 3, releasing sRAGE by TEV protease; step 4, removal of TEV protease by HisLink™ resin and step 5, recovery of tag-free sRAGE protein.

3.2.6.4 Concentration and dialysis of protein

Purified sRAGE was concentrated using 15 mL Amicon Ultra 10,000 MWCO centrifugal filter devices (Merck Millipore) centrifuged at 13,000 g for 15 minutes. To remove excess salt from the purified sRAGE, overnight dialysis was performed against 500 mL of 50 mM HEPES pH 7.5 and 10 mM NaCl buffer at 4 °C using 12 - 14 kDa dialysis tubing (Livingstone International Pty Ltd.).

3.2.7 Large scale expression and purification of sRAGE in four different expression strains of *E. coli*

The sRAGE construct was transformed into three additional *E. coli* strains: BL21 (DE3), C41 (DE3), and Rosetta-gami and compared to the KRX strain to determine the strain with the highest yield.

3.2.7.1 Expression of sRAGE in different expression strains of E. coli

Competent cells of the *E. coli* strains (BL21 (DE3), C41 (DE3), and Rosetta-gami) were thawed on ice before addition of the DNA/ligation reaction mixture. Heat shock transformation was carried out as per the method described in section 3.2.3, except that the Rosetta-gami cells were plated on LB agar plates supplemented with 100 μg mL^{-1} chloramphenicol in addition to 30 μg mL^{-1} kanamycin. Positive colonies were PCR screened as per the method described in section 3.2.4.

3.2.7.2 Extraction of sRAGE from the four strains

Starter cultures of the four strains (BL21 (DE3), C41 (DE3), KRX and Rosetta-gami) were prepared as per the method in section 3.2.6.1, except for the following changes:

A freshly transformed colony was used to inoculate 10 mL LB liquid medium (two starter cultures per strain) supplemented with 30 μg mL^{-1} of kanamycin or 100 μg mL^{-1} chloramphenicol and 30 μg mL^{-1} kanamycin for the Rosetta-gami culture. The overnight starter cultures were added to 2 L baffled conical flasks containing 0.8 L of LB liquid medium. The diluted cultures were supplemented with 30 μg mL^{-1} of kanamycin or 100 μg mL^{-1} chloramphenicol. The cultures were grown at 37 °C with shaking at 225 rpm until they reached an OD$_{600}$ of 0.8 - 1.0. Cells were harvested according to the method outlined section 3.2.6.2. The optimal selected strain was grown as above, and sRAGE protein extracted from a total of 2 L of cell cultures. The yields of sRAGE (mg) obtained from

0.8 L and 2 L of cell cultures were converted to mg L^{-1}, to allow the comparison of the yields extracted from different cell culture volumes. A French press was used to efficiently and quickly disrupt the cell pellets produced by the large scale expression of the four strains and 2 L cell cultures as follows;

The cultures were centrifuged at 17,000 g for 15 minutes at 4 °C and the cell pellet was resuspended in 50 mL of Halo-Tag purification buffer containing one cOmplete EDTA-free Protease Inhibitor (Roche) tablet, 5 mM of PMSF (Sigma,) and 1 mM DTT (Promega). The cells were incubated on a tube rotator with end-over-end mixing at room temperature for 20 minutes. The cells were lysed by EmulsiFlex-C5 cell disruptor (French Press; Avestin, Canada) and the cell lysate centrifuged at 17,000 g for 15 minutes at 4 °C. The supernatant was transferred to fresh tubes and centrifuged at 17,000 g for 15 minutes at 4 ºC. After centrifugation the supernatant was again transferred to fresh tubes on ice.

Further purification was carried out as per the batch method for HaloTag® protein purification in section 3.2.6.3., except 70 mL of prepared cell lysate supernatant was added to 1 mL of settled HaloLink™ resin and mixed by inverting the tube on a tube rotator for 1 hour at room temperature. Furthermore, TEV cleavage was extended to overnight.

3.2.7.3 E. coli-made sRAGE purification by size-exclusion chromatography

The *E. coli*-made sRAGE purified by HaloTag® purification method was further purified using size-exclusion chromatography. Following HaloTag® purification, fractions containing sRAGE were pooled and concentrated to ~1 - 2 mL using 15 mL Amicon Ultra 10,000 MWCO, centrifugal filter devices (Merck Millipore). A Superdex 200 10/300 pre-packed column (GE Healthcare) was attached to a FPLC (ÄKTA, GE Healthcare) and equilibrated with buffer containing 50 mM HEPES pH 7.5, 150 mM NaCl and 5 % glycerol. The HaloTag fractions were loaded onto the SEC column at a rate of 1 mL min^{-1}. sRAGE was eluted in 50 mM HEPES pH 7.5, 150 mM NaCl and 5 % glycerol at a rate of 1 mL min^{-1}. *E. coli*-made sRAGE was quantified by sandwich ELISA (see 2.2.5.2) and protein samples were diluted 1:40,000 and 1:80,000.

3.2.8 Characterisation of *E. coli*-made sRAGE by native polyacrylamide gel electrophoresis

E. coli-made sRAGE was analysed by native polyacrylamide gel electrophoresis. sRAGE samples were prepared in a non-reducing and non-denaturing sample buffer, thus allowing it to maintain its secondary structure and the native charge density. Aliquots of 15 µL of each of the samples were transferred to fresh tubes and 5 µL of 4X native loading buffer lacking SDS and 10 % β-mercaptoethanol (Appendix III) added to each tube. The samples and protein molecular mass markers (7 µL; Bio-Rad, Precision plus Protein™ Dual Xtra standard) were loaded onto a 12 % PAGE gel and run at 90 V for 90 minutes using the native running buffer (Appendix III). Protein samples were visualised by staining with Coomassie Brilliant Blue R-250 for 30 minutes and destained.

3.2.9 Mass spectrometry of SEC-purified sRAGE

The SEC-purified putative monomeric form of sRAGE was concentrated to ~1 mg mL^{-1}, using 15 mL Amicon Ultra 10,000 MWCO, centrifugal filter devices (Merck Millipore). Concentrated sample (20 µL) was subjected to MALDI TOF/TOF, 4700 Proteomics Analyser (Applied Biosystems Foster City, CA, USA) at the Monash Biomedical Proteomic Facility, Monash University. Mass spectral data were analysed by 4000 Series Explorer version 3.0.

Desalted sample was mixed 1:1 with Matrix, 10 mg mL^{-1} a-cyano-4-hydroxycinnamic acid (Laser BioLabs, Sophia-Antipolis, France) in 50 % Acetonitrile, 0.1 % TFA) and spotted onto the MALDI target plate. Proteins were analysed in Linear mode with a mass range of 20 kDa to 80 kDa and a focus mass of 40 kDa. Laser shots are fired randomly across the sample spot at a rate of 125 shots per spectrum and accumulated to a total of 2500 shots/spectrum. The spectrum was externally calibrated against Bovine Serum Albumin using 2 point calibrate masses, 66431 Da and 33216 Da.

3.3 RESULTS

Results of this chapter are discussed in terms of sRAGE produced on a small scale (50 mL culture) and on a large scale (2 L of cell cultures).

3.3.1 Characterisation and quantification of sRAGE expressed on a small scale

sRAGE, expressed in the KRX bacterial strain, was produced on a small scale in 50 mL of Terrific broth. sRAGE extracted from the cell pellet was purified by HaloTag® purification method. Molecular weight of the protein was determined by SDS-PAGE (see 2.2.4.1) and the yield of sRAGE was calculated by ELISA (see 2.2.5.2). This was repeated several times with variable yields of sRAGE.

The final OD_{600} of the culture was found to be 2.207 and 0.86 g of cell pellet was harvested from 50 mL of Terrific broth. The *E. coli*-made sRAGE was purified by the HaloTag® purification method. sRAGE eluted in fractions E1 and E2 are shown in lanes 4 and 5 respectively (Figure 3.3). One major band at ~37 kDa was observed for E1 and E2. Lane 1 shows the cell lysate supernatant representing the total soluble proteins loaded onto the HaloLink™ resin. The band for sRAGE after dialysis (lane 6) was less intense than E2 (lane 5) and may be due to dilution as a result of adding the buffer during dialysis.

A total yield of 1.2 mg of sRAGE was obtained (1.2 mg / 50 mL) from experiment 1 as determined by ELISA. However, in subsequent purification experiments yield was markedly reduced (Table 3.2). Various parameters were tested, including the induction temperature of the *E. coli* cultures expressing sRAGE. A temperature range of 15 ºC to 25 ºC was recommended by Promega for protein induction using Flexi vectors. Therefore, during the next purification the culture temperature after induction was changed from 18 ºC to 25 ºC to determine the effect of temperature on the yield of sRAGE. However, the total yield remained consistently low.

Figure 3.3 Analysis of HaloTag® purification steps of Experiment 1 by SDS-PAGE. Lane M, protein molecular mass markers (kDa); lane 1, clarified cell lysate extract with expressed sRAGE; lane 2, fraction after cleavage of sRAGE from the HaloTag®; lane 3, flow-through; lane 4, eluent 1 (E1); lane 5, eluent 2 (E2); lane 6, E2 after dialysis. The proteins were visualised with Coomassie Brilliant Blue.

Table 3.2 The yields of sRAGE expressed in *E. coli*-KRX strain grown on a small scale

Experiment Number	Yield of sRAGE mg / 50 mL	
1 - Initial expression experiment	1.2	
2 - Same glycerol stock as in the experiment 1	0.089	
3 - Same glycerol stock as in the experiment 1	0.034	
4 - Different glycerol stocks to experiment 1	**Colony 1**	**Colony 2**
	0.06	0.05
5 - Newly transformed competent cells	0.07	
6 - Induction temperature increased up to 25 ºC	0.09	

3.3.2 Quantification of large scale expressed sRAGE in four different strains of *E. coli*

To optimise the protocol and produce a higher yield of sRAGE protein, a pilot study was carried out using 0.8 L of LB medium and four different *E. coli* expression strains: BL21 (DE3), C41 (DE3), Rosetta-gami and KRX (Promega). The intention was to identify the strain that would produce the highest yield of protein and then use this *E. coli* strain to produce sRAGE required to perform the *in vitro* ligand binding studies. The best yielding

strain would be grown on a large scale using the facilities available in Prof. Matthew Wilce's laboratory, School of Biomedical Science, Monash University.

3.3.2.1 SDS-PAGE analysis

The cell lysates and the purified sRAGE from the *E. coli* strains (BL21 (DE3), C41 (DE3), Rosetta-gami and KRX) were subjected to SDS-PAGE analysis (see 2.2.4.1). The results are depicted in Figure 3.4. *E. coli*-BL21 (DE3) (lane 1) and Rosetta-gami (lane 4) showed equally intense bands corresponding to the molecular size of sRAGE protein (~37 kDa) (Figure 3.4). However, corresponding bands for the C41 (DE3) strain (lane 2) and KRX strain (lane 3) were very faint. Apart from the major band at ~37kDa, several bands were also present at ~75 kDa, ~65 kDa, ~25 kDa and ~5 kDa in lanes 1 to 4 (Figure 3.4). The higher molecular weight bands seen at ~75 kDa and ~65 kDa could have resulted from multimeric forms of sRAGE and the lower molecular weight bands (~25 kDa and ~5 kDa) could possibly have resulted either from cleaved products of sRAGE or impurities.
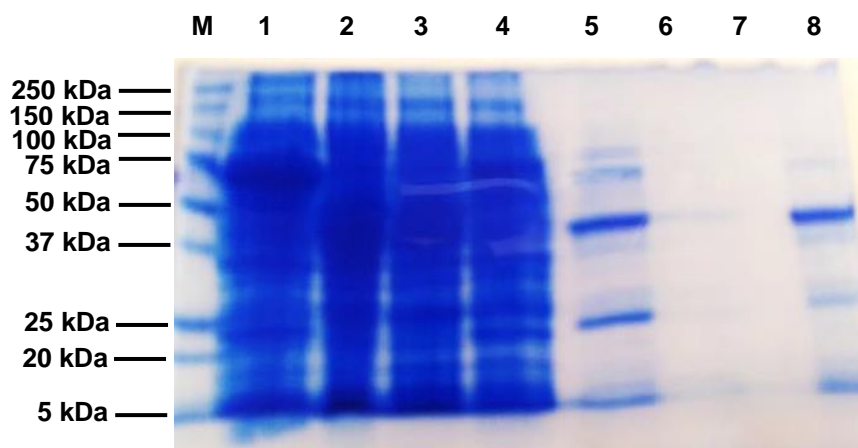
Figure 3.4 Analysis of HaloTag® purified sRAGE obtained from four different *E. coli* strains using SDS-PAGE. Lane M, protein molecular mass markers (kDa); lane 1, cell lysate of BL21 (DE3); lane 2, cell lysate of C41 (DE3); lane 3, cell lysate of KRX; lane 4, cell lysate of Rosetta-gami; lane 5-8, E2 fractions of BL21 (DE3), C41 (DE3), KRX and Rosetta-gami, respectively. The proteins were visualised with Coomassie Brilliant Blue.

3.3.2.2 Yields of sRAGE: a comparison

The total yield of sRAGE produced by each of the strains, BL21 (DE3), C41 (DE3), KRX and Rosetta-gami, was determined using ELISA as per the method in section 2.2.5.2; the yields are shown in Figure 3.5 as mg L^{-1} of culture.
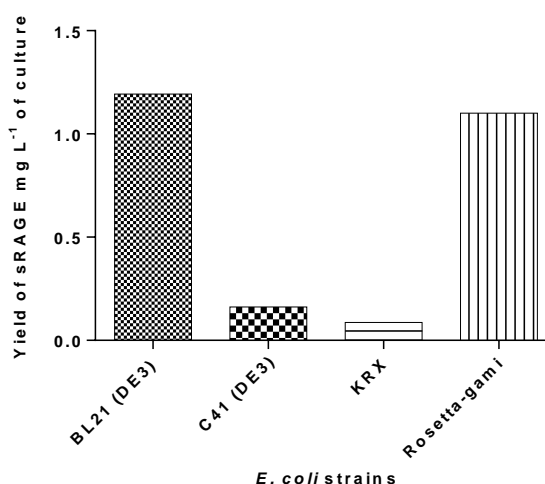
Figure 3.5 Yields of sRAGE in *E. coli* strains; BL21 (DE3), C41 (DE3), KRX and Rosetta-gami. Data shown in the graph are from a single experiment.

Of the four *E. coli* strains, 1.2 mg L^{-1} of sRAGE obtained from BL21 (DE3) was the highest yield. Rosetta-gami produced a similar yield of 1.1 mg L^{-1}. Lower yields of sRAGE were generated by C41 (DE3) and KRX strains (0.16 and 0.08 mg L^{-1} respectively). Rosetta-gami is known to express eukaryotic proteins with the proper folding (Hatahet *et al.*, 2010) and combined with the high yield of sRAGE this strain was selected to express sRAGE on a large scale.

3.3.3 Characterisation and quantification of large scale expressed sRAGE in *E. coli* Rosetta-gami strains

sRAGE was expressed in *E. coli*-Rosetta-gami strains, grown on a large scale to give a final OD_{600} of 2.777. sRAGE was extracted from ~8 g of cell pellet obtained after centrifugation.

3.3.3.1 SDS-PAGE and western blot analysis

sRAGE expressed in the *E. coli*-Rosetta-gami strain, was purified by the HaloTag® purification system and the resulting fractions were analysed by SDS-PAGE (see 2.2.4.1). Purified sRAGE produced by the Rosetta-gami strain appeared at ~37 kDa on the SDS-PAGE gel (Figure 3.6; lanes 4 and 5). A small amount of sRAGE was retained in the HaloLink™ resin (Figure 3.6, lane 6), however, no effort was made to recover this small amount of resin bound sRAGE.

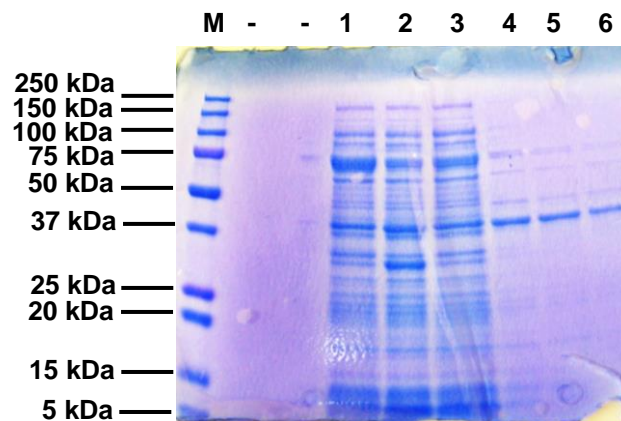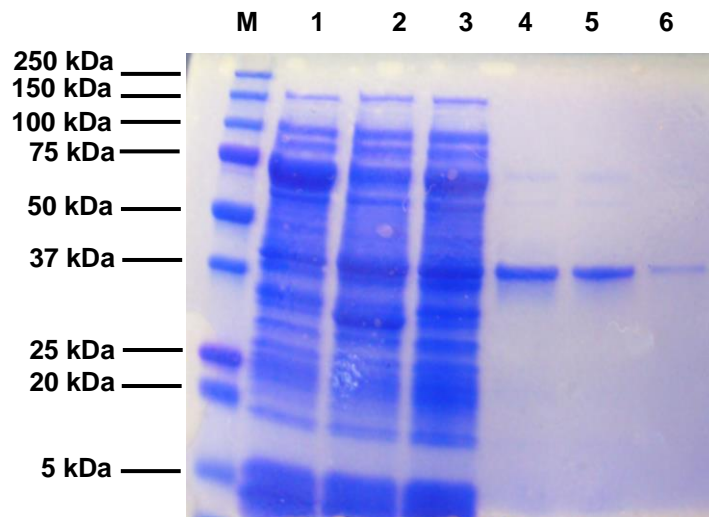**Figure 3.6 Analysis of HaloTag® purification steps using SDS-PAGE. Lane M, protein molecular mass markers (kDa); lane 1, clarified cell lysate extract with expressed sRAGE; lane 2, fraction after cleavage of sRAGE from the HaloTag® ; lane 3, flow-through; lane 4, E1; lane 5, E2; lane 6, heated resin containing any sRAGE bound to the resin. The proteins were visualised with Coomassie Brilliant Blue.**

HaloTag® purified sRAGE was further analysed by western blotting to verify the authenticity of the purified sRAGE (Figure 3.7). Eluted fractions E1 (lane 1) and E2 (lane 2) appeared as a ~37 kDa band on the western blot. Protein bound to the resin was also confirmed to be sRAGE with a band size of ~37 kDa (Figure 3.7).
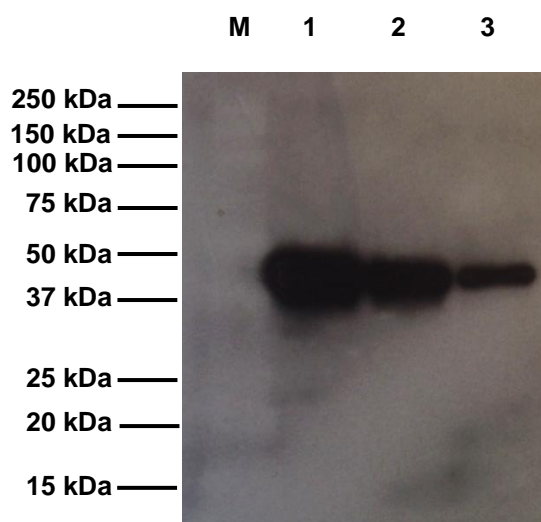
Figure 3.7 Analysis of HaloTag® purification steps using western blotting. Lane M, protein molecular mass markers (kDa); lane 1, E1; lane 2, E2; lane 3, heated resin containing any sRAGE bound to the resin. The location of the molecular weight markers were defined following alignment of the western blot and X-ray film.

3.3.3.2 Analysis of sRAGE after size-exclusion chromatography purification

HaloTag® purified sRAGE from *E. coli*-Rosetta-gami strains was further purified by size-exclusion chromatography to remove any impurities. The major peak eluting at 42 mL fraction may represent putative soluble aggregates of sRAGE. The peak eluting at 85 mL may represent the putative monomeric form of sRAGE (Figure 3.8). The red trace of the resulting chromatogram shows the absorbance of proteins at 280 nm, whilst, the blue trace shows the absorbance at 254 nm. The blue trace may have resulted from the interaction of sRAGE and the bacterial DNA. RAGE has been shown to interact with DNA as well as with RNA (Sirois, 2013).

When the protein from each of these peaks was quantified with ELISA (as per the method in 2.2.5.2) the yield of the putative monomeric form was found to be 0.3 mg L^{-1} and for the putative soluble aggregates fraction, 0.25 mg L^{-1} of sRAGE. However, from the peak area of the size-exclusion chromatogram it would suggest that the yield of putative soluble aggregates should be higher than the putative monomeric form (Figure 3.8).
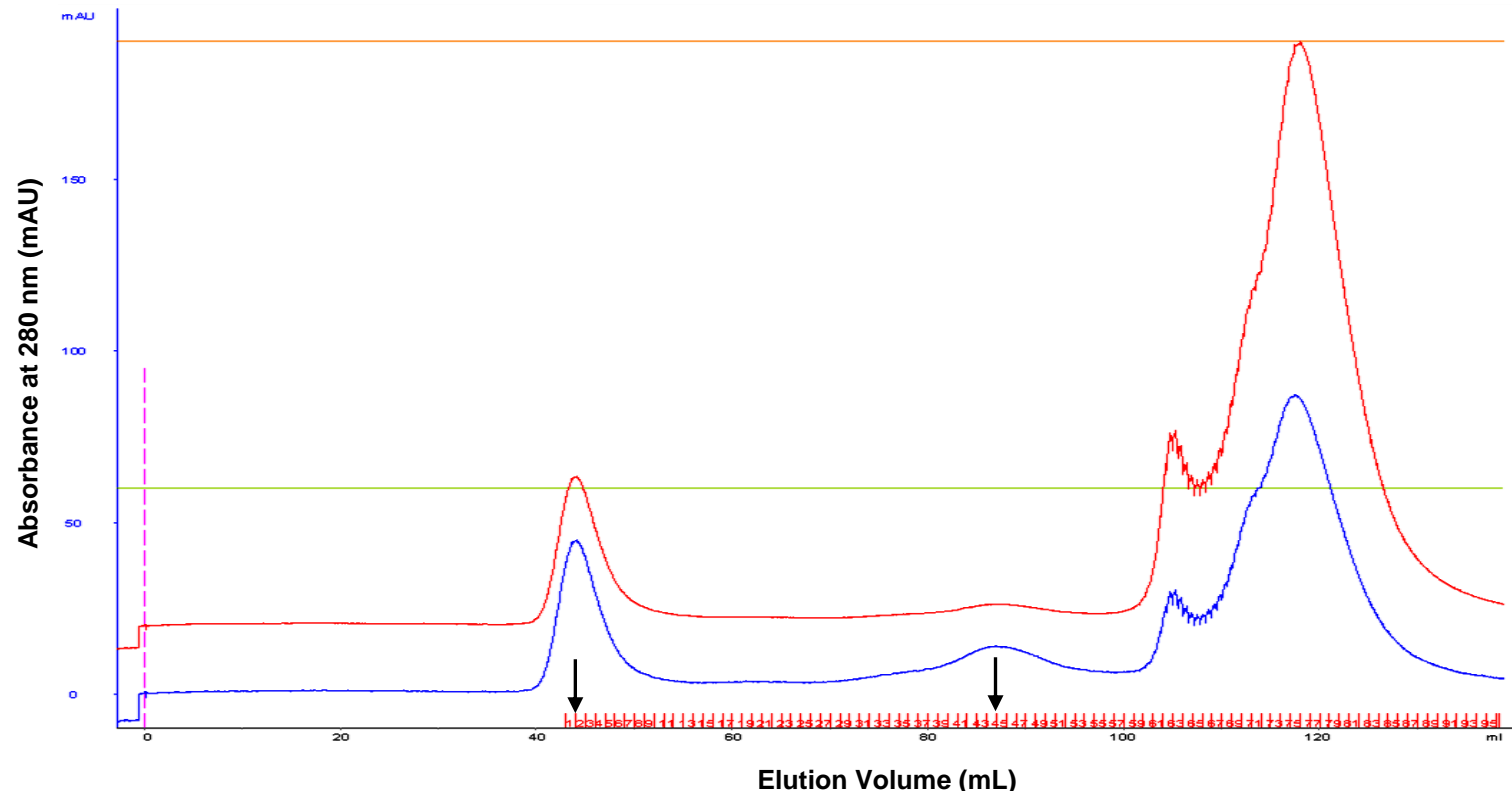
Figure 3.8 For size-exclusion chromatography, HaloTag® purified sRAGE of *E. coli*-Rosetta-gami strains was applied to a Superdex 200 10/300 pre-packed column (GE Healthcare) and eluted with 50 mM HEPES pH 7.5, 150 mM NaCl and 5 % glycerol buffer at 1 mL min⁻¹. Protein elution is monitored by measuring absorbance at 280 nm, using an ÄKTA purifier FPLC system (GE Healthcare). Red trace represents the products at 280 nm, the blue trace represented the 254 nm products.

SEC-purified sRAGE was further analysed by SDS-PAGE (see 2.2.4.1) to determine the purity of the final product and to examine the size difference between the putative monomeric form and the putative soluble aggregates of sRAGE (Figure 3.9).
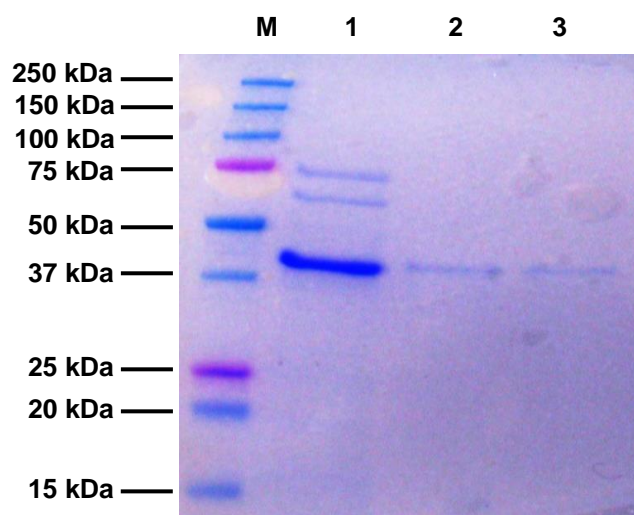
Figure 3.9 Analysis of SEC purified putative monomeric form and the putative soluble aggregates of sRAGE compared to the HaloTag® purified sRAGE using SDS-PAGE. Lane M, protein molecular mass markers (kDa); lane 1, HaloTag® purified sRAGE (10 µg); lane 2, putative monomeric form of sRAGE (3 µg) after size-exclusion purification; lane 3, putative soluble aggregates of sRAGE (3 µg) after size-exclusion purification. The proteins were visualised with Coomassie Brilliant Blue.

HaloTag® purified sRAGE showed an intense band for sRAGE at ~37 kDa with some impurities at ~75 kDa and ~60 kDa (Figure 3.9). The putative monomeric form and the putative soluble aggregates of sRAGE also appeared as ~37 kDa bands. However, a higher molecular weight band was expected to be observed for the putative soluble aggregates. The reduction of the putative aggregated sample by adding β-mercaptoethanol and then denaturation by heating (95 ºC for 5 minutes) prior to SDS-PAGE, may have caused the putative aggregated protein to appear as a band at ~37 kDa. The putative monomeric form and putative soluble aggregates of sRAGE were subjected to native polyacrylamide gel electrophoresis (Figure 3.10) to distinguish the size difference between them. Both samples were loaded onto the native polyacrylamide gel with and without additional denaturation by heating at 95 ºC to examine the effect of temperature on the size of the protein.
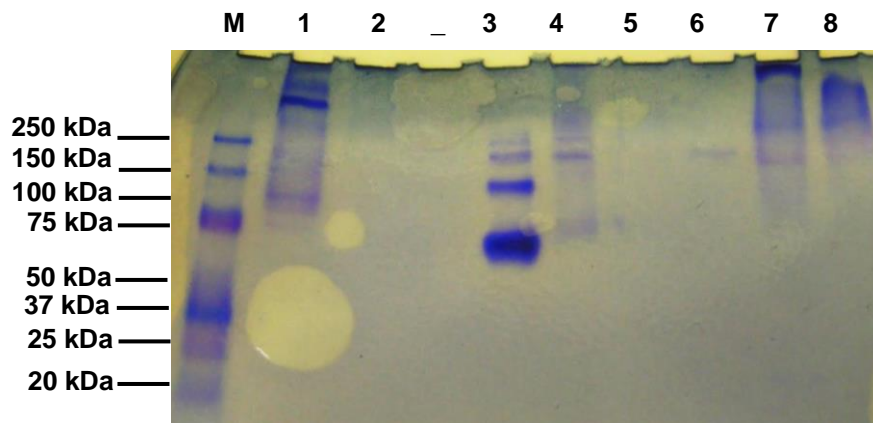
Figure 3.10 Analysis of SEC-purified sRAGE compared to a positive control and bovine serum albumin (BSA) by native-PAGE. Lane M, protein molecular mass markers (kDa); lane 1, putative monomeric form of sRAGE without heating (10 µg); lane 2, putative monomeric form of sRAGE after heating(10 µg); lane 3, BSA without heating (10 µg); lane 4, BSA after heating (10 µg); lane 5, positive control (recombinant human sRAGE Fc Chimera) without heating (10 µg); lane 6, positive control after heating (10 µg); lane 7, putative soluble aggregates of sRAGE without heating (10 µg); lane 8, putative soluble aggregates of sRAGE after heating (10 µg). The proteins were visualised with Coomassie Brilliant Blue.

The protein molecular mass markers were well separated by native polyacrylamide gel electrophoresis (Figure 3.10). The separation of the non-heated monomeric form of sRAGE resulted in the visualisation of several bands, the major one greater than 250 kDa, (Figure 3.10, lane 1). No bands were observed for the putative monomeric form of sRAGE when the sample was heated (lane 2). It would be expected that the putative soluble aggregates of sRAGE would be observed as larger bands compared to the monomeric form and this is shown for both non-heated (lane 7) and heated (lane 8) samples. The predominant monomeric band of BSA (~66 kDa) was observed to be clearly distinct from its dimeric and trimeric forms. However, those bands were less intense when the BSA sample was heated. The positive control should be observed to be ~80 kDa but a band approximately twice the size (~160 kDa) was observed upon heating. No bands were present in the absence of heating. The observation of higher molecular weights of sRAGE was similar to the findings of Hanford *et al.* (2004), when mouse sRAGE was separated by SDS-PAGE. Under non-denaturing and non-reducing conditions, purified mouse sRAGE runs at ~200 kDa (Hanford *et al.* 2004). Although the intensities of the bands (Figure 3.10) were not strong, the molecular weight of the putative monomeric

form and the putative soluble aggregates of sRAGE are different from each other following native PAGE.

3.3.3.3 Western blot analysis of sRAGE purified by size-exclusion chromatography

The fractions containing the putative monomeric form of sRAGE were pooled and concentrated using 15 mL Amicon Ultra 10,000 MWCO, centrifugal filter devices (Merck Millipore). The sample was analysed using western blotting (see 2.2.4.2) to confirm its authenticity and purity.
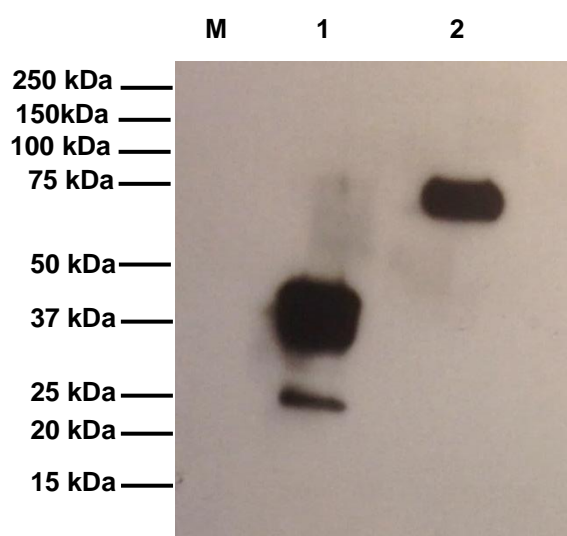
Figure 3.11 Analysis of SEC-purified sRAGE using western blotting. Lane M, protein molecular mass markers (kDa); lane 1, putative monomeric form of sRAGE; lane 2, positive control with ELISA kit (recombinant human sRAGE Fc Chimera). The location of the molecular weight markers were defined following alignment of the western blot and X-ray film.

Purified sRAGE appeared as a major band of ~37 kDa (Figure 3.11), with a faint band of ~25 kDa also present. The ~25 kDa band may be due to a cleavage product of sRAGE. The positive control, (recombinant human sRAGE Fc Chimera (R & D system)) showed a band at ~75 - 80 kDa, which was consistent with the expected size of an Fc-sRAGE chimeric protein.

3.3.3.4 Mass spectrometry

The putative monomeric form of sRAGE was subjected to MALDI TOF/TOF mass spectroscopy to determine if its molecular mass matched the expected molecular mass of sRAGE in its monomeric form. The molecular mass was determined to be 33 kDa (Figure 3.12), which is comparable to the theoretical molecular mass of monomeric sRAGE based on ExPASy analysis (http://web.expasy.org/compute_pi/) expressed in *E. coli* expression systems. The peaks observed at ~11 kDa and ~16 kDa may have resulted from impurities in the sample. However, the results from the mass spectrum data confirmed that the putative monomeric form of sRAGE was in the monomeric form.
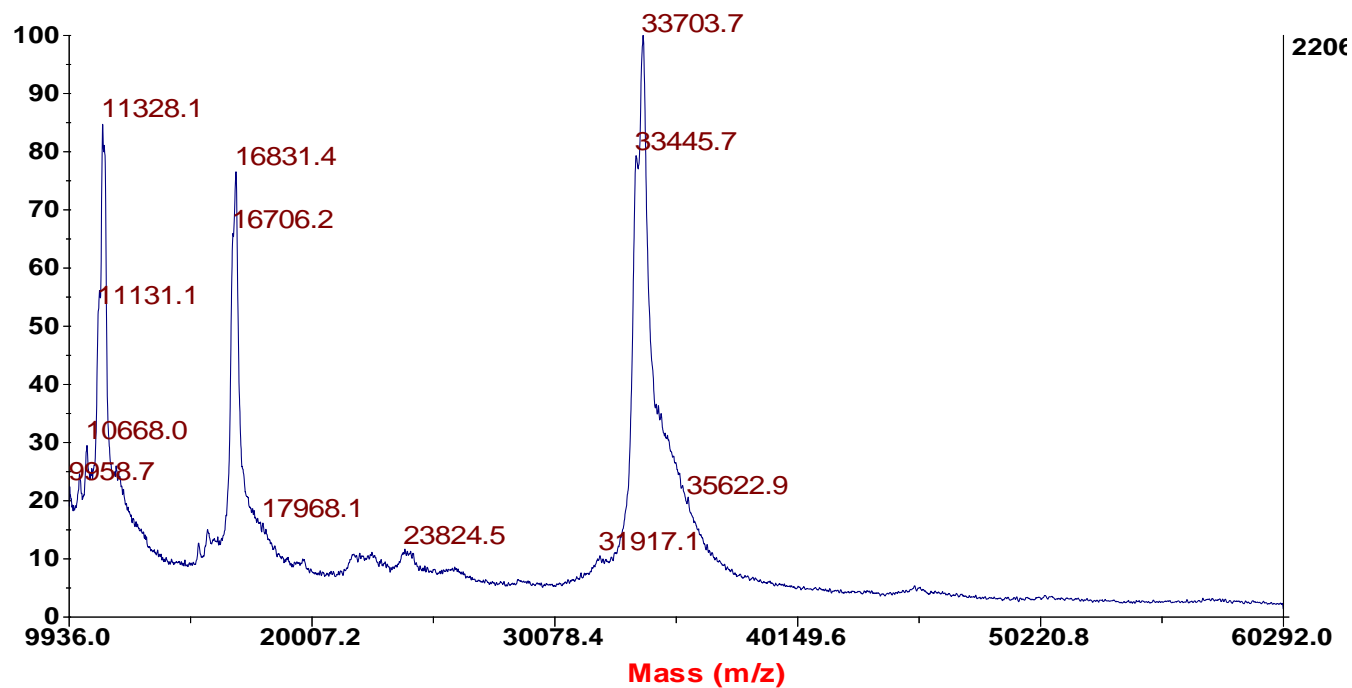
Figure 3.12 MALDI TOF/TOF mass spectrometry, to determine accurate mass of putative monomeric form of sRAGE. Desalted sample is mixed 1:1 with Matrix, 10 mg mL^{-1} a-cyano-4-hydroxycinnamic acid (Laser BioLabs, Sophia-Antipolis, France) in 50 % Acetonitrile, 0.1 % TFA) and spotted onto the MALDI target plate of MALDI TOF/TOF, 4700 Proteomics Analyser (Applied Biosystems Foster City, CA, USA).

3.4 DISCUSSION

The full-extracellular domain of human sRAGE devoid of the native signal peptide was expressed on a small scale in the *E. coli*-KRX strain using the pFN18K HaloTag® T7 Flexi® vector (Promega) encoding an N-terminal HaloTag®. Initially, a yield of 1.2 mg / 50 mL of sRAGE (experiment 1; 24 mg L^{-1}) was obtained using this expression system and was higher than the yield of sRAGE obtained by Kumano-Kuramochi *et al*. (2009) which was approximately 10 fold lower (2.2 mg L^{-1}), when a minimum stable structure of sRAGE was expressed in *E. coli*-Origami (DE3) strains. The initial yield of 1.2 mg / 50 mL; (24 mg L^{-1}) is similar to the yield of exRAGE (Ala23-Gly340) expressed in *E. coli*-JM83 strains (24 mg L^{-1}) in a study by Wilton *et al*. (2006).

sRAGE was also expressed in four different *E. coli* expression strains, KRX, BL21 (DE3), C41 (DE3) and Rosetta-gami (0.8 L culture per strain) to determine the strain with the highest yield of sRAGE. The scaled-up cultures and the different strains did not result in a substantial increase in the yield of sRAGE as expected (1.2 mg L^{-1} of sRAGE from BL21 (DE3), 1.1 mg L^{-1} from Rosetta-gami and 0.16 mg L^{-1} for C41 (DE3) and 0.08 mg L^{-1} from KRX strain). There is no guarantee that protein yield will increase with the scaling up of the cultures. Scaling up is a much more complex procedure, which involves manipulation of important parameters (single parameters alone or multiple parameters in combination) that affect the microbial growth, including increasing the volume of the culture medium, introducing different culture media, changing the composition of the culture media, introducing different host strains and, operating the oxygen transfer of the cultures (Routledge *et al*., 2011; Ukkonen *et al*., 2011; Ukkonen *et al*., 2013). This was true for sRAGE when expressed on a large scale in *E. coli* expression strains; KRX, BL21 (DE3), C41 (DE3) and Rosetta-gami that showed low yields of sRAGE. However, the BL21 (DE3) and Rosetta-gami strains produced higher yields compared to the C41 (DE3) and KRX strains.

Several *E. coli* strains have been developed to express recombinant proteins. *E. coli*-KRX has been developed as the host strain to express human proteins using the HaloTag® expression system by Promega and it serves as a cloning as well as an expression strain. BL21 (DE3) is popular and has been widely used as an expression strain to produce many proteins (Costa *et al*., 2014). Being deficient in both *lon* and *ompT* proteases, it has the ability to degrade the majority of the misfolded proteins in the presence of Lon protease

(Hatahet *et al*., 2010; Rosen *et al*., 2002). C41 (D3), a mutant host strain derived from BL21 (DE3) has the ability to produce elevated levels of proteins and lacks the toxic effect of target proteins on the growth of the bacterial cells which is the major drawback of BL21 (D3) strain (Dumon-Seignovert *et al*., 2004). Rosetta-gami combines the advantages of Origami and the rare tRNA genes of Rosetta and are better at expressing eukaryotic proteins (Hatahet *et al*., 2010). Rosetta-gami strains contain thioredoxin reductase (*trxB*) and glutathione reductase (*gor*) mutations for disulphide bond formation and improved protein yield *in vivo* (De Marco, 2009; Hatahet *et al*., 2010). Therefore, Rosetta-gami strains were selected for this study due to their high yield of recombinant protein expression and superior ability to express eukaryotic proteins that are properly folded (Hatahet *et al*., 2010).

Despite the HaloTag® being a soluble tag, the T7 RNA polymerase being a strong promoter, and Rosetta-gami being a strain with *trxB/gor* mutations for disulphide bond formation and improved protein folding *in vivo*, a considerable amount of expressed sRAGE was shown to form putative soluble aggregates. Rosetta-gami produced an equal yield of putative soluble aggregates and the putative monomeric form of sRAGE resulting in 0.3 mg L^{-1} of putative monomeric form and 0.25 mg L^{-1} of putative soluble aggregates based on the ELISA calculations. However, it seems that the yield of putative soluble aggregates is higher than the putative monomeric form with respect to the peak area of the resulted size-exclusion chromatogram (Figure 3.8). Putative soluble aggregates may have prevented the antibody recognition, meaning that the ELISA could have underestimated the yield of sRAGE (Janssen *et al*., 2015). However, the yield would be sufficient to carry out ligand binding studies with HMGB-1 and S100A8/A9 complex.

The full-extracellular domain of human sRAGE is comprised of three immunoglobulin-like domains: V1, C1 and C2. Each domain carries two cysteine residues (Appendix I), which are involved in disulphide bond formation and subsequent folding of sRAGE (Kumano-Kuramochi *et al*., 2009). *E. coli* Rosetta-gami strains possess thioredoxin reductase (*trxB*) and glutathione reductase (*gor*) mutations, which facilitate disulphide bond formation and improved protein yield *in vivo*. However*, w*hen sRAGE was expressed in the cytoplasm of the Rosetta-gami strains a considerable amount of putative soluble aggregates was produced. However, we do not know whether sRAGE was folded correctly in *E. coli* expression strains. Circular dichroism (CD) spectroscopy will

determine whether sRAGE was properly folded in the Rosetta-gami strains in the future studies.

The native disulphide bond formation in eukaryotes commonly occurs in the endoplasmic reticulum and intermembrane space of mitochondria and in the periplasmic space of prokaryotes. Native disulphide bond formation is a rate-limiting factor in protein folding. It is one of the most common post-translational modifications taking place in living cells (Hatahet *et al*., 2010). The cytoplasm of *E. coli* carries no components to catalyse native disulphide bond formation and contains a system that reduces protein disulphide bonds (Woycechowsky & Raines, 2000). Therefore, proteins with native disulphide bonds like sRAGE are thought to be difficult to express in the cytoplasm of *E. coli* (Ke, & Berkmen, 2014). Therefore, in future studies, secretion of sRAGE could be targeted to the periplasmic space of *E. coli* that has disulphide bond isomerases which assist in formation of the correct disulphides (Gleiter & Bardwell, 2008). Studies by Wilton *et al*. (2006) demonstrated that when sRAGE was targeted to the periplasmic space of *E. coli*, it mainly existed in a monomeric form and folded properly: this is thought to be due to the oxidising environment of the periplasmic space.

The production of putative soluble aggregates may have contributed to the low yields of sRAGE observed in almost all of the *E. coli* strains. It was speculated that, the β-sheet rich nature of sRAGE may have contributed to this putative soluble aggregate formation because β-sheet rich proteins are prone to aggregation (Budyak *et al*., 2013; Fink, 1999; Przybycien *et al*., 1994). There is an inevitable competition between protein folding and aggregation and this competition is linked to the energy landscapes of these two processes. The concept of energy landscapes explains the progression of unfolded polypeptide chains along an energy landscape towards the compact native structure (Budyak *et al*., 2013). The energy landscape for protein folding varies depending on the complexity of the protein. The protein folding landscape of small proteins appears to be funnel-like and the polypeptide sequences fold rapidly and reliably towards a unique native state. Whilst larger polypeptide sequences have rougher energy landscapes, and therefore, the population of partially folded species may be in an on- or off-pathway to the native state (Jahn and Radford, 2008). β-sheet proteins in particular have sharp folding energy landscapes, and form populations of intermediate states leading to increased susceptibility for aggregation (Budyak *et al*., 2013).

Protein aggregation is a frequent drawback in recombinant protein expression in *E. coli* expression systems (Schultz *et al*., 2006). The interaction between exposed hydrophobic surfaces of the neighbouring domains of proteins may have resulted in the production of large assemblies of proteins known as aggregates. These hydrophobic surfaces are ordinarily buried in the core of the protein but they tend to be exposed in an unfolded protein (Rosen *et al*., 2002). It is assumed that misfolded proteins are refolded by chaperones or else degraded by proteases. However, misfolded proteins could potentially escape from these quality control mechanisms and form non-functional aggregates (Rosen *et al*., 2002). Therefore, many strategies have been undertaken to prevent protein aggregation, which is a common problem when eukaryotic proteins are expressed in prokaryotic systems like in *E. coli* (Costa *et al*., 2014).

Co-expression of proteins with chaperones and/or with foldases prevent protein aggregation. Molecular chaperones promote proper isomerisation and cellular targeting of the proteins of interest by transiently interacting with folding intermediates. GroES-GroE, DnaK-DnaJ and GrpE-ClpB are some of the well-characterised *E. coli* chaperones systems (reviewed by Mogk *et al*., 2002). Foldases on the other hand accelerate rate-limiting steps along the folding pathway. Peptidyl prolyl *cis/trans* isomerases (PPI's), disulfide oxidoreductase (DsbA), disulfide isomerase (DsbC) and protein disulfide isomerase (PDI) are commonly known foldases (De Marco, 2013; Thomas *et al*., 1997). However, increased production of monomers of the proteins by over-expression of chaperones is protein dependent (Haacke *et al*., 2009). The crystal structure of human RAGE ectodomain was deduced by co-expressing sRAGE with *exA* leaderless *E. coli* chaperone/disulfide-isomerase (DsbC) to aid the proper disulfide bond formation (Park *et al*., 2010).

Affinity tags enhance the solubility of their fusion partners and therefore, sometimes promote the proper folding of the protein (Hammarstrom *et al*., 2002). However, the underlying mechanism for how solubility tags enhance the solubility of their fusion partners remains unclear (Waugh, 2005). *E. coli* maltose-binding proteins (MBP) (Kapust & Waugh 1999) and N-utilisation substance A (NusA) (Davis *et al*., 1999) are the most highly validated solubility-enhancing proteins so far. The solubility enhancing activity of these two tags is triggered only when fused to the N-terminus of a recombinant protein.

N-terminus tags improve the recombinant protein yield through efficient translation initiation (Sachdev & Chirgwin, 1998).

In future studies, solubility of the proteins could be enhanced by manipulating a number of parameters in combination: the protocol can be modified in regards to growth conditions of the *E. coli* (temperature, growth media, time of induction, aeration) (Berrow *et al*., 2006; Francis & Page, 2010), type of vector constructs, host strains, fusion tags and co-expression with molecular chaperones or foldases (De Marco & De Marco, 2004; Hammarstrom *et al*., 2002; Knaust & Nordlund., 2001; Waugh, 2005; Yasukawa *et al*., 1995).

3.5 CONCLUSION

The present study successfully produced sRAGE using an *E. coli* expression system to obtain non-glycosylated sRAGE to conduct *in vitro* ligand binding assays and then to compare the results with the similar assays performed with plant-made glycosylated sRAGE. sRAGE was over-expressed as a HaloTag® fusion protein in *E. coli*-KRX strain (Promega). The yield of sRAGE was not consistent and therefore, protein expression and purification protocols were optimised to generate a higher yield of sRAGE. This optimisation involved the expression of newly transformed bacterial colonies rather than use of glycerol stocks, change of the growth temperature of the cultures, and use of different *E. coli* expression strains: BL21 (DE3), C41 (DE3), Rosetta-gami in addition to KRX, to identify the strain that would produce the highest yield of protein.

The scaled up cultures of the *E. coli*-Rosetta-gami strains generated the highest yield of sRAGE (0.25 mg L^{-1} of putative monomeric form) with ~90 % of purity. The production of putative soluble aggregates was the major issue when sRAGE was expressed in *E. coli* expression systems and may have contributed to the lower yields of sRAGE observed in almost all of the *E. coli* strains including the Rosetta-gami strains. The putative monomeric form of sRAGE was confirmed to be monomeric with a molecular mass of 33 kDa as confirmed by MALDI TOF/TOF mass spectrometry. The yield of this monomeric form of sRAGE was adequate to perform *in vitro* ligand binding assays with the ligands of interest: HMGB-1 and S100A8/A9 complex (see Chapter 4).

CHAPTER 4

The binding activity of plant and *E. coli*-made recombinant human sRAGE to HMGB-1 and S100A8/A9 complex

4.1 INTRODUCTION

sRAGE was expressed in hairy root cultures of *Nicotiana tabacum* plants and in *E. coli* to obtain glycosylated and non-glycosylated sRAGE, respectively. The expressed proteins were used for *in vitro* ligand binding studies and then to compare the affinities of plant-made sRAGE and *E. coli*-made sRAGE to the ligands of interest; HMGB-1 and S100A8/A9 complex. The effect of glycosylation of sRAGE on HMGB-1 or S100A8/A9 complex was evaluated by performing *in vitro* ligand binding studies with deglycosylated (non-denatured) plant-made sRAGE. The effect of extracellular components (EDTA, divalent cations) and conditions (pH) on sRAGE binding to HMGB-1 and S100A8/A9 complex were also evaluated.

HMGB-1 is the only member of the high mobility box protein family that has been shown to interact with RAGE and develop disease pathologies, including cell death (Muhammad *et al.*, 2008), inflammation and infection (Andersson & Tracey, 2011). Although many studies have shown that the RAGE and HMGB-1 axis is related to disease pathology development (Andrassy *et al.*, 2008; Choi *et al.*, 2011), the underlying structural features that might affect the affinity between RAGE/sRAGE and HMGB-1 are not clearly understood. Therefore, the effect of glycosylation of sRAGE on the affinity of HMGB-1 was investigated here.

The S100A8/A9 complex, belonging to the calcium binding S100 protein family, is expressed in a wide variety of cell types, including circulating neutrophils and monocytes (Odink *et al.*, 1987; Roth *et al.*, 2003). The S100A8/A9 complex is known to mediate tumor-stromal interactions via RAGE, leading to inflammation associated colon carcinogenesis (Turovskaya *et al.*, 2008) and cardiomyocyte dysfunction (Boyd *et al.*, 2008). However, there is very limited information on *in vitro* binding studies of RAGE and S100A8/A9 complex in the literature (Eue *et al.*, 2002; Poulsom *et al.*, 2002).

Therefore, S100A8/A9 complex was selected as the second ligand of interest to perform *in vitro* binding studies with sRAGE.

The determination of the affinities of plant-made sRAGE and *E. coli*-made sRAGE to the ligands of interest (HMGB-1 and the S100A8/A9 complex), with respect to glycosylation of sRAGE protein and also on extracellular components and conditions, would help in determining the most feasible production system in terms of affinity, yield and purity to generate recombinant human sRAGE as a potential therapeutic in future.

4.2 MATERIALS AND METHODS

4.2.1 Enzymatic *N*-linked deglycosylation of plant and *E. coli*-made sRAGE

An enzymatic *N*-linked deglycosylation assay was performed to determine if the purified sRAGE samples were glycosylated. Plant and *E. coli*-made sRAGE were subjected to enzymatic *N*-linked deglycosylation to cleave *N*-linked glycans using the commercially available PNGase F enzyme kit (New England Bio Labs, P0704S). The control sample was comprised of non-deglycosylated sRAGE, which was prepared using the same protocol as the deglycosylated samples, except the enzyme PNGase F was not added. Concentrated sRAGE (20 µg) was mixed with 1 µL of 10X glycoprotein denaturing buffer (New England Bio Labs) and adjusted to 10 µL by adding Milli-Q water. The reaction mixture was denatured by boiling at 100 ℃ for 10 minutes, allowed to cool at room temperature for 10 minutes and then 2 µL of 10X G7 reaction buffer (0.5 M Sodium Phosphate, pH 7.5), 2 µL of 10 % NP-40 (4-Nonylphenyl-polyethylene glycol) and 2 µL of PNGase F was added. Finally, the total reaction volume was adjusted to 20 µL by adding Milli-Q water and incubated at 37 ℃ for 2.5 hours. Both the glycosylated and deglycosylated samples were loaded onto a 12 % SDS-PAGE, subjected to gel electrophoresis (see 2.2.4.1) and analysed by western blotting (see 2.2.4.2).

4.2.1.1 Enzymatic N-linked deglycosylation of plant-made sRAGE under non-denaturation

Deglycosylation of plant-made sRAGE was carried out as per the method stated in section 4.2.1 except it was not denatured by boiling. Therefore, the sRAGE was expected to retain activity in the ELISA-based ligand binding assays with HMGB-1 or S100A8/A9 complex.

4.2.1.2 Mass spectrometry of plant-made sRAGE

Plant-made sRAGE samples were concentrated to ~2 mg mL^{-1}, using 0.5 mL Amicon Ultra 3,000 MWCO, centrifugal filter devices (Merck Millipore) and subjected to deglycosylation as per the methods stated in section 4.2.1 or 4.2.1.1. Concentrated glycosylated and deglycosylated (non-denatured) plant-made sRAGE (20 μL of each) were subjected to analysis by the MALDI TOF/TOF, 4700 Proteomics Analyser (Applied Biosystems Foster City, CA, USA) at Monash University Biomedical Proteomic Facility, to determine the accurate molecular masses of the resultant fractions/bands. The mass spectral data was analysed by 4000 Series Explorer version 3.0 (see 3.2.9).

4.2.2 Ligand binding assays of sRAGE to HMGB-1 and S100A8/A9 complex

The enzyme-linked immunosorbent (ELISA) assay developed by Webster & Pickering (pers. comm.), and used to quantify the amount of sRAGE present in the hairy roots of *N. tabacum* plants (Chapter 2), was also used as the basis for developing an ELISA-based *in vitro* ligand binding assay to determine the affinity of sRAGE to HMGB-1 or to the S100A8/A9 complex. Plant-made sRAGE and the monomeric form of *E. coli*-made sRAGE were used to perform the *in vitro* ligand binding studies with the expectation of comparing the binding affinities to the ligands; HMGB-1 or S100A8/A9 complex. *E. coli* also produces putative soluble aggregates of sRAGE but these were not used to perform the *in vitro* ligand binding studies.

4.2.2.1 Binding affinity and Dissociation constant

The binding affinity is defined as the strength of the interaction between two or more molecules that bind or interact reversibly. The binding affinity is then translated into a physico-chemical term: the dissociation constant (K_d). The dissociation constant is the ligand concentration needed to occupy a half-maximum binding of protein at equilibrium (Kastritis & Bonvin, 2013). The dissociation constant is commonly used to describe the affinity between a ligand and a protein and explains how tightly a ligand binds to a particular protein.

By convention, the protein present in fixed and limited amounts will be termed the receptor protein (A), whereas the reaction component that is varied will be termed the ligand protein (B).

For a simple reversible reaction between proteins A and B we can write,
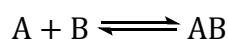
$$A + B \rightleftharpoons AB$$

When the system is at equilibrium, K_d is defined as,

$$K_d = \frac{[A]\ [B]}{[AB]}$$

Where, [A] and [B] denote the concentrations of the free proteins (reactants), whereas [AB] denotes the concentration of their bound complex (product) (Kastritis & Bonvin, 2013).

Three independent ELISA assays, each with duplicate samples were run to determine the *in vitro* binding of sRAGE and HMGB-1 or sRAGE and S100A8/A9 complex. The absorbance values were measured at a wavelength of 620 nm using a plate reader (Multiskan Ascent, Thermo Fisher Scientific). The absorbance values (absorbance values are directly proportional to the concentration of the product) were corrected by subtracting the non-specific binding of PBS buffer (PBS was used to prepare sRAGE solutions) to obtain the corrected binding values. Then, these binding values were subjected to nonlinear regression analysis using the Prism software (GraphPad prism), using the model, one-site specific binding (Figure 4.1) to obtain three independent K_d values, three independent B_{max} values and three independent goodness of fit (R^2) values. Then, the mean values (mean of three experiments) of K_d, B_{max} and the associated standard error of these mean values (SEM) were calculated using GraphPad Prism version 6. K_d, B_{max}, R^2 and SEM values of all the binding curves presented in this thesis are reported as the means of 3 individual experiments.

Model (one-site specific binding) used to analyse data in GraphPad prism version 6

$$Y = B_{max} * X / (K_d + X)$$
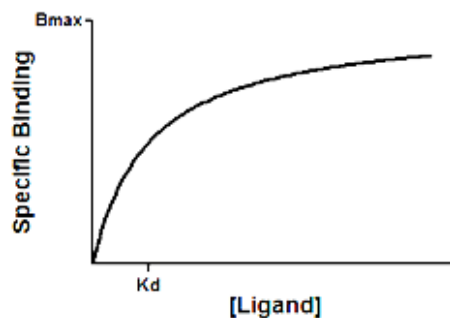
Figure 4.1 Model to show one-site specific binding curve of a protein and a ligand, after nonlinear regression analysis using the GraphPad prism software (Adapted from GraphPad curve fitting guide).

The maximum specific binding (B_{max}) is the specific binding extrapolated to very high concentrations of ligand, and therefore, its value is almost always higher than any specific binding measured in the experiment. It has the same units as the Y axis of the graph.

The dissociation constant (K_d), is the ligand concentration needed to achieve a half-maximum binding at equilibrium. It has the same units as the X axis of the graph.

R^2 is a measure of goodness of fit.

4.2.2.2 sRAGE to HMGB-1 binding assay

A high binding 96 well ELISA plate (Interpath Services) was coated with 100 μL of recombinant human HMGB-1 (Sigma, Catalogue No: H4652) prepared in the coating buffer (0.1 M NaHCO$_3$ and 0.1 M Na$_2$CO$_3$, pH 9.8) at varying concentrations (34.0 nM, 64.0 nM, 136.0 nM, 270.0 nM, 405.0 nM, 540.0 nM, 676.0 nM, 811 nM and 946.0 nM) and incubated overnight at 4 ℃. Recombinant human HMGB-1 used in this assay has a molecular weight of 25 kDa and is comprised of two homologous HMG boxes, and an acidic tail at the carboxy-terminus. Wells were aspirated and washed three times with PBS with 0.05 % tween 20 (PBST). The plate was blocked with 200 μL of 4 % skim milk in PBST (Appendix III) and incubated for 2 hours at 37 ℃ and washed with PBST three times. One hundred microliters of the monomeric form of sRAGE (*E. coli*-made, plant-made or deglycosylated (non-denatured) plant-made sRAGE) (338 nM prepared in PBS,

pH 7.4) and the control (PBS) were added in duplicate, incubated for 2 hours at 37 ℃ and then washed three times with PBST. Anti-human RAGE biotinylated antibody (R & D System) and HRP-conjugated streptavidin (R & D System) was diluted 1:500 and 1:1000 respectively with 0.5 % skim milk in PBST. Anti-human RAGE biotinylated antibody (100 μL; R & D System) was added, incubated for 1 hour at 37 ℃ and washed three times with PBST, followed by the addition of 100 μL of HRP-conjugated streptavidin (R & D System), the plate was incubated for 1 hour at 37 ℃ and washed three times with PBST. TMB (3,3′,5,5′-tetramethylbenzidine, 100 μL; Sigma) substrate was added and incubated for 30 minutes at room temperature. Finally, the absorbance was measured at a wavelength of 620 nm using a plate reader (Multiskan Ascent, Thermo Fisher Scientific). Corrected absorbance values of sRAGE to HMGB-1 binding were calculated by subtracting the values obtained for the control (PBS). This experiment was repeated three times and each experiment was with two technical repeats.

4.2.2.3 sRAGE to S100A8/A9 binding assay

The S100A8/A9 complex generally exists either in dimeric or tetrameric forms. Being the most stable and probably the biologically relevant form, the tetrameric form of S100A8/A9 complex was utilised in the experiments detailed here (Vogl *et al*., 1999; Vogl *et al*., 2006). Prior to the binding assays the molecular weight of the tetrameric form of S100A8/A9 complex (MyBioSource, Catalogue No: MBS702466) used in this assay was confirmed by SDS-PAGE.

sRAGE binding to S100A8/A9 complex assay was performed in the presence of calcium ions and zinc ions. Previous findings have emphasised the importance of calcium and zinc ions on *in vitro* binding studies of S100A8/A9 complex; *in vitro* binding of human dermal microvascular endothelial cells (HMEC-1) to S100A8/A9 complex was demonstrated to depend on calcium ions (1 mM of Ca^{2+}) (Eue *et al*., 2002) and RAGE binding to S100A9 homodimer was also shown to be strictly dependent on calcium ions (1.0 mM of Ca^{2+}) and zinc ions (0.1 mM of Zn^{2+}) (Björk *et al*., 2009). Therefore, sRAGE binding to S100A8/A9 complex assay was performed in the presence of 1.0 mM of Ca^{2+} and 0.1 mM of Zn^{2+}. sRAGE to S100A8/A9 complex binding assay was carried out as per the method stated in section 4.2.2.2, but with the following modifications:

Varying concentrations (5 nM, 20 nM, 35 nM, 50 nM, 65 nM, 80 nM, 95 nM, 110 nM and 125 nM) of recombinant S100A8/A9 complex (MyBioSource, Catalogue No:

MBS702466) were prepared in the coating buffer, (0.1 M $NaHCO_3$ and 0.1 M Na_2CO_3, pH 9.8). sRAGE (100 μL at 338 nM prepared in PBS, pH 7.4) and 100 μL of the control (PBS) were added to the high binding 96 well ELISA plate, along with calcium and zinc, at final concentrations of 1.0 mM Ca^{2+} and 0.1 mM Zn^{2+}.

4.2.3 Effect of extracellular components and conditions on sRAGE ligand binding

As part of the ligand binding studies the effects of extracellular components and conditions on sRAGE-ligand interactions, such as ethylenediaminetetraacetic acid (EDTA), divalent cations and pH were evaluated. EDTA has the ability to sequester metal ions such as Ca^{2+}, Zn^{2+}, Mg^{2+} and Fe^{3+} and as a metal chelating agent EDTA is widely used in protein interaction studies (Nyborg & Peersen, 2004). Researchers have postulated that metal chelation might promote beneficial results in Alzheimer's disease (AD) patients by inhibiting Al and/or Cu, Zn deposition in the brain (Hegde *et al*., 2009). Divalent cations in particular are found in many mechanisms, playing either structural or catalytic roles, or acting as mediators in protein-ligand complexes (Dudev & Lim, 2003; Nayal & Di Cera, 1994; Yamasita *et al*., 1990). pH significantly impacts ligand-receptor interactions by modifying the ionic nature of intermolecular interactions, which promote the ligand-receptor complex (Griko & Remeta, 1999; Lohman & Mascotti, 1992). Considering the importance of extracellular components and conditions on protein binding to ligands, the effect of EDTA, divalent cations and pH on sRAGE binding to HMGB-1 and S100A8/A9 complex was evaluated using *in vitro* ligand binding assays.

4.2.3.1 Effect of EDTA on sRAGE binding to HMGB-1

The effect of EDTA on sRAGE binding was only determined for HMGB-1. RAGE binding to S100 family proteins such as S100A9 homodimer and S100A8/A9 complex have been shown to be dependent on the both Ca^{2+} and Zn^{2+} ions (Björk *et al*., 2009; Eue *et al*., 2002). Therefore, the effect of EDTA on sRAGE binding to S100A8/A9 complex was not determined considering the necessity of Ca^{2+} and Zn^{2+} to perform the binding assay. The effect of EDTA on the binding of plant-made sRAGE or *E. coli*-made sRAGE to HMGB-1 was determined by performing an ELISA-based *in vitro* ligand binding assay (see 4.2.2.2), with the following modifications:

A high binding 96 well ELISA plate (Interpath Services) was coated with 100 μL of HMGB-1 (4 nM) (Sigma, Catalogue No: H4652) prepared in a coating buffer (0.1 M

NaHCO$_3$ and 0.1 M Na$_2$CO$_3$, pH 9.8) and kept overnight at 4 ºC. 100 µL of sRAGE (338 nM prepared in PBS, pH 7.4) along with 0.25 mM, 0.5 mM, 1.0 mM, 2.0 mM, 4.0 mM or 8.0 mM of EDTA as the final concentration and the control (sRAGE devoid of EDTA) were added in duplicate, and incubated for 2 hours at 37 ºC. This experiment was repeated three times and each experiment included two technical repeats.

4.2.3.2 Effect of divalent cations on sRAGE binding to HMGB-1 or S100A8/A9 complex

S100A8 and S100A9 are the calcium and zinc binding proteins of the S100 protein family (Schäfer & Heizmann, 1996). The importance of calcium and zinc ions for their activity has been implicated in previous studies; S100A8/A9 complex binds heparan sulfate on endothelial cells in a zinc-dependent manner (Poulsom *et al.*, 2002) and S100A9 binds to RAGE in the presence of calcium and zinc ions (Björk *et al.*, 2009). However, the structure of HMGB-1 does not show any Ca^{2+} or Zn^{2+} ion binding sites. Therefore, it is possible to speculate that the presence of these cations will not affect the *in vitro* binding assays between sRAGE and HMGB-1. The effects of divalent cations on sRAGE binding to HMGB-1 or S100A8/A9 complex was determined by performing the ELISA-based *in vitro* binding assay (as stated in the previous section) in the presence of different combinations of cations; Ca^{2+} and Zn^{2+}, Mg^{2+} and Zn^{2+} or Ca^{2+}, Mg^{2+} and Zn^{2+}. However, some modifications to the original protocol were made:

A high binding 96 well ELISA plate (Interpath Services) was coated with 100 µL of HMGB-1 (4 nM) or 100 µL of S100A8/A9 complex (2 nM) prepared in a coating buffer (0.1 M NaHCO$_3$ and 0.1 M Na$_2$CO$_3$, pH 9.8) and kept overnight at 4 ºC. 100 µL of sRAGE (338 nM prepared in PBS, pH 7.4) along with 1.0 mM of Ca^{2+}, 1.0 mM of Mg^{2+} or 0.1 mM of Zn^{2+} and the control (sRAGE devoid of divalent cations) were added in duplicate (EDTA was not added). This experiment was repeated three times and each experiment had two technical repeats.

4.2.3.3 Effect of pH on sRAGE binding to HMGB-1 or S100A8/A9 complex

Acetate-MES-Tris (AMT) buffer (Appendix III) was selected to prepare a range of pH solutions to investigate the effect of pH on the binding of sRAGE to HMGB-1 or S100A8/A9 complex. AMT buffer provides a constant ionic strength over the required pH range, which is important when studying pH dependent processes (Ellis & Morrison,

1982). The assay to determine the effect of pH on sRAGE to HMGB-1 or S100A8/A9 complex binding was performed as per the methods in section 4.2.2.2 and 4.2.2.3 respectively, but with the following modifications:

A pH series ranging from 5.0 to 9.0 (5.0, 5.5, 6.0 6.5, 7.0, 7.5, 8.0, 8.5 and 9.0) was prepared using AMT buffer adjusted to the appropriate pH with NaOH or HCl (Appendix III). sRAGE was added to the AMT buffer series to a final concentration of 338 nM and 100 µL used in the binding assay. AMT buffer at each pH, without sRAGE, was used as controls. This experiment was repeated three times and each experiment contained two technical repeats.

4.2.4 Data analysis

The effects of extracellular components and conditions on sRAGE binding to HMGB-1 or S100A8/A9 complex were statistically analysed using GraphPad Prism version 6. The two-tailed paired t-test was performed to evaluate statistical differences between the two data groups. A p-value of <0.05 was considered to be statistically significant.

4.3 RESULTS

4.3.1 Enzymatic *N*-linked deglycosylation

4.3.1.1 Deglycosylation and western blot analysis of plant-made sRAGE

Plant-made sRAGE was subjected to enzymatic *N*-linked deglycosylation and western blot analysis to determine whether the protein had undergone glycosylation. The resultant western blot of putative glycosylated and deglycosylated plant-made sRAGE samples are shown below (Figure 4.1).

Figure 4.1 Western blot analysis of deglycosylated plant-made sRAGE. Lane M, protein molecular mass markers (kDa); lane 1, putative glycosylated sRAGE; lane 2, deglycosylated sRAGE. The protein molecular weight markers were visible on the western blot and were marked on the X-ray following alignment.

The putative glycosylated sRAGE showed two bands corresponding to the molecular weights of ~45 kDa and ~37 kDa (Figure 4.1, lane 1). The expected size of sRAGE, based on the amino acid sequence, is 34.5 kDa. Proteins expressed in plant systems are likely to be *N*-glycosylated, which would result in the larger proteins observed. This is supported by the visualisation of four bands following deglycosylation (lane 2): band 1 aligned at ~43 kDa: band 2 appeared at ~37 kDa; bands 3 and 4 at ~36 kDa and ~33 kDa, respectively. Similar changes in protein patterns were observed by Hanford *et al.* (2004) in the analysis of mouse sRAGE. These results indicate that the plant made sRAGE is glycosylated.

4.3.1.2 Mass spectral analysis of plant-made sRAGE

The deglycosylated (non-denatured) plant-made sRAGE and glycosylated plant-made sRAGE were subjected to MALDI TOF/TOF mass spectroscopy, to determine the molecular masses of the proteins. It was expected that this would provide an estimate of the the molecular mass of the *N*-linked glycans by comparing the molecular mass of deglycosylatd (non-denatured) plant-made sRAGE and glycosylated plant-made sRAGE. However, data was only obtained for deglycosylated sRAGE and lower mass peaks than expected were observed, with the two major peaks at ~11 kDa and ~23 kDa (Figure 4.2). The reasons for the appearance of these low mass peaks are not known and due to circumstances at Monash University these experiments could not be repeated. Mass spectral data was successfully obtained for *E. coli*-made sRAGE (Figure 3.12).
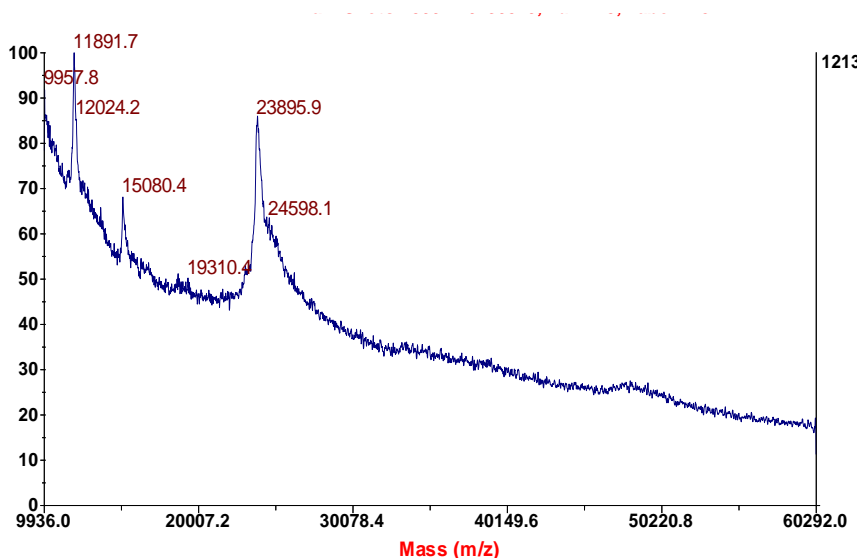
Figure 4.2 MALDI TOF/TOF mass spectrometry, to determine the accurate mass of deglycosylated (non-denatured) plant-made sRAGE. Desalted sample is mixed 1:1 with Matrix, 10 mg mL^{-1} a-cyano-4-hydroxycinnamic acid (Laser BioLabs, Sophia-Antipolis, France) in 50 % Acetonitrile, 0.1 % TFA) and spotted onto the MALDI target plate of MALDI TOF/TOF, 4700 Proteomics Analyser (Applied Biosystems Foster City, CA, USA).

4.3.1.3 Deglycosylation and western blot analysis of E. coli-made sRAGE

E. coli-made sRAGE were subjected to enzymatic *N*-linked deglycosylation as per the method stated in section 4.2.1. Putative non-glycosylated *E. coli*-made sRAGE and deglycosylated sRAGE samples were subjected to western blot analysis (Figure 4.3) to determine the molecular weights of the bands.
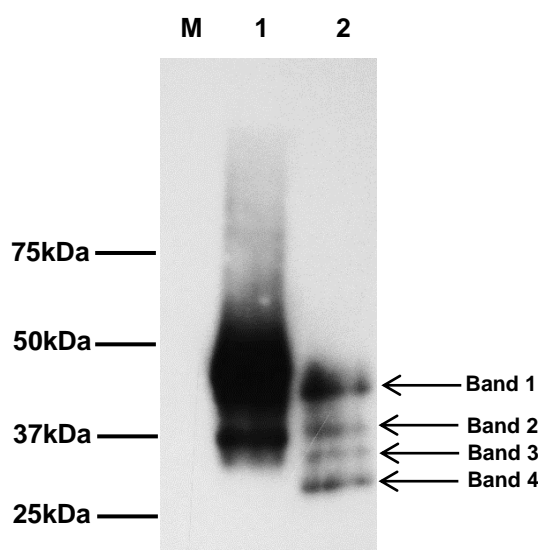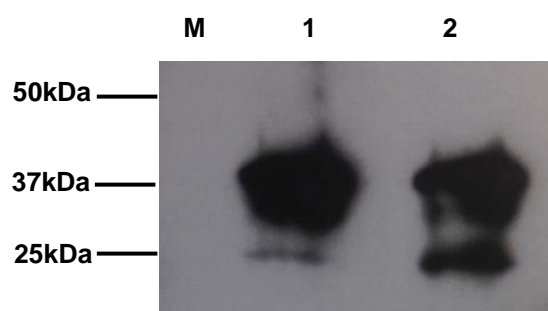

Figure 4.3 Western blot analysis of deglycosylated *E. coli*-made sRAGE. Lane M, protein molecular mass markers (kDa); lane 1, non-deglycosylated sRAGE; lane 2, deglycosylated sRAGE. The protein molecular weight markers were visible on the western blot and were marked on the X-ray following alignment.

E. coli-expressed sRAGE appeared predominantly as a ~37 kDa band (Figure 4.3). The ~25 kDa band may have resulted as a cleavage product of sRAGE and was also observed previously (Chapter 3) where the molecular mass of the monomeric form of *E. coli*-made sRAGE was determined to be 33 kDa based on MALDI TOF/TOF mass spectrometry, (Figure 3.12). The intensity of the ~37 kDa band in lane 1 and 2 was similar, whilst, the intensity of the ~25 kDa band was lower in lane 2, than in lane 1. However, there was no apparent difference between the molecular weights of the bands before (lane 1) and after deglycosylation (lane 2). This similarity suggests that *E. coli*-expressed sRAGE has not undergone *N*-linked glycosylation, which would be expected as in general *E. coli* made sRAGE is not glycosylated.

4.3.2 sRAGE binding to HMGB-1

The binding of the different forms of sRAGE to the HMGB-1 ligand was modelled using one-site specific binding. Glycosylated and deglycosylated plant-made sRAGE, and *E. coli*-made sRAGE was subjected to an ELISA-based binding assay in the presence of varying concentrations of human HMGB-1.

The K_d value of glycosylated plant-made sRAGE to HMGB-1 binding was 129.6 nM ± 18.8 nM (Figure 4.4A). The maximum specific binding (B_{max}) value was 0.54 ± 0.01 and the measure of goodness of fit (R^2) value was 0.97 ± 0.01. The K_d value of the plant-made deglycosylated sRAGE to HMGB-1 was 227.8 nM ± 38.0 nM. The maximum specific binding (B_{max}) value was 0.63 ± 0.03 and the measure of goodness of fit (R^2) value was 0.94 ± 0.01 (Figure 4.4B). When compared to the glycosylated plant-made sRAGE to HMGB-1 binding (129.6 nM ± 18.8 nM, Figure 4.4A); deglycosylated (non-denatured) plant-made sRAGE showed a significantly (P<0.05) lower affinity to HMGB-1.

In the analysis of the binding between *E. coli*-made sRAGE and HMGB-1 the last two data points (1008 nM and 1220 nM) were trending downwards (Figure 4.4, inset D). Therefore, the data set excluding these two data points was re-analysed to obtain a new one-site specific binding curve (Figure 4.4C). The K_d value of *E. coli*-made sRAGE to HMGB-1 binding was 201.4 nM ± 14.5 nM. The maximum specific binding (B_{max}) value was 1.19 ± 0.06 and the measure of goodness of fit (R^2) value was 0.963 ± 0.005 (Figure 4.4C). The affinity of *E. coli*-made sRAGE to HMGB-1 was significantly lower (P<0.05) than that of glycosylated plant-made sRAGE (129.6 nM ± 18.8 nM) but not significantly different from deglycosylated (non-denatured) plant-made sRAGE to HMGB-1 (227.8 nM ± 38.0 nM).
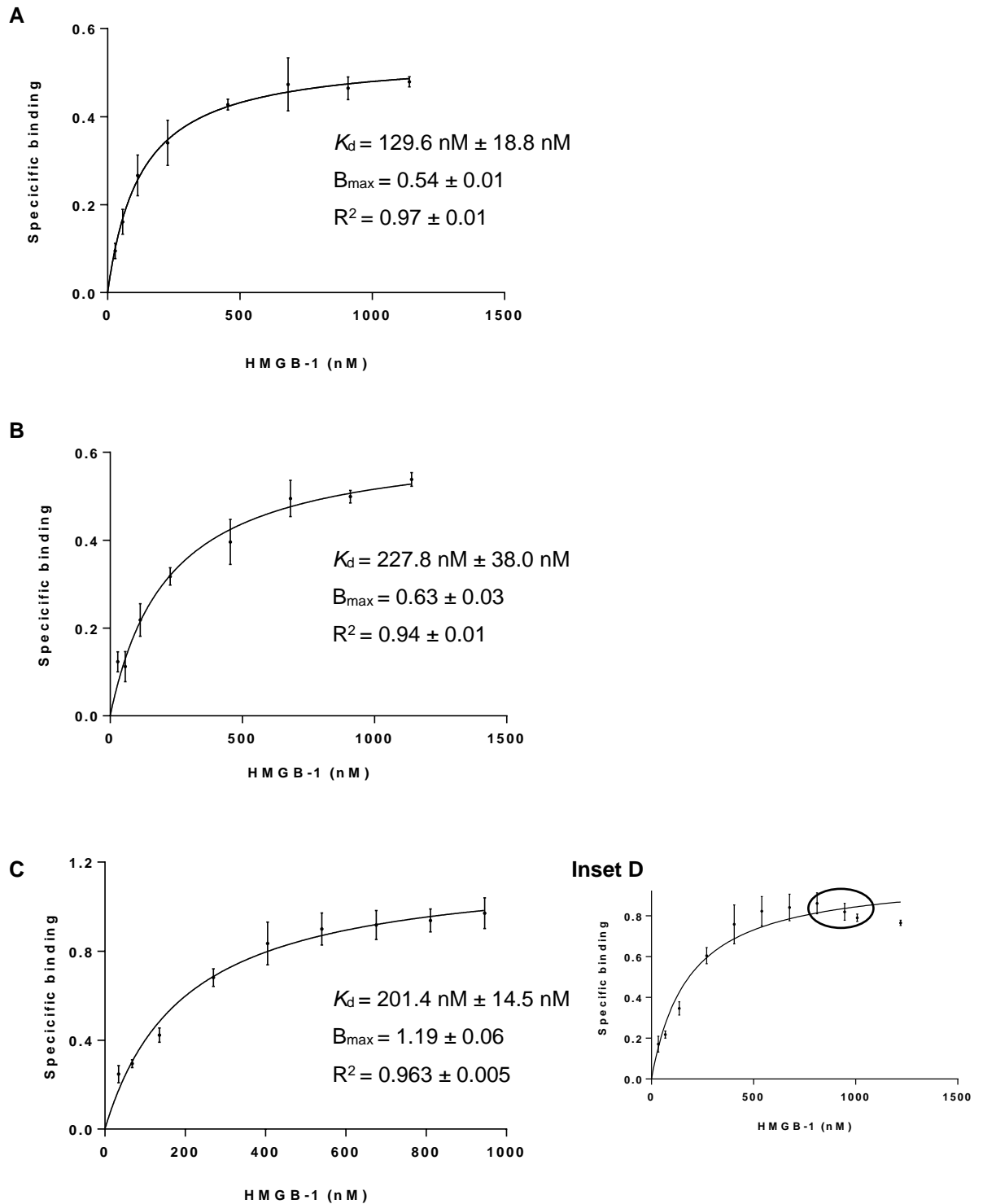
Figure 4.4 One-site specific binding curves of sRAGE to HMGB-1. A. Glycosylated plant-made sRAGE; B. Deglycosylated (non-denatured) plant-made sRAGE to HMGB-1; C. *E. coli*-**made sRAGE to HMGB-1; inset D. shows the two last data points of one-site specific binding curve of** *E. coli*-**made sRAGE to HMGB-1 trending downwards. Error bars show the standard error of the mean calculated from 3 experiments, each experiment is with 2 technical repeats.**

4.3.3 The effects of extracellular components on sRAGE binding to HMGB-1

The effects of extracellular components on sRAGE binding to HMGB-1 were determined by performing ELISA-based *in vitro* ligand binding assays, as per the methods stated in section 4.2.3.1, 4.2.3.2 and 4.2.3.3.

4.3.3.1 The effect of EDTA on plant-made sRAGE to HMGB-1 binding

The effect of EDTA on plant-made sRAGE to HMGB-1 was assessed using ELISA-based *in vitro* ligand binding assay, as per the method stated in section 4.2.3.1. The data was compared to the no-EDTA control (Figure 4.5A).

Higher concentrations of EDTA, greater than 2 mM, significantly inhibited binding between sRAGE and HMGB-1 (Figure 4.5A). The no-EDTA control demonstrated the highest degree of ligand binding (0.74 ± 0.08). The binding values in the presence of relatively low concentrations of EDTA; 0.25 mM (0.61 ± 0.01), 0.5 mM (0.55 ± 0.04) and 1.0 mM (0.58 ± 0.03) were similar to the no-EDTA control treatment. These binding values were not statistically different from each other (Figure 4.5A). There was a negative correlation between binding affinities and increasing concentrations of EDTA (2.0 mM to 8.0 mM) with values (2.0 mM of EDTA= 0.34 ± 0.02, 4.0 mM of EDTA= 0.34 ± 0.03 and 8.0 mM of EDTA= 0.36 ± 0.03) significantly lower than that of the no-EDTA control.

4.3.3.2 The effect of EDTA on E. coli-made sRAGE to HMGB-1 binding

The effect of EDTA on *E. coli*-made sRAGE to HMGB-1 was assessed using ELISA. The data was compared to the no-EDTA control (Figure 4.5B). The highest binding was observed in the absence of EDTA (0.76 ± 0.03). The binding values in the presence of lower concentrations of EDTA; 0.25 mM (0.73 ± 0.03), 0.5 mM (0.71 ± 0.01) and 1.0 mM (0.70 ± 0.02) were similar and not significantly different from one another (Figure 4.5B). Furthermore, these binding values were not significantly different to the no-EDTA control. However, with the increased concentrations of EDTA; 2 mM (0.58 ± 0.02), 4 mM (0.45 ± 0.02), and 8 mM (0.41 ± 0.06), there was a significant reduction in the mean binding values when compared to the no-EDTA control.

A

B
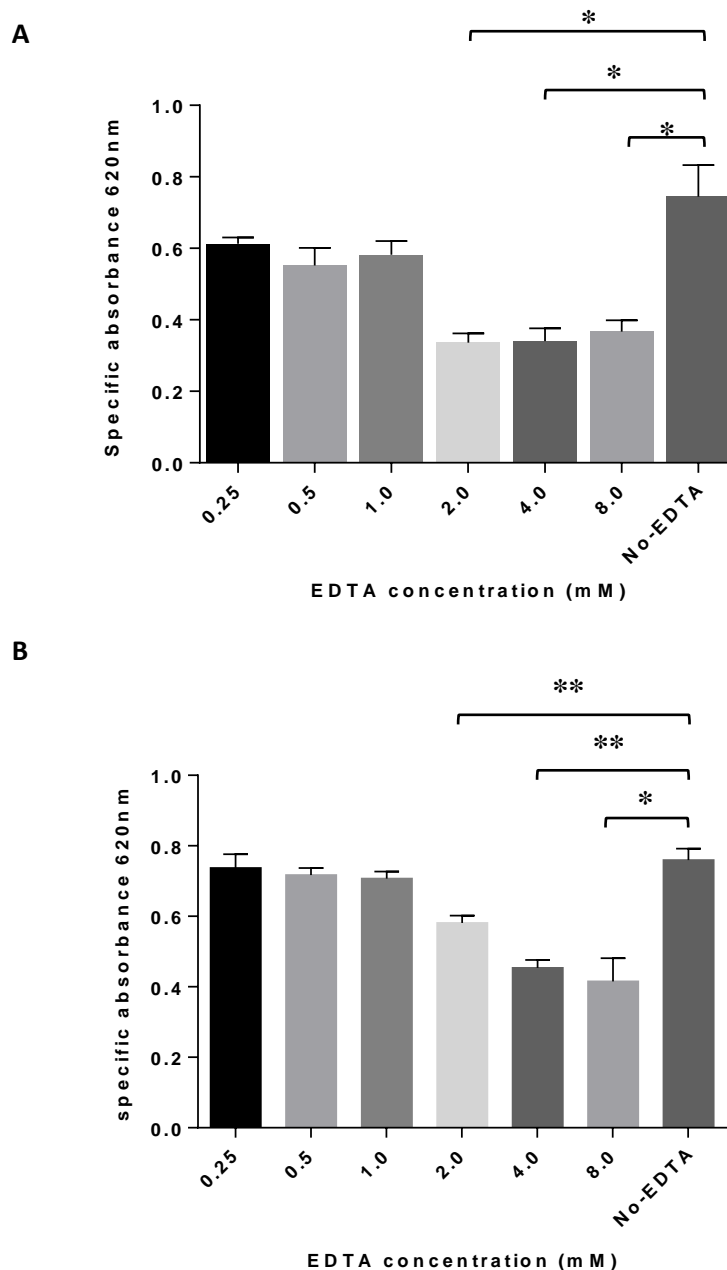
Figure 4.5 The effect of EDTA on sRAGE binding to HMGB-1. A. plant-made sRAGE; B *E. coli*-made sRAGE. Error bars show the standard error of the mean calculated from 3 experiments, each experiment is with 2 technical repeats. Binding values under different EDTA concentrations were compared to the no-EDTA control. Statistical significance is denoted by an asterisk (*P<0.05, **P<0.01, by *t*-test).

4.3.3.3 The effect of divalent cations on plant-made sRAGE to HMGB-1 binding

The effect of divalent cations on plant-made sRAGE to HMGB-1 binding was determined in the presence of three divalent cations (Ca^{2+}, Mg^{2+} and Zn^{2+}) in different combinations. The data were compared with the no-divalent cations control (Figure 4.6A). The highest

mean binding (0.65 ± 0.04) was observed in the control reaction that didn't contain any additional cations. The mean binding values in the presence of any combination of cations were statistically similar and significantly lower than the no-divalent cation control reaction (Figure 4.6A). The combination of two cations gave similar binding values (Ca^{2+}/Zn^{2+} (0.17 ± 0.09) and Mg^{2+}/Zn^{2+} (0.18 ± 0.07)), whilst the lowest binding value was observed in the presence of all three cations, Ca^{2+}, Mg^{2+} and Zn^{2+} (0.13 ± 0.01).

4.3.3.4 The effect of divalent cations on E. coli-made sRAGE to HMGB-1 binding

The highest binding for *E. coli*-made sRAGE to HMGB-1 was observed in the absence of divalent cations (0.76 ± 0.03). The mean binding values in the presence of any combination of cations were significantly lower compared to the no-divalent cations control (Figure 4.6B). However, binding in the presence of the three cations combination, $Ca^{2+}/Mg^{2+}/Zn^{2+}$ (0.50 ± 0.01) was significantly higher than that of cations-pairs Ca^{2+}/Zn^{2+} ($P<0.001$) and also Mg^{2+}/Zn^{2+}. In comparing the cations-pairs, *E. coli*-made sRAGE to HMGB-1 binding was significantly lower in the presence of Ca^{2+}/Zn^{2+} (0.21 ± 0.01) than Mg^{2+}/Zn^{2+} (0.35 ± 0.03).
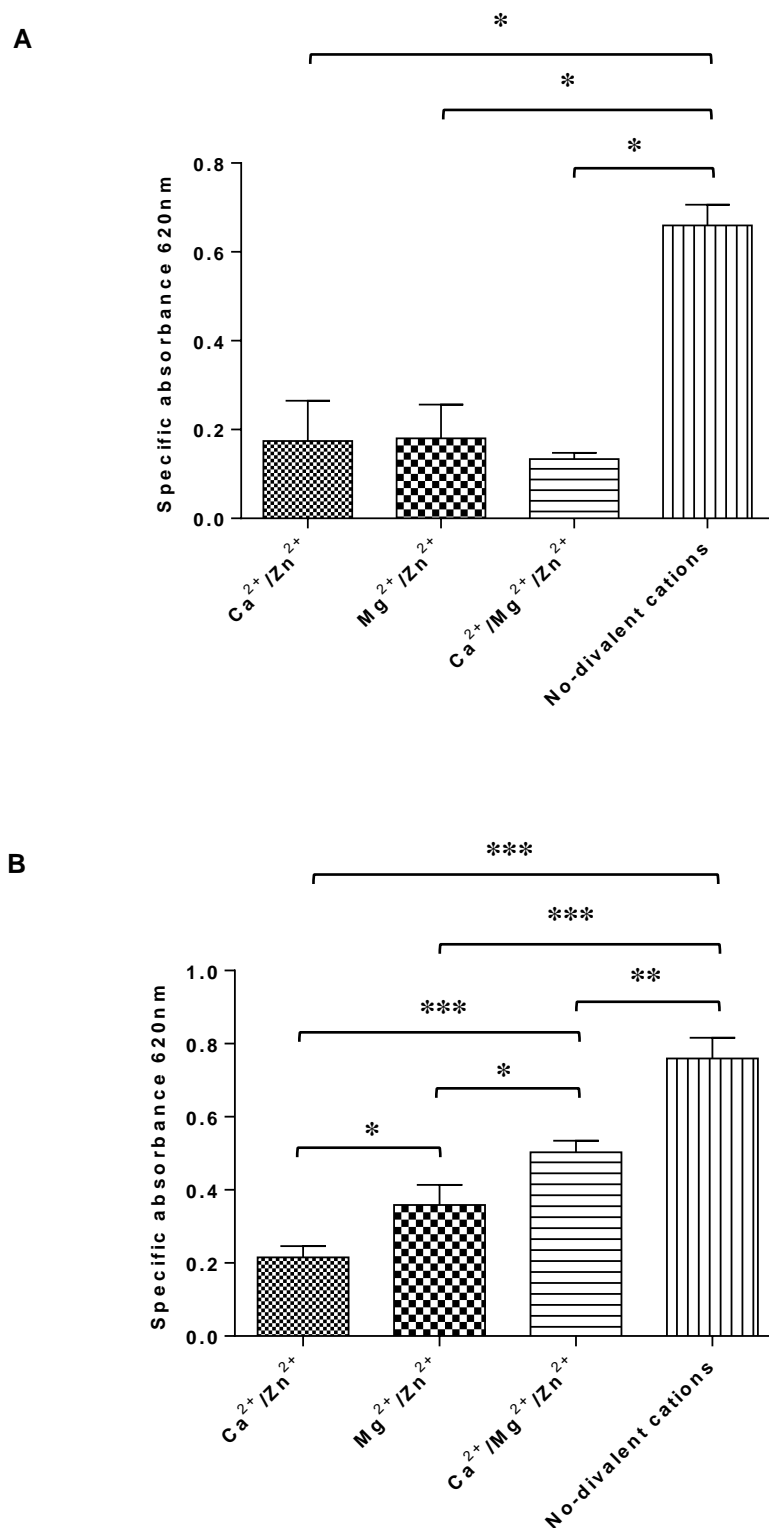
Figure 4.6 The effect of divalent cations on sRAGE binding to HMGB-1. A. plant-made sRAGE; B *E. coli*-made sRAGE. Binding values under different divalent cations were compared with the no-divalent cations control. Error bars show the standard error of the mean calculated from 3 experiments, each experiment is with 2 technical repeats. Statistical significance is denoted by asterisks (* P<0.05, ** P<0.01, *** P<0.001 by *t*-test).

4.3.3.5 The effect of pH on plant-made sRAGE to HMGB-1 binding

The effect of pH on plant-made sRAGE binding to HMGB-1 was assessed using an ELISA-based *in vitro* ligand binding assay under a series of pH values. The data was compared with the results of binding under neutral pH 7.0 conditions (Figure 4.7A).

The highest binding (1.66 ± 0.07) was observed at an acidic pH value of 5.5 and this value was statistically significant to that observed at pH 7.0 (0.58 ± 0.12). The binding values observed for pH 5.0 (1.33 ± 0.02) and pH 6.0 (1.40 ± 0.03) were also statistically significant when compared with the binding observed at pH 7.0. Binding values decreased as the pH values became more basic (pH 8.0= 0.44 ± 0.07, pH 8.5= 0.36 ± 0.07 and pH 9.0= 0.35 ± 0.09) but it was not significantly different from that at pH 7 (Figure 4.7A).

4.3.3.6 The effect of pH on E. coli-made sRAGE to HMGB-1 binding

The highest binding (1.20 ± 0.03) was observed at a slightly acidic pH value of 6.5 and this was the only absorbance value that was significant when compared to control conditions at neutral pH 7.0 (1.04 ± 0.01). As conditions became more acidic (below pH 6.5) binding decreased. There was no significant difference in binding with increasing pH (Figure 4.7B).
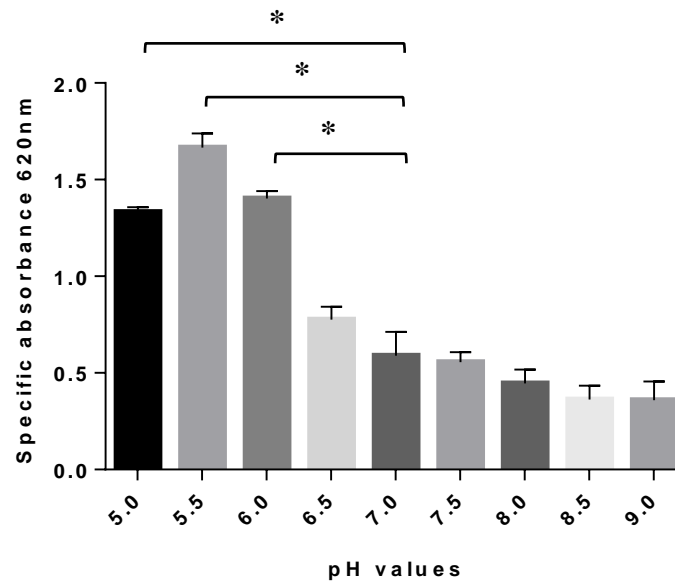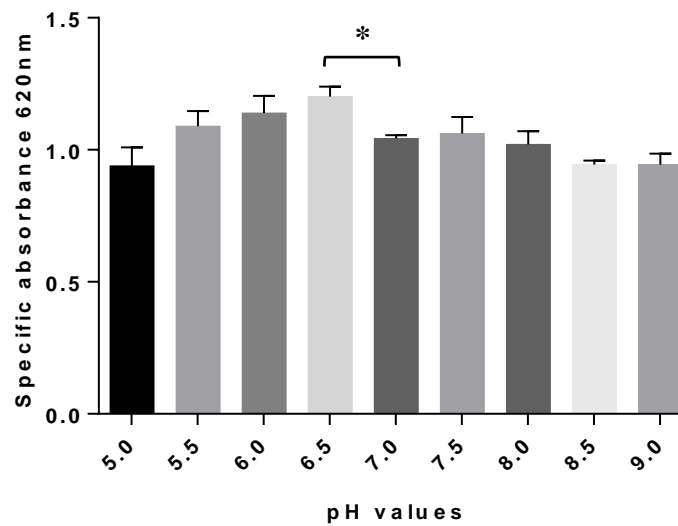
Figure 4.7 The effect of pH on sRAGE binding to HMGB-1. A. plant-made sRAGE; B. *E. coli*-made sRAGE. Binding values as a result of different pH concentrations were compared to binding value in a neutral pH 7.0. Error bars show the standard error of the mean calculated from 3 experiments, each experiment is with 2 technical repeats. Statistical significance is denoted by an asterisk (* P<0.05, by *t*-test).

4.3.4 sRAGE binding to S100A8/A9 complex

Prior to the binding assays the molecular weight of the tetrameric form of S100A8/A9 complex (MyBioSource, Catalogue No: MBS702466) used in this assay was confirmed by SDS-PAGE to be ~50 kDa (Figure 4.8).
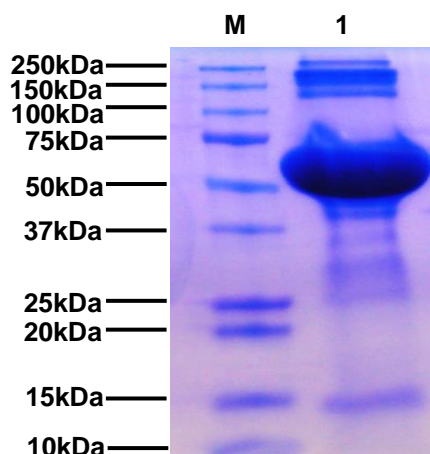
Figure 4.8 Analysis of tetrameric form of S100A8/A9 complex used to perform *in vitro* ligand binding assays with sRAGE. Lane M, protein molecular mass markers (kDa); lane 1, tetrameric form of S100A8/A9 complex. The proteins were visualised with Coomassie Brilliant Blue.

sRAGE binding to S100A8/A9 complex was determined by performing an ELISA-based *in vitro* ligand binding assay in the presence of varying concentrations of S100A8/A9 complex (see 4.2.2.3).

The dissociation constant value (K_d) of glycosylated plant-made sRAGE binding to S100A8/A9 complex was found to be 4.8 nM ± 2.4 nM. The maximum specific binding (B_{max}) value was 0.64 ± 0.05 and the measure of goodness of fit (R^2) value was 0.84 ± 0.04 (Figure 4.9A).

The dissociation constant value (K_d) of deglycosylated plant-made sRAGE binding to S100A8/A9 complex was 14.3 nM ± 2.6 nM. The maximum specific binding (B_{max}) value was 0.58 ± 0.03 and the measure of goodness of fit (R^2) value was 0.88 ± 0.05 (Figure 4.9B). However, the binding potentials (K_d values) of glycosylated and deglycosylated plant-made sRAGE to S100A8/A9 complex were not statistically different from each other.

The dissociation constant value (K_d) for *E. coli*-made sRAGE binding to S100A8/A9 complex was found to be 6.1 nM ± 1.9 nM. The maximum specific binding (B_{max}) value was 0.94 ± 0.14 and the measure of goodness of fit (R^2) value was 0.62 ± 0.09 (Figure 4.9C). However, the binding potential of *E. coli*-made sRAGE binding to S100A8/A9 complex was not statistically different to that of glycosylated plant-made sRAGE (K_d = 4.8 nM ± 2.4 nM) or deglycosylated (non-denatured) plant-made sRAGE (K_d = 14.3 nM ± 2.6 nM).
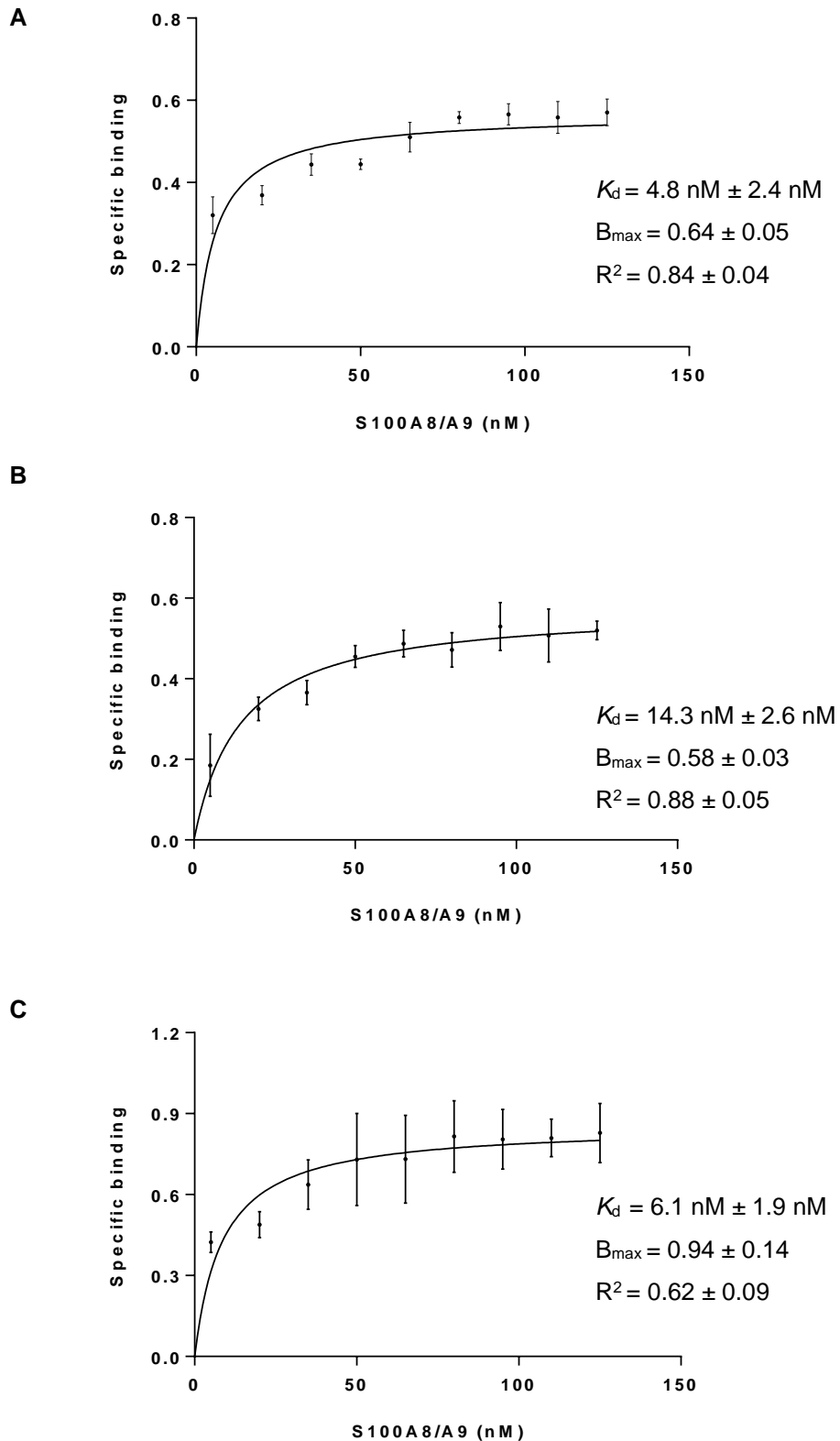
Figure 4.9 One-site specific binding curve of sRAGE to S100A8/A9 complex. A. glycosylated plant-made sRAGE; B. deglycosylated (non-denatured) plant-made sRAGE; C. *E. coli*-made sRAGE. Error bars show the standard error of the mean calculated from 3 experiments, each experiment is with 2 technical repeats.

4.3.5 The effects of extracellular components on sRAGE binding to S100A8/A9 complex

The effects of extracellular components on sRAGE binding to S100A8/A9 complex were determined by performing ELISA-based *in vitro* ligand binding assays, as per the methods stated in section 4.2.3.1, 4.2.3.2 and 4.2.3.3.

4.3.5.1 The effect of divalent cations on plant-made sRAGE to S100A8/A9 binding

The effect of divalent cations on plant-made sRAGE binding to S100A8/A9 complex is shown in Figure 4.10A. The data was compared with the no-divalent cations control.

The binding value (0.10 ± 0.01) of plant-made sRAGE to S100A8/A9 complex were significantly lower in the absence of divalent cations (Figure 4.10A), which is in contrast to HMGB-1 binding where lower binding values were observed in the presence of divalent cations (Figure 4.6A). All three combinations of divalent cations; Ca^{2+}/Zn^{2+} (0.91 ± 0.02), Mg^{2+}/Zn^{2+} (0.94 ± 0.02) and $Ca^{2+}/Mg^{2+}/Zn^{2+}$ (0.85 ± 0.20) generated significantly higher binding values than that observed in the no-divalent cations control (Figure 4.10A. There was no statistical difference between the different combinations of cations and sRAGE binding to S100A8/A9 complex.

4.3.5.2 The effect of divalent cations on E. coli-made sRAGE binding to S100A8/A9 complex

For *E. coli*-made sRAGE, the lowest binding to S100A8/A9 complex was observed in the absence of divalent cations (0.05 ± 0.004). All three combinations of divalent cations; Ca^{2+}/Zn^{2+} (0.78 ± 0.04), Mg^{2+}/Zn^{2+} (0.79 ± 0.07) and $Ca^{2+}/Mg^{2+}/Zn^{2+}$ (0.74 ± 0.08) demonstrated significantly increased binding between *E. coli*-derived sRAGE and S100A8/A9 complex when compared to the no-divalent cations control (Figure 4.10B).

Figure 4.10 The effect of divalent cations on sRAGE binding to S100A8/A9 complex. A. Plant-made sRAGE; B. *E. coli*-made sRAGE. Binding values under different divalent cations were compared with the no-divalent cations control. Error bars show the standard error of the mean calculated from 3 experiments, each experiment is with 2 technical repeats. Statistical significance is denoted by asterisks (** P<0.01, *** P<0.001, **** P<0.0001 by *t*-test).

4.3.5.3 The effect of pH on plant-made sRAGE binding to S100A8/A9 complex

The effect of pH on plant-made sRAGE binding to S100A8/A9 complex was determined by performing *in vitro* ligand binding assay in the presence of a series of pH solutions as per the method stated in section 4.2.3.3. The data was compared with neutral pH 7.0 (Figure 4.11A).

The lowest binding was observed at the neutral pH 7.0 (0.45 ± 0.02) with binding increasing with both decreases and increases in pH. The binding values observed in an acidic pH range from 5.0 to 6.0 were lower than the binding values observed at basic pH values of 7.5 to 9.0. Binding at pH 5.0 (0.62 ± 0.02) and 5.5 (0.64 ± 0.02) were statistically higher than binding at pH 7.0 (0.44 ± 0.01). The binding observed at pH 6.5 (0.45 ± 0.02) was significantly lower than binding observed at pH 5.0 and 5.5 but there was no significant difference for pH 6.0 and 7.0. From pH 7.5 (physiological pH) (0.64 ± 0.11) binding affinity increased as the solution became more alkaline until it reached the maximum at pH 9.0 (1.28 ± 0.07) (Figure 4.11A).

4.3.5.4 The effect of pH on E. coli-made sRAGE binding to S100A8/A9 complex

The effect of pH on *E. coli*-made sRAGE to S100A8/A9 complex was assessed using ELISA. The data was compared to neutral pH of 7.0 (Figure 4.11B).

For *E. coli*-made sRAGE binding to S100A8/A9 complex, there was generally no impact of pH on the receptor-ligand interaction within the pH range of 5.5 to 9.0: binding fluctuated in a narrow range of 0.6 to 0.7 nm. The highest binding of sRAGE to S100A8/A9 complex was observed at pH 5.0 (1.60 ± 0.07) and this value is more than double that observed at pH 5.5 to 9.0. One could argue that this value may be an outlier. Therefore, this pH point was repeated with more replicates several times but similar absorbance values were observed. Therefore, this higher binding observed at pH 5.5 should not be ignored. The binding values at pH 5.5 to 6.5 were not significantly different from one another, but the binding observed at pH 5.0 (1.60 ± 0.07) and 5.5 (0.70 ± 0.02) were significantly different to binding observed at pH 7.0 (0.62 ± 0.03). The binding at physiological pH of 7.5 was 0.73 ± 0.02. The binding observed at pH 8.0 was significantly higher than that observed at pH 7.0. Binding at pH 8.5 (0.68 ± 0.04) and 9.0 (0.68 ± 0.05) was almost similar (Figure 4.11B).

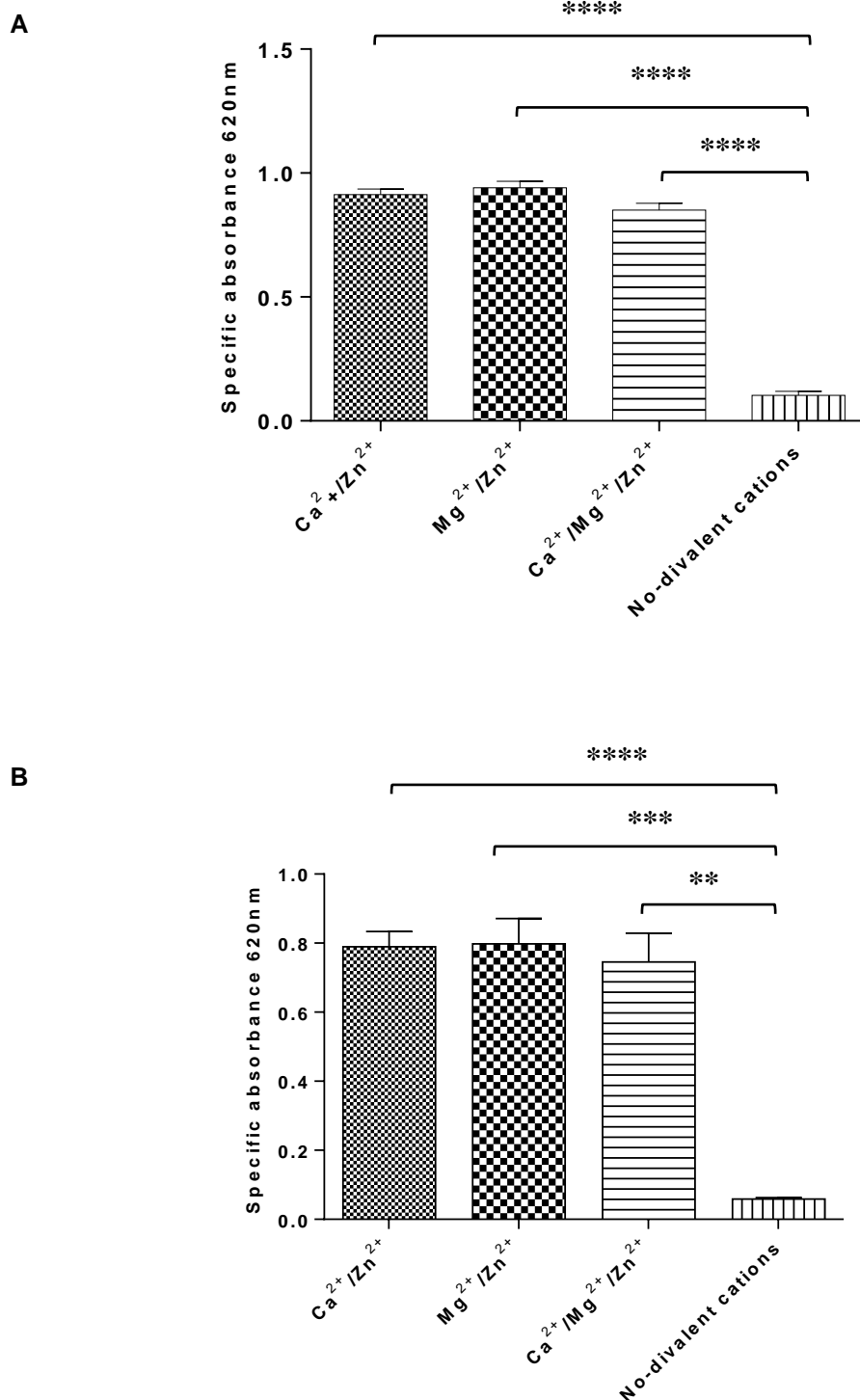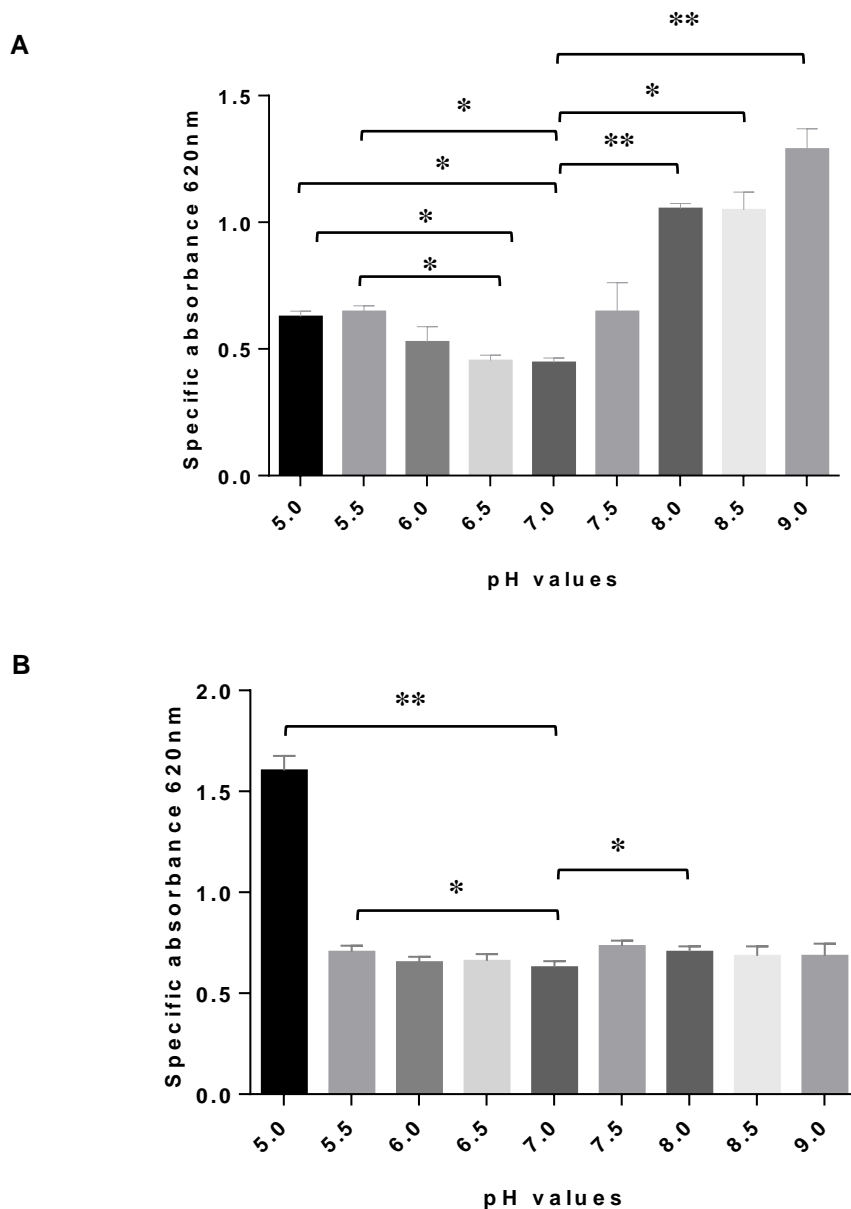**Figure 4.11 The effect of pH on sRAGE binding to S100A8/A9 complex. A. Plant-made sRAGE; B. *E. coli*-made sRAGE. Binding values under different pH solutions were compared with pH 7.0. Error bars show the standard error of the mean calculated from 3 experiments, each experiment is with 2 technical repeats. Statistical significance is denoted by asterisks (* P<0.05, ** P<0.01 by *t*-test).**

4.4 DISCUSSION

Investigating the structural basis for the interaction between recombinant sRAGE and the ligands, HMGB-1 or S100A8/A9 complex, and also the determination of the full-extracellular domain of plant-made sRAGE were major aims of this research project. To accomplish these objectives sRAGE was expressed in the hairy roots of *Nicotiana tabacum* plants and in an *E. coli* expression system to obtain glycosylated and non-glycosylated sRAGE, respectively. High mobility group box family proteins (HMGB-1) and the calgranulin family proteins (S100A8/A9 complex), were selected as the ligands of interest in this study; firstly, the structures of these ligands are less heterologous than other ligands of RAGE, such as advanced glycation end products (AGEs) and, secondly, due the limited information in the current literature on the binding of sRAGE to HMGB-1 and S100A8/A9 complex.

An ELISA-based *in vitro* binding assay was performed to determine the affinity of the glycosylated plant-made sRAGE, the *E. coli*-made (non-glycosylated) sRAGE and deglycosylated (non-denatured) plant-made sRAGE to HMGB-1 or S100A8/A9 complex. The ELISA-based binding assay is an indirect method that can be used to measure binding of protein-protein or protein-ligand interactions where the assumption is made that the measured signal is directly proportional to the concentration of the product, assuming that the proteins exist in only two states: the free and the bound populations, with each having its unique optical characteristic (Kastritis & Bonvin, 2013). ELISA-based 96 well microtiter plate assays serve as a quick, cheap and reproducible method for determining protein-ligand interactions compared to other methods such as surface plasmon resonance (SPR), isothermal titration calorimetry (ITC), and bead-based pull-down assays using affinity tags. SPR and ITC are powerful methods for assaying protein-ligand interactions, but are expensive to implement. Alternatively, bead-based pull-down assays using affinity tags require no specialist equipment and, therefore, are the most popular method for analysing protein-protein interactions but time-consuming and prone to variability (Craig *et al*., 2004).

Then the effect of glycosylation of sRAGE on HMGB-1 or S100A8/A9 binding was evaluated by comparing the binding affinities of glycosylated sRAGE and non-glycosylated and deglycosylated sRAGE to the ligands. As part of the ligand binding

studies the effects of extracellular components and conditions on sRAGE-ligand interactions, such as the presence of EDTA, divalent cations and pH, were evaluated.

Glycosylated plant-made sRAGE showed a significantly higher affinity to HMGB-1 (K_d = 129.6 nM ± 18.8 nM, Figure 4.4A) compared to non-glycosylated *E. coli*-made sRAGE (K_d = 201.4 nM ± 14.5 nM, Figure 4.4C). These dissociation constant (K_d) values are higher compared to the reported dissociation constant value of 97 nM generated as a result of HMGB-1 and RAGE interaction based on surface plasmon resonance (SPR) studies (Ling *et al.*, 2009). However, the dissociation constant values (K_d) of the present study are lower than a value of 710 nM reported in a previous study that used an ELISA-based binding assay to determine the affinity of *E. coli*-made sRAGE to HMGB-1 (Liu *et al.*, 2009). Another study that used an ELISA-based binding assay to determine the affinity of bovine lung RAGE binding to recombinant rat HMGB-1 has reported a dissociation constant value of 10.2 nM (Hori *et al.*, 1995). These differences may be due to variations in experimental conditions. Similarly, glycosylated plant-made sRAGE showed a higher affinity to S100A8/A9 (K_d = 4.8 nM ± 2.4 nM, Figure 4.9A) compared to *E. coli*-made sRAGE (K_d = 6.1 nM ± 1.9 nM, Figure 4.9C). However, these K_d values were not significantly different from each other. Dissociation constant values observed for S100A8/A9 binding in the present study are comparable to a dissociation constant value of 9.4 nM that was observed when RAGE binding to S100A9 homodimer was performed (Björk *et al.*, 2009) and a K_d value of 6 nM observed for heparin binding to S100A8/A9 complex (Robinson *et al.*, 2002). S100A8/A9 complex is a member of S100 protein family and these generally have higher affinities for their target proteins, such as RAGE (reviewed in Santamaria-Kisiel *et al.*, 2006).

The affinity of plant-made sRAGE to HMGB-1 as well as to S100A8/A9 complex decreased with the deglycosylation of sRAGE (Table 4.1). The binding potential of deglycosylated (non-denatured) plant-made sRAGE to HMGB-1 (227.8 nM ± 38.0 nM) was significantly lower than that of glycosylated plant-made sRAGE (129.6 nM ± 18.8 nM). Similarly, a lower affinity of plant-made sRAGE to S100A8/A9 complex (14.3 nM ± 2.6 nM, Figure 4.9B) was observed in the absence of glycosylation. However, the binding potential of deglycosylated (non-denatured) plant-made sRAGE to S100A8/A9 complex was not significantly different from glycosylated plant-made sRAGE to S100A8/A9 complex (4.8 nM ± 2.4 nM) (Table 4.1). These results suggest that

glycosylation of sRAGE protein has influenced its ligand binding, particularly in relation to binding to HMGB-1.

Table 4.1 Dissociation constant (K_d) and P values of sRAGE binding to HMGB-1 and S100A8/A9 complex.

Type of sRAGE	K_d values		P Values
	HMGB-1	S100A8/A9	
Glycosylated plant-made sRAGE - **(1)**	129.6 nM ± 18.8 nM	4.8 nM ± 2.4 nM	
Deglycosylated (non-denatured) plant-made sRAGE - **(2)**	227.8 nM ± 38.0 nM	14.3 nM ± 2.6 nM	(1) vs (2)-HMGB-1 binding = P<0.05
E. coli-made sRAGE (non-glycosylated) - **(3)**	201.4 nM ± 14.5 nM	6.1 nM ± 1.9 nM	(1) vs (3)-HMGB-1 binding = P<0.05

An alternative explanation for the higher affinity of plant-made sRAGE to ligands observed in the present study may be related to the oligomerization of the receptor (here it is sRAGE). However, as we utilised the monomeric form of sRAGE in the *in vitro* binding assays this is unlikely, unless binding of sRAGE to the ligands facilitates oligomerization of the receptor. A higher affinity of RAGE towards its ligands can be attributed to the presence of either an oligomerized form of the ligand or the oligomerized form of the receptor (Ostendorp *et al*., 2007; Sitkiewicz *et al*., 2013). Many other cell-surface receptors are also known to be activated by a ligand-induced multimerisation process, such as Toll-like receptors (Hu *et al*., 2004; De Bouteiller *et al*., 2005) or the receptor for tumour necrosis factor α (Bazzoni *et al*., 1995). Surface Plasmon Resonance (SPR)-based binding studies performed using recombinant human sRAGE fused at the C-terminus to the glutathione-S-transferase (GST) protein, demonstrated that tetrameric S100B bound to sRAGE with an eight-fold higher affinity (K_d = 1.1 mM) compared with dimeric S100B (K_d = 8.3 mM) (Ostendorp *et al*., 2007). The stoichiometric analysis of S100B and the V-domain (13 kDa) of human RAGE complexes by analytical ultracentrifugation, substantiated that the S100B tetramer (41 kDa) may have triggered

RAGE dimerization by binding to the V-domain of two receptor molecules resulting in a complex of 67 kDa (Ostendorp *et al*., 2007). However, in the present study, the enhanced binding potential of plant-made sRAGE could not be related to oligomerization of the receptor (sRAGE), since only the monomeric form of plant-made sRAGE was used in the ELISA-based *in vitro* ligand binding assays, unless binding of ligands favour the formation of oligomerized form of sRAGE. However, since the same ligands were utilised to perform the binding assay for plant-made sRAGE and *E. coli*-made sRAGE, the higher affinity of plant-made sRAGE towards the ligands tested here suggests that the glycosylation of sRAGE protein is important for activity.

N-linked glycosylation is known to improve the biological activity and stability of proteins and this may be the reason for the enhanced affinity of glycosylated plant-made sRAGE towards the ligands, HMGB-1 and S100A8/A9 complex. *N*-glycans contribute to the hydrodynamic volume and net charge of glycoproteins in circulation, which may be important for ligand binding and conformational stability (Agarwal *et al*., 2008; Hu *et al*., 1994; Hu & Norrby, 1994; Srikrishna *et al*., 2002). Bone morphogenetic protein (BMPR2), natural killer cell receptor 2B4 protein (CD244) and mouse interleukins (mILs) are examples that show that enhanced ligand binding is associated with the *N*-linked glycosylation of the protein (Gao *et al*., 2008; Lowery *et al.,* 2014; Margraf-Schönfeld *et al*., 2011. The *N*-linked glycosylation of the extracellular domains of bone morphogenetic protein (BMPR2) has been shown to enhance its ability to bind BMP2 ligand (Lowery *et al.,* 2014). BMPR2 plays an important role in the development of bone and cartilage and is strongly implicated in human diseases. 2B4 (CD244) is an important activating receptor for the regulation of natural killer (NK) cell responses (Margraf-Schönfeld *et al*., 2011) and it has been demonstrated that the extracellular domain of *N*-linked glycosylated 2B4 (CD244) protein is essential for binding to its ligand, CD48 (Margraf-Schönfeld *et al*., 2011). The enhanced biological activity of mouse interleukins (mILs) has been shown to relate to *N*-glycosylation of the protein (Gao *et al*., 2008). Similarly, the effect of glycosylation on RAGE binding to HMGB-1 has been previously reported, where glycosylation of bovine RAGE was shown to enhance its ligand binding capacity to HMGB-1 compared to non-glycosylated RAGE (Srikrishna *et al*., 2001; Srikrishna *et al*., 2002). Based on these publications it is clear that *N*-linked glycosylation of sRAGE has significantly enhanced HMGB-1 binding.

At this stage we do not know the mechanism behind the enhanced ligand binding potential due to *N*-linked glycosylation of sRAGE. However, based on the previous studies by Srikrishna *et al.* (2010), it was speculated that *N*-glycans attached to the sRAGE protein may have enhanced the binding potential by promoting receptor oligomerization and subsequent signalling events following HMGB-1 or S100A8/A9 binding. Srikrishna *et al.* (2010) demonstrated that carboxylated glycan-enriched population of RAGE forms higher order multimeric complexes with S100A12. However, this multimerisation is reduced upon deglycosylation or by using non-glycosylated sRAGE expressed in *E. coli*. Further studies implicated that an antibody against carboxylated glycans (mAbGB3.1) blocks S100A12-mediated NF-kB signalling in HeLa cells expressing full-length RAGE (Srikrishna *et al.*, 2010). Based on these results it was concluded that carboxylated *N*-glycans present on RAGE increase binding potential and promote receptor clustering and subsequent signalling events following oligomeric S100A12 binding (Srikrishna *et al.*, 2010). However, the mechanism behind improved ligand binding potential due to *N*-linked glycosylation of sRAGE in this study should be empirically verified in future studies.

We know that glycosylation of sRAGE has an influence on ligand binding. However, at present we do not know the exact molecular masses or the structure of the *N*-linked glycans of plant-made sRAGE. The western blot analysis showed that plant-made sRAGE has undergone *N*-linked glycosylation while *E. coli*-made sRAGE has not. Plant-made sRAGE showed two bands corresponding to ~45 kDa and ~37 kDa before deglycosylation (Figure 4.1, lane 1). The calculated molecular weight of expressed sRAGE is 34.5 kDa as determined by ExPASy-Compute pI/Mw tool. After deglycosylation of plant-made sRAGE four bands (~43 kDa, ~37 kDa, ~36 kDa and ~33 kDa) were observed, suggesting that at least partial deglycosylation occurred. It may also be that there is some residual structure of sRAGE after denaturation with SDS and reduction with β-mercaptoethanol, making sRAGE appear larger in SDS gels (Hanford *et al.*, 2004). However, these results indicate that the plant made sRAGE is glycosylated. Therefore, the ~45 kDa protein may have undergone *N*-linked glycosylation and it was assumed that the two *N*-linked glycosylation sites present (Park *et al.*, 2011) in the V-domain of RAGE (sRAGE) have been utilised within the plant expression system. Hanford *et al.* (2004) extracted sRAGE from mouse lungs, where it would also be expected to be glycosylated, and observed a protein of 45 kDa by SDS-PAGE. After

deglycosylation of the 45 kDa sRAGE Hanford *et al*. (2004) observed two bands on a SDS gel, which is similar to our results. They concluded that these two bands were produced as a result of utilisation of the two potential *N*-glycosylation sites present in mouse sRAGE. These two *N*-linked glycosylation sites are known to be occupied by complex *N*-glycans (Turovskaya *et al*., 2008).

In future studies, the accurate molecular masses of the glycosylated and deglycosylated plant-made sRAGE should be determined by mass spectroscopy, to confirm that the plant-made sRAGE was subjected to *N*-linked glycosylation *in planta* as suggested by SDS-PAGE results. Identification of the glycans could be determined by tryptic digestion of the plant-made sRAGE followed by HPLC or analysis by MALDI-MS in reflector mode before and after enzymatic *N*-linked deglycosylation in the presence of PNGase F (reviewed by Roth *et al*., 2012; Zaia, 2010). Alternatively, it is possible to assign the putative structures of free *N*-linked glycans based on mass spectral data, once these are derivatized with fluorescent markers, such as 2-aminobenzamine (2AB) or with methyl groups (permethylation), to increase the sensitivity of detection (Kailemia *et al*., 2014). This method facilitates the detection of low abundance glycan species.

One limitation of the ELISA-based *in vitro* ligand binding assay was the downward trend observed for the last two data points of *E. coli*-made sRAGE to HMGB-1 binding. The high concentration of HMGB-1 may have inhibited the binding of *E. coli*-made sRAGE (concentration of sRAGE is constant for the assay) to the RAGE specific antibody (anti-human RAGE biotinylated antibody, R & D System) used in the assay. However, this kind of decrease in binding activity in the presence of high concentrations of HMGB-1 was not observed for either glycosylated or deglycosylated plant-made sRAGE (Figure 4.4A and Figure 4.4B). An alternative hypothesis may be that the decreased binding is a consequence of the inability of deglycosylated sRAGE (*E. coli*-made sRAGE) to recognise anti-human RAGE biotinylated antibody in the presence of high concentrations of HMGB-1. However, this downward trend was not observed for *E. coli*-made sRAGE binding to high concentrations of the S100A8/A9 complex. The cross reaction of RAGE specific anti-human RAGE biotinylated antibody to glycosylated versus deglycosylated RAGE is not known. However, the observed variations of data points in binding curves in the present study are similar to the dissociation binding curves of RAGE (cytoplasmic tail) and mammalian diaphanous 1, in the presence of small molecule inhibitors (Manigrasso *et al*., 2016). Another limitation of this ELISA-based *in vitro* binding assay

was the lower goodness of fit (R^2) values observed (0.6 to 0.8) for sRAGE binding to S100A8/A9 complex. However, this ELISA-based *in vitro* binding assay still serve as a quick method with increased throughput to determine the affinity of sRAGE and HMGB-1 or S100A8/A9 binding.

When the effect of EDTA on sRAGE binding to HMGB-1 was determined (Figure 4.5A and Figure 4.5B), maximum binding was observed in the absence of EDTA and, this was true for both the plant-made sRAGE and *E. coli*-made sRAGE. The binding values in the presence of lower concentrations of EDTA (0.25 mM to 1.0 mM) were statistically similar to that of no-EDTA control. However, higher EDTA concentrations (2.0 mM to 8.0 mM) significantly inhibited the binding of HMGB-1 to sRAGE. Our study suggests that sRAGE binding to HMGB-1 is not dependent on the presence of divalent cations such as Ca^{2+}, Mg^{2+} and Zn^{2+}. This may be because the structure of HMGB-1 does not show any Ca^{2+}/Zn^2 binding sites. This binding inhibition by EDTA above 1 mM should not arise as a result of sequestering metal ions. HMGB-1 is not a calcium binding protein and therefore, metal ions are not needed for protein function to occur. Therefore, the underlying mechanism of inhibitory effect of EDTA above 1 mM concentration on sRAGE to HMGB-1 is not known. Thus, one could argue that EDTA could be tested as a potential therapeutic target to break the RAGE-HMGB-1 axis and associated pathologies. EDTA chelation therapy is already popular as a safe, effective and relatively inexpensive treatment for coronary heart disease, atherosclerosis and other age-related diseases (Seely *et al*., 2005). However, thorough investigation is needed to prove that EDTA is a potential candidate to break the RAGE-HMGB-1 axis.

In the present study the effect of divalent cations on sRAGE binding to HMGB-1 and S100A8/A9 complex was also determined. The results revealed that divalent cations inhibit the binding of both the plant and *E. coli*-made sRAGE to HMGB-1 and these binding values were significantly lower when compared to the no-divalent cations control (Figure 4.6A and Figure 4.6B). The maximum binding was observed in the absence of divalent cations and this was true for both the plant and *E. coli*-made sRAGE to HMGB-1 binding. sRAGE binding to HMGB-1 was not enhanced by any of the cations combinations: our observations were similar to previous findings by Liu *et al*. (2009), where maximum binding of RAGE and HMGB-1 was observed in the absence of cations. In contrast, higher binding values were obtained for sRAGE binding to S100A8/A9 complex in the presence of any combination of divalent cations (Figure 4.10A and Figure

4.10B). The binding values in the presence of Ca^{2+}/Zn^{2+} or Mg^{2+}/Zn^{2+} were almost equal and were significantly higher than the no-divalent cations control. These results showed that Mg^{2+} ions are equally important as Ca^{2+} ions for sRAGE-S100A8/A9 binding to occur. Binding was slightly lower in the presence of all three cations, $Ca^{2+}/Mg^{2+}/Zn^{2+}$, compared to that of any two cations (Ca^{2+}/Zn^{2+} or Mg^{2+}/Zn^{2+}) in combination. However, the combination of the three cations was still significantly higher than the no-divalent cations control. Previous studies have shown that RAGE binding to the calcium protein family requires divalent cations: it was suggested that the presence of Ca^{2+} and Zn^{2+} ions are required for binding of RAGE to S100A9 (Björk *et al*., 2009) and S100A12 (Liu *et al*., 2009; Spyropoulos, 2005). The calcium-dependent signalling roles of the S100 proteins arise because their affinities for calcium are comparable with the free calcium concentration in the cytoplasm during a calcium wave ($\sim 1~\mu M$) (Santamaria-Kisiel *et al*., 2006). The present finding also suggests the importance of divalent cations, such as Ca^{2+} and Zn^{2+}, for RAGE binding to S100 family proteins to occur. However, our results indicated that Mg^{2+} ions are equally as important as Ca^{2+} ions for sRAGE-S100A8/A9 binding by showing almost similar binding values in the presence of Ca^{2+}/Zn^{2+} and Mg^{2+}/Zn^{2+}.

The pH of the binding reaction affects sRAGE ligand binding in a ligand dependent way. Highest binding values for plant made sRAGE to HMGB-1 was observed at acidic pH. Generally, proteins attain a net positive charge when the pH is below their isoelectric points (pI). The pI of sRAGE is 7.6. Therefore, at acidic pH, positively charged sRAGE may have strongly bound to negatively charged HMGB-1 (Knapp *et al*., 2004; Ueda *et al*., 2004). At physiological pH of 7.5 slightly negative charged sRAGE may have bound less tightly to negatively charged HMGB-1 showing significantly lower binding values compared to that of neutral pH of 7.0. Our observation is comparable to recent findings of Park *et al*. (2010). Competition experiments using gel shift assays show that RAGE interaction with AGE is driven by the recognition of negative charges on the AGE-protein rather than interaction with distinct glycation moieties on the amino acid side chains of proteins (Park *et al*., 2010). These findings suggest that structurally different ligands are bound to RAGE through charge-charge interactions, made possible by complementary charge of the ligands and the receptor (Park *et al*., 2010).

Plant-made sRAGE binding to S100A8/A9 complex showed significantly higher binding values at pH above 7.5 compared to that at neutral pH of 7.0. Interestingly, the maximum binding was observed at pH 9.0. At basic pH, most proteins obtain a net negative charge, which can cause unfolding or even protein aggregation (Melo *et al*., 1997; Monahan *et al*., 1995). The high pH values cause denaturation or unfolding of the protein due to ionisation of carboxyl, phenolic and sulfhydryl groups within the proteins. The higher binding affinity observed at basic pH suggests that ionisation of these groups either modifies or improves the affinity of plant-made sRAGE towards S100A8/A9 complex and thus opens up avenues for intervention. However, for *E. coli*-made sRAGE the highest binding for S100A8/A9 was observed at a slightly acidic pH value (6.5). Why plant and *E. coli*-made sRAGE behave differently in terms of acidic and basic pH values is a question that remains unanswered. Further analysis of sRAGE binding to ligands, under different pH conditions should be conducted using electrophoretic techniques or NMR (Nuclear Magnetic Resonance) spectroscopy studies (Beringhelli *et al*., 2002).

4.5 CONCLUSION

The data presented here show that an ELISA-based *in vitro* ligand binding assay was successfully developed to determine the affinity of sRAGE to HMGB-1 or S100A8/A9 complex, based on preliminary work by Webster & Pickering (pers. comm.). By utilising plant and *E. coli*-made sRAGE, we showed for the first time that plant-made sRAGE has a higher affinity to both the ligands: HMGB-1 and S100A8/A9 complex than *E. coli*-made sRAGE. However, only the binding potential of plant-made sRAGE to HMGB-1 was significantly higher than that of *E. coli*-made sRAGE. The enhanced affinity of plant-made sRAGE is likely to be related to the *N*-linked glycosylation of sRAGE that occurred within the plant expression system. We showed that plant or *E. coli*-made sRAGE binding to S100A8/A9 complex is strictly dependent either on Ca^{2+}/Zn^{2+} or Mg^{2+}/Zn^{2+} by showing higher binding values in the presence of these divalent cations compared to the no-divalent cations control. However, sRAGE and HMGB-1 binding was not influenced by divalent cations, instead higher binding values were observed in the absence of divalent cations. This may have resulted due to the absence of any Ca^{2+}/Zn^{2+} binding sites in HMGB-1. EDTA above 1 mM concentration was also shown to inhibit binding of sRAGE to HMGB-1. At acidic pH, both plant and *E. coli*-made sRAGE strongly bound to HMGB-1. The effect of pH on sRAGE binding to S100A8/A9 complex was different; plant-made

sRAGE showed highest binding values at a basic pH (9.0) and for *E. coli*–made sRAGE it was at a slightly acidic pH (6.5).

Plant expression systems are well suited for the expression of large complex recombinant proteins because they are relatively low cost production systems which are versatile and easily scalable (Klimyuk *et al*., 2005). In addition, plant systems offer the molecular components necessary for splicing introns, subcellular targeting and post-translational modifications which are lacking in prokaryotic expression systems, like *E. coli* (Di Fiore *et al*., 2002; Fisher *et al*., 2004; Lorkovic *et al*., 2000; Vitale & Denecke, 1999).

Using hairy roots produced reasonable protein yields but significant amounts of protein were lost during purification. An alternative system is transient expression in *Nicotiana benthamiana* leaves, which has been used to generate higher yields of recombinant proteins (Janssen & Gardner, 1990; Vaquero *et al*., 2002; Webster *et al*., 2009; Wroblewski *et al*., 2005). Experiments expressing sRAGE transiently in *N. benthamiana* leaves, using the MagnICON® deconstructed viral vector system (Marillonnet *et al*., 2004) and targeting the apoplast, cytoplast and chloroplast, resulted in protein production but the yield was low. The maximum yield of 0.02 % of TSP was observed for cytoplasmic targeted construct containing a SEKDEL sequence to retain in ER. This is lower than the yield (0.6 % total soluble protein, (TSP)) achieved in the study presented here.

The results of the *in vitro* binding assays presented here, suggests that *E. coli* is a potential expression system to produce milligram quantities of recombinant sRAGE of high purity (90 %) on a large scale if sRAGE were to be used as a potential therapeutic in future. However, the results also show that glycosylation is important for ligand binding and this is only achieved through the plant based system. Mammalian systems will also glycosylate proteins but the major disadvantage is that it is more expensive than a plant based system.

sRAGE has the potential to be an important therapeutic protein as it is capable of competing with full-length RAGE for ligand binding and thereby blunts the RAGE-dependent signal transductions and subsequent development of RAGE related pathologies (Sturchler *et al*., 2008; Taguchi *et al*., 2000; Yamagishi *et al*., 2008). The advantage of the plant-made sRAGE is that it shows higher affinity towards HMGB-1 and the S100A8/A9 complex than *E. coli*-made sRAGE, making it a better therapeutic

agent. Interestingly, HMGB-1 binding to the glycosylated plant made sRAGE, was significantly higher than the *E. coli*-made sRAGE. The enhanced ligand binding ability caused by *N*-linked glycosylated plant-made sRAGE could be used in future studies to improve the activity of sRAGE through glycoengineering to develop a better potential therapeutic protein.

CHAPTER 5

General Discussion

The receptor for advanced glycation end-products (RAGE), a member of the immunoglobulin (Ig) super family of cell surface receptors is the best studied receptor of advanced glycation end-products (AGEs). In addition to the interaction with AGEs, RAGE is also known to interact with matrix proteins, members of the S100/calgranulin protein family and high mobility group family proteins. The interaction between RAGE and its ligands is thought to result in pro-inflammatory gene activation and are hypothesised to have a causative effect in a range of inflammatory diseases, including diabetic complications (Barlovic *et al*., 2011; Ramasamy *et al*., 2011; Sakurai *et al*., 2003; Zong *et al*., 2011), Alzheimer's disease (Leclerc *et al*., 2010) and even some tumors (Logsdon *et al*., 2007; Kang *et al*., 2012; Sparvero *et al*., 2009). The soluble receptor of RAGE (sRAGE) competes with full-length RAGE for ligand binding and thereby, blunts the RAGE-dependent signal transductions (Ding & Keller, 2005). Thus, sRAGE is believed to have therapeutic potential in RAGE-dependent pathologies (Buckley & Ehrhardt, 2010).

With the availability of the crystal structure of VC1-domains of RAGE, it was shown that the 'V' domain and 'C1' domain are responsible for ligand recognition and binding (Koch *et al*., 2010; Park *et al*., 2010). Apart from the involvement of the VC1-domains, post-translational modifications, in particular glycosylation, has been shown to be important for RAGE-ligand interactions (Srikrishna *et al*., 2002 & Srikrishna *et al*., 2010). However, most of the ligand binding studies have been carried out using non-glycosylated RAGE expressed in an *E. coli* expression system. Therefore, in the present study, a comparative *in vitro* ligand binding study was performed using glycosylated plant-made sRAGE and non-glycosylated *E. coli*-made sRAGE in the presence of two ligands of RAGE; HMGB-1 and S100A8/A9 complex. This is the first study of plant-made sRAGE as well as the first comparative binding study that compared sRAGE produced in a plant expression system to sRAGE from an *E. coli* expression system. This thesis describes the expression, purification, and characterisation of sRAGE from *E. coli* and plant (hairy roots of *Nicotiana tabacum*) expression systems. *In vitro* ligand binding studies of plant-made

sRAGE and *E. coli*-made sRAGE to HMGB-1 or S100A8/A9 complex were undertaken to understand the effect of glycosylation of sRAGE on ligand binding and to analyse the impact of extracellular components and conditions on sRAGE-ligand interactions. Determination of the full-extracellular domain structure of plant-made sRAGE was also part of the initial aim but due to resource constraints at Monash University this could not be attempted. However, it is an important aspect and should be part of future studies.

The protein extraction and purification (by anion-exchange and size exclusion chromatography, AEC and SEC, respectively) protocol was optimised to obtain a sufficient yield of plant-made sRAGE from hairy roots of *N. tabacum*. Key improvements to the protocol included decreasing the speed and time of centrifugation, lowering the concentration of Triton X-100, and dialysis and concentration of the protein prior to AEC and SEC. This improved protocol resulted in purified plant-made sRAGE of ~414 µg from ~100 g of hairy roots (Figure 2.6). The expression and purification of the plant-made sRAGE is important as it can provide a less expensive production system for glycosylated sRAGE as a potential therapeutic protein. ELELYSO™ (Taliglucerase alfa) is such therapeutic protein produced in carrot root cell cultures by Pfizer Inc. and Protalix BioTherapeutics. It is the first FDA approved therapeutic protein produced in a plant expression system. Interestingly, this expression system does not require additional processing for postproduction glycosidic modifications of the protein. ELELYSO is used as an injection for adult and pediatric patients with a confirmed diagnosis of Type 1 Gaucher disease (Grabowski *et al*., 2014). The production of high-value proteins in plants is a developing area and as a result the production of experimental Ebola treatments in tobacco plants are also underway (Sack *et al*., 2015).

The full-extracellular domain of the sRAGE gene was fused with a SEKDEL sequence and expressed in stable hairy root cultures of *N. tabacum* plants. The SEKDEL sequence allowed sRAGE to be retained in the ER of the plant cells, where the core glycans, which are the same in plants and mammals, are added (Gomord & Faye, 2004). Therefore, the present study shows the effects of core glycans of sRAGE protein on the *in vitro* ligand binding. *N*-linked glycosylation of RAGE is important for the regulation of ligand binding (Srikrishna *et al*., 2010; Park *et al*., 2011). Therefore, it is important for sRAGE to be glycosylated for the efficient binding to ligands, if it is to be used to prevent binding of the FL-RAGE to these ligands and, therefore, prevent subsequent development of pathological conditions. There have been no published reports on sRAGE, however,

previous studies have indicated that the complex post-translational modifications of RAGE protein have an effect on its activity, including enhancing ligand-binding potential. RAGE molecules from bovine lung modified by carboxylated glycans were shown to partially enhance binding to HMGB-1 (Srikrishna *et al*., 2002). In another study, a subpopulation of RAGE enriched for carboxylated glycans showed a 100-fold increase in binding potential (B_{max}/K_d) for S100A8/A9 complex (Turovskaya *et al*., 2008). These findings suggest that carboxylated glycans form critical binding sites for the HMGB-1 and S100A8/A9 ligands on RAGE (Turovskaya *et al*., 2008). Similarly, a subpopulation of RAGE enriched for carboxylated glycans showed a ligand binding potential for S100A12 that was more than 10-fold higher than the total RAGE. Further research has shown that mAbGB3.1 (an antibody against carboxylated glycans) blocks S100A12-mediated NF-kB signalling in HeLa cells expressing full-length RAGE. This explains the importance of carboxylated *N*-glycans on receptor clustering and subsequent signalling (Srikrishna *et al*., 2010; Srikrishna *et al*., 2005). The above studies have shown that post-translational modifications, such as carboxylated glycans, can affect both structural and functional aspects of RAGE. However, the effects of carboxylated glycans on sRAGE and ligand binding is not known. This could be tested using human cell lines and this information could be useful in developing potential therapeutic agents including sRAGE for RAGE mediated disease pathologies.

The enzymatic *N*-linked deglycosylation studies and western blot analysis detailed in the studies presented here, suggest that the plant-made sRAGE was *N*-glycosylated. Future studies should include the confirmation of the glycosylated state of the plant-made sRAGE and also the identification of the structure of the glycans. The mass of the *N*-glycans could be determined by comparing the masses of proteins, before and after enzymatic *N*-linked deglycosylation in the presence of PNGase F by MALDI-MS (Hanford *et al*., 2004). Identification of the glycans could be determined by tryptic digestion of the deglycosylated plant-made sRAGE in the presence of PNGase F, and subjecting this peptides to MS/MS (reviewed by Roth *et al*., 2012; Zaia, 2010). An entire *N*-glycan moiety of a glycoprotein is removed in the presence of PNGase F and results in the conversion of Asn to Asp corresponding to a shift of one mass unit for each *N*-glycosylation site. Therefore, when a deglycosylated protein is further digested with trypsin, the peptides that are bound to the glycan moiety will be 1 Da higher than the expected theoretical mass. By subjecting these peptides to MS/MS, each peptide that

possesses Asp (instead of Asn) is identified as formerly attached to the glycan moiety (reviewed by Roth *et al*., 2012). However, the analysis of protein glycans is a complicated process in the presence of large number of potential glycosylation combinations, as a single protein has the ability to undergo a number of *N*-glycosylations. The microheterogeneity; the ability of the same glycosylation site to be occupied by different glycans, make glycan analysis more complex (reviewed by Roth *et al*., 2012). Protein glycosylation analysis is also made difficult by the significantly lower proportion of glycopeptides in comparison to other peptides obtained after glycoprotein digestion. The suppression of the glycopeptide mass spectral signal, in the presence of other peptides, further complicates the analysis (Ongay *et al*., 2012). To overcome these issues, it is possible to assign the putative structures of free *N*-linked glycans based on mass spectral data, once these are derivatized with fluorescent markers, such as 2-aminobenzamine (2AB) or with methyl groups (permethylation), to increase the sensitivity of detection (Kailemia *et al*., 2014). This method facilitates the detection of low abundance glycan species. Therefore, all these methods should be taken into account when glycosylation studies of plant-made sRAGE are conducted in the future.

Characterisation by SDS-PAGE and western blot analysis showed that plant-made sRAGE exists mainly in its monomeric form. However, we do not know at this stage whether our plant-made sRAGE is properly folded. Circular Dichroism (CD) spectroscopy based studies would have to be performed to determine the folding patterns of plant-made sRAGE. This was not done in the present study due to time constraints.

sRAGE was also expressed in an *E. coli* expression system to obtain non-glycosylated sRAGE for comparison with the plant-made sRAGE in *in vitro* ligand binding studies with HMGB-1 and S100A8/A9 complex. Protein characterisation by SDS-PAGE and western blot analysis showed that *E. coli*-made sRAGE, is in the form of both putative aggregates and monomeric forms. This is a disadvantage of using *E. coli* made sRAGE (Costa *et al*., 2014; Rosen *et al*., 2002; Schultz *et al*., 2006). The monomeric form has to be used in the ligand binding assays and the yield of the purified monomeric form of *E. coli*-made sRAGE (based on ELISA calculations) was relatively low, at 0.3 mg L^{-1}. However, the purity of the monomeric form of sRAGE was 90 % (based on SDS-PAGE analysis), and the protein was used in the *in vitro* binding studies with HMGB-1 and S100A8/A9 complex.

A goal of this study was to examine the effect of glycosylation of sRAGE on the binding of HMGB-1 and S100A8/A9, which has not been reported previously. Very few binding studies of RAGE and S100A8/A9 complex have been recorded in the present day literature (Turovskaya *et al*., 2008; Yin *et al*., 2013). Recombinant human HMGB-1 (~25 kDa) (Sigma, Catalogue No: H4652) and the hetero-tetrameric form of S100A8/A9 complex (~50 kDa) (MyBioSource, Catalogue No: MBS702466) were used to conduct ELISA-based *in vitro* ligand binding assays. Comparative *in vitro* binding studies performed using the monomeric forms of plant and *E. coli*-made sRAGE with the ligands HMGB-1 and S100A8/A9 complex highlights the importance of sRAGE glycosylation. Further studies were carried out in the presence of EDTA, divalent cations or pH alterations to examine the impact of the extracellular components and conditions on sRAGE binding to these ligands.

Plant-made sRAGE demonstrated a higher affinity for the ligands, (HMGB-1 and S100A8/A9 complex) than the *E. coli*-made sRAGE. Prior to the experiments we speculated that the higher affinity of plant-made sRAGE was due to the glycosylation of the protein. Our results support this hypothesis as in subsequent experiments the ligand-binding affinity of plant-made sRAGE markedly dropped after deglycosylation. The affinity of deglycosylated plant-made sRAGE to HMGB-1 and S100A8/A9 complex was lower than that of the glycosylated plant-made sRAGE. The affinity of glycosylated plant-made sRAGE to HMGB-1 was significantly higher than that of *E. coli* made sRAGE. The binding affinity of glycosylated plant-made sRAGE to S100A8/A9 was also higher but not significantly so, compared to both the *E. coli* and deglycosylated plant-made sRAGE. Our finding of sRAGE and HMGB-1 binding is similar to research by Srikrishna *et al*., (2002), where RAGE and HMGB-1 assays were carried out before and after *N*-linked deglycosylation (non-denatured). They reported that purified RAGE specifically bound HMGB-1 with a K_d of 10.7 nM ± 1.7 nM while deglycosylation significantly reduced the binding potential (K_d of 18.2 nM ± 5.3 nM). The ligand binding studies detailed in here, could be compared with similar assays performed with commercially available sRAGE.

Binding of RAGE to HMGB-1 has been associated with development of disease pathologies including cell death, brain damage, ischemia-reperfusion injury of the heart, cancer and lupus nephritis (Andrassy *et al*., 2008; Choi *et al*., 2011; Lu *et al*., 2015; Muhammad *et al*., 2008). Many studies have focused on the effect of sRAGE on lupus

nephritis development (Lee *et al*., 2013; Martens *et al*., 2012; Wu *et al*., 2012; Yu *et a*l., 2015). The effect of HMGB1/DNA/RAGE-mediated innate inflammatory responses in patients with lupus nephritis has been evaluated in the presence of FL-RAGE and sRAGE. It was shown that the level of sRAGE in the plasma, negatively correlated with the systemic lupus erythematosus (SLE) disease activity index. This finding highlights the importance of plasma sRAGE as a potential biomarker for disease activity and a future therapeutic target in SLE (Yu *et a*l., 2015). Animal studies have also shown that sRAGE injected intraperitoneally (2 µg) into mouse models, significantly improved nephritis-prone mice compared to the standard induction treatment for lupus nephritis (Lee *et al*., 2013). They have injected mouse sRAGE-Fc, which was expressed in HEK 293E cells and purified on a protein A–Sepharose column after testing the endotoxin level. Interestingly, not only sRAGE interrupted the nuclear translocation of NF-ƙB in the kidney but the subsequent reduction of the expression of downstream genes of NF-ƙB (Lee *et al*., 2013). They concluded that sRAGE could be used as a new therapy for this disease, based on these findings. Our plant-made glycosylated sRAGE could be tested in mouse models in a similar way, to see the efficacy of the protein.

In our study we found that extracellular environmental components and conditions had an impact on sRAGE-ligand binding. We used three divalent cations in different combination (Ca^{2+} or Mg^{2+}=1.0 mM and Zn^{2+}= 0.1 mM) to find out the effect on sRAGE binding to S100A8/A9 complex and HMGB-1. Our results showed that in the absence of divalent cations, the binding affinity of plant and *E. coli*-made sRAGE to S100A8/A9 complex was reduced. Significantly higher binding values were observed for both plant-made and *E. coli*-made sRAGE compared to the no-divalent control in the presence of any combination of divalent cations: Ca^{2+}/Zn^{2+}, Mg^{2+}/Zn^{2+} or $Ca^{2+}/Mg^{2+}/Zn^{2+}$. The binding values of the different cation combinations were statistically similar to one another. The importance of Ca^{2+} (1.0 mM) and Zn^{2+} (0.1 mM) has been previously shown for RAGE binding to S100A9 (Björk *et al*., 2009) and recombinant human S100A12 (Ca^{2+}=1.0 mM and Zn^{2+}=10 µM) (Liu *et al*., 2009). However, our study showed that Mg^{2+} ions are equally as important as Ca^{2+} ions by demonstrating almost identical binding values. In contrast, significantly higher binding values between sRAGE and HMGB-1 were observed in the absence of divalent cations. Our results were similar to previous research, which found that the binding of sRAGE to HMGB-1 was not affected by any combination of divalent cations (Liu *et al*., 2009).

Higher concentrations of EDTA (2.0 mM to 8.0 mM) significantly inhibited both plant and *E. coli* derived sRAGE binding to HMGB-1. Therefore, higher concentrations of EDTA could be a potential inhibitory agent, preventing binding between RAGE and HMGB-1 and thus potentially preventing the development of disease pathologies. Many studies have focused on the identification of potential inhibitory compounds that directly bind to HMGB-1, ranging from small natural or synthetic molecules, such as glycyrrhizin and gabexate mesilate, HMGB1-specific antibodies, peptides, proteins as well as bent DNA-based duplex, as potential therapeutic agents in HMGB1-related pathologies (reviewed by Musumeci *et al*., 2014). Some of these compounds are expected to be used in *in vivo* assays using animal models to investigate the effect on HMGB-1-related pathologies (reviewed by Musumeci *et al*., 2014). The observed inhibitory effect of EDTA on sRAGE binding to HMGB-1 could be tested in human cell cultures or in mouse models in the future (Gwak *et al*., 2012; Lee *et al*., 2013).

Final comments

In summary, sRAGE expressed in stable hairy root cultures of *N. tabacum,* bound to the ligands HMGB-1 and S100A8/A9 complex, indicating that it is biologically active. This is the first report that features the production of recombinant sRAGE in a plant expression system and determination of its binding to selected ligands. *In vitro* ligand binding studies revealed that glycosylated plant-made sRAGE bound to both the ligands with a higher affinity than the *E. coli*-made sRAGE. The affinity of plant-made sRAGE to HMGB-1 and S100A8/A9 complex decreased after *N*-linked deglycosylation of the sRAGE protein. Our results showed that glycosylation of sRAGE enhanced its ligand affinity. The *E. coli*-made recombinant sRAGE was also biologically active as it bound to HMGB-1 and S100A8/A9 complex. The lower ligand affinity of *E. coli*-made sRAGE may be due to the absence of sRAGE glycosylation in the *E. coli* expression system. The significance of glycosylation of RAGE on the efficient binding of HMGB-1 has been previously documented (Srikrishna *et al*., 2002). The results presented in this thesis and the results of Srikrishna *et al.* (2002) highlights the importance of glycosylation of all forms of RAGE.

Our study showed that enhanced ligand binding occurred in the plant-expressed sRAGE as a result of *N*-linked glycosylation. Glycosylated plant-made sRAGE demonstrated a

higher affinity than the non-glycosylated *E. coli*-made sRAGE or deglycosylated plant-made sRAGE. Due to the retention of sRAGE in ER of plant cells, only core glycans are supposed to be added to the proteins (Bosch *et al.*, 2013; Gomord & Faye, 2004). Therefore, the present study shows the effects of these core glycans of sRAGE on its ligand binding. Thus, in future, the effects of complex glycan could be tested using plant-made sRAGE. Alternatively, considering the importance of glycosylation of RAGE on the affinity of its ligands, glycoengineering could be used in future studies to improve sRAGE as a potential therapeutic protein. This involves the elimination or disruption of the plant specific xylose and core α1,3-fucose or addition of mammalian sialic acid residues to sRAGE (Castilho *et al.*, 2010; Strasser *et al.*, 2004). The presence of plant specific glycans are considered as unwanted moieties of the proteins intended for therapeutic use. Alternatively, sialylated oligosaccharides are required for the optimal therapeutic potency (Castilho *et al.*, 2010). sRAGE modified with glycoengineering could enhance the heterogeneity and immunogenicity of sRAGE. Therefore, the relationship between the primary sequence of sRAGE and cellular machineries should be critically looked at before attempting glycoengineering to produce a better potential therapeutic protein.

The effects of extracellular components and conditions on sRAGE-ligand binding such as EDTA, divalent cations and pH could open up new avenues of research on the regulation of RAGE-ligand binding. The importance of Ca^{2+}/Zn^{2+} cations for RAGE binding to S100A9 has been reported previously (Björk *et al.*, 2009). However, in our study it was found that Mg^{2+}/Zn^{2+} facilitates *in vitro* binding of sRAGE to S100A8/A9 complex with a similar capacity to Ca^{2+}/Zn^{2+}. The inhibitory effect of EDTA (2.0 mM) that was observed in our *in vitro* binding assay could be tested in human cell cultures or in mouse models (Gwak *et al.*, 2012; Lee *et al.*, 2013), with the aim of developing EDTA as a potential treatment for RAGE-HMGB-1 mediated inflammatory diseases. This could be a promising treatment because EDTA chelation therapy is already popular as a safe, effective and relatively inexpensive treatment for coronary heart disease, atherosclerosis and other age-related diseases (Seely *et al.*, 2005).

sRAGE is believed to have therapeutic potential in RAGE-dependent pathologies because it competes with full-length RAGE for ligand binding and thereby, blunts the RAGE-dependent signal transductions, effectively neutralising the detrimental effects of RAGE signalling (Buckley & Ehrhardt, 2010). If sRAGE is to be used as a therapeutic treatment

in the future then the results presented here suggests that it is important that it is glycosylated. *E. coli* could be a potential expression platform, as it has the potential to produce large quantities at high purity (reviewed by Rosano & Ceccarelli, 2014). However, the sRAGE produced from *E. coli* would not be glycosylated because it has the disadvantage of lacking post-translational modifications such as generating or attaching mammalian-like glycosylation chains (Jenkins & Curling, 1994; reviewed by Rosano & Ceccarelli, 2014), and hence likely to have lower binding affinities and be less effective as a treatment option.

Hairy root cultures of *N. tabacum* successfully produced the monomeric form of sRAGE that are biologically active. This plant-made sRAGE has the potential for therapeutic use to inhibit the RAGE and ligand mediated disease pathologies.

References

Agarwal, S., Singh, R., Sanyal, I. and Amla, D. (2008). Expression of modified gene encoding functional human alpha-1-antitrypsin protein in transgenic tomato plants. *Transgenic Res.* **17**:881–896.

Akiyama, N., Ohno, Y., Fukuda, T., Manome, Y. and Saito, S. (2009). Enhancing activity of N-glycosylation for constitutive proteins secretions in non-polarized cells. *Biochem. Biophys. Res. Commun.* **381**:612–618.

Alberts, B., Johnson, A., Lewis, J., Raff, M., Roberts, K. and Walter, P. (2002). Molecular Biology of the Cell. 4th Edition. New York: Garland Science.

Alderson, P., Bunn, F., Lefebvre, C., Li, W. P., Li, L., Roberts, I. and Schierhout, G. (2004). Human albumin solution for resuscitation and volume expansion in critically ill patients. *Cochrane Database Syst. Rev*. **18**:1–40.

Al-Senaidy, A. M. (2011). Purification and characterization of membrane-bound peroxidase from date palm leaves (*Phoenix dactylifera* L.). *Mohammad A. Ismael Saudi Journal of Biological Sciences*, **18**:293–298.

Altamirano, C., Paredes, C., Cairo, J. J. and Godia, F. (2000). Improvement of CHO cell culture medium formulation: simultaneous substitution of glucose and glutamine. *Biotechnol. Prog.* **16**:69–75.

Andersen, D. C. and Krummen, L. (2002). Recombinant protein expression for therapeutic applications. *Curr. Opin. Biotechnol.* **13**:117–123.

Andersson, U. and Tracey K. J. (2011). HMGB-1 is a therapeutic target for sterile inflammation and infection. *Annu. Rev. Immunol.* **29**:139–162.

Andrassy, M., Volz, H. C., Igwe, J. C., Funke, B., Eichberger, S. N. and *et al*. (2008). High-mobility group box-1 in ischemia-reperfusion injury of the heart. *Circulation* **117**:3216–3226.

Apweiler, R., Hermjakob, H. and Sharon, N. (1999). On the frequency of protein glycosylation, as deduced from analysis of the SWISS-PROT database. *Biochimica et Biophysica Acta* (BBA)-General Subjects **1473**:4–8.

Arakawa, T., Chong, D. K. X., Merritt, J. L. and Langridge, W. H. R. (1997). Expression of cholera toxin B subunit oligomers in transgenic potato plants. *Transgenic Res*. **6**:403–413.

Aricescu, A. R., Lu, W. and Jones, E. Y. (2006). A time and cost-efficient system for high-level protein production in mammalian cell. *Acta Cryst.* **D62**:1243–1250.

Arlen, P. A., Falconer, R., Cherukumilli, S., Cole, A., Cole, A. M., Oishi, K. K. and Daniell, H. (2007). Field production and functional evaluation of chloroplast-derived interferon-α2b. *Plant Biotechnol J.* **5**:511–525.

Arumugam, T., Simeone, D. M., Schmidt, A. M. and Logsdon, C. D. (2004). S100P stimulates cell proliferation and survival via receptor for activated glycation end products (RAGE). *J. Biol. Chem.* **279**:5059–5065.

Assenberg, R., Wan, P.T., Geisse, S. and Mayr, L. M. (2013). Advances in recombinant protein expression for use in pharmaceutical research. *Curr. Opin. Struct. Biol.* **23**:393–402.

Baker, J. L., Celik, E. and DeLisa, M. P. (2013). Expanding the Glycoengineering toolbox: the rise of bacterial N-linked protein glycosylation. *Trends in Biotechnology* **31**:313–323.

Baneyx, F. (1999). Recombinant protein expression in *Escherichia coli*. *Curr. Opin. Biotechnol*. **10**:411–421.

Baneyx, F. and Mujacic, M. (2004). Recombinant protein folding and misfolding in *Escherichia coli*. *Nat. Biotechnol.* **22**:1399–1408.

Baneyx, F. and Palumbo, J. L. (2003). Improving Heterologous Protein Folding via Molecular Chaperone and Foldase Co-Expression. *Methods Mol. Biol.* **205**:171–197.

Barlovic, D. P., Soro-Paavonen, A. and Jandeleit-Dahm, K. A. (2011). RAGE biology, atherosclerosis and diabetes. *Clin. Sci. (Lond)*. **121**:43–55.

Barta, A., Sommergruber, K., Thompson, D., Hartmuth, K., Matzke, M. A. and Matzke, A. J. M. (1986). The expression of a nopaline synthase-human growth hormone chimaeric gene in transformed tobacco and sunflower callus tissue. *Plant Mol. Biol.* **6**:347–357.

Barth, H. G. and Boyes, B. E. (1992). Size-exclusion chromatography. *Anal. Chem.* **64**:428–442.

Bartling, B., Hofmann, H. S., Weigle, B., Silber, R. E. and Simm, A. (2005). Down-regulation of the receptor for advanced glycation end-products (RAGE) supports non-small cell lung carcinoma. *Carcinogenesis* **26**:293–301.

Basta, G. (2008). Receptor for advanced glycation end products and atherosclerosis: from basic mechanisms to clinical implications. *Atherosclerosis* **196**:9–21.

Bazzoni, F., Alejos, E. and Beutler, B. (1995). Chimeric tumor necrosis factor receptors with constitutive signaling activity. *Proc. Natl. Acad. Sci. USA* **92**:5376–5380.

Beringhelli, T., Eberini, I., Galliano, M., Pedoto, A., Perduca, M., Sportiello, A., Fontana, E., Monaco, H. L. and Gianazza, E. (2002). pH and ionic strength dependence of protein (un)folding and ligand binding to bovine β-lactoglobulins A and B. *Biochemistry* **41**:15415–15422.

Berrow, N. S., Bussow, K., Coutard, B., Diprose, J., Ekberg, M., Folkers, G. E., Levy, N., Lieu, V., Owens, R. J., Peleg, Y., Pinaglia, C., Quevillon-Cheruel, S., Salim, L., Scheich, C., Vincentelli, R. and Busso, D. (2006). Recombinant protein expression and solubility screening in *Escherichia coli*: a comparative study. *Acta Cryst.* **62**:1218–1226.

Beutler, E., Dale, G. L., Guinto, E. and Kuhl, W. (1977). Enzyme replacement therapy in Gaucher's disease: preliminary clinical trial of a new enzyme preparation. *Proc. Natl. Acad. Sci. USA* **74**:4620–4623.

Bhattacharya, P., Pandey, G., Srivastava, P. and Mukherjee, K. J. (2005). Combined effect of protein fusion and signal sequence greatly enhances the production of recombinant human GM-CSF in *Escherichia coli. Mol. Biotechnol*. **30**:103–116.

Bierhaus, A., Hofmann, M. A., Ziegler, R., Nawroth, P. P. (1998). AGEs and their interaction with AGE-receptors in vascular disease and diabetes mellitus. I. The AGE concept. *Cardiovasc. Res.* **37**:586–600.

Björk, P., Björk, A., Vogl, T., Stenstrom, M., Liberg, D., Olsson, A., Roth, J., Ivars, F. and Leanderson, T. (2009). Identification of human S100A9 as a novel target for treatment of autoimmune disease via binding to quinoline-3-carboxamides. *PLoS Biol*. **7**:0800–0812.

Bonnerjea, J., Oh, S., Hoare, M., and Dunnill, P. (1986). Protein Purification: The Right Step at the Right Time. *Nature Biotechnol*. **4**:954–958.

Bopp, C., Bierhaus, A., Hofer, S., Bouchon, A., Nawroth, P. P., Martin, E., Weigand, M. A. (2008). Bench-to-bedside review: The inflammation-perpetuating pattern-recognition receptor RAGE as a therapeutic target in sepsis. *Crit Care*. **12**:201.

Bosch, D., Castilho, A., Loos, A., Schots, A., and Steinkellner, H. (2013). *N*-Glycosylation of Plant-produced Recombinant Proteins. *Curr. Pharm. Des.* **19**:1–10.

Bowie, J. U. (2001). Stabilizing membrane proteins. *Curr Opin Struct Biol.* **11**:397–402.

Boyd, J. H., Kan, B., Roberts, H., Wang, Y. and Walley, K. R. (2008). S100A8 and S100A9 mediate endotoxin-induced cardiomyocyte dysfunction via the receptor for advanced glycation end products. *Circ. Res.* **102**:1239–1246.

Boynton, J. E., Gillham, N. W., Harris, E. H., Hosler, J. P., Johnson, A. M., Jones, A. R., Randolph-Anderson, B. L., Robertson, D., Klein, T. M., Shark, K. B. *et al*. (1998). Chloroplast transformation in *Chlamydomonas* with high velocity microprojectiles. *Science* **240**:1534–1538.

Braakman, I., Helenius, J. and Helenius, A. (1992). Manipulating disulfide bond formation and protein folding in the endoplasmic reticulum. *The EMBO Journal* **11**:1717–1722.

Brownlee, M. Vlassara, H. and Cerami, A. (1985). Nonenzymatic glycosylation products on collagen covalently trap low-density lipoprotein. *Diabetes* **34**:938–941.

Buckley, S. T. and Ehrhardt, C. (2010). The receptor for advanced glycation end products (RAGE) and the lung. *J. Biomed. Biotechnol.* **2010**:1–11.

Budyak, I. L., Krishnan, B., Marcelino-Cruz, A. M., Ferrolino, M. C., Zhuravleva, A. and Gierasch, L. M. (2013). Early folding events protect aggregation-prone regions of a β-rich protein. *Structure* **21**:476–485.

Cardarelli, M., Mariotti, D., Pomponi, M., Spanò, L., Capone, I. and Costantino, P. (1987). "*Agrobacterium rhizogenes* T-DNA genes capable of inducing hairy root phenotype". *Mol Gen Genet* **209**:475–480.

Carrillo, C., Wigdorovitz, A., Oliveros, J. C., Zamorano, P. I., Sadir, A. M., Gomez, N., Salinas, J., Escribano, J. M. and Borca, M. V. (1998). Protective Immune Response to Foot-and-Mouth Disease Virus with VP1 Expressed in Transgenic Plants. *J. Virol.* **72**:1688–1690.

Casademunt, E., Martinelle, K., Jernberg, M., Winge, S., Tiemeyer, M., Biesert, L., Knaub, S., Walter, O. and Schröder, C. (2012). The first recombinant human coagulation factor VIII of human origin: human cell line and manufacturing characteristics. *Eur J Haematol*. **89**:165–176.

Castilho, A., Strasser, R., Stadlmann, J., Grass, J., Jez, J., Gattinger, P., Kunert, R., Quendler, H., Pabst, M., Leonard, R., and Steinkellner, H. (2010). In planta protein sialylation through overexpression of the respective mammalian pathway. *J. Biol. Chem* **285**:15923–15930.

Chen, Q., Lai, H., Hurtado, J., Stahnke, J., Leuzinger, K. and Dent, M. (2013). Agroinfiltration as an Effective and Scalable Strategy of Gene Delivery for Production of Pharmaceutical Proteins. *Adv. Tech. Biol. Med.* **1**:1–9.

Chichester, J. A., Manceva, S. D., Rhee, A., Coffin, M. V., Musiychuk, K., Mett, V., Shamloul, M., Norikane, J., Streatfield S. J. and Yusibov V. (2013). A plant-produced protective antigen vaccine confers protection in rabbits against a lethal aerosolized challenge with *Bacillus anthracis* Ames spores. *Hum Vaccin Immunother.* **9**:544–552.

Chilton, M. D., Drummond, M. J., Merlo, D. J. Sciaky, D., Montoya, A. L., Gordon, M. P. and Nester, E. W. (1977). Stable incorporation of plasmid DNA into higher plant cells: the molecular basis of crown gall tumorigenesis. *Cell* **11**:263–271.

Chilton, M. D., Tepfer, D. A., Petit, A., David, C., Casse-Delbart, F. and Tempé, J. (1982). *Agrobacterium rhizogenes* insert T-DNA into the genome of the host plant root cells. *Nature* **295**:432–434.

Chintapakorn, Y and Hamill, J. D. (2003). Antisense-mediated down-regulation of putrescine N-methyltransferase activity in transgenic *Nicotiana tabacum* L. can lead to elevated levels of anatabine at the expense of nicotine. *Plant Mol. Biol.* **53**:87–105.

Choi, J., Lee, M. K., Oh, K. H., Kim, Y. S., Choi, H. Y., Baek, S. K., Jung, K. Y., Woo, J. S., Lee, S. H. and Kwon, S. Y. (2011). Interaction effect between the receptor for advanced glycation end products (RAGE) and high-mobility group box-1 (HMGB-1) for the migration of a squamous cell carcinoma cell line. *Tumori.* **97**:196–202.

Chumanov, R. S., Kuhn, P. A., Xu, W. and Burgess, R. R. (2011). Expression and purification of full-length mouse CARM1 from transiently transfected HEK293T cells using HaloTag technology. *Protein Expr. Purif.* **76**:145–153.

Colhoun, H. M., Betteridge, D. J., Durrington, P., Hitman, G., Neil, A., Livingstone, S., Charlton-Menys, V., Bao, W., DeMicco, D. A., Preston, G. M., Deshmukh, H., Tan, K. and Fuller, J. H. (2011). Total soluble and endogenous secretory receptor for

advanced glycation end products as predictive biomarkers of coronary heart disease risk in patients with type 2 diabetes. *Diabetes* **60**:2379–2385.

Costa, S., Almeida, A., Castro, A., Domingues, L. (2014). Fusion tags for protein solubility, purification and immunogenicity in Escherichia coli: the novel Fh8 system. *Front Microbiol.* **5**:63.

Craig, T. J., Ciufo, L. F. and Morgan, A. (2004). A protein–protein binding assay using coated microtitre plates: increased throughput, reproducibility and speed compared to bead-based assays. *J. Biochem. Biophys. Methods* **60**:49–60.

Cremer, F., and Van de Walle, C. (1985). Method for extraction of proteins from green plant tissues for two-dimensional polyacrylamide gel electrophoresis. *Anal Biochem.* **147**:22–26.

Daffu, G., Hurtado del Pozo, C., O'Shea, K. M., Ananthakrishnan, R., Ravichandran, R., and Schmidt, A. M. (2013). Radical Roles for RAGE in the Pathogenesis of Oxidative Stress in Cardiovascular Diseases and Beyond. *Int. J. Mol. Sci.* **14**:19891–19910.

Daniell, H. (2006). Production of biopharmaceuticals and vaccines in plants via the chloroplast genome. *Biotechnol. J.* **1**:1071–1079.

Dash, P. K. (2013). High quality RNA isolation from ployphenol, polysaccharide and protein-rich tissues of lentil (*Lens culinaris*). *3 Biotech* **3**:109–114.

Dattilo, B. M., Fritz, G., Leclerc, E., Kooi, C. W. V., Heizmann, C. W. and Chazin, W. J. (2007). The extracellular region of the receptor for advanced glycation end product is comprised of two independent structural units. *Biochemistry* **46**:6957–6970.

Davis, G. D., Elisee, C., Newham, D. M. and Harrison, R. G. (1999). New fusion protein systems designed to give soluble expression in *Escherichia coli. Biotechnol. Bioeng.* **65**:382–388.

De Bouteiller, O., Merck, E., Hasan, U. A., Hubac, S., Benguigui, B., Trinchieri, G., Bates, E. E. and Caux, C. (2005). Recognition of double stranded RNA by human toll-like receptor 3 and downstream receptor signalling requires multimerization and an acidic pH. *J. Biol. Chem.* **280**:38133–38145.

De Cosa, B., Moar, W., Lee, S. B., Miller, M. and Daniell, H. (2001). Overexpression of the Bt cry2Aa2 operon in chloroplasts leads to formation of insecticidal crystals. *Nat Biotechnol* **19**:71–74.

De Marco, A. (2009). Strategies for successful recombinant expression of disulphide bond-dependent proteins in *Escherichia coli. Microb. Cell Fact.* **8**:1–8.

De Marco, A. (2013). Recombinant polypeptide production in *E. coli*: towards a rational approach to improve the yields of functional proteins. *Microb Cell Fact.* **12**: 101.

De Marco, A. and De Marco, V. (2004). Bacterial co-transformed with recombinant proteins and chaperones cloned in independent plasmids are suitable for expression tuning. *J. Biotechnol.* **109**:45–52.

Deane, R., Singh, I., Sagare, A. P., Bell, R. D., Ross, N. T., LaRue, B., Love, R., Perry, S., Paquette, N., Deane, R. J., Thiyagarajan, M., Zarcone, T., Fritz, G., Friedman, A. E., Miller, B. L. and Zlokovic, B. V. (2012). A multimodal RAGE-specific inhibitor reduces amyloid β–mediated brain disorder in a mouse model of Alzheimer disease. *J. Clin. Invest.* **122**:1377–1392.

Demain, A. L. and Vaishnav, P. (2009). Production of recombinant proteins by microbes and higher organisms. *Biotechnol Adv.* **27**:297–306.

Di Fiore, S., Li, Q., Leech, M. J., Schuster, F., Emans, N., Fischer, R. And Schillberg, S. (2002). Targetting tryptophan decarboxylase to selected subcellular compartments of tobacco plants affects enzyme stability and *in vivo* function and leads to a lesion-mimic phenotype. *Plant Physiol.* **129**:1160–1169.

Ding, Q. and Keller, J. N. (2005). Evaluation of RAGE isoforms, ligands, and signalling in the brain. *Biochim. Biophys. Acta.* **1746**:18–27.

Dong, J. L., Liang, B. G., Jin, Y. S., Zhang, W. J. and Wang, T. (2005). Oral immunization with pBsVP6-transgenic alfaalfa protects mice against rotavirus infection. *Virology* **339**:153–163.

Dudev, T. and Lim, C. (2003). Principles governing Mg, Ca, and Zn binding and selectivity in proteins. *Chem Rev.* **103**:773–788.

Dumon-Seignovert, L., Cariot, G., and Vuillard, L. (2004). The toxicity of recombinant proteins in *Escherichia coli*: a comparison of overexpression in BL21 (DE3), C41 (DE3), and C43 (DE3). *Protein Expr. Purif.* **37**:203–206.

Duong-Ly, K. C. and Gabelli, S. B. (2014). Using ion-exchange chromatography to purify a recombinantly expressed protein. *Methods Enzymol.* **541**:95–103.

Ecamilla-Trevino, L. L., Viader-Salvado, J. M., Barrera-Saldana, H. A. and Guerrero-Olazaran, M. (2000). Biosynthesis and secretion of recombinant human growth hormone in *Pichia pastoris. Biotechnol. Lett.* **22**:109–114.

Ellis, K. J. and Morrison, J. F. (1982). Buffers of constant ionic strength for studying pH- dependent processes. *Meth. Enzymol.* **87**:405–426.

Englert, J. M., Hanford, L. E., Kaminski, N., Tobolewski, J. M., Tan, R. J., Fattman, C. L., Ramsgaard, L., Richards, T. J., Loutaev, I., Nawroth, P. P., Kasper, M., Bierhaus, A. and Oury, T. D. (2008). A role for the receptor for advanced glycation end products in idiopathic pulmonary fibrosis. *Am. J. Pathol.* **172**:583–591.

Eue, I., König, S., Pior, J. and Sorg, C. (2002). S100A8, S100A9 and the S100A8/A9 heterodimer complex specifically bind to human endothelial cells: identification and characterization of ligands for the myeloid-related proteins S100A9 and S100A8/A9 on human dermal microvascular endothelial cell line-1 cells. *Int Immunol.* **14**:287–297.

Falcone, C., Bozzini, S., D'Angelo, A., Buzzi, M. P., Totaro, R., Falcone, R. and Pelissero, G. (2013). Soluble receptor for advanced glycation end-products levels in chronic heart failure and its correlation to left ventricular ejection function. *J. Clin. Exp. Cardiolog.* **4**:1000275.

Fass, D. (2012). Disulphide Bonding in Protein Biophysics. *Annu. Rev. Biophys.* **41**:3–79.

Ferrer-Miralles, N., Domingo-Espin, J., Corchero, J. L., Vazquez, E. and Villaverde, A. (2009). Microbial factories for recombinant pharmaceuticals. *Microb. Cell Fact.* **8**:1–8.

Fink, A. L. (1999). Chaperone-Mediated Protein Folding. *Physiol. Rev.* **79**:425–449.

Fischer, R., Stoger, E., Schillberg, S., Christou, P. and Twyman, R. M. (2004). Plant-based production of biopharmaceuticals. *Curr. Opin. Plant Biol.* **7**:152–158.

Fischer, R., Stoger, E., Schillberg, S., Christou, P. and Twyman, R. M. (2004). Plant-based production of biopharmaceuticals. *Curr. Opin. Plant Biol.* **7**:152–158.

Fisher, A. C., Haitjema, C. H., Guarino, C., Çelik, E., Endicott, C. E., Reading, C. A., Merritt, J. H., Ptak, A. C., Zhang, S. and DeLisa, M. P. (2011). Production of secretory and extracellular N-linked glycoproteins in *Escherichia coli*. *Appl. Environ. Microbiol.* **77**:871–881.

Food and Drug Administration (1982). Human insulin receives FDA approval. *FDA Drug Bull.* **12**:18–19.

Forbes, J. M., Cooper, M. E., Oldfield, M. D. and Thomas M. C. (2003). Role of advanced glycation end products in diabetic nephropathy. *J. Am. Soc. Nephrol.* **14**:S254–S258.

Fortis, F., Girot, P., Brieau, O., Boschetti, E., Castagna, A. and Righetti, P. G. (2005). Amphoteric, buffering chromatographic beads for proteome prefractionation. I: theoretical model. *Proteomics* **5**:620–628.

Fox, J. L. (2012). First plant-made biologic approved. *Nat. Biotechnol.* **30**:472.

Francis, D. M. and Page, R. (2010). Strategies to optimize protein expression in *E. coli*. *Curr Protoc Protein Sci.* Chapter 5:Unit 5.24.1–29.

Fritz, G. (2011). RAGE: a single receptor fits multiple ligands. *Trends Biochem. Sci.* **36**:625–632.

Gao, Z. Q., Yang, C., Wang, Y. Y., Wang, P., Chen, H. L., Zhang, X. D., Liu, R., Li , W. L., Qin, X. J., Liang, X. and Hai, C. X. (2008). RAGE up regulation and nuclear factor-kappa B activation associated with ageing rat cardiomyocyte dysfunction. *Gen. Physiol. Biophys.* **27**:152–158.

Garavito, R. M. and Ferguson-Miller, S. (2001). Detergents as tools in membrane biochemistry. *J. Biol. Chem.* **276**:32403–32406.

Garboczi, D. N., Hung, D. T. and Wiley, D. C. (1992). HLA-A2-peptide complexes: refolding and crystallization of molecules expressed in *Escherichia coli* and complexed with single antigenic peptides. *Proc. Natl. Acad. Sci*. USA **89**:3429–3433.

Gaume, A., Komarnytsky, S., Borisjuk, N. and Raskin, I. (2003). Rhizosecretion of recombinant proteins from plant hairy roots. *Plant Cell Rep*. **21**:1188–1193.

Geiger, T., Wehner, A., Schaab, C., Cox, J. and Mann, M. (2012). Comparative proteomic analysis of eleven common cell lines reveals ubiquitous but varying expression of most proteins. *Mol. Cell Proteomics* **11**:M111.014050.

Geroldi, D., Falcone, C. and Emanuele, E. (2006). Soluble Receptor for Advanced Glycation End Products: From Disease Marker to Potential Therapeutic Target. *Curr. Med. Chem.* **13**:1971–1978.

Ghavami, S., Rashedi, I., Dattilo, B. M., Eshraghi, M., Chazin, W. J., Hashemi, M., Wesselborg, S., Kerkhoff, C. and Los, M. (2008). S100A8/A9 at low concentration promotes tumor cell growth via RAGE ligation and MAP kinase-dependent pathway. *J. Leuckoc. Biol.* **83**:1484–1492.

Gilbert, T. W., Tiffany L. Sellaro, T. L., Badylak, S. F. (2006). Decellularization of tissues and organs. *Biomaterials* **27**:3675–3683.

Gils, M., Kandzia, R., Marillonnet, S., Klimyuk, V. and Gleba, Y. (2005). High-yield production of authentic human growth hormone using a plant-virus based expression system. *Plant Biotechnol. J.* **3**:613–620.

Giri, A. and Narasu, M. L. (2000). Transgenic hairy roots. Recent trends and applications. *Biotechnol Adv* **18**:1–22.

Gleba, Y., Klimyuk, V. and Marillonnet, S. (2005). Magnifection-a new platform for expressing recombinant vaccines in plants. *Vaccine* **23**:2042–2048.

Gleba, Y., Klimyuk, V. and Marillonnet, S. (2007). Viral vectors for the expression of proteins in plants. *Curr. Opin. Biotechnol.* **18**:134–141.

Gleiter, S., and Bardwell, J. C. A. (2008). Disulfide bond isomerization in prokaryotes. *Biochim Biophys Acta.* **1783**:530–534.

Gohon, Y. and Popot, J. L. (2003). Membrane protein-surfactant complexes. *Curr Opin Colloid Interface Sci.* **8**:15–22.

Goldin, A., Beckman, J. A., Schmidt, A. M. and Creager, M. A. (2006). Advanced glycation end products: sparking the development of diabetic vascular injury. *Circulation* **114**:597–605.

Gomord, V and Faye, L. (2004). Post-translational modification of therapeutic proteins in plants. *Curr Opin Plant Biol.* **7**:171–181.

Gomord, V., Fitchette, A. C., Menu-Bouaouiche, L., Saint-Jore-Dupas, C., Plasson, C., Michaud, D. and Faye, L. (2010). Plant-specific glycosylation patterns in the context of therapeutic protein production. *Plant Biotechnol. J.* **8**:564–87.

Goova, M. T., Li, J., Kislinger, T., Qu, W., Lu, Y., Bucciarelli, L. G., Nowygrod, S., Wolf, B. M., Caliste, X., Yan, S. F., Stern, D. M. and Schmidt, A. M. (2001). Blockade of receptor for advanced glycation end-products restores effective wound healing in diabetic mice. *Am. J. Pathol.* **159**:513–525.

Gowik, U. and Westhoff, P. (2011). The path from C_3 to C_4 Photosynthesis. *Plant Physiol.* **155**:56–63.

Grabowski G. A., Golembo, M. and Shaaltiel, Y. (2014). Taliglucerase alfa: an enzyme replacement therapy using plant cell expression technology. *Mol Genet Metab.* **112**:1–8.

Graumann, K. and Premstaller, A. (2006). Manufacturing of recombinant therapeutic proteins in microbial system. *Biotechnol. J.* **1**:164–186.

Griko, Y. V. and Remeta, D. P. (1999). Energetics of solvent and ligand-induced conformational changes in alpha-lactalbumin. *Protein Sci.* **8**:554–561.

Guillon, S., Tremouillaux-Guiller, J. and Pati, P. K. (2006). Harnessing the potential of hairy roots: dawn of a new era. *Trends Biotechnol*. **24**:403–409.

Guzman, G. De., Shepherd, R. P. and Walmsley, A. M. (2011). Immunoassays in Veterinary Plant-Made Vaccines. Immunoassays in Agricultural Biotechnology. John Wiley & Sons, Inc. 289–308.

Gwak, G-Y., Moon, T. G., Lee, D. H. and Yoo, B. C. (2012). Glycyrrhizin attenuates HMGB1-induced hepatocyte apoptosis by inhibiting the p38-dependent mitochondrial pathway. *World J Gastroenterol*. **18**: 679–684.

Haacke, A., Fendrich, G., Ramage, P. and Geiser, M. (2009). Chaperone over-expression in *Escherichia coli*: apparent increased yields of soluble recombinant protein kinases are due mainly to soluble aggregates. *Protein Expr. Purif.* **64**:185–193.

Hammarstrom, M., Hellgren, N., van Den Berg, S., Berglund, H. and Hard, T. (2002). Rapid screening for improved solubility of small human proteins produced as fusion proteins in *Escherichia coli. Protein Sci*. **11**:313–321.

Hanford, L. E., Enghild, J. J., Valnickova, Z., Petersen, S. V., Schaefer, L. M., Schaefer, T. M., Reinhart, T. A. and Oury, T. D. (2004). Purification and characterization of mouse soluble receptor for advanced glycation end products (sRAGE). *J. Biol. Chem.* **279**:50019–50024.

Haq, T. A., Mason, H. S., Clements, J. D. and Arntzen, C. J. (1995). Oral immunization with a recombinant bacterial antigen produced in transgenic plants. *Science* **268**:714–716.

Harja, E., Bu, D-X., Hudson, B. I., Chang, J. S., Shen, X., Hallam, K., Kalea, A. Z., Lu, Y., Rosario, R. H., Oruganti, S., Nikolla, Z., Belov, D., Lalla, E., Ramasamy, R., Yan, S. F. and Schmidt A. M. (2008). Vascular and inflammatory stresses mediate atherosclerosis via RAGE and its ligands in *apoE-/-*mice. *J. Clin. Invest.* **118**:183–194.

Harrison, R. L. and Jarvis, D. L. (2006). Protein N-glycosylation in the baculovirus-insect cell expression system and engineering of insect cells to produce "mammalianized" recombinant glycoproteins. *Adv. Virus Res.* **68**:159–91.

Hatahet, F., Nguyen, V. D., Salo, K. E. and Ruddock L. W. (2010). Disruption of reducing pathways is not essential for efficient disulphide bond formation in the cytoplasm of *E. coli*. *Microb. Cell Fact.* **9**:1–9.

Hayashi, I. and Sato, G. H. (1976). Replacement of serum by hormones permits growth of cells in a defined medium. *Nature* **259**:132–134.

Hegab, Z., Gibbons, S., Neyses, L. and Mamas, M. A. (2012). Role of advanced glycation end products in cardiovascular disease. *World J. Cardiol*. **4**:90–102.

Hegde, M. Bharathi, P., Suram, A., Venugopa, C., Jagannathan, R., Poddar, P., Srinivas, P., Sambamurti, K., Rao, K. J., Scancar, J., Messori, L., Zecca, L. and Zatta, P. (2009). Challenges Associated with Metal Chelation Therapy in Alzheimer's Disease. *J Alzheimers Dis*. **17**:457–468.

Heizmann, C. W., Fritz, G. and Schafer, B. W. (2002). S100 proteins: structure, functions and pathology. *Front. Biosci.* **7**:d1356–d1368.

Higgs, H. N. (2005). Formin proteins: a domain-based approach. *Trends Biochem. Sci.* **30**:342–353.

Hjelmeland, L. M. and Chrambach, A. (1984). Solubilization of functional membrane-bound receptors. In: Venter, J. C. and Harrison, L. C. editors. Receptor Biochemistry and Methodology. Alan R. Liss; New York. 35–46.

Hofmann, M. A., Drury, S., Fu, C., Qu, W., Taguchi, A., Lu, Y., Avila, C., Kambham, N., Bierhaus, A., Nawroth, P., Neurath, M. F., Slattery, T., Beach, D., McClary, J., Nagashima, M., Morser, J., Stern, D. and Schmidt, A. M. (1999). RAGE mediates a novel proinflammatory axis: a central cell surface receptor for S100/calgranulin polypeptides. *Cell* **97**:889–901.

Hollister, J., Grabenhorst, E., Nimtz, M., Conradt, H. and Jarvis, D. L. (2002). Engineering the protein N-glycosylation pathway in insect cells for production of biantennary, complex N-glycans. *Biochemistry* **41**:15093–15104.

Holtz, B. R., Berquist, B. R., Bennett, L. D., Kommineni, V. J. M., Munigunti, R. K., White, E. L., Wilkerson, D. C., Wong, K. I., Ly, L. H. and Marcel, S. (2015). Commercial-scale biotherapeutics manufacturing facility for plant-made pharmaceuticals. *Plant Biotechnol.* **13**:1180–1190.

Hori, O., Brett, J., Slattery, T., Cao, R., Zhang, J., Chen, J. X., Nagashima, M., Lundh, E. R., Vijay, S., Nitecki, D., Morser, J., Stern, D. and Schmidt, A. M. (1995). The receptor for advanced glycation end products (RAGE) is a cellular binding site for amphoterin. Mediation of neurite outgrowth and co-expression of RAGE and amphoterin in the developing nervous system. *J. Biol. Chem.* **270**:25752–25761.

Hu, A. and Norryby, E. (1994). Role of individual cysteine residues in the processing and antigenicity of the measles virus haemagglutinin protein. *J. Gen. Virol.* **75**:2173–2181.

Hu, A., Cattaneo, R., Schwartz, S. and Norrby, E. (1994). Role of N-linked oligosaccharide chains in the processing and antigenicity of measles virus haemagglutinin protein. *J. Gen. Virol.* **75**:1043–1052.

Hu, X., Yagi, Y., Tanji, T., Zhou, S. and Ip, Y. T. (2004) Multimerization and interaction of Toll and Spätzle in *Drosophila*. *Proc. Natl. Acad. Sci. USA* **101**:9369–9374.

Huang, J. S., Guh, J. Y., Hung, W. C., Yang, M. L., Lai, Y. H., Chen, H. C. and Chuang, L. Y. (1999). Role of the Janus kinase (JAK)/signal transducters and activators of transcription (STAT) cascade in advanced glycation end-product-induced cellular mitogenesis in NRK-49F cells. *Biochem J.* **342**:231–238.

Hudson, B. I., Carter, A. M., Harja, E., Kalea, A. Z., Arriero, M., Yang, H., Grant, P. J. and Schmidt, A. M. (2008b). Identification, classification, and expression of *RAGE* gene splice variants. *FASEB J.* **22**:1572–1580.

Hudson, B. I., Kalea, A. Z., Del Mar Arriero, M., Harja, E., Boulanger, E., D'Agati, V. and Schmidt, A. M. (2008a). Interaction of the RAGE cytoplasmic domain with diaphanous-1 is required for ligand-stimulated cellular migration through activation of Rac1 and Cdc42. *J. Biol. Chem.* **283**:34457–34468.

Hunter, M. J. and Chazin, W. J. (1998). High level expression and dimer characterization of the S100 EF-hand proteins, migration inhibitory factor-related proteins. *J. Biol. Chem.* **273**:12427–12435.

Huttunen, H. J., Fages, C. and Rauvala, H. (1999). Receptor for advanced glycation end products (RAGE)-mediated neurite outgrowth and activation of NF-κB require the cytoplasmic domain of the receptor but different downstream signalling pathways. *J. Biol. Chem.* **274**:19919–19924.

Huttunen, H. J., Fages, C., Kuja-Panula, J., Ridley, A. J. and Rauvala, H. (2002). Receptor for advanced glycation end products-binding COOH-terminal motif of amphoterin inhibits invasive migration and metastasis. *Cancer Res.* **62**:4805–4811.

Irzyk, C. P. and Fuerst, E. P. (1993). Purification and Characterization of a Glutathione S-Transferase from Benoxacor-Treated Maize (*Zea mays*). *Plant Physiol.* **102**:803–810.

Ishihara, K., Tsutsumi, K., Kawane, S., Nakajima, M. and Kasaoka, T. (2003). The receptor for advanced glycation end-products (RAGE) directly binds to ERK by a D-domain-like docking site. *FEBS Lett*. **550**:107–113.

Jacobs, P. P. and Callewaert, N. (2009). N-glycosylation engineering of biopharmaceutical expression systems. *Curr. Mol. Med.* **9**:774–800.

Jahn, T. R. and Radford, S. E. (2008). Folding *versus* aggregation: Polypeptide conformations on competing pathways. *Arch Biochem Biophys*. **469**: 100–117.

Jana, S. and Deb, J. K. (2005). Strategies for efficient production of heterologous proteins in *Escherichia coli*. *Appl. Microbiol. Biotechnol.* **67**:289–298.

Janssen, B. J. and Gardner, R. C. (1990). Localized transient expression of GUS in leaf discs following co-cultivation with *Agrobacterium*. *Plant Mol. Biol.* **14**:61–72.

Janssen, L., Sobott, F., De Deyn, P. P., Dam, D. V. (2015). Signal loss due to oligomerization in ELISA analysis of amyloid-beta can be recovered by a novel sample pre-treatment method. *MethodsX* **2**:112–123

Jenkins, N. and Curling, E. M. (1994). Glycosylation of recombinant proteins: problems and prospects. *Enzyme Microb. Technol*. **16**:354–364.

Joh, L. D. and VanderGheynst, J. S. (2006). Perspective Agroinfiltration of plant tissues for production of high-value recombinant proteins: an alternative to production in transgenic crops. *J. Sci. Food Agric*. **86**:2002–2004.

Kailemia, M. J., Ruhaak, L. R., Lebrilla, C. B. and Amster, I. J. (2014). Oligosaccharide Analysis by Mass Spectrometry: A Review of Recent Developments. *Anal. Chem.* **86:**196–212.

Kang, R.*,* Loux, T., Tang, D., Schapiro, N. E., Vernon, P., Livesey, K. M., Krasinskas, A., Lotze, M. T. and Zeh H. J. (2012). The expression of the receptor for advanced glycation endproducts (RAGE) is permissive for early pancreatic neoplasia. *Proc. Natl. Acad. Sci. USA* **109**:7031–7036.

Kapila, J., De Rycke, R., Montagu, M. V. and Angenon, G. (1997). An *Agrobacterium*-mediated transient gene expression system for intact leaves. *Plant Sci.* **122**:101–108.

Kapust, R. B. and Waugh, D. S. (1999). *Escherichia coli* maltose-binding protein is uncommonly effective at promoting the solubility of polypeptides to which it is fused. *Protein Sci.* **8**:1668–1674.

Kastritis, P. L. and Bonvin, A. M. J. J. (2013). On the binding affinity of macromolecular interactions: daring to ask why proteins interact. *J R Soc Interface* **10**:20120835.

Ke, N. and Berkmen, M. (2014). Production of Disulfide-Bonded Proteins in *Escherichia coli. Curr Protoc Mol Biol.* **108**:I:16.1B:16.1B.1–16.1B.21.

Khoudi, H., Laberge, S., Ferullo, J. M., Bazin, R., Darveau, A., Castonguay, Y., Allard, G., Lemieux, R. and Vezina, L. P. (1999). Production of a diagnostic monoclonal antibody in perennial alfalfa plants. *Biotechnol. Bioeng*. **64**:135–143.

Kislinger, T., Fu, C., Huber, B., Qu, W., Taguchi, A., Du Yan, S., Hofmann, M., Yan, S. F., Pischetsrieder, M., Stern, D. and Schmidt, A. M. (1999). Nε-(carboxymethyl)lysine adducts of proteins are ligands for receptor for advanced glycation end products that activate cell signalling pathways and modulate gene expression. *J. Biol. Chem.* **274**:1740–31749.

Kjeldsen, T. (2000). Yeast secretory expression of insulin precursors. *Appl Microbiol Biotechnol.* **54**:277– 286.

Klimyuk, V., Marillonnet, S., Knaeblein, J., McCaman, M. and Gleba Y. (2005). Production of recombinant proteins in plants. *In Modern Biopharmaceuticals* (Knaeblein J & Mulller RH eds), Chap. VI. Weinheim: WILEY-WCH Verlag GmbH & Co.KgaA.

Knapp, S., Müller, S. Digilio, G., Bonaldi, T., Bianchi, M. E. and Musco, G. (2004). The Long Acidic Tail of High Mobility Group Box 1 (HMGB1) Protein Forms an Extended and Flexible Structure That Interacts with Specific Residues within and between the HMG Boxes. *Biochemistry* **43:**11992–11997.

Knaust, R. K. and Nordlund, P. (2001). Screening for soluble expression of recombinant proteins in a 96-well format. *Anal. Biochem.* **297**:79–85.

Koch, M., Chitayat, S., Dattilo, B. M., Schiefner, A., Diez, J., Chazin, W. J. and Fritz, G. (2010). Structural basis for ligand recognition and activation of RAGE. *Structure* **18**:1342–1352.

Koley, D. and Bard A. J. (2010). Triton X-100 concentration effects on membrane permeability of a single HeLa cell by scanning electrochemical microscopy (SECM). *Proc. Natl. Acad. Sci*. USA **107**:16783–16787.

Komaraiah, P., Reddy, G. V., Reddy, P. S., Raghavendra, A. S., Ramakrishna, S. V. and Reddanna, P. (2003). Enhanced production of antimicrobial sesquiterpenes and lipoxygenase metabolites in elicitor-treated hairy root cultures of *Solanum tuberosum*. *Biotechnol. Lett*. **25**:593–597.

Kondo, A., Kohda, J., Endo, Y., Shiromizu, T., Kurokawa, Y., Nishihara, K., Yanagi, H., Yura, T. and Fukuda, H. (2000). Improvement of productivity of active horseradish peroxidase in *Escherichia coli* by coexpression of Dsb proteins. *J. Biosci. Bioeng*. **90**:600–606.

Korndorfer, I. P., Brueckner, F. and Skerra, A. (2007). The crystal structure of the human (S100A8/S100A9)2 heterotetramer, calprotectin, illustrates how conformational changes of interacting alpha-helices can determine specific association of two EF-hand proteins. *J. Mol. Biol.* **370**:887–898.

Koya, V., Moayeri, M., Leppla, S. H. and Daniell, H. (2005). Plant-based vaccine: mice immunized with chloroplast-derived anthrax protective antigen survive anthrax lethal toxin challenge infect. *Infect. Immun.* **73**:8266–8274.

Kumano-Kuramochi, M., Ohnishi-Kameyama, M., Xie, Q., Niimi, S., Kubota, F., Komba, S. and Machida, S. (2009). Minimum stable structure of the receptor for advanced glycation end product possesses multi ligand binding ability. *Biochem. Biophys. Res. Commun.* **386**:130–134.

Lam, J. K., Wang, Y., Shiu, S. W., Wong, Y., Betteridge, D. J. and Tan, K. C. (2013). Effect of insulin on the soluble receptor for advanced glycation end products (RAGE). *Diabet. Med.* **30**:702–709.

Lampson, G. P. and Tytell, A. A. (1965). A simple method for estimating isoelectric points. *Anal. Biochem.* **11**:374–377.

Lanctot, P. M., Leclerc, P. C., Clement, M., Auger-Messier, M., Escher, E., Leduc, R. and Guillemette, G. (2005). Importance of N-glycosylation positioning for cell-surface expression, targeting, affinity and quality control of the human AT_1 receptor. *Biochem. J.* **390**:367–376.

Lander, H. M., Tauras, J. M., Ogiste, J. S., Hori, O., Moss, R. A. and Schmidt, A. M. (1997). Activation of the receptor for advanced glycation end products triggers a p21(ras)-dependent mitogen-activated protein kinase pathway regulated by oxidant stress. *J. Biol. Chem.* **272**:17810–17814.

Leader, B., Baca, Q. J. and Golan D. E. (2008). Protein therapeutics: a summary and pharmacological classification. *Nat. Rev. Drug Discov.* **7**:21–39.

Leclerc, E., Fritz, G., Vetter, S. W. and Heizmann, C. W. (2009). Binding of S100 proteins to RAGE: An update. *Biochim. Biophys. Acta.* **1793**:993–1007.

Leclerc, E., Fritz, G., Weibel, M., Heizmann, C. W. and Galichet, A. (2007). S100B and S100A6 differentially modulate cell survival by interacting with distinct RAGE (receptor for advanced glycation end products) immunoglobulin domains. *J. Biol. Chem.* **282**:31317–31331.

Leclerc, E., Sturchler, E. and Vetter, S. W. (2010). The S100B/RAGE Axis in Alzheimer's disease. *Cardiovas. Psychiatry Neurol.* **2010**:1–11.

Lee, L. Y. and Gelvin, S. B. (2008). T-DNA Binary Vectors and Systems. *Plant Physiol.* **146**:325–332.

Lee, S-W., Park, K-H., Park, S., Kim, J-H., Hong, S-Y., Lee, S-K., Choi, D. and Park, Y-B. (2013). Soluble Receptor for Advanced Glycation End Products Alleviates Nephritis in (NZB/NZW)F1 Mice. *Arthritis Rheum.* **65**:1902–1912.

Leukert, N., Vogl, T., Strupat, K., Reichelt, R., Sorg, C. and Roth, J. (2006). Calcium-dependent tetramer formation of S100A8 and S100A9 is essential for biological activity. *J. Mol. Biol.* **359**:961–972.

Leuzinger, K., Dent, M., Hurtado, J., Stahnke, J., Lai, H., Zhou, X. and Chen, Q. (2013). Efficient agroinfiltration of plants for high-level transient expression of recombinant proteins. *J. Vis. Exp.* **77**:1–9, e50521.

Li, F., Vijayasankaran, N., Shen, A., Kiss, R., Amanullah, A. (2010). Cell culture processes for monoclonal antibody production. *mAbs* **2**:466–477.

Li, J. H., Wang, W., Huang, X. R., Oldfield, M., Schmidt, A. M., Cooper, M. E. and Lan, H. Y. (2004). Advance glycation end products induce tubular epithelial-myofibroblast transition through the RAGE-ERK1/2 MAP kinase signalling pathway. *Am. J. Pathol.* **164**:1389–1397.

Lico, C., Chen, Q. and Santi, L. (2008). Viral vectors for production of recombinant proteins in plants. *J. Cell Physiol.* **216**:366–377.

Lih-Fen, L., Walker, D. G., Jacobson, S. and Sabbagh, M. (2009). Receptor for Advanced Glycation End Products: It's Role in Alzheimer's disease and Other Neurological Diseases. *Future Neurol.* **4**:167–177.

Lin, H. W., Kwok, K. H. and Doran, P. M. (2003). Production of podophyllotoxin using cross-species coculture of *Linum flavum* hairy roots and *Podophyllum hexandrum* cell suspensions. *Biotechnol. Prog.* **19**:1417–1426.

Liu, H. L., Li, W. S., Lei, T., Zheng, J., Zhang, Z., Yan, X. F., Wang, Z. Z., Wang, Y. L. and Si, L. S. (2005). Expression of human papillomavirus type 16 L1 protein in transgenic tobacco plants. *Acta Biochim Biophys Sin (Shanghai).* **37**:153–158.

Liu, R., Mori, S., Wake, H., Zhang, J., Liu, K., Izushi, Y., Takahashi, H. K., Peng, B. and Nishibori, M. (2009). Establishment of *in vitro* binding assay of high mobility group box-1 and S100A12 to receptor for advanced glycation endproducts: heparin's effect on binding. *Acta. Med. Okayama.* **63**:203–211.

Lodish, H., Berk, A., Zipursky, S. L. *et al.* Molecular Cell Biology. 4th edition. New York: W. H. Freeman; 2000. Available from: http://ncbi.nlm.nih.gov/books/NBK21475/.

Logsdon, C. D., Fuentes, M. K., Huang, E. H. and Arumugam, T. (2007). RAGE and RAGE ligands in Cancer. *Curr. Mol. Med.* **7**:777–789.

Lohman, T. M. and Mascotti, D. P. (1992). Thermodynamics of ligand-nucleic acid interactions. *Methods Enzymol.* **212**:400–424.

Loos, A. and Steinkellner, H. IgG-Fc glycoengineering in non-mammalian expression hosts. (2012). *Arch Biochem Biophys.* **526**:167–173.

Lorkovic, Z. L., Kirk, D. A. W., Lambermon, M. H. and Filipowicz, W. (2000). Pre-mRNA splicing in higher plants. *Trends Plant Sci.* **5**:160–167.

Lowery, J. W., Amich, J. M., Andonian, A. and Rosen, V. (2014). N-linked glycosylation of the bone morphogenetic protein receptor type 2 (BMPR2) enhances ligand binding. *Cell Mol Life Sci.* **71**:3165–3172.

Lu, M., Yu, S., Xu, W., Gao, B. and Xiong, S. (2015). HMGB1 Promotes Systemic Lupus Erythematosus by Enhancing Macrophage Inflammatory Response. *J Immunol Res.* **2015**:946748.

Lue, L. F., Walker, D. G., Brachova, L., Beach, T. G., Rogers, J., Schmidt, A. M., Stern, D. M. and Yan, S. D. (2001). Involvement of microglial receptor for advanced glycation endproducts (RAGE) in Alzheimer's disease: identification of a cellular activation mechanism. *Exp. Neurol.* **171**:29–45.

Ma, J. K. and Lehner, T. (1990). Prevention of colonization of *Streptococcus* mutans by topical application of monoclonal antibodies in human subjects. *Arch. Oral Biol.* **35**:115S-122S.

Ma, J. K. C., Drake, P. M. W. and Christou, P. (2003). Genetic modification: The production of recombinant pharmaceutical proteins in plants. *Nat. Rev. Genet.* **4**:794–805.

Ma, J. K., Barros, E., Bock, R., Christou, P., Dale, P. J., Dix, P. J., Fischer, R., Irwin, J., Mahoney, R., Pezzotti, M., Schillberg, S., Sparrow, P., Stoger, E. and Twyman, R. M. (2005). Molecular farming for new drugs and vaccines. Current perspectives on the production of pharmaceuticals in transgenic plants. *EMBO Rep.* **6**:593–599.

Ma, J. K., Hiatt, A., Hein, M., Vine, N. D., Wang, F., Stabila, P., van Dolleweerd, C., Mostov, K. and Lehner, T. (1995). Generation and assembly of secretory antibodies in plants. *Science* **268**:716–719.

Ma, J. K., Hikmat, B. Y., Wycoff, K., Vine, N. D., Chargelegue, D., Yu, L., Hein, M. B. and Lehner, T. (1998). Characterization of a recombinant plant monoclonal secretory antibody and preventive immunotherapy in humans. *Nat. Med.* **4**:601–606.

Maclean, J., Koekemoer, M., Olivier, A. J., Stewart, D., Hitzeroth, I. I., Rademacher, T., Fischer, R., Williamson, A. L. and Rybicki, E. P. (2007). Optimization of human papillomavirus type 16 (HPV-16) L1 expression in plants: comparison of the suitability of different HPV-16 L1 gene variants and different cell-compartment localization. *J Gen Virol.* **88**:1460–1469.Madanala, R., Gupta, V., Pandey, A. K.,

Srivastava, S., Pandey, V., Singh, P. K. and Tuli, R. (2015). Tobacco Chloroplasts as Bioreactors for the Production of Recombinant Superoxide Dismutase in Plants, an Industrially Useful Enzyme. *Plant Mol Biol Rep*. **33**:1107–1115.

Magdeldin, S. and Moser, A. (2012). Affinity Chromatography: Principles and Applications, Affinity Chromatography, Dr. Sameh Magdeldin (Ed.), ISBN: 978-953-51-0325-7, InTech, Available from:http://www.intechopen.com/books/affinity-chromatography/affinity-chromatography-principles-and-applications.

Maire, M. le., Viel, A., Møller, J. V. (1989). Size-exclusion chromatography and universal calibration of gel columns. A*nal. Biochem.* **177**:50–56.

Manigrasso, M. B., Pan, J., Rai, V., Zhang, J., Reverdatto, S., Quadri, N., DeVita, R. J., Ramasamy, R., Shekhtman, A. and Schmidt, A. M. (2016). Small Molecule Inhibition of Ligand-Stimulated RAGE-DIAPH1 Signal Transduction. *Sci Rep.* **6**:22450.

Margraf-Schönfeld, S., Böhm, C. and Watzl, C. (2011). Glycosylation Affects Ligand Binding and Function of the Activating Natural Killer Cell Receptor 2B4 (CD244) Protein. *J. Biol. Chem.* **286**:24142–24149.

Marillonnet, S., Giritch, A., Gils, M., Kandzia, R., Klimyuk, V. and Gleba, Y. (2004). *In planta* engineering of viral RNA replicons: Efficient assembly by recombination of DNA modules delivered by *Agrobacterium. Proc. Natl. Acad. Sci. USA* **101**:6852–6857.

Marillonnet, S., Thoeringer, C., Kandzia, R., Klimyuk, V. and Gleba, Y. (2005). Systemic *Agrobacterium tumefaciens*-mediated transfection of viral replicons for efficient transient expression in plants. *Nat. Biotechnol.* **23**:718–723.

Martens, H. A., Nienhuis, H. L., Gross, S., van der Steege, G., Brouwer, E., Berden, J. H., de Sévaux, R. G., Derksen, R. H., Voskuyl, A. E., Berger, S. P., Navis, G. J., Nolte, I. M., Kallenberg, C. G. and Bijl, M. (2012). Receptor for advanced glycation end products (RAGE) polymorphisms are associated with systemic lupus erythematosus and disease severity in lupus nephritis. *Lupus* **21**:959–968.

Martinez, C., Petruccelli, S., Giulietti, A. M. and Alvarez, M. A. (2005). Expression of the antibody 14D9 in *Nicotiana tabacum* hairy roots. *Electron J. Biotechnol.* **8**:170–176.

Mason, H. S., Ball, J. M., Shi, J. J., Jiang, X., Estes, M. K. and Arntzen, C. J. (1996). Expression of Norwalk virus capsid protein in transgenic tobacco and potato and its oral immunogenicity in mice. *Proc. Natl. Acad. Sci. USA* **93**:5335–5340.

McGarvey, P. B., Hammond, J., Dienelt, M. M., Hooper, D. C., Fu, Z. F., Dietzschold, B., Koprowski, H. and Michaels, F. H. (1995). Expression of the rabies virus glycoprotein in transgenic tomatoes. *Biotechnol. (NY)* **13**:1484–1487.

Melo, E. P., Aires-Barros, M. R., Costa, S. M. and Cabral, J. M. (1997). Thermal unfolding of proteins at high pH range studied by UV absorbance. *J Biochem Biophys Methods.* **34**:45–59.

Mogk, A., Mayer, M. P. and Deuerling, E. (2002). Mechanisms of protein folding: molecular chaperones and their applications in biotechnology. *Chembiochem* **3**:807–814.

Monahan, F. J., German, J. B. and Kinsella, J. E. (1995). Effect of pH and Temperature on Protein Unfolding and Thiol/Disulfide Interchange Reactions during Heat-Induced Gelation of Whey Proteins. *J. Agric. Food Chem.* **43**:46–52.

Mortimer, E., Maclean, J. M., Mbewana, S., Buys, A., Williamson, A-L., Hitzeroth, I. I. and Rybicki, E. P. (2012). Setting up a platform for plant-based influenza virus vaccine production in South Africa. *BMC Biotechnology.* **12**:14.

Moy, K. A., Jiao, L., Freedman, N. D., Weinstein, S. J., Sinha, R., Virtamo, J., Albanes, D. and Stolzenberg-Solomon, R. Z. (2013). Soluble receptor for advanced glycation end products and risk of liver cancer. *Hepatology* **57**:2338–2345.

Moyano, E., Jouhikainen, K., Tammela, P., Palazon, J., Cusido, R. M., Pinol, M. T., Teeri, T. H. and Oksman-Caldentey, K. M. (2003). Effect of pmt gene overexpression on tropane alkaloid production in transformed root cultures of *Datura metel* and *Hyoscyamus muticus*. *J. Exp. Bot*. **54**:203–211.

Muhammad, S., Barakat, W., Stoyanov, S., Murikinati, S., Yang, H., Tracey, K. J., Bendszus, M., Rossetti, G., Nawroth, P. P., Bierhaus, A. and Schwaninger, M. (2008). The HMGB1 Receptor RAGE Mediates Ischemic Brain Damage. *J. Neurosci.* **28**:12023–12031.

Musumeci, D., Roviello, G. N. and Montesarchio, D. (2015). An overview on HMGB1 inhibitors as potential therapeutic agents in HMGB1-related pathologies. *Pharmacol Ther.* **141**:347–357.

Nagels, B., Weterings, K., Callewaert, N. and Van Damme, E. J. M. (2012). Production of Plant Made Pharmaceuticals: From Plant Host to Functional Protein. *Crit Rev in Plant Sci* **31**:148–180.

Nayal, M. and Di Cera, E. (1994). Predicting Ca^{2+}-binding sites in proteins. *Proc. Natl. Acad. Sci. USA* **91**:817–821.

Neeper, M., Schmidt, A. M., Brett, J., Yan, S. D., Wang, F., Pan, Y. C., Elliston, K., Stern, D. and Shaw, A. (1992). Cloning and expression of a cell surface receptor for advanced glycosylation end products of proteins. *J. Biol. Chem.* **267**:14998–15004.

Nybo, K. (2010). Protein Purification: Ion Exchange. *Bio Techniques* **49**:869–871.

Nyborg, J. K. and Olve B. Peersen, O. B. (2004). That zincing feeling: the effects of EDTA on the behaviour of zinc-binding transcriptional regulators. *Biochem. J.* **381**:e3–e4.

Odink, K., Cerletti, N., Bruggen, J., Clerc, R. G., Tarcsay, L., Zwadlo, G., Gerhards, G., Schlegel, R. and Sorg, C. (1987). Two calcium-binding proteins in infiltrate macrophages of rheumatoid arthritis. *Nature* **330**:80–82.

Ohana, R. F., Encell, L. P., Zhao, K., Simpson, D., Slater, M. R., Urh, M. and Wood K. V. (2009). HaloTag7: a genetically engineered tag that enhances bacterial expression

of soluble proteins and improves protein purification. *Protein Expr. Purif.* **68**:110–120.

Okazaki, F., Aoki, J., Tabuchi, S., Tanaka, T., Ogino, C. and Kondo, A. (2012). Efficient heterologous expression and secretion in *Aspergillus oryzae* of a llama variable heavy-chain antibody fragment V(HH) against EGFR. *Appl Microbiol Biotechnol.* **96**:81–88.

Ongay, S., Boichenko, A., Govorukhina, N. and Bischoff, R. (2012). Glycopeptide enrichment and separation for protein glycosylation analysis. *J. Sep. Sci.* **35**:2341–2372.

Origlia, N., Righi, M., Capsoni, S., Cattaneo, A., Fang, F., Stern, D. M., Chen, J. X., Schmidt, A. M., Arancio, O., Yan, S. D. and Domenici, L. (2008). Receptor for advanced glycation end product-dependent activation of p38 mitogen-activated protein kinase contributes to amyloid-beta-mediated cortical synaptic dysfunction. *J. Neurosci.* **28**:3521–3530.

Ostendorp, T., Leclerc, E., Galichet, A., Koch, M., Demling, N., Weigle, B., Heizmann, C. W., Kroneck, P. M. H and Fritz, G. (2007). Structural and functional insights into RAGE activation by multimeric S100B. *EMBO J.* **26**:3868–3878.

Ostendorp, T., Weibel, M., Leclerc, E., Kleinert, P., Kroneck, P. M. H., Heizmann, C. W. and Fritz, G. (2006). Expression and purification of the soluble isoform of human receptor for advanced glycation end products (sRAGE) from *Pichia pastoris.* *Biochem. Biophys. Res. Commun.* **347**:4–11.

Park, H., Adsit, F. G. and Boyington, J. C. (2010). The 1.5A° crystal structure of human Receptor for advanced glycation end products (RAGE) ectodomains reveals unique features determining ligand binding. *J. Biol. Chem.* **285**:40762–40770.

Park, I. H., Yeon, S. I., Youn, J. H., Choi, J. E., Sasaki, N., Choi, I. H. and Shin J. S. (2004). Expression of a novel secreted splice variant of the receptor for advanced glycation end products (RAGE) in human brain astrocytes and peripheral blood mononuclear cells. *Mol. Immunol.* **40**:1203–1211.

Park, S. J., Kleffmann, T. and Hessian, P. A. (2011). The G82S polymorphism promotes glycosylation of the receptor for advanced glycation end products (RAGE) at asparagine 81: comparison of wild-type RAGE with the G82S polymorphic variant. *J. Biol. Chem.* **286**:21384–21392.

Paul, M. and Ma, J. K. C. (2011). Plant-made pharmaceuticals: Leading products and product platforms. *Biotechnol Appl Biochem.* **58**:58–67.

Penfold, S. A., Coughlan, M. T., Patel, S. K., Srivastava, P. M., Sourris, K. C., Steer, D., Webster, D. E., Thomas, M. C., Maclsaac, R. J., Jerums, G., Burrell, L. M., Cooper, M. E. and Forbes J. M. (2010). Circulating high-molecular-weight RAGE ligands activate pathways implicated in the development of diabetic nephropathy. *Kidney Int.* **78**:287–295.

Pengelly, J. J. L., Forster, B., von Caemmerer, S., Badger, M. R., Price, G. D. and Whitney, S. M. (2014). Transplastomic integration of a cyanobacterial bicarbonate transporter into tobacco chloroplasts. *J. Exp. Bot.* **65**:3071–3080.

Peters, R. T., Low, S. C., Kamphaus, G. D., Dumont, J. A., Amari, J. V., Lu, Q., Zarbis-Papastoitsis, G., Reidy, T. J., Merricks, E. P., Nichols, T. C. and Bitonti, A. J. (2010). Prolonged activity of factor IX as a monomeric Fc fusion protein. *Blood*. **115**:2057–2064.

Porro, D., Sauer, M., Branduardi, P. and Mattanovich, D. (2005). Recombinant protein production in yeasts. *Mol Biotechnol*. **31**:245–259.

Poulsom, R., Hogg, N., Robinson, M. J. and Tessier, P. (2002). The S100 family heterodimer, MRP-8/14, binds with high affinity to heparin and heparan sulfate glycosaminoglycans on endothelial cells. *J. Biol. Chem*. **277**:3658–3665.

Propper, C., Huang, X., Roth, J., Sorg, C. and Nacken, W. (1999). Analysis of the MRP8-MRP14 protein–protein interaction by the two-hybrid system suggests a prominent role of the C-terminal domain of S100 proteins in dimer formation. *J. Biol. Chem.* **274**:183–188.

Przybycien, T. M., Dunn, J. P., Valax, P. and Georgiou, G. (1994). Secondary structure characterization of beta-lactamase inclusion bodies. *Protein Eng*. **7**:131–136.

Putalun, W., Taura, F., Qing, W., Matsushita, H., Tanaka, H. and Shoyama Y. (2003). Anti-solasodine glycoside single-chain Fv antibody stimulates biosynthesis of solasodine glycoside in plants. *Plant Cell Rep*. **22**:344–349.

Queisser, M. A., Kouri, F. M., Konigshoff, M., Wygrecka, M., Schubert, U., Eickelberg, O. and Preissner, K. T. (2008). Loss of RAGE in pulmonary fibrosis: molecular relations to functional changes in pulmonary cell types. *Am. J. Respir. Cell Mol. Biol.* **39**:337–345.

Rai, V., Maldonado, A. Y., Burz, D. B., Reverdatto, S., Yan, S. F., Schmidt, A. M. and Shekhtman, A. (2012). Signal transduction in receptor for advanced glycation end products (RAGE): solution structure of C-terminal RAGE (ctRAGE) and its binding to mDia1. *J. Biol. Chem.* **287**:5133–5144.

Ramasamy, R., Yan, S. F. and Schmidt, A. M. (2011). Receptor for AGE (RAGE): signaling mechanisms in the pathogenesis of diabetes and its complications. *Ann. NY Acad. Sci*. **1243**:88–102.

Rauch, C., Feifel, E., Amann, E. M., Spotl, H. P., Schennach, H., Pfaller, W. and Gstraunthaler, G. (2011). Alternatives to the use of fetal bovine serum: platelet lysates as a serum substitute in cell culture media. *ALTEX* **28**:305–316.

Read, C. M., Cary, P. D., Crane-Robinson, C., Driscoll, P. C. and Norman, D. G. (1993). Solution structure of a DNA-binding domain from HMG1. *Nucleic Acids Res*. **21**:3427–3436.

Redkiewicz, P., Sirko, A., Kamel, K. A. and Gora-Sochacka, A. (2014). Plant expression systems for production of hemagglutinin as a vaccine against influenza virus. *Acta Biochim Pol*. **61**:551–560.

Renard, C., Chappey, O., Wautier, M. P., Nagashima, M., Lundh, E., Morser, J. Zhao, L., Schmidt, A. M., Scherrmann, J. M. and Wautier, J. L. (1997). Recombinant

Advanced Glycation End Product Receptor Pharmacokinetics in Normal and Diabetic Rats. *Mol Pharmacol.* **52**:54–62.

Richter, L. J., Thanavala, Y., Arntzen, C. J and Mason, H. S. (2000). Production of hepatitis B surface antigen in transgenic plants for oral immunization. *Nat. Biotechnol.* **18**:1167–1171.

Richter, W., Hermsdorf, T., Kronbach, T. and Dettmer, D. (2002). Refolding and purification of recombinant human PDE7A expressed in *Escherichia coli* as inclusion bodies. *Protein Expr. Purif.* **25**:138–148.

Rigano, M. M., De Guzman, G., Walmsley, A. M., Frusciante, L. and Barone, A. (2013). Production of Pharmaceutical Proteins in *Solanaceae* Food Crops. *Int. J. Mol. Sci.* **14**:2753–2773.

Ritchie, C. (2012). Protein Purification. *MATER METHODS*. **2**:134.

Robinson, M. J., Tessier, P., Poulsom, R. and Hogg, N. (2002). The S100 family heterodimer, MRP-8/14, binds with high affinity to heparin and heparan sulfate glycosaminoglycans on endothelial cells. *J. Biol. Chem.* **277**:3658–3665.

Rosano, G. L. and Ceccarelli E. A. (2009). Rare codon content affects the solubility of recombinant proteins in a codon bias-adjusted *Escherichia coli* strain. *Microb. Cell Fact.* **8**:1–9.

Rosano, G. L. and Ceccarelli, E. A. (2014). Recombinant protein expression in *Escherichia coli*: advances and challenges. *Front Microbiol.* **5**:172.

Rosen, R., Biran, D., Gur, E., Becher, D., Hecker, M. and Ron E. Z. (2002). Protein aggregation in *Escherichia coli*: role of proteases. *FEMS Microbiol. Lett.* **207**:9–12.

Roth, J., Vogl, T., Sorg, C. and Sunderkotter, C. (2003). Phagocyte-specific S100 proteins: a novel group of proinflammatory molecules. *Trends Immunol.* **24**:155–158.

Roth, Z., Yehezkel, G. and Khalaila, I. (2012). Identification and Quantification of Protein Glycosylation. *Int. J. Carbohydr. Chem.* **2012**: 10.

Routledge, S. J., Hewitt, C. J., Bora, N. and Bill, R. M. (2011). Antifoam addition to shake flask cultures of recombinant *Pichia pastoris* increases yield. *Microb. Cell Fact.* **10**:1–11.

Ruhlman, T., Ahangari, R., Devine, A., Samsam, M. and Daniell, H. (2007). Expression of cholera toxin B-proinsulin fusion protein in lettuce and tobacco chloroplasts--oral administration protects against development of insulitis in non-obese diabetic mice. *Plant Biotechnol J.* **5**:495–510.

Sachdev, D. and Chirgwin, J. M. (1998). Order of fusions between bacterial and mammalian proteins can determine solubility in *Escherichia coli. Biochem. Biophys. Res. Commun.* **244**:933–937.

Sack, M., Hofbauer, A., Fischer, R. and Stoger, E. (2015). The increasing value of plant-made proteins. *Curr Opin Biotech*. **32**:163–170.

Sack, M., Hofbauer, A., Fischer, R. and Stoger, E. The increasing value of plant-made proteins. (2015). *Curr Opin Chem Biol.* **32**:163–170.

Sainsbury, F. and Lomonossoff, G. P. (2008). Extremely High-Level and Rapid Transient Protein Production in Plants without the Use of Viral Replication. *Plant Physiol.* **148**:1212–1218.

Sainsbury, F. and Lomonossoff, G. P. (2014). Transient expressions of synthetic biology in plants. *Curr. Opin. Plant Biol.* **19**:1–7.

Saint-Jore-Dupas, C., Faye, L. and Gomord, V. (2007). From planta to pharma with glycosylation in the toolbox. *Trends Biotechnol.* **25**:317–323.

Sakurai, S., Yonekura, H., Yamamoto, Y., Watanabe, T., Tanaka, N., Li, H., Rahman, A. K., Myint, K. M., Kim, C. H. and Yamamoto, H. (2003). The AGE-RAGE system and diabetic nephropathy. *J. Am. Soc. Nephrol.* **14**:S259–S263.

Sanford, J. C. (1990). Biolistic plant transformation. *Physiol. Plant* **79**:206–209.

Santamaria-Kisiel, L., Rintala-Dempsey, A. C. and Shaw G. S. (2006). Calcium-dependent and independent interactions of the S100 protein family. *Biochem J.* **396**:201–214.

Santi, L., Giritch, A., Roy, C. J., Marillonnet, S., Klimyuk, V., Gleba, Y., Webb, R., Arntzen, C. J. and Mason, H. S. (2006). Protection conferred by recombinant *Yersinia pestis* antigens produced by a rapid and highly scalable plant expression system. *Proc. Natl. Acad. Sci. USA* **103**:861–866.

Sarkany, Z., Ikonen, T. P., Ferreira-da-Silva, F., Saraiva, M. J., Svergun, D. and Damas, A. M. (2011). Solution structure of the soluble receptor for advanced glycation end products (sRAGE). *J. Biol. Chem.* **286**:37525–37534.

Schäfer, B. W. and Heizmann, C. W. (1996). The S100 family of EF-hand calcium-binding proteins: functions and pathology. *Trends Biochem Sci.* **21**:134–140.

Schedin-Weiss, S., Winblad, B. and Tjernberg, L. O. (2014). The role of protein glycosylation in Alzheimer disease. *FEBS* **281**:46–62.

Schein, C. H. (1989). Production of soluble recombinant proteins in bacteria. *Nat. Biotechnol.* **7**:1141–1149.

Schell, J., Van Montagu, M., De Beuckeleer, M., De Block, M., Depicker, A., De Wilde, M., Engler, G., Genetello, C., Hernalsteens, J. P., Holsters, M., Seurinck, J., Silva, B., Van Vliet, F, Villarroel R. (1979). Interactions and DNA transfer between *Agrobacterium tumefaciens*, the Ti-plasmid and the plant host. *Proc R Soc Lond B Biol Sci.* **204**:251–266.

Schellekens, H. (2002). Immunogenicity of therapeutic proteins: clinical implications and future prospects. *Clin. Ther.* **24**:1720–1740.

Schlegel, S., Rujas, E., Ytterberg, A. J., Zubarev, R. A., Luirink, J. and Jan-Willem de Gier. (2013). Optimizing heterologous protein production in the periplasm of *E. coli* by regulating gene expression levels. *Microb Cell Fact.* **12**:1–12.

Schlueter, C., Hauke, S., Flohr, A. M., Rogalla, P. and Bulle, J. (2003). Tissue-specific expression patterns of the RAGE receptor and its soluble forms–a result of regulated alternative splicing? *Biochim. Biophys. Acta.* **1630**:1–6.

Schmidt, A. M. (2015). Soluble RAGEs-Prospects for treating & tracking metabolic and inflammatory disease. *Vascul. Pharmacol.* **72**:1–8.

Schmidt, A. M., Hori, O., Brett, J., Yan, S. D., Wautier, J. L. and Stern, D. (1994). Cellular receptors for advanced glycation end products: Implications for induction of oxidant stress and cellular dysfunction in the pathogenesis of vascular lesions. *Arterioscler. Thromb.* **14**:1521–1528.

Schmidt, A. M., Vianna, M., Gerlach, M., Brett, J., Ryan, J., Kao, J., Esposito, C., Hegarty, H., Hurley, W., Clauss, M., Wangl, F., Pan, Y-C. E., Tsang, T. C. and Stern, D. (1992). Isolation and characterization of two binding proteins for advanced glycosylation end products from bovine lung which are present on the endothelial cell surface. *J. Biol. Chem.* **267**:14987–14997.

Schmidt, A. M., Yan, S. D., Yan, S. F. and Stern, D. M. (2000). The biology of the receptor for advanced glycation end products and its ligands. *Biochim. Biophys. Acta.* **1498**:99–111.

Schmidt, A. M., Yan, S. D., Yan, S. F. and Stern, D. M. (2001). The multiligand receptor RAGE as a progression factor amplifying immune and inflammatory responses. *J. Clin. Invest.* **108**:949–955.

Schrödel, A. and de Marco, A. (2005). Characterization of the aggregates formed during recombinant protein expression in bacteria. *BMC Biochemistry.* **6**:10.

Schultz, T., Martinez, L. and de Marco, A. (2006). The evaluation of the factors that cause aggregation during recombinant expression in *E. coli* is simplified by the employment of an aggregation-sensitive reporter. *Microb. Cell Fact.* **5**:1–9.

Seely, D. M. R., Wu, P. and Mills E. J. (2005). EDTA chelation therapy for cardiovascular disease: a systematic Review. *BMC Cardiovasc. Disord.* **5**:32.

Sessa, L., Gatti, E., Zeni, F., Antonelli, A., Catucci, A., Koch, M., Pompilo, G., Fritz, G., Raucci, A. and Bianchi, M. (2014). The Receptor for Advanced Glycation End-Products (RAGE) Is only Present in Mammals, and Belongs to a Family of Cell Adhesion Molecules (CAMS). *PLoS one* **9**:1–13, e86903.

Sevon, N. and Oksman-Caldentey, K. M. (2002). *Agrobacterium rhizogenes*-mediated transformation: root cultures as a source of alkaloids. *Planta Med.* **68**:859–868.

Shacter, E. (2000). Quantification and significance of protein oxidation in biological samples. *Drug Metab Rev.* **32**:307–326.

Sharma, P., Padh, H. and Shrivastava, N. (2013). Hairy root cultures: A suitable biological system for studying secondary metabolic pathways in plants. *Eng Life Sci.* **13**:62–75.

Sharp, J. M. and Doran, P. M. (2001). Strategies for enhancing monoclonal antibody accumulation in plant cell and organ cultures. *Biotechnol. Prog.* **17**:979–992.

Sharpe, J. and London, E. (1997). Inadvertent concentrating of EDTA by ion exchange chromatography: avoiding artefacts that can interfere with protein purification. *Anal. Biochem.* **250**:124–125.

Shirano, Y. and Shibata, D. (1990). Low temperature cultivation of *Escherichia coli* carrying a rice lipoxygenase L-2 cDNA produces a soluble and active enzyme at a high level. *FEBS Lett.* **271**:128–130.

Sinclair, A. M. and Elliott, S. (2005). Glycoengineering: the effect of glycosylation on the properties of therapeutic proteins. *J. Pharm. Sci.* **94**:1626–1635.

Sirois, C. M., Jin, T., Miller, A. L., Bertheloot, D., Nakamura, H., Horvath, G. L., Mian, A., Jiang, J., Schrum, J., Bossaller, L., Pelka, K., Garbi, N., Brewah, Y., Tian, J., Chang, C. S., Chowdhury, P. S., Sims, G. P., Kolbeck, R., Coyle, A. J., Humbles, A. A., Xiao, T. S. and Latz, E. (2013). RAGE is a nucleic acid receptor that promotes inflammatory responses to DNA. *J Exp Med.* **210**:2447–2463.

Sitia, R. and Braakman, I. (2003). Quality control in the endoplasmic reticulum protein factory. *Nature* **426**:891–894.

Sitkiewicz, E., Tarnowski, K., Poznanski, J., Kulma, M. and Dadlez, M. (2013). Oligomerization interface of RAGE receptor revealed by MS-monitored hydrogen deuterium exchange. *PLoS one* **8**:e76353.

Smelko, J. P., Wiltberger, K. R., Hickman, E. F., Morris, B. J., Blackburn, T. J. and Ryll, T. (2011). Performance of high intensity fed-batch mammalian cell cultures in disposable bioreactor systems. *Biotechnol. Prog.* **27**:1358–1364.

Smith, S. A. and Morrissey, J. H. (2004). Rapid and efficient incorporation of tissue factor into liposomes. *J. Thromb. Haemost.* **2**:1155–1162.

Sorensen, H. P. and Mortensen, K. K. (2005). Soluble expression of recombinant proteins in the cytoplasm of *Escherichia coli. Microb. Cell Fact.* **4**:1–8.

Sourris, K. C., Morley, A. L., Koitka, A., Samuel, P., Coughlan, M. T., Penfold, S. A., Thomas, M. C., Bierhaus, A., Nawroth, P. P., Yamamoto, H., Allen, T. J., Walther, T., Hussain, T., Cooper, M. E. and Forbes, J. M. (2010). Receptor for AGEs (RAGE) blockade may exert its renoprotective effects in patients with diabetic nephropathy via induction of the angiotensin II type 2 (AT2) receptor. *Diabetologia* **53**:2442–2451.

Sparvero, L. J., Asafu-Adjei, D., Kang, R., Tang, D., Amin, N., Im, J., Rutledge, R., Lin, B., Amoscato, A. A., Zeh, H. J. and Lotze, M. T. (2009). RAGE (Receptor for Advanced Glycation Endproducts), RAGE ligands, and their role in cancer and inflammation. *J. Transl. Med.* **7**:1–21.

Spyropoulos, A. C. (2005). Pharmacologic therapy for the management of thrombosis: Unfractionated heparin or low-molecular-weight heparin? *Clin. Cornerstone.* **7**:39–48.

Srikrishna, G., Huttunen, H. J., Johansson, L., Weigle, B., Yamaguchi, Y., Rauvala, H. and Freeze, H. H. (2002). *N*-Glycans on the receptor for advanced glycation end

products influence amphoterin binding and neurite outgrowth. *J. Neurochem.* **80**:998–1008.

Srikrishna, G., Nayak, J., Weigle, B., Temme, A., Foell, D., Hazelwood, L., Olsson, A., Volkmann, N., Hanein, D. and Freeze, H. H. (2010). Carboxylated *N*-glycans on RAGE promotes S100A12 binding and signalling. *J. Cell Biochem.* **110**:645–659.

Srikrishna, G., Panneerselvam, K., Westphal, V., Abraham, V., Varki, A. and Freeze, H. H. (2001). Two proteins modulating transendothelial migration of leukocytes recognize novel carboxylated glycans on endothelial cells. *J. Immunol.* **166**:4678–4688.

Srikrishna, G., Turovskaya, O., Shaikh, R., Newlin, R., Foell, D., Murch, S., Kronenberg, M. and Freeze, H. H. (2005). Carboxylated Glycans Mediate Colitis through Activation of NF- kB. *J Immunol* **175**:5412–5422.

Srivastava , S. and Srivastava, A. K. (2007). Hairy root culture for mass-production of high-value secondary metabolites. *Crit Rev Biotechnol.* **27**:29–43.

Staub, J. M., Garcia, B., Graves, J., Hajdukiewicz, P. T., Hunter, P., Nehra, N., Paradkar, V., Schlittler, M., Carroll, J. A., Spatola, L., Ward, D., Ye, G. and Russell, D. A. (2000). High-yield production of a human therapeutic protein in tobacco chloroplasts. *Nat. Biotechnol.* **18**:333–338.

Stern, D. M., Yan, S. D., Yan, S. F. and Schmidt, A. M. (2002). Receptor for advanced glycation endproducts (RAGE) and the complications of diabetes. *Ageing Res. Rev.* **1**:1–15.

Stitt, A. W. (2010). AGEs and diabetic retinopathy. *Invest. Ophthalmol. Vis. Sci.* **51**:4867–4874.

Stoger, E., Fischer, R., Moloney, M., and Ma, J. K. C. (2014). Plant Molecular Pharming for the Treatment of Chronic and Infectious Diseases. *Ann. Rev. Plant Biol.* **65**:743–768.

Stogsdill, J. A., Stogsdill, M. P., Porter, J. L., Hancock, J. M., Robinson, A. B. and Reynolds, P. R. (2012). Embryonic overexpression of receptors for advanced glycation end-products by alveolar epithelium induces an imbalance between proliferation and apoptosis. *Am. J. Respir. Cell Mol. Biol.* **47**:60–66.

Strasser, R., Altmann, F., Mach, L., Glössl, J. and Steinkellner, H. (2004). Generation of *Arabidopsis thaliana* plants with complex N-glycans lacking beta1,2-linked xylose and core alpha1,3-linked fucose. *FEBS Lett* **561**:132–136.

Striegel, A. M., Yau, W. Y., Kirkland, J. J. and Bly, D. D. (2009). Modern Size-Exclusion Liquid Chromatography-Practice of Gel Permeation and Gel Filtration Chromatograph. 2nd Edition. John Wiley & Science, Hoboken. New Jersey.

Strupat, K., Rogniaux, H., Van Dorsselaer, A., Roth, J. and Vogl, T. (2000). Calcium-induced noncovalently linked tetramers of MRP8 and MRP14 are confirmed by electrospray ionization-mass analysis. *J. Am. Soc. Mass Spectrom.* **11**:780–788.

Sturchler, E., Galichet, A., Weibel, M., Leclerc, E. and Heizmann, C. W. (2008). Site-Specific Blockade of RAGE-Vd Prevents Amyloid-β Oligomer Neurotoxicity. *J. Neurosci.* **28**:5149–5158.

Sudha, C. G., Obul Reddy, B., Ravishankar, G. A. and Seeni, S. (2003). Production of ajmalicine and ajmaline in hairy root cultures of *Rauvolfia micrantha* Hook f., a rare and endemic medicinal plant. *Biotechnol. Lett.* **25**:631–636.

Sugaya, K., Fukagawa, T., Matsumoto, K., Mita, K., Takahashi, E., Ando, A., Inoko, H. and Ikemura, T. (1994). Three genes in the human MHC class III region near the junction with the class II: gene for receptor of advanced glycosylation end products, PBX2 homeobox gene and a notch homolog, human counterpart of mouse mammary tumor gene int-3. *Genomics* **23**:408–419.

Sun, P., Tropea, J. E. and Waugh, D. S. (2011). Enhancing the solubility of recombinant proteins in *Escherichia coli* by using hexahistidine-tagged maltose-binding protein as a fusion partner. *Methods Mol. Biol.* **705**:259–274.

Svab, Z and Maliga, P. (1993). High-frequency plastid transformation in tobacco by selection for a chimeric aadA gene. *Proc. Natl. Acad. Sci. USA.* **90**:913–917.

Swartz, J. R. (2001). Advances in *Escherichia coli* production of therapeutic proteins. *Curr. Opin. Biotechnol.* **12**:195–201.

Szymanski, C. M., Yao, R., Ewing, C. P., Trust, T. J. and Guerry P. (1999) Evidence for a system of general protein glycosylation in *Campylobacter jejuni. Mol. Microbiol.* **32**:1022–1030.

Taguchi, A., Blood, D. C., del Toro, G., Canet, A., Lee, D. C., Qu, W., Tanji, N., Lu, Y., Lalla, E., Fu, C., Hofmann, M. A., Kislinger, T., Ingram, M., Lu, A., Tanaka, H., Hori, O., Ogawa, S., Stern, D. M. and Schmidt, A. M. (2000). Blockade of RAGE-amphoterin signalling suppresses tumour growth and metastases. *Nature* **405**:354–360.

Tan, A. L., Forbes, J. M. and Cooper, M. E. (2007). AGE, RAGE, and ROS in diabetic nephropathy. *Semin. Nephrol.* **27**:130–143.

Tekoah, Y., Shulman, A., Kizhner, T., Ruderfer, I., Fux, L., Nataf, Y., Bartfeld, D., Ariel, T., Gingis–Velitski, S., Hanania, U. and Shaaltiel, Y. (2015). Large-scale production of pharmaceutical proteins in plant cell culture—the protalix experience. *Plant Biotechnol J.* **13**:1199–1208.

Thomas, C. T. and McNamee, M. G. (1990). Purification of membrane proteins. *Methods Enzymol.* **182**:499–520.

Thomas, J. G., Ayling, A. and Baneyx, F. (1997). Molecular chaperones, folding catalysts, and the recovery of active recombinant proteins from *E. coli* to fold or to refold. *Appl Biochem. Biotechnol.* **66**:197–238.

Thomas, J. O. (2001). HMG1 and 2: architectural DNA-binding proteins. *Biochem. Soc. Trans.* **29**:395–401.

Thomas, J. O. and Travers, A. A. (2001). HMG1 and 2, and related 'architectural' DNA-binding proteins. *Trends Biochem. Sci.* **26**:167–174.

Thomas, M. C. (2011). Advanced glycation end-products. *Contrib. Nephrol.* **170**:66–74.

Thomas, M. C., Soderlund, J., Lehto, M., Maikinen, V. P., Moran, J. L., Cooper, M. E., Forsblom, C. and Groop, P. H. (2011). Soluble receptor for AGE (RAGE) is a novel independent predictor of all-cause and cardiovascular mortality in type 1 diabetes. *Diabetologia* **54**:2669–2677.

Tregoning, J. S., Nixon, P., Kuroda, H., Svab, Z., Clare, S., Bowe, F., Fairweather, N., Ytterberg, J., van Wijk, K. J., Dougan, G. and Maliga, P. (2003). Expression of tetanus toxin Fragment C in tobacco chloroplasts. *Nucleic Acids Res.* **31**:1174–1179.

Trivedi, M. V., Laurence, J. S. and Siahaan, T. J. (2009). The role of thiols and disulfides on protein stability. *Curr. Protein Pept. Sci.* **10**:614–625.

Turovskaya, O., Foell, D., Sinha, P., Vogl, T., Newlin, R., Nayak, J., Nguyen, M., Olsson, A., Nawroth, P. P., Bierhaus, A., Varki, N., Kronenberg, M., Freeze, H. H. and Srikrishna, G. (2008). RAGE, carboxylated glycans and S100A8/A9 play essential roles in colitis-associated carcinogenesis. *Carcinogenesis* **29**:2035–2043.

Ueda, T., Chou, H., Kawase, T., Shirakawa, H. and Yoshida, M. (2004). Acidic C-tail of HMGB1 is required for its target binding to nucleosome linker DNA and transcription stimulation. *Biochemistry* **43**:9901–9908.

Uemura, K., Suzuki, Y., Shikanai, T., Wadano, A., Jensen, R. G. Chmara, W. and Yokota, A. (1996). A Rapid and Sensitive Method for Determination of Relative Specificity of RuBisCO from Various Species by Anion-Exchange Chromatography. *Plant Cell Physiol.* **37**:325–331.

Ukkonen, K., Vasala, A., Ojamo, H. and Neubauer, P. (2011). High-yield production of biologically active recombinant protein in shake flask culture by combination of enzyme-based glucose delivery and increased oxygen transfer. *Microb. Cell Fact.* **10**:1–9.

Ukkonen, K., Veijola, J., Vasala, A. and Neubauer, P. (2013). Effect of culture medium, host strain and oxygen transfer on recombinant Fab antibody fragment yield and leakage to medium in shaken *E. coli* cultures. *Microb. Cell Fact.* **12**:1–14.

Unger, T. and Peleg, Y. (2012). Recombinant protein expression in the baculovirus-infected insect cell system. *Methods Mol Biol.* **800**:187–199.

Vanz, A. N. L. S., Renard, G., Palma, M. S., Chies, J. M., Dalmora, S. L., Basso, L. A., and Santos, D. S. (2008). Human granulocyte colony stimulating factor (hG-CSF): cloning, overexpression, purification and characterization. *Microb. Cell Fact.* **7**:1–12.

Vaquero, C., Sack, M., Schuster, F., Finnern, R., Drossard, J., Schumann, D., Reimann, A. and Fischer, R. (2002). A carcinoembryonic antigen-specific diabody produced in tobacco. *FASEB J.* **16**:408–410.

Verch, T., Yusibov, V. and Koprowski, H. (1998). Expression and assembly of a full-length monoclonal antibody in plants using a plant virus vector. *J. Immunol. Methods* **220**:69–75.

Vitale, A. and Denecke, J. (1999). The endoplasmic reticulum-gateway of the secretory pathway. The *Plant Cell* **11**:615–628.

Vogl, T., Leukert, N., Barczyk, K., Strupat, K. and Roth, J. (2006). Biophysical characterization of S100A8 and S100A9 in the absence and presence of bivalent cations. *Biochim. Biophys. Acta* **1763**:1298–1306.

Vogl, T., Roth, J., Sorg, C., Hillenkamp, F. and Strupat, K. (1999). Calcium-induced noncovalently linked tetramers of MRP8 and MRP14 detected by ultraviolet matrix-assisted laser desorption/ionization mass spectrometry. *J. Am. Soc. Mass Spectrom.* **10**:1124–1130.

Walker, K. W., Lyles, M. M. and Gilbert, H. F. (1996). Catalysis of oxidative protein folding by mutants of protein disulfide isomerase with a single active-site cysteine. *Biochemistry* **35**:1972–1980.

Wallar, B. J. and Alberts, A. S. (2003). The formins: active scaffolds that remodel the cytoskeleton. *Trends Cell Biol.* **13**:435–446.

Walsh, G. (2014). Biopharmaceutical benchmarks. *Nat. Biotechnol.* **32**:992–1000.

Wang, L., Webster, D. E., Campbell, A. E., Dry, I. B., Wesselingh, S. L. and Coppel, R. L. (2008). Immunogenicity of *Plasmodium yoelii* merozite surface protein 4/5 produced in transgenic plants. *Int. J. Parasitol.* **38**:103–110.

Wang, W., Tai, F. and Chen, S. (2008). Optimizing protein extraction from plant tissues for enhanced proteomics analysis. *J. Sep. Sci.* **31**:2032–2039.

Ward, M., Lin, C., Victoria, D. C., Fox, B. P., Fox, J. A., Wong, D. L., Meerman, H. J., Pucci, J. P., Fong, R. B., Heng, M. H., Tsurushita, N., Gieswein, C., Park, M. and Wang H. (2004). Characterization of humanized antibodies secreted by *Aspergillus niger*. *Appl Environ Microbiol.***70**:2567–2576.

Ward, W. W. and Swiatek, G. (2009). Protein Purification. *Curr. Anal. Chem.* **5**:1–21.

Watson, J., Koya, V., Leppla, S. H. and Daniell, H. (2004). Expression of *Bacillus anthracis* protective antigen in transgenic chloroplasts of tobacco, a non-food/feed crop. *Vaccine* **22**:4374–4384.

Waugh, D. S. (2005). Making the most of affinity tags. *Trends Biotechnol.* **23**:316–320.

Webster, D. E. and Thomas, M. C. (2012). Post-translational modification of plant-made foreign proteins; glycosylation and beyond. *Biotech. Adv.* **30**:410–418.

Webster, D. E., Cooney, M. L., Huang, Z., Drew, D. R., Ramshaw, I. A., Dry, I. B., Strugnell, R. A., Martin, J. L. and Wesselingh, S. L. (2002). *J. Virol.* **76**:7910–7912.

Webster, D. E., Thomas, M. C., Huang, Z. and Wesselingh, S. L. (2005). The development of a plant-based vaccine for measles. *Vaccine*. **23**:1859–1865.

Webster, D. E., Wang, L., Mulcair, M., Ma, C., Santi, L., Mason, H. S., Wesselingh, S. L. and Coppel, R. L. (2009). Production and characterisation of an orally immunogenic Plasmodium antigen in plants using a virus-based expression system. *Plant Biotechnol. J.* **7**:846–855.

Werner, S., Breus, O., Symonenko, Y., Marillonnet, S. and Gleba, Y. (2011). High-level recombinant protein expression in transgenic plants by using a double-inducible viral vector. *Proc. Natl. Acad. Sci. USA* **108**:14061–14066.

Wildt, S. and Gerngross, T. U. (2005). The humanization of *N*-glycosylation pathways in yeast. *Nat. Rev. Microbiol.* **3:**119–128.

Wilton, R., Yousef, M. A., Saxena, P., Szpunar, M. and Stevens, F. J. (2006). Expression and purification of recombinant human receptor for advanced glycation end products in *Escherichia coli*. *Protein Expr. Purif.* **47**:25–35.

Woodard, S. L., Mayor, J. M., Bailey, M. R., Barker, D. K., Love, R. T., Lane, J. R., Delaney, D. E., McComas-Wagner, J. M., Mallubhotla, H. D., Hood, E. E., Dangott, L. J., Tichy, S. E. and Howard, J. A. (2003). Maize (*Zea mays*)-derived bovine trypsin: characterization of the first large-scale, commercial protein product from transgenic plants. *Biotechnol. Appl. Biochem*. **38**:123–130.

Woycechowsky, K. J. and Raines, R. T. (2000). Native Disulfide Bond Formation in Proteins. *Curr Opin Chem Biol*. **4**: 533.

Wroblewski, T., Tomczak, A. and Michelmore, R. (2005). Optimization of *Agrobacterium*-mediated transient assays of gene expression in lettuce, tomato and *Arabidopsis*. *Plant Biotechnol. J.* **3**:259–273.

Wu, T and Mohan, C. (2012). Lupus nephritis - alarmins may sound the alarm? *Arthritis Res Ther*. **14**:129.

Wurm, F. M. (2004). Production of recombinant protein therapeutics in cultivated mammalian cells. *Nat. Biotechnol.* **22**:1393–1398.

Xie, J., Burz, D. S., He, W., Bronstein, I. B., Lednev, I. and Shekhtman, A. (2007). Hexameric calgranulin C (S100A12) binds to the receptor for advanced glycation end products (RAGE) using symmetric hydrophobic target-binding patches. *J. Biol. Chem.* **282**:4218–4231.

Xie, J., Mendez, J. D., Mendez-Valenzuela, V. and Aguilar-Hernandez, M. M. (2013). Cellular signalling of the receptor for advanced glycation end products (RAGE). *Cell Signal*. **25**:2185–2197.

Xue, J., Rai, V., Singer, D., Chabierski, S., Xie, J., Reverdatto, S., Burz, D. S., Schmidt, A. M., Hoffmann, R. and Shekhtman, A. (2011). Advanced glycation end product recognition by the receptor for AGEs. *Structure* **19**:722–732.

Yamagishi, S., Nakamura, K., Matsui, T., Noda, Y. and Imaizumi, T. (2008). Receptor for advanced glycation end products (RAGE): a novel therapeutic target for diabetic vascular complication. *Curr Pharm Des*. **14**:487-495.

Yamamoto, Y., Harashima, A., Saito, H., Tsuneyama, K., Munesue, S., Motoyoshi, S., Han, D., Watanbe, T., Asano, M., Takasawa, S., Okamoto, H., Shimura, S., Karasawa, T., Yonekura, H. and Yamamoto, H. (2011). Septic shock is associated with receptor for advanced glycation end products ligation of LPS. *J. Immunol.* **186**:3248–3257.

Yamashita, N., Ciani, S. and Hagiwara, S. (1990). Effects of internal Na^+ on the Ca channel outward current in mouse neoplastic B lymphocytes. *J. Gen. Physiol.* **96**:559–579.

Yan, S. D., Zhu, H., Fu, J., Yan, S. F., Roher, A., Tourtellotte, W. W., Rajavashisth, T., Chen, X., Godman, G. C., Stern, D. and Schmidt, A. M. (1997). Amyloid-beta peptide-receptor for Advanced Glycation End product interaction elicits neuronal expression of macrophage-colony stimulating factor: a proinflammatory pathway in Alzheimer's disease. *Proc. Natl. Acad. Sci. USA* **94**:5296–5301.

Yao, J., Weng, Y., Dickey, A., and Wang, K. Y. (2015). Plants as Factories for Human Pharmaceuticals: Applications and Challenges. *Int J Mol Sci.* **16**:28549–28565.

Yasukawa, T., Kanei-Ishii, C., Maekawa, T., Fujimoto, J., Yamamoto, T. and Ishii, S. (1995). Increase of Solubility of Foreign Proteins in *Escherichia coli* by Coproduction of the Bacterial Thioredoxin. *J. Biol. Chem.* **270**:25328–25331.

Yeh, C. H., Sturgis, L., Haidacher, J., Zhang, X. N., Sherwood, S. J., Bjercke, R. J., Juhasz, O., Crow, M. T., Tilton, R. G. and Denner, L. (2001). Requirement for p38 and p44/p42 mitogen-activated protein kinases in RAGE-mediated nuclear factor-κB transcriptional activation and cytokine secretion. *Diabetes* **50**:1495–1504.

Yin, C., Li, H., Zhang, B., Liu, Y., Lu, G., Lu, S., Sun, L., Qi, Y., Li, X. And Chen, W. (2013). RAGE-binding S100A8/A9 promotes the migration and invasion of human breast cancer cells through actin polymerization and epithelial–mesenchymal transition. *Breast Cancer Res Treat* **142**:297–309.

Yonchuk, J. G., Silverman, E. K., Bowler, R. P., Agustí, A., Lomas, D. A., Miller, B. E., Tal-Singer, R. and Mayer, R. J. (2015). Circulating soluble receptor for advanced glycation end products (sRAGE) as a biomarker of emphysema and the RAGE axis in the lung. *Am. J. Respir. Crit. Care Med.* **192**:785–792.

Yonekura, H., Yamamoto, Y., Sakurai, S., Petrova, R. G., Abedin, M. J., Li, H., Yasui, K., Takeuchi, M., Makita, Z., Takasawa, S., Okamoto, H., Watanabe, T. and Yamamoto, H. (2003). Novel splice variants of the receptor for advanced glycation end-products expressed in human vascular endothelial cells and pericytes, and their putative roles in diabetes-induced vascular injury. *Biochem. J.* **370**:1097–1109.

Yu, S. L., Wong, C. K., Szeto, C. C., Li, E. K., Cai, Z. and Tam, L. S. (2015). Members of the receptor for advanced glycation end products axis as potential therapeutic targets in patients with lupus nephritis. *Lupus* **24**:675–686.

Yusibov, V., Streatfield, S. J. and Kushnir, N. (2011). Clinical development of plant-produced recombinant pharmaceuticals, vaccines, antibodies and beyond. *Hum Vaccines.* **7**:313-321.

Zaia, J. (2010). Mass Spectrometry and Glycomics. *OMICS.* **14**: 401–418.

Zhang, L., Wu, G., Tate, C. G., Lookene, A. and Olivecrona, G. (2003). Calreticulin promotes folding/dimerization of human lipoprotein lipase expressed in insect cells. (Sf21). *J. Biol. Chem.* **278**:29344–29351.

Zhuo, Q., Piao, J. H., Wang, R. and Yang, X. G. (2005). Refolding and purification of non-fusion HPT protein expressed in *Escherichia coli* as inclusion bodies. *Protein Expr. Purif.* **41**:53–60.

Zong, H., Ward, M. and Stitt, A. W. (2011). AGEs, RAGE, and diabetic retinopathy. *Curr. Diab. Rep.* **11**:244–252.

Appendix I

Amino acid sequences of sRAGE expressed in hairy roots

```
         10         20         30         40         50         60
MAAGTAVGAW VLVLSLWGAV VGAQNITARI GEPLVLKCKG APKKPPQRLE WKLNTGRTEA

         70         80         90        100        110        120
WKVLSPQGGG PWDSVARVLP NGSLFLPAVG IQDEGIFRCQ AMNRNGKETK SNYRVRVYQI

        130        140        150        160        170        180
PGKPEIVDSA SELTAGVPNK VGTCVSEGSY PAGTLSWHLD GKPLVPNEKG VSVKEQTRRH

        190        200        210        220        230        240
PETGLFTLQS ELMVTPARGG DPRPTFSCSF SPGLPRHRAL RTAPIQPRVW EPVPLEEVQL

        250        260        270        280        290        300
VVEPEGGAVA PGGTVTLTCE VPAQPSPQIH WMKDGVPLPL PPSPVLILPE IGPQDQGTYS

        310        320        330        340
CVATHSSHGP QESRAVSISI IEPGEEGPTA GHHHHHHHHS EKDEL
```
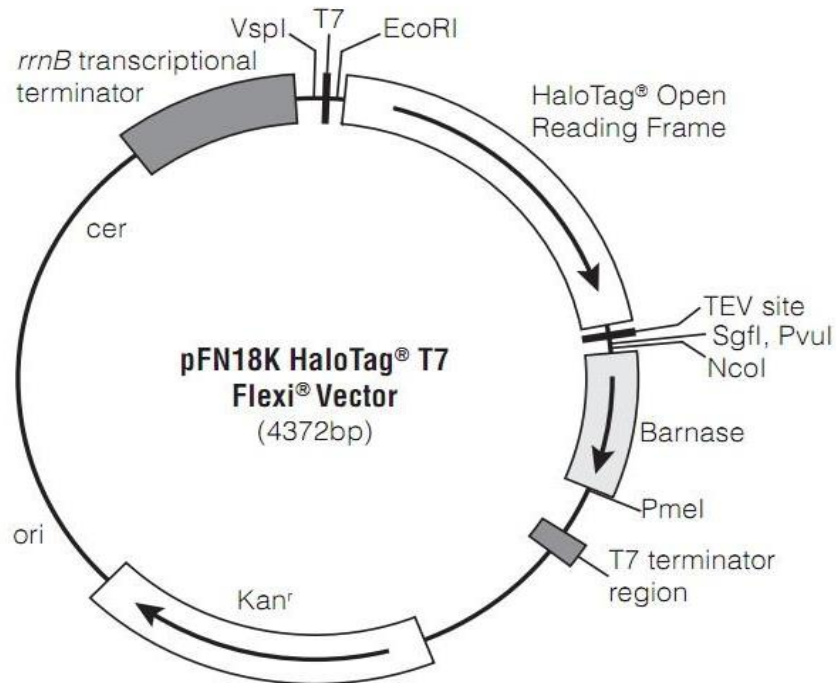
Histidine-Tag (eight) and the SEKDEL sequence is indicated in blue and red colour respectively. The underlined sequence is the signal peptide. Cysteine residues are indicated in brown colour. *N*-glycosylation sites are within the boxes.

Appendix II

pFN18K Halo-Tag® T7 Flexi® vector (Promega) circle map and the sequence reference points. sRAGE gene is inserted between _Nco_I and _Pme_I restriction enzyme sites (complete sequence; http://www.ncbi.nlm.nih.gov/nuccore/EU545993).

Appendix III

Murashige and Skoog medium (MS)

4.43 g / L^{-1} of MS medium with Vitamins (Catalogue No: M519: PhytoTechnologies Laboratories, LLC^{TM}) with selection using 100 μg mL^{-1} cefotaxime and 25 μg mL^{-1} kanamycin

Phosphate Buffered Saline (PBS)

8 % NaCl, 0.2 % KCl, 1.44 % Na_2HPO4, and 0.24 % KH_2PO_4, pH 7.4

PBST

PBS with 0.05 % tween 20

Luria Bertani (LB) agar

1% Bacto tryptone, 0.5% Bacto yeast extract, 0.5% NaCl, 1.5% agar, pH 7.5

Terrific broth

1.2 % Bacto tryptone, 2.4 % Bacto yeast extract, 0.4 % glycerol and 1 % filter sterile 0.89M potassium phosphate

1X Tris-acetate-EDTA (TAE) buffer

40 mM Tris (Merck Millipore), 20 mM acetic acid (Ajax Finechem Pty Ltd.), 1 mM EDTA (pH 8.0, Merck)

1 % agarose gel

1 g of molecular grade agarose (Bioline) in 100 mL of 1X TAE buffer

4X Native loading buffer

125 mM Tris-HCl pH 6.8, 0.01 % bromophenol blue and 10 % glycerol

Native running buffer

25 mM Tris, 192 mM glycine

Acetate-MES-Tris (AMT) buffer for pH profiles

100 mM acetate, 100 mM MES, 200 mM Tris, 4 mM EDTA

9.76 g MES (2-(*N*-morpholino) ethanesulfonic acid (monohydrate free acid)) and 12.12 g Tris were dissolved in 350 mL ddH$_2$O. 2.86 mL glacial acetic acid and 3.2 mL 0.5 M EDTA were added to the solution. The final volume was adjusted to 400 mL with ddH$_2$O. 40 mL aliquots were adjusted to the appropriate pH with NaOH or HCl and made up to 50 mL with ddH$_2$O.